REMOVAL BEHAVIOUR OF IRON COATED SAND (ICS) AND MANGANESE COATED SAND (MCS) FOR HEAVY METAL TOXIC IONS FROM AQUEOUS SOLUTIONS

A Thesis submitted

in partial fulfilment of the requirements for the Degree of

Doctor of Philosophy

in Chemistry

By

C. LALDAWNGLIANA

DEPARTMENT OF CHEMISTRY
SCHOOL OF PHYSICAL SCIENCES
MIZORAM UNIVERSITY
TANHRIL, AIZAWL-796004

June, 2012

REMOVAL BEHAVIOUR OF IRON COATED SAND (ICS) AND MANGANESE COATED SAND (MCS) FOR HEAVY METAL TOXIC IONS FROM AQUEOUS SOLUTIONS

A Thesis submitted

in partial fulfilment of the requirements for the Degree of

Doctor of Philosophy

in Chemistry

By

C. LALDAWNGLIANA

Regd. No. & date: MZU/Ph.D/196/17.12.2007

DEPARTMENT OF CHEMISTRY
SCHOOL OF PHYSICAL SCIENCES
MIZORAM UNIVERSITY
TANHRIL, AIZAWL-796004

June, 2012

MIZORAM UNIVERSITY
(A Central University under the Act of Parliament)
Department of Chemistry
School of Physical Sciences

Dr. Diwakar Tiwari
Professor & Head

Certificate

This is to certify that the thesis entitled '*Removal behaviour of iron coated sand (ICS) and manganese coated sand (MCS) for heavy metal toxic ions from aqueous solutions'* submitted by ***Shri C. Laldawngliana***, for the degree of ***Doctor of Philosophy*** of the Mizoram University, Aizawl, embodies the record of original investigations carried out by him under my supervision. He has been duly registered and the thesis presented is worthy of being considered for the award of the Ph.D. degree. This work has not been submitted for any degree of any other university.

Dated: 28th June 2012 (Diwakar Tiwari)
` Supervisor

Tanhril Campus, Aizawl (Mizoram) 796004, India; Ph. 0389-2330832 (O); Cell: 09862323015; Fax: 0389-2330834;
E.Mail:diw_tiwari@yahoo.com

Declaration of the Candidate

I, C. Laldawngliana, a Ph.D. Scholar in Chemistry Department, Mizoram University, Aizawl, do hereby solemnly declare that the subject matter of this thesis is the record of the work done by me. I have duly worked on my Ph.D. thesis under the supervision of Professor Diwakar Tiwari, Department of Chemistry, Mizoram University, Aizawl. This is being submitted to the Mizoram University for the degree of Doctor of Philosophy in Chemistry and that I have not submitted this work to any other University or Institute for any other degree.

I also declare that the present investigation relates to bonafide research works done by me and the title of the thesis is **'REMOVAL BEHAVIOUR OF IRON COATED SAND (ICS) AND MANGANESE COATED SAND (MCS) FOR HEAVY METAL TOXIC IONS FROM AQUEOUS SOLUTIONS'.**

Dated: 28th June 2012

(C. LALDAWNGLIANA)

Candidate

Acknowledgements

It is my pleasure to express my sincere gratitude to my Research Supervisor, *Dr. Diwakar Tiwari*, Professor and Head, Department of Chemistry, Mizoram University, for his reverend, dynamic and unceasing guidance throughout this research work. His expertise and immense knowledge in this field of research boost me carrying out this research work, imparting deeper knowledge of scientific technology to the present field of research.

I extend my sincere thanks to *Professor Seung Mok Lee* and his team, Department of Environmental Engineering, Kwandong University, Gangneung, Korea for allowing me utilizes their sophisticated instruments *viz.*, Scanning Electron Microscope (SEM), Atomic Absorption Spectrophotometer (AAS), X – Ray Diffractometer (XRD), etc. to carry out the analysis of my sample. Their valuable help in every possible ways to the success of my research is greatly acknowledged.

I express my sense of gratitude to present and former Deans *Professor R.K. Thapa* and *Professor R. P. Tiwari*, School of Physical Sciences, MZU for their support and encouragements accomplishing the research work in the department. I also thank to the former Head, *Dr. Muthukumaran, R.*, Department of Chemistry, MZU for his support and providing all necessary facilities required to carry out experiments in the department.

I convey my sincere thanks to the former and present Principals, *Mr. V. Suakbuanga* and *Mr. Lalnunmawia*, Govt. Champhai College for allowing me pursue my research programme at MZU.

I also convey my heartfelt gratitude to all the faculty members viz., *Dr. Zodinpuia Pachuau, Dr. N. Mohondas Singh, Dr. Rajkumar Mishra, Dr. Ved Prakash Singh*, Department of Chemistry, MZU for their continuous inspiration, support and innovative suggestions while carrying out my research work.

The valuable support and encouragement that I had received from my colleagues in Govt. Champhai College during my research career is worth to be mentioned. I would like to mention in particular, the efforts and dedication which my colleagues *Dr. Goutam Bit, Mr. Zirsangliana, Mr. Lijumon Lalremsanga* and *Miss Lalchhingpuii* of Chemistry Department, Govt. Champhai College, had taken during my absence. I extend my heartfelt gratitude to them.

Acknowledgements

I would like to acknowledge the *Higher and Technical Education Department, Govt. of Mizoram, Aizawl* for granting me three years of study leave to carry out my research work.

Further, I also wish to acknowledge *Mizoram Scholarship Board*, for their financial assistance during my research work.

I am indebted to my fellow research scholars of Chemistry Department, *Miss Lalramnghaki Pachuau, Mr. Lalhmunsiama, Miss Rebecca Lalmuanpuii, Mr. Samuel Lallianrawna , Mr Lalrosanga, Mr. Joseph Lalhruaitluanga* and others for their support, encouragement and helping hand which had been rendered while carrying out my research work. It is my pleasure to mention *Mr. John Vanlalhruaia* and *Miss Lalthuammawii* for their efficient help in all the administrative related works. I put forth my deep sense of gratitude to them.

I express my deep sense of gratitude to *Mrs. Alka Tiwari*, for her kind hospitality and encouragements throughout my research work.

I am happy to express the endless love, support, encouragements, prayers and enthusiasm from my parents and my family. I feel extremely thankful to my wife *Mrs. Lalmuanpuii* and our four children**,** *C. Lalbiaknunga, C. Lalnunsangi, C. Lalrohlui* and *C. Lalduhsaki* who stand beside me in every nooks and corners of my life. Their smilingly face always inspire me to overcome the hardship and take up the challenge of life.

Above all, I thank the Almighty God for his blessings, fellowship and guidance which steer me through the hard days of my life. I dedicated this work for His glory.

C. Laldawngliana

CONTENTS

Pages

APPENDIX PUBLISHED JOURNAL PAPERS

REMOVAL BEHAVIOUR OF IRON COATED SAND (ICS) AND MANGANESE COATED SAND (MCS) FOR HEAVY METAL TOXIC IONS FROM AQUEOUS SOLUTIONS

CHAPTER
1
Introduction

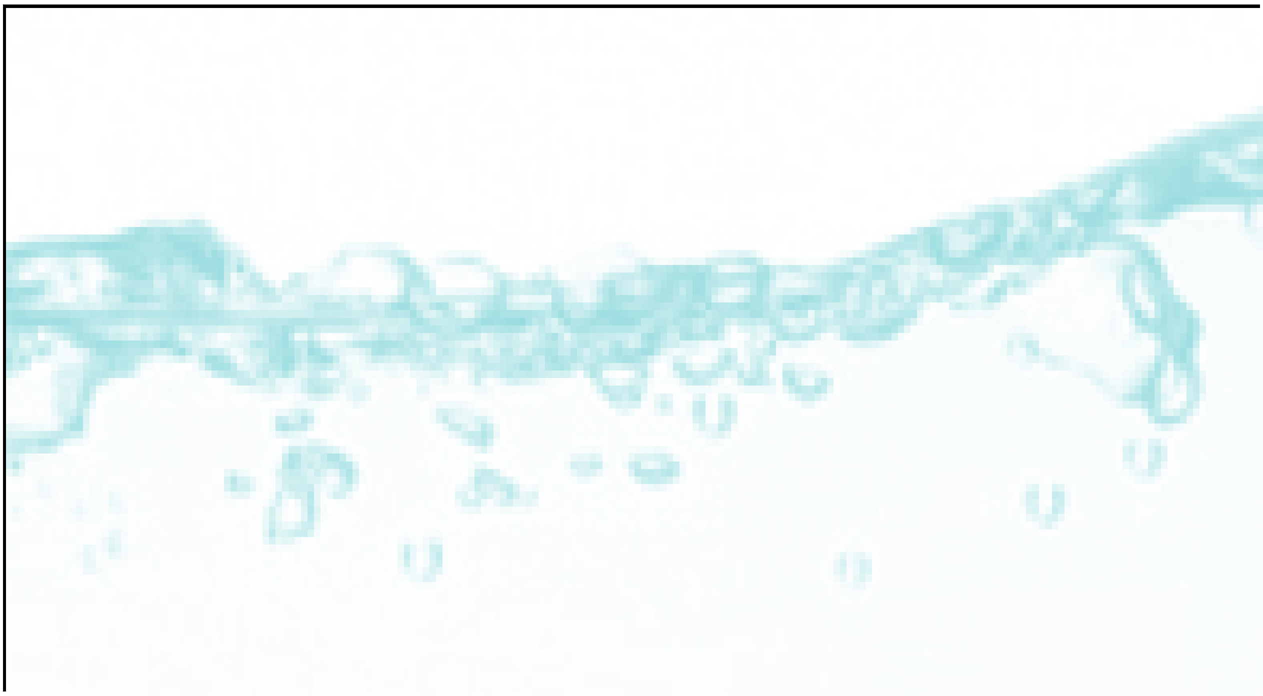

INTRODUCTION

Water is an important and essential component of living being, which is increasingly polluted from day to day. Water pollution requires ongoing evaluation and revision of water resource policy at all levels (international down to individual aquifers and wells). It was observed that the use of deleterious quality of water caused for various diseases or even deaths throughout the globe (Daniel, 2006). In addition to the acute problems of water pollution in developing countries or even industrialized countries continue to struggle with the strategies to adopt in the remediation policies for decontamination of polluted water bodies.

Water is typically referred to as polluted when it is impaired by anthropogenic contaminants and either does not support a human use, such as drinking water, and/or undergoes a marked shift in its ability to support its constituent biotic communities. Natural phenomena such as volcanoes, algae blooms, storms, and earthquakes also cause major changes in water quality and the ecological status of aquatic environment. The reclaimed water often contained with the contaminants of emerging concerns (CECs) that includes pharmaceuticals, household chemicals, personal care products, disinfectants, insecticides, heavy metal toxic ions etc., which poses a serious concern to maintain the water quality standards (Laws *et al.*, 2011; Ternes *et al.*, 1998; Kolpin *et al.*, 2004; Wells *et al.*, 2009).

Many chemicals undergo reactive decay or chemical change especially over long periods of time in groundwater reservoirs. A noteworthy class of such chemicals is the chlorinated hydrocarbons such as trichloroethylene (used in electronic industries for metal degreasing) and tetrachloroethylene used in the dry cleaning industry (note latest advances in liquid carbon dioxide in dry cleaning that avoids use of chemicals). Both of these chemicals which are known to be potential carcinogens, undergo only partial decomposition, leading to new hazardous chemicals (including dichloroethylene and vinyl chloride).

Groundwater pollution is much more difficult to abate than surface water pollution since groundwater moves greater distances through unseen aquifers. Micro or meso-porous aquifers such as clays partially purify the water from bacteria by simple filtration (adsorption and absorption), dilution, and, in some cases, chemical reactions and biological activity: however, in some cases, the pollutants merely transform to soil contaminants. Groundwater that moves through cracks and caverns is not filtered and can be transported as easily as surface water. In fact, this can be aggravated by the human tendency to use natural sink holes as dumps in areas of Karst topography.

There is variety of secondary effects stemming not from the original pollutant, but a derivative condition. An example is silt-bearing surface runoff, which can inhibit the penetration of sunlight through the water column, hampering photosynthesis in aquatic plants.

The contamination of surface/ground waters by heavy metal toxic ions is a serious environmental and public concern because of the fact that these ions are virtually non-biodegradable and tend to accumulate within the bio-system, causing various biological disorders (Martin, 1985). Increasing use of toxic metals in various industrial process leads to the contamination of our aquatic environment. Besides the toxic and harmful effects to the aquatic life the extended perseverance of these pollutants in the biological systems and accumulating in the biosphere through the food chain results in the environmental and occupational hazards (Martins, 2004; Rout *et al.*, 2009). Contamination of water bodies with heavy metals arises mainly from the aqueous waste streams of industries *viz.*, metal plating, mining operations, tanneries, etc. Toxic metals such as mercury, cadmium, arsenic, copper and many other species tend to accumulate with the sediments from which they may be released by various processes of remobilization which further can move up to the biologic chain, thereby reaching human beings where they produce chronic and acute ailments (Förstner *et al.*, 1981). Leachates emanating from old mines often contain higher concentrations of dissolved metals like iron, manganese, aluminium, zinc, etc. and sulphate which could even contain high acidity (Bamsforth *et al.*, 2006; Manzano *et al.*, 1999; Younger, 2002). Heavy metals form compounds in the body that can be carcinogenic and mutagenic even at very low levels (Ruiz-Manriques *et al.*, 1998). Inorganic micro-pollutants are of considerable concern since these are non-biodegradable, highly toxic and perhaps cause for carcinogenic effect (Cimino *et al.*, 1990; Madoni *et al.*, 1996). The increased level of industrialization/urbanization is known to be an additional source of contamination of fresh water. Although, several heavy metals are reported to be essential at trace level concentration however, an increased level of intake caused for adverse effects towards the living beings. Heavy metals such as cadmium (Cd), chromium (Cr), copper (Cu), lead (Pb), arsenic (As) etc. often present in industrial waste/effluent waters which is a potential hazard to the aquatic ecosystem and poses human health risk.

1.1. TOXICITY OF HEAVY METALS

1.1.1. Chromium

Chromium is usually found in industrial effluent. The most common sources of chromium includes with steelworks, chromium electroplating, leather tanning, chemical manufacturing and textile industries etc. (Sankararamakrishnan *et al.*, 2006; Stasinakis *et al.*, 2003; Raji and Anirudhan, 1998; Balasubramanian and Pugalenthi, 1999; Liang *et al.*, 2003; Gopi Krishna *et al.*, 2004; Adria-Cerezo *et al.*, 2000; Deng and Bai, 2004). Chromium(VI) is poisonous to most living organisms but has many applications including in wood preservation (Lakatos *et al.*, 2002; Chwastowska *et al.*, 2005; Sankararamakrishnan *et al.*, 2006). Humans are exposed to excessive amount of Cr(VI) through food, drinking water, and inhaling air that may contain chromium particles. The average daily intake from air, water, and food is estimated to be 0.01 – 0.03 µg, 2.0 µg/L and 60.0 µg, respectively (Donais *et al.*, 1999). Cr(VI) is known to be toxic to both plants and animals, as a strong oxidizing agent and potential carcinogen (Costa and Klein, 2006). Cr(VI) is considered by the IARC (International Agency for Research on Cancer) as a potential carcinogenic agent that modifies the DNA transcription process causing important chromosomic aberrations (IARC, 1982). The NIOSH (National Institute for Occupational Safety and Health) recommends that the levels of Cr(VI) in water should be reduced to 10^{-3} mg/m^3 (Muir, 1977). The discharge of Cr(VI) to surface water is regulated to below 0.05 mg/L by the US EPA (Baral, 2002). The inhalation of chromium compounds has been associated with the development of cancer in workers in the chromate industry. The relative risk for developing lung cancer was calculated to be as much as 30 times that of controls (Hayes, 1982; Leonard and Lauwerys, 1980; Langard, 1983). There is also evidence for an increased risk of developing nasal, pharyngeal and gastrointestinal carcinomas (Hamilton and Wetterhahn,1988). Quantitative epidemiological data were obtained by Mancuso and Hueper, (1951), they observed an increase in deaths (18.2 %; $P < 0.01$) from respiratory cancer among chromate workers compared with 1.2 % deaths with controls. In a follow-up study, conducted when more than 50 % of the workers were died, the observed incidents for lung cancer deaths were increased to approximately 60% (Mancuso, 1975). The workers were exposed to total chromium of 1-8 mg/m^3/year. Mancuso (1975) observed a dose response for total chromium exposure and attributed to the lung cancer deaths on exposure to insoluble Cr(III), soluble Cr(VI) and total chromium.

1.1.2. Arsenic

Arsenic is generally found as a contaminant in soil and water systems due to various anthropogenic sources, geologic variance, the arsenic mine drenching, the dissolution of ground rock along with the human activities such as mining, metallurgy, leather process, dyeing industry, use of pesticide and insecticide etc. (Chakravarty *et al.*, 2002; Smedley *et al.*, 2002; Bhumbla *et al.*, 1994; Kim *et al.*, 2002).

Arsenic occurrence in the environment, its toxicity, health hazards, and the techniques used for speciation analysis is well reviewed elsewhere (Penrose, 1974; Bodek *et al.*, 1998; Jain and Ali, 2000; Matschullat, 2000; Bissen and Frimmel, 2003). Long-term drinking water exposure caused for skin, lung, bladder, and kidney canceras well as pigmentation changes, skin thickening (hyperkeratosis) neurological disorders, muscular weakness, loss of appetite, nausea etc. (Jain and Ali, 2000; Kiping, 1997; WHO, 1981; Mandal and Suzuki, 2002). This differs from acute poisoning, which typically caused for vomiting, oesophageal and abdominal pain, and bloody “rice water” diarrhea (Jain and Ali, 2000; Kiping, 1997; WHO,1981; Desesso *et al.*, 1998; Duker *et al.*, 2005; Ng *et al.*, 2003). Arsenic in natural waters is a worldwide problem. Arsenic pollution reported in various countries including USA, China, Chile, Bangladesh, Taiwan, Mexico, Argentina, Poland, Canada, Hungary, New Zealand, Japan and India (Burkel & Stoll, 1999; Cebrian *et al.*, 1983; Dhar *et al.*, 1997; Karim, 2000). The largest population at risk among the 21 countries with known groundwater arsenic contamination is in Bangladesh, followed by West Bengal in India (Das *et al.*, 1995; Jain and Ali, 2000; Chatterjee *et al.*, 1995)

Arsenic is classified as a Group A carcinogen by the United States Environmental Protection Agency (USEPA). The toxic effects ranged from acute lethality to chronic effects, such as cancer and diseases of the vascular system (Borum *et al.*, 1994; Saha *et al.*, 1999). It was reported that serious health problems, such as cancers, skin alteration, etc., was linked to arsenic ingestion even at a low concentration (20–50 mg/l) (O'Connor, 2002). Extensive epidemiological studies showed that chronic ingestion of high levels of inorganic arsenic caused skin cancer (National Research Council, 1999). It was found that Arsenic exposure also caused cancers of the nasal cavity, trachea, bronchus, lung, liver, bladder, colon, kidney, prostate, brain, the lymphatic and hematopoietic tissues as well as the nervous system (Chen and Lin, 1994; Naqvi *et al.*, 1994; Remembrance, 2003). Recent report by the United States National Academy of Science and United States National Research Council revealed that even at 3µg/L of arsenic, the risk of bladder and lung cancer was between four and seven deaths per 10,000 people. At 10 µg/L, the risk was increased to between 12 and 23 deaths per 10,000 people (NRC, 2001). In addition, arsenic can cause high blood pressure and diabetes. The US EPA announced its ruling in October 2001 to lower the maximum contaminant level (MCL) from 50 µg/L to 10 µg/L (An *et al*, 2005; EPA, 2000). China has adopted a new standard of arsenic in drinking water which was promulgated by National Standard Committee and Sanitation Ministry, lowered the arsenic level from 50 µg/L to 10 µg/L. The World Health Organization (WHO) also recommended lowering the As -drinking water standard to 10 µg/L (WHO, 2001).The improved drinking water standard posed new challenges to water treatment technique.

1.1.3. Cadmium

Cadmium (Cd) is a toxic element whose presence in the environment, mainly due to the industrial processes and phosphate fertilizers through which it is transferred to the food chain (Pinto *et al.*, 2004). Cadmium enters into surface water with the discharge of industrial effluents/wastes from metal plating, smelting, paint pigments, batteries, fertilizers, metallurgical alloying, mining, ceramics and other industrial operations (Davis *et al.*, 2000; Iqbal and Edyvean, 2005) or by leaching of soil, to which sewage sludge is added. It is biologically very reactive and therefore gives rise to both acute and chronic poisoning. Nariagu (1983) emphasized the effects of cadmium on aquatic organisms. It became popularized in late 1940's in Japanese villages causing a condition known as the "itai-itai" or ouch-ouch bone degenerative disease (Aoshima, 2003**;** Kasuya, 2000; Hutton, 1983). Cadmium toxicity was observed by a variety of syndromes and effects including renal dysfunction, hypertension, hepatic injury, lung damage and teratogenic effects (Hajialigol *et al.*, 2006). It was reported that cadmium found to be carcinogenic and caused for lung fibrosis and dyspnea (Sud *et al.*, 2008). Chronic exposure to elevated levels of cadmium caused for bone degeneration, liver damage etc. (Iqbal *et al.*, 2007). Acute exposure to cadmium fumes may cause flu like symptoms including chills, fever, and muscle ache sometimes referred to as "the cadmium blues". More severe exposures can cause tracheal bronchitis, pneumonitis and pulmonary edema. Symptoms of inflammation may start hours after the exposure and include cough, dryness and irritation of the nose and throat, headache, dizziness, weakness, fever, chills, and chest pain. Cigarettes are also a source of cadmium exposure. Although there is generally less cadmium in tobacco than in food, but lungs absorb cadmium more efficiently than the stomach (Jarup, 1998). Workers exposed to cadmium-containing fumes were reported to develop acute respiratory distress syndromes (ARDS) (Barbee and Prince, 1999). Intake of cadmium-contaminated food caused acute gastro- intestinal effects, such as vomiting and diarrhoea (Nordberg, 2004).The IARC (International Agency for Research on Cancer) decided to classify cadmium as one of human carcinogen group I. Latest data however, supported the assumption that only an uptake of cadmium via the respiratory system has carcinogenic potential (Jin *et al.*, 2002).

1.1.4. Copper

The primary sources of copper includes with the effluents aroused from printed circuit boards, metal surface treatments and mining operations. Copper in small amount known to be an essential element of humans and living organism where it is an important catalyst for heme synthesis and iron absorption. However, higher concentrations of copper in the biological systems possessed with several toxic effects (Benaissa and Elouchdi, 2007). Copper can cause severe mucosal irritation and corrosion, widespread capillary damage central nervous system irritation, stomach and intestinal distress, liver and kidney damage, and anemia (Gardea-Torresdey *et al.*, 1996; Ajmal *et al.*, 1998). The human body has a natural mechanism for maintaining the proper level of copper. However, children fewer than one year old do not show such mechanism therefore is more vulnerable to the toxic effects of copper. People with Wilson's disease also showed a problem with maintaining the proper balance and taking care to limit the exposure of copper. Concentration of copper in drinking water with level of 5 to 8 mg/L make the water undrinkable (HDR Engineering Inc, 2001). Maximum Contaminated Level (MCL) for copper is 1.3 mg Cu/L based on taste and to a lesser extent on limited toxicity data (Donald *et al.*, 1999).

1.1.5. Lead

Lead is one of potential toxic heavy metals and once absorbed into the body showed several biological disorder (Friberg *et al.*, 1979).Lead contamination of the environment is primarily due to anthropogenic activities making it the most ubiquitous toxic metal in the environment (Environmental health criteria 165 1995, Amdur *et al.*, 1991). Research on lead (Pb) becomes an important topic of research for environmental and medical scientists for the reasons: (1) It has no known biological use and (2) It is toxic to most living beings. Lead readily bio accumulates in the human-rich surface layer of the soils due to its complexation with organic matter. It is the least mobile heavy metal in soils under reducing or non-acidic conditions. Furthermore, it is one of the most common trace metal contaminants in urban soils due to atmospheric deposition from industries and automobile emission. The sources of lead in the environment is mainly because of waste streams of battery manufacturing, acid metal plating and finishing, ammunition, tetraethyl lead manufacturing, ceramic and glass industries printing, painting, dying, and other industries (An *et al.*, 2001; Li *et al.*, 2002). Lead has been well recognized for its negative effect on the environment where it accumulates readily in living systems. Lead is non-biodegradable and can accumulate in living tissues, thus becoming concentrated throughout the food chain and can be readily absorbed into the human body (Wong *et al.*, 2003). The presence of lead in drinking water even at low concentration level may cause diseases such as anemia, encephalopathy, hepatitis and nephritic syndrome (Lo et *al.*, 1999). Severe exposure to lead was associated with sterility, abortion, stillbirths and neo-natal deaths (Goel *et al.*, 2005). When Lead is ingested, there is rapid uptake into red blood cells forming PbB, then into soft tissues (kidney, bone marrow, liver and brain) and followed by a slow redistribution to mineralizing tissues (bones and teeth) (Nriagu, 1988; Environmental health criteria 165, 1995; Lum Max *et al.*, 1994). Current Environmental Protection Agency (EPA) guidelines indicated that the maximum limit of lead in drinking water is 0.05 mg/L, but a level of 0.02 mg/L is proposed which is under review (Groffman *et al.*, 1992). According to the Indian Standard Institution, the tolerance limit for discharge of lead into drinking water is 0.05 mg/L and in land surface water is 0.1 mg/L (I.S.I., 1982).

1.2. REMOVAL TECHNIQUES OF HEAVY METALS

The removal of heavy metal toxic ions from wastewaters has received an increased attention in recent decade for global awareness of the underlying detriment of heavy metals in the environment. The tighter national and international regulations on water pollution and the discharge of heavy metals make it necessary to develop efficient and cost effective technologies for their effective and efficient removal. Various treatment technologies were developed for the removal of heavy metals from water. The commonly used technologies for removing metallic impurities from effluents include with chemical precipitation, lime coagulation, ion exchange (Gode *et al.*, 2005; Chakravarti *et al.*, 1995; Qdais *et al.*, 2004), electro dialysis, reverse osmosis membrane filtration (Low *et al.*, 1999; Lacour *et al.*, 2001; Juang *et al.*, 2000), electro winning (Gode *et al.*, 2006), solvent extraction, adsorption (Gode *et al.*, 2006; Leinonen *et al.*, 2000; Yu *et al.*, 2003), complexation/sequestration, electro-chemical operation and biological treatment etc. (Kiffs, 1987; Namasivayam, 1995). Chemical precipitation was traditionally employed to remove heavy metal toxic ions from aqueous solutions. However, metal removal via coagulation/flocculation is, in many cases, insufficient to meet strict regulatory requirements (Lee and Davis, 2001). Iron oxide-coated sand was used to remove the toxic metal ions (Thirunavukkarasu *et al.*, 2003). The applications of traditional treatment techniques thus need enormous cost and continuous input of chemicals, which become impracticable and unconventional and also caused for further environmental damage (Tiwari *et al.*, 2007b).

Among several methods available, ion exchange is an attractive process as its application is relatively simple and safe. Ion exchange is the exchange of ions between a liquid phase and a porous solid phase, which may be synthetic or natural (Wartelle and Marshall, 2006; Korngold *et al.*, 2003). Ion-exchangers play a prominent role for the removal

/speciation of several cationic/anionic species in waste waters and if the adsorbent is chosen so carefully and the solution chemistry adjusted accordingly, it can provide an effective waste treatment even at wide range of solution pH (Benjamin and Leckie, 1982; Davis and Leckie, 1978; Elliot and Huang, 1980; Mishra *et al.*, 2004). The low-cost exchangers like zeolite etc. is used, the method is reported to be cost – effective (Inglezakis *et al.*, 2004; Inglezakis *et al.*, 2005; Yebra-Biurrun *et al.*, 1995; Dabrowski *et al.*, 2004). Synthetic ion exchangers are often used in elimination of heavy metal pollutants (Patterson *et al.*, 1975; Schwuger and Smolka, 1976; Schore, 1972; Higgins, 1973). During treatment, ion exchange involves the reversible exchange of ions between a solution and a solid phase that are in direct contact (Dean, 1985).

The biosorption process which is an innovative technology using living or dead biomasses to remove toxic heavy metals from aqueous solutions offers potential advantages such as low operating cost, minimization of chemical or biological sludge, relatively high efficiency of heavy metal removal from diluted solutions, regeneration of biosorbents, possibility of metal recovery and environment friendly (Ahluwalia and Goyal, 2007).

Several natural and synthetic hydrous solids have been investigated as adsorbents of heavy metals. Among these, metal oxides (Benjamin and Leckie, 1981; Elliott and Huang, 1984; Davis and Bhatnagar, 1995) and activated carbon (Tan and Teo, 1987; Corapcioglu and Huang, 1987; Seco *et al.*, 1997) are the most extensively employed. However, the high cost of these materials limit their large-scale use for the removal of metals. Hence, the interest lies for more effective, economic and eco-friendly techniques to be developed for the fine-tuning of effluent/waste water treatment (Chiron *et al.*, 2003; Kadirvelu and Namasivayam, 2003). Therefore, numerous approaches are intended for the development of cheap metal trapping materials, such as fly ash (Sen and De, 1987), peat (Gosset *et al.*, 1986), activated sludge

(Fristoe and Nelson, 1983; Tien and Huang, 1987), waste slurry (Srivastava *et al.*, 1989) and biosorbents (Huang *et al.*, 1990 &1991).

It is reported that the adsorption phenomena can remove metals over a wide pH range and lower concentrations than precipitation (Lo *et al.*, 1997)**.** Green-Pedersen and Pind (2000) reported that a ferrihydrite-coated montmorillonite surface possessed large specific surface area and an increased sorption capacity for Ni(II) compared to the bare surface of montmorilllonite. Meng and Letterman (1996) discussed the adsorption properties of oxide mixtures and correlated the metal uptake by relative amount of metal oxide components. Meng and Letterman (1993) also reported adsorption of heavy metal ions onto the aluminum oxide-coated silica and the adsorption was modeled with uniform coverage of the oxide rather than using two distinct surfaces. Lo and Chen (1997a) determined the effect of Al oxide mineralogy, amount of oxide coating, and acid- and alkali-resistance on the removal of selenium from water. Brandao and Galembecket (1990) reported that the impregnation of cellulose acetates with manganese dioxide resulted in high removal efficiency of Cu(II), Pb(II), and Zn(II) from aqueous solutions. Al-Degs and Khraisheh (2000) had reported that diatomite and manganese oxide modified diatomite were effective adsorbents for removing Pb^{2+}, Cu^{2+}, and Cd^{2+} ions. The sorption capacity of Mn-diatomite was considerably increased compared to the original material in removing the studied metals. Filtration quality of diatomite was significantly increased after modification with Mn-oxides.

Numerous researchers investigated the use of activated carbon to remove heavy metals from aqueous solutions (Alfarra *et al.*, 2004; Kononova *et al.*, 2005; Park and Kim, 2005; Puziy *et al.*, 2004; Sekar *et al.*, 2004). Granular activated carbon (GAC) used in a column process could eliminate separation problems and minimize sludge production. Activated carbon, however, showed relatively lesser adsorption capacity and affinity for metals (Fan and Anderson, 2005). Huang *et al.,* (1975 &1977, 1978) found that the removal of Cr(III) and Cr(VI) from aqueous solutions by different heat-treated charcoal and activated carbons depends largely on the solution pH and chromium concentrations. Oxides were widely used for the removal of heavy metal toxic ions from aqueous solutions. Relative to GAC, oxides have higher metal exchange capacities. Furthermore, oxides have the ability to remove metals even up to trace levels and the adsorbed metals can be recovered and solids can be reused. However, solid separation and sludge management after the adsorption process is seemingly difficult, because the oxides are usually in colloidal forms. One possible solution to this problem is to prepare a granular adsorbent that can be used in column process. Composite adsorbents of this type include Fe^{2+} treated activated carbon (Huang and Van, 1989), Fe-coated sand (Edwards and Benjamin, 1989; Lai *et al.*, 1994; Lo *et al.*, 1997; Satpathy and Chaudhuri, 1995; Stahl and James, 1991a), granular iron oxides (Theis *et al.*, 1992), Fe-coated GAC (Wang, 1995) and Mn oxide coated sand etc. (Stahl and James, 1991b).

Sand is one of the natural filter media and widely used in the waste water treatment plant for pre-filtration and it was reported that during the treatment, manganese or iron, which is present in the wastewater, is deposited on the surface of sand in the form of oxides. Recently, several researchers have developed techniques for coating metal oxides onto the surface of sand to overcome the problem of using metal oxides powders in water treatment. Many reports have shown the importance of these surface coatings in controlling metal distribution in soils and sediments (Zacharra *et al.*, 1995; Fuller *et al.*, 1996; Edwards and Benjamin, 1989). In recent years, coated minerals are widely studied because of their potential application as effective sorbents (Zacharra *et al.*, 1995; Lo *et al.*, 1997; Kuan *et al.*, 1998).

Merkle *et al.,* (1996 & 1997) reported that manganese dioxide coated sand was effective for removal of arsenic from ground water in column experiments. Merkle *et al.*, (1996) developed a manganese oxide coating method on anthracite to improve the removal of Mn^{2+} from drinking water and hazardous waste effluent. They generated a filter media with an increased surface area after coating with manganese oxide and found manganese oxide coated media have the ability to adsorb and co-precipitate a variety of inorganic species. Stahl and James (1991 b) found that manganese oxide coated sands generated a larger surface area and increased adsorption capability with increasing pH as compared to uncoated silica sand. The removal of As(III) and lead(II) from aqueous solutions was studied using manganese coated sand and the equilibrium study and competitive adsorption was further carried out (Han *et al.*, 2006). The removal of copper using manganese coated sand in a liquid fluidized-bed reactor was carried out by Lee *et al.,* (2004). Similarly, manganese coated sand was studied by Guha *et al.*, (2001).

Iron oxide coated materials for heavy metal removal was employed successfully for the enhancement of removal capacity and efficiency comparing to uncoated filter media, such as silica sand (Sansalone *et al.*, 1995; Sansalone *et al.*, 1999; Khaodhia *et al.*, 2000; Joshi *et al.*, 1996; Benjamin *et al.*, 1996), granular activated carbon (Reed *et al.,* 1996) and polymeric media (Liu *et al.*, 2001 a; Edwards and Benjamin, 1989) etc. It was observed that coated media possessed with significant higher removal capacity for several heavy metals toxic ions over a wide pH range. Bailey *et al.*, (1992) used iron oxide coated sand to remove hexavalent chromium from a synthetic waste stream. The influent contained with 20 mg/L of Cr(VI) and more than 99% of Cr(VI) was removed. It was found that iron(III) coated sand can be used for the removal of both cationic and anionic heavy metals, such as Cu(II), Pb(II), As(III), As(V), Sr(II) and Se(IV) (Huang and Liu, 1997; Lo and Chen, 1997a; Yang *et al.*, 2005).

The oxidation and adsorption of Co(III)-EDTA complex subsurface materials using iron oxide coated and manganese oxide coated grains was performed by Zachara *et al.* (1995). Mn(II) was removed from aqueous solutions using manganese coated sand and the removal efficiency was greatly enhanced in presence of sodium hypo-chlorite (Tiwari *et al.*, 2007b).

Iron oxides, hydroxides and oxide hydroxides consist of arrays of Fe ions and O^{2-} or OH^{-} ions. In comparison with minerals existing in soil, iron oxides have relatively high surface area and surface charge, and they often regulate free metal concentration in soil through adsorption reactions (Scwertmann and Taylor, 1989**.** It was affirmed that, in recent years, many researchers have applied the iron oxide to the treatment of heavy metals from metal-bearing tap or wastewater (Benjamin and Leckie, 1981b). Most of iron oxides are available only as fine powders or are being generated in aqueous suspension as hydroxide floc or gel. In such forms, they retain their desirable adsorptive properties for the trace metals but are limited to reactor configurations incorporating large sedimentation basins or a filtration unit. Under such conditions, the solid/liquid separation is fairly difficult. Besides, the iron oxide alone is not suitable as a filter medium because of its low hydraulic conductivity (Theis *et al.*, 1992). Many researchers have studied the adsorption characteristics of anions, cations, and organics onto the iron oxide surface in recent decades. Adsorption is capable of removing metals over a wider pH range and to much lower concentrations than precipitation (Benjamin and Leckie, 1981b; Schultz *et al.*, 1987). It was reported that iron oxide could be regenerated and reused at least 50 times without a noticeable loss in treatment efficiency (Edwards and Benjamin, 1989). Iron – coated sand was tested for removal of cationic as well as anionic metals from synthetic and real waste waters (Theis *et al.*, 1992; Edwards and Benjamin, 1989; Stahl and James, 1991; Bailey *et al.*, 1992; Lai *et al.*, 1994). The results from these studies confirm the utilization of iron-coated sand for trace removal of metal ions from water is worth to be developed for future wastewater treatment strategy. The applications of iron-coated sand are influenced by the coating techniques. Iron oxide formed from $Fe(NO_3)_3$ is composed of mainly amorphous iron oxides and a small amount of crystalline iron oxides (Lo *et al.*, 1994a; Lo *et al.*, 1994b). But the type of iron oxide coating produced depends on the physical and chemical environments at which iron oxide was prepared and coated.

1.3. ADSORPTION

Adsorption is the adhesion of atoms, ions, or molecules from a gas, liquid, or dissolved solid to a surface (Glossary, 2009). This process differs from absorption, in which a fluid (the adsorbate) permeates or is dissolved by a liquid or solid i.e., the absorbent (Absorption Chemistry, 2010). The exact nature of the bonding depends on the details of the species involved, but the adsorption process is generally classified as physi-sorption (characteristic of weak van der Waals forces) or chemisorption (characteristic of covalent bonding). It may also occur due to electrostatic attraction (Ferrari *et al.*, 2010). A liquid or a solid substance which is present in the bulk of the substance is being attracted uniformly from all sides by the neighbouring molecules and hence there is no net force acting on the molecule hence there is no unbalanced force around molecule. On the other hand, if a molecule is present near the surface, such a molecule is not bonded to other molecules from all sides but has some unutilized valencies because there are no neighbouring molecules above the surface to which it can be bonded. As a result of these unbalanced forces the molecules present at the solid or liquid surfaces tends to satisfy their residual forces by attracting and retaining on their surface, the molecules of other species when brought in contact with them. These results in increase in concentration of the substance near the surface compared with the bulk phases. A substance which has different concentration at the surface than in the bulk phases is said to adsorb and the existence of a substance at a surface in a different concentration than in the adjoining bulk phases is adsorption.

The material upon whose surface the adsorption takes place is called an adsorbent while the molecular species that get adsorbed are called adsorbate. Adsorption is not necessarily a physical phenomenon always. It maybe said a chemical process involving a chemical interaction between the adsorbent and adsorbate. When the molecules of the adsorbate are held to the surface of the adsorbent by chemical forces, the adsorption is called chemisorption.

Adsorption is different from absorption. In absorption, the molecules of a substance are uniformly distributed in the bulk of the other, whereas in adsorption molecules of one substance are present in higher concentration at the surface of the other substance. But in some cases adsorption and absorption occur together. In such cases, the substances gets uniformly distributed into the bulk of the solid but at the same time, its concentration is higher at the surface than in the bulk, such phenomenon is called “sorption”. Instead of using an adsorption, the term sorption and bio-sorption is used since the adsorption phenomenon is not clear. Bio-sorption can be defined as a non-directed physio-chemical interaction that may occur between metal species and the biological materials.

1.4. CLASSIFICATION OF ADSORPTION

Adsorption has been classified mainly on the basis of the nature of interactions between the atoms, molecules or ions of the adsorbates and the adsorbents.

1.4.1. Physisorption

Physisorption, also called physical adsorption, is a process in which the electronic structure of the atom or molecule is barely perturbed upon adsorption (Oura *et al.*, 2003; Desjonqueres *et al.*, 1993; Hans Luth, 1993). This type of adsorption depends on the result of dispersion or Van der Waal forces of attraction between the adsorbent and the adsorbate. It is generally resulting with the binding of the adsorbate particles ion several consecutive layers which is usually favours the lowering of temperature. Physisorption is a spontaneous, rapid and reversible process, which requires small activation energy and the corresponding enthalpy change ranges up to 20 kJ/mol (Bond, 1984; Yoyutsky, 1978).

1.4.2. Chemisorption

Chemisorption is a sub-class of adsorption, driven by a chemical reaction occurring at the exposed surface. A new chemical species is generated at the adsorbent surface (e.g. corrosion, metallic oxidation). The strong interaction between the adsorbate and the substratesurface creates new types of electronic bonds - ionic or covalent, depending on the reactive chemical species involved (Oura *et al.*, 2003). Chemisorption is based on the chemical forces which arise due to transfer or sharing of electrons between the adsorbate and the adsorbent. The energy of attachment is much greater as compared to the physisorption and may be comparable to the energies of the chemical bond formations. Chemisorption behaves to be irreversible, slow and temperature dependent which indicates the presence of an activation energy. The enthalpy of chemisorption is usually in the range of 40 – 800 kJ/mol (Volkenshtein *et al.*, 1949; Robers, 1935).

1.4.3. Electrostatic Adsorption

This type of adsorption is mainly due to the attractive coulombic forces between electrically charged adsorbent surface and the oppositely charged adsorbate species which is mostly observed in adsorption from aqueous solutions. It is usually the ionic exchange type; however, ion exchange need not be necessarily an electrostatic process. The ion exchange adsorption is specific, not always reversible and occurs slowly and the heat of adsorption is usually smaller than that of chemisorption (Helfferich, 1962).

In many systems, the mechanism of adsorption cannot be definitely specified and several mechanisms may be involved simultaneously (Ottewill and Shaw, 1968; Mishra *et al.*, 1991).

The adsorption of trace elements is difficult to interpret as some of the physical methods used to distinguish among the adsorption mechanisms *viz.*, calorimetry, infrared spectroscopy etc. fail entirely to detect micro and sub micro concentrations of the adsorbate species. However, it is well established that the mechanism of adsorption for trace elements depends upon their state in solutions. Simple ions are adsorbed by ion exchange mechanism whereby ions of the similar charge form part of the surface crystal layer of the adsorbent or the outer part of the electrical double layer which exists on the surface of most of the adsorbents (counter ions). The former mechanism is basically primary adsorption on crystalline precipitates (Wahl *et al.*, 1951) and is mostly due to isomorphous ion replacement. The latter (secondary adsorption) can occur with the major site of the adsorbents (Grebenshesikova *et al.*, 1972).

1.5. FACTORS INFLUENCING ADSORPTION PROCESS

Adsorption at solid – solution interface is influenced by several parameters *viz*., nature of adsorbent, nature of adsorbate, temperature, pH and concentration of the adsorbate and the presence of foreign species.

1.5.1. Nature of Adsorbent

The efficiency of an adsorbent depends on two factors. One is the specific surface area of the adsorbent and the other is the adsorption affinity of 1 cm^2 of the adsorbent. Generally, an increase in specific surface area of adsorbent enhances the adsorption due to increase in the number of sites available for adsorption (Kurbatov, 1948; Petrov, 1958). Adsorbents with higher surface charge will have a greater tendency to adsorb oppositely charged trace elements (King *et al.*, 1974; Skulskii *et al.*, 1971) while similar charged trace elements (adsorbate) results in lesser uptake by the adsorbent (Benes *et al.*, 1972). The adsorption of hydrolysed or slightly dissociated species normally increases with the increase in hydrophobic character of the adsorbent (Rydberg *et al.*, 1952).

1.5.2 Nature of Adsorbate

The adsorption process also depends on the size, shape and chemical nature of the adsorbate. The uptake of the adsorbate depends upon the polarity and the presence of active sites on the adsorbent. The presence of hydroxyl groups in a molecule is reported to enhance its adsorb ability (Stryker *et al.*, 1968).

1.5.3. Influence of Temperature

Temperature influences the kinetics and the final values of adsorption (Benes *et al.*, 1980). The uptake of the adsorbate normally increases with the increase in temperature which could be used in evaluating the activation energies (Gutsanu *et al.*, 1990; Kikuchi *et al.*, 1979; Kato *et al.*, 1981; Pakholkov *et al.*, 1983). On the other hand, the effect of temperature on trace adsorption was found to be small and is nearly constant over a wide range of temperature (Dyck, 1968; Mishra *et al.*, 1986). It was observed that the physisorption decreased with the increase in temperature (Mishra *et al.*, 1987 a; Taylor *et al.*, 1932). The increase in adsorption with the rise in temperature was attributed to the acceleration of some steps which are originally slow or even due to the change in the adsorption mechanism towards the chemisorption (Taylor, 1932; Mishra *et al.*, 1992).

1.5.4. Influence of pH on Sorptive Solutions

The pH is an important parameter for adsorption of trace elements as their state in solutions is strongly depends on the pH of the solution. The pH can extensively affect the surface charge of the adsorbent which in turn direct the electrostatic adsorption of ions and colloids. Organic polymers are negatively charged in the pH range of 2–3 due to the dissociation of their surface active groups or due to adsorption of OH^- ions (Benes *et al.*, 1971). The acidity and basicity of solution can influence the composition and properties of adsorbent surface and this in turn put forth some effect on adsorption (Rozovskaya, 1960; Suhybani, 1989; Kenta *et al.*, 1984). The anions or cations of hydroxides used for adjustment of pH compete with trace ions in ion exchange process which is particularly observed in the adsorption of monovalent or bivalent ions (Benes and Kucerra, 1972).

Generally, the adsorption of cations takes place at higher pH values whereas the anions are adsorbed at lower pH values. Therefore, adsorption of most trace cations is observed in negligible quantity at lower pH i.e., strongly acidic solutions (Ahmad, 1969). Under certain conditions the increase in pH may even increase the uptake of anions (Burclova *et al.*, 1973).

1.5.5. Influence of Sorptive Concentration

The adsorption at solid–solution interface obviously depends on the bulk sorptive concentrations. The concentration of trace quantity adsorption often conform either Langmuir or Freundlich adsorption isotherms. The later has been successfully utilized by several researchers for the adsorption study of cations and anions on solid surfaces (Upien, 1986; Aksoyoglu, 1989; Clark, 1970; Mishra and Tiwary, 1991). However, Freundlich isotherm fails in some cases wherein Sips formulation is obtained for a better fit to such cases (Sips, 1948).

1.6. THEORIES OF ADSORPTION

Various theories have been put forward from time to time to explain the process of adsorption which is discussed briefly below:

1.6.1. Chemical Theory

The chemisorption may involve sharing or transfer of electrons between the adsorbate and the adsorbent resulting in the formation of a chemical bond. Considering a covalent bonding model, Pauling derived an empirical formula for bonds between single atoms and extended to adsorption bonds in the case of covalent bonding (Pauling, 1939).

1.6.2. Capillary Condensation Theory

The condensation of the adsorptive species on to the pores of the adsorbent to form a thin layer of the molecules is the basis of this theory. The concept of this theory is comparable to the idea proposed by Zsingmondy (1911) and Foster (1932). The theory was extended further by Patric and Long (1925) to explain the physical adsorption. However, the elementary theory of capillary condensation does not take into account the specific action of surfaces and it also differs from poly-molecular physical adsorption by the fact that the latter may occur on plane surface while capillary condensation cannot.

1.6.3. Residual Valence Theory

Haber (1914) proposed this theory assuming that the upper surfaces of adsorbents generally possess residual valencies, as a result of which adsorptive species are attracted towards the surface of adsorbents. This theory was further elaborated by Langmuir (Langmuir, 1918) assuming that the adsorption forces are homogeneously distributed all over the surface forming a monolayer coverage. However, the bonds are weaker than the true chemical bonds.

1.6.4. Polarization Theory

The polarization theory is based on the notations of de Boer and Zwikker (1929) and Bradly (1936) where the surface of a polar adsorbent polarizes the molecules of a non-polar adsorbate which are adsorbed in the first adsorption layer. The induced dipoles further induce secondary dipoles in the second layer and the process extends to several layers. Modern spectroscopic data point to the substantial polarization of the adsorbed molecules and atoms. This theory is successfully utilized in explaining the adsorption of organic molecules and noble gases on metals, graphite and alumina (Fridrikhsberg, 1986) which has been supported by the works of Cassel (1931) and Imre (1934).

1.6.5. Potential Theory

This theory was proposed by Polanyi (1914) and extended by several workers (Berenyi, 1920; Williams, 1918). It is based on the assumption that there is a potential field at the surface of adsorbents responsible for mono- and multi-layer adsorption. The potential energy of interacted gas molecule with the particles of the lattice is the sum of all the individual interactions:

$$U = \Sigma U(r_i) \qquad \text{-----(1)}$$

Where $U(r_i)$ is the potential energy of interaction of the gas molecules with the i^{th} particle of the lattice at a distance r_i.. U is a function of X, Y and Z coordinates of adsorbed molecule. If X and Y coordinates of the adsorbed molecule are kept constant, while Z varies, U(z) will have shape of the potential energy curve with minimum such as that given by Lennard-Jones intermolecular pair i.e.

$$U(r) = \frac{A}{r^{12}} - \frac{C}{r^{6}} \qquad \text{-----(2)}$$

where A and C are the constants and r is the distance perpendicular to the surface. The value of U(z) above a particle of the solid will be different from U(z) between two particles. Specifically, U_m, the potential minimum of U(z) will vary periodically in both X and Y directions. Thus, a plot of U_m against X and Y will give a curve with maxima and minima. The energy difference between the energy of minima and that of molecules in the gas phase is the energy of adsorption (U_0) and the difference between energy of minima and maxima is the energy required for surface diffusion (V_0). In the simple case of localized adsorption and adsorbed molecule is considered to be held at the bottom of a potential well whose depth is much greater than *kT*. All the potential wells at the surface are assumed to be equal in depth and regularly spaced. Molecules in such positions have practically no chance of lateral movement across the surface. However, localized adsorption may be mobile or immobile depending on the nature of the surface. When the adsorptive species are free to migrate along the surface, the adsorption is generally classified as mobile or non-localized. This theory was further modified for the adsorption from solutions of sparingly soluble solute (Polanyi, 1920).

1.6.6. BET Theory

Brunauer, Emmett and Teller (Brunauer *et al.*, 1938) extended the Langmuir concept to the multilayer adsorptions and derived an equation which is known as BET equation. It represents the first effective attempt to explain physical adsorption from monolayer regions through the multilayer regions. The equation is:

$$\frac{C}{(Cx-C)Qc} = \frac{1}{BQ^0} + \frac{B-1}{BQ^0} \cdot \frac{C}{Cs} \qquad \text{---(3)}$$

where Cs is the saturation concentration of the solute on adsorbent, C is the measured concentration in solution at equilibrium, Q^0 is the number of moles of solute adsorbed per unit weight of adsorbent inferring a complete monolayer on the surface, Qc is the number of moles of solute adsorbed per unit weight of adsorbent at concentration C, and B is a constant, expressive of the energy of interaction with the surface. This equation is helpful in determining the nature of adsorption isotherm, heat of adsorption and the amount of adsorbate required to form a complete monolayer. This theory has been extensively used for the determination of the surface area of solid materials.

1.6.7. Boundary – Layer Theory

This theory was reported by Aigrain and Dugas (1952) and Hauffe and Engell (1952) and Weisz (1953). The electron transfer between the adsorbing gas and adsorbent (semiconductor) is the basis of boundary layer theory of adsorption (Mott and Gurney, 1950; Garner *et al.*, 1952) when a neutral atom ‘c’ is brought to the surface of solid (n-type semiconductor), electron near the surface is transferred from conduction band to the electron accepting level of ‘c’ giving, a negative ion ’c’. As the process of adsorption continues, a positive space charge is developed in the semiconductor underneath the surface and the surface accumulates the negatively charged adsorbate molecules. After the setting up of negative field, the surface layer of semiconductor starts repelling the electrons and prevents an accumulation process. In view of the fact that the electrons available from the upper conduction band or impurity levels are depleted and then adsorption remains confined to a monolayer, this type of adsorption is known as ‘depletive chemisorption’. The process of adsorption is followed by a decrease in conductivity of adsorbent. An example of such behaviour is the adsorption of oxygen on zinc oxide (Mott and Gurney, 1950). This theory predicts the direction of change of conductivity accompanying adsorption. It also explains the adsorption due to the presence of impurities in the adsorbent. The major disadvantage of this theory is that it considers only those types of adsorption processes which result from the transfer of charge.

1.6.8. Electron Theory

This theory was developed by Wolkenstein to explain chemisorptions and catalysis on semiconductors (Wolkentein and Peshev, 1965). He considered a process in which transfer of charge occurs with resulting change in conduction and also adsorption in which no transfer of charge occurs. Electron theory indicated that two or more types of adsorption may occur simultaneously. The adsorption of CO on Cu_2O and ZnO/Cr_2O_3 were explained with this theory (Green *et al.*, 1957). Wolkenstein and Peshev, (1965) has further defined ‘weak’ and ‘strong’ chemisorption.

i) In weak chemisorption, no change occurs in the number of electrons in the conduction band or positive holes in the valence band of the material. The chemisorbed particle with its adsorption center remains electrically neutral.

ii) In strong chemisorption either donation or capture of an electron by the chemisorbed particle will occur. Thus, the number of electrons in the conduction band or positive holes in the valence band of the crystal will change. There are two types of ‘strong’ chemisorption bonds’ donor bonds when the chemisorbed particles donate electrons (capture positive holes) to the crystal and acceptor bonds, when the particles capture free electrons from the crystal. Each of these bonds may be purely ionic, purely covalent or intermediate.

1.7. ADSORPTION ISOTHERM

The adsorption of compound onto adsorbent can be described mathematically by an adsorption isotherm; adsorption isotherm simply defined as the quantity of adsorption that can be bound up on a particular of adsorbent is a function of the concentration of an adsorbate and the temperature.

Although several isotherms have been developed for use in modeling the adsorption isotherms, only two isotherms are considered the most common equation used to describe the equilibrium between an adsorbent (surface) and an adsorbate (chemical in solution). These isotherms are the Freundlich and Langmuir adsorption equations.

1.7.1. Freundlich isotherm equation

In 1906, Freundlich presented the earliest known adsorption isotherm equation. Freundlich is an empirically derived logarithmic model that attempts to factor in the effects of various adsorption energy levels. The model assumes that the number of sites associated with a particular free energy of adsorption decreases approximately as the free energy level increases, this empirical model can be applied to non – ideal sorption on heterogeneous surfaces as well as multilayer adsorption. The model can be described by the following equation (4) (Alley, 2002; Ho *et al.*, 2002**)**:

$$q_e = K_f\, C_e^{1/n} \qquad \text{…. (4)}$$

where:

q_e=Equilibrium loading on the adsorbent (mg/g)

K_f=Adsorption capacity at unit concentration (mg/g)

C_e= Equilibrium concentration of adsorbate (mg/L)

1/n= Adsorption intensity

The equation fit to straight line when plotted on Log– Log basis, the above equation can be written in following form as equation (5):

$$\text{Log } q_e = \text{Log } K_f + [1/n] \text{ Log } C_e \qquad \text{…. (5)}$$

1.7.2. Langmuir Isotherm Equations

In 1915 Langmuir developed equation to describe the interaction between the adsorbent and adsorbate as a linear, reversible and mono layer chemical reaction, this equation is relatively a straight forward model that assume that the adsorbent surface is completely homogeneous, that each adsorbent site can bind a maximum of one adsorbate molecule, and that their no lateral interaction take place between molecules of the adsorbate(Alley, 2000).

This model can describe theoretically by following equation (6) (Ho *et al.*, 2005):

$$q_e = \frac{q_m\, K_a\, C_e}{1 + K_a\, C_e} \qquad \text{----- (6)}$$

where:

q_e = Equilibrium loading on the adsorbent (mg/g)

C_e= Equilibrium concentration of adsorbate (mg/L)

$q_m$and K_a = characteristics Langmuir constants

Constant q_e and K_a can be determined from linearized form of equation (7), represented as:

$$\frac{C_e}{q_e} = \frac{1}{q_m + K_a} + \frac{C_e}{q_m} \qquad \text{--- (7)}$$

A plot of C_e/q_e *vs* C_e could indicate a straight line of slope $1/q_m$ and an intercept of $1/ (K_a q_m)$. Advantage of the Langmuir equation includes simplicity and the applicability to a wide range of data. Limitations to the model include the monolayer assumption the reversibility of bonding and the constant uptake rate.

1.8. SCOPE OF THE PRESENT INVESTIGATION

Sand itself is widely used as a filter media for the treatment of wastewaters and it was found that during the treatment, manganese and iron, if present in wastewater, is to be deposited on the surface of sand in the form of their oxides. Hence, the application of iron coated sand or manganese coated sand may provide more viable, eco-friendly and cost effective treatment technology. The present research work is an alternative treatment technology for the removal of heavy metal toxic ions from the aqueous solutions by employing the artificially obtained manganese coated sand (MCS) or iron coated sand (ICS). Further, the manganese or iron coated sand is a type of silica medium coated with manganese or iron oxides, formed from the sorption of manganese or iron oxides during long-term filtration via the process of rapid sand filtration, followed by aeration on a water treatment plant. This study was conducted to build the basic data for coating hydrated manganese or iron oxide on the sand surface to utilize the adsorbent properties of the coating and the filtration properties of the sand in the low level removal of various heavy metal ions.

The wide range of waste water treatment strategies to be adopted for the effective/efficient low level removal of several heavy metal toxic ions is a current area of research. The cost effective and more environment friendly processes are inevitable for the treatment methods. Hence keeping in view the proposed study is an attempt to exploit fully the natural sand materials in order to obtain the manganese or iron coated sand which further be used for the low level removal of several heavy metal toxic ions viz., Cr(VI), As(III), As(V), Cd(II), Cu(II) and Pb(II). The materials employed were likely to be cost effective and perhaps environmentally benign. Further, the studies were extended to understand the mechanism involved at solid/solution interface carrying the various parametric studies viz., effect of sorptive pH, concentration and ionic strength, etc.

The practical applicability of these methods could better be demonstrated under the dynamic experimentation i.e., column studies. Hence, the column experimentation were included in the present investigation. The basic data to be obtained by the column experiments could be used finally to develop the Pilot Plant or the Large Scale Treatment Plant for the treatment of waste/effluent waters contaminated of these polluting ions.

CHAPTER

2

Methodology

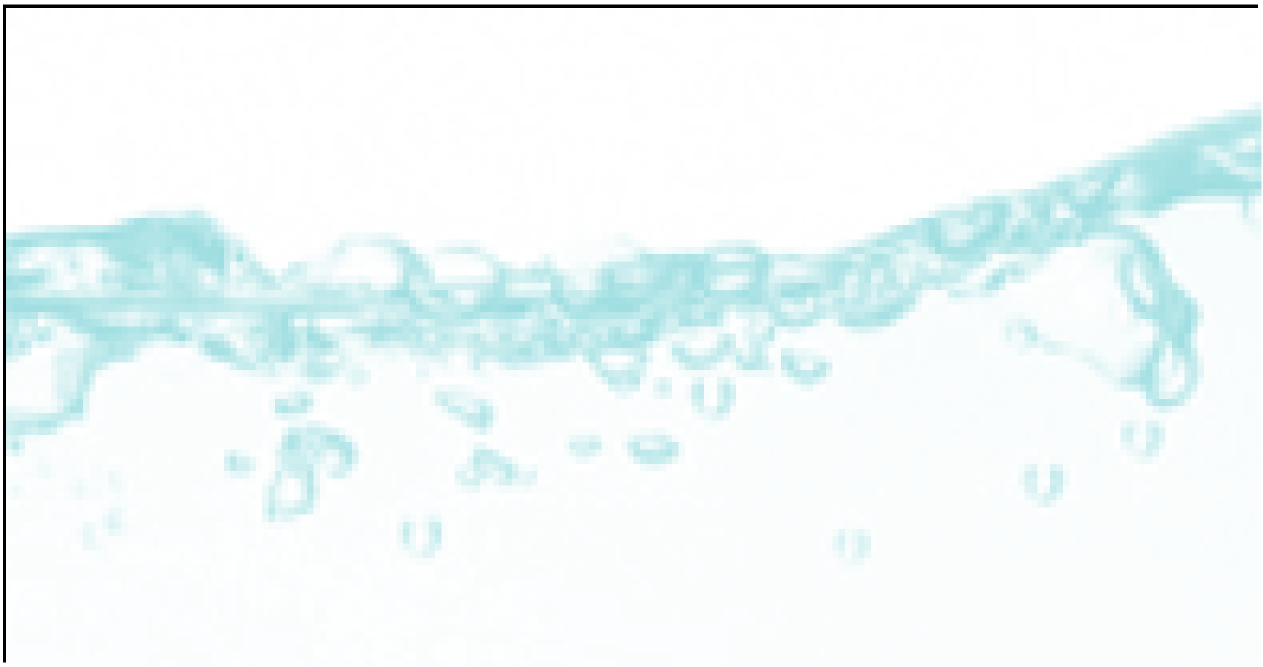

METHODOLOGY

2.1. MATERIALS

Sand was obtained from the local river Tlawng at the Sairang site, Aizawl, Mizoram, India. It was washed thoroughly with water followed by 0.2 mol/L HNO_3 to remove any mud dirt or other adhering impurities. It was again washed with plenty of distilled water and dried. The dried sample was sieved to obtain the 30 – 60 BSS standard Mesh size using the mechanical sieve. The chemicals used for the experiment were manganese nitrate as $Mn(NO_3)_2.6H_2O$ (97% Extra Pure, Junsei Chemicals, Japan); ferric nitrate ($Fe(NO_3)_3.5H_2O$, AR grade, E. Merck, Germany); potassium dichromate $K_2Cr_2O_7$, AR grade, E. Merck Germany); cadmium nitrate ($Cd(NO_3)_2$; copper sulphate ($CuSO_4.5H_2O$)(both GR Reagent, Duksan Pure Chemicals Co. Ltd., Korea); lead nitrate ($Pb(NO_3)_2$, GR Reagent, Shinyo Pure Chemicals Co. Ltd., Japan); sodium meta arsenite ($NaAsO_2$) and sodium arsenate (Na_3AsO_4)(both GR Reagent, Himedia, India). These chemicals were obtained and used without any further purification. HNO_3 and NaOH used were of AR grade and the water was used as de-ionized distilled water (18MΩ-cm) using the Millipore water purification system (Milli-Q+).

2.1.1. UV- Visible Spectroscopy

Ultraviolet–visible spectroscopy refers to absorption spectroscopy or reflectance spectroscopy in the ultraviolet - visible spectral region. This means it uses light in the visible and adjacent (near-UV and near-infrared (NIR) regions. The absorption or reflectance in the visible range directly affects the perceived color of the chemicals involved. In this region of the electromagnetic spectrum, molecules undergo electronic transitions. This technique is complementary to fluorescence spectroscopy, in that fluorescence deals with transitions from the excited state to the ground state, while absorption measures transitions from the ground state to the excited state (Skoog *et al.*, 2007). The principle of this technique lies to the fact that molecules containing π-electrons or non-bonding electrons (n-electrons) can absorb the energy in the form of ultraviolet or visible light to excite these electrons to higher anti-bonding molecular orbitals (Mehta, 2011). The more easily excited the electrons (i.e. lower energy gap between the HOMO and the LUMO) the longer the wavelength of light it can absorb.

The alternative title for this technique is Electronic Spectroscopy since it involves the promotion of electrons from the ground state to the higher energy state. The amount of light absorbed by the sample is as a function of the wavelength (nm unit) is called the absorption spectrum which generally consists of absorption bands. The spectrum consists of a sharp peaks and each peak will corresponds to the promotion of electron from one electronic level to another. But, actually sharp peaks are seldom observed and instead, broad absorption bands are recorded. It is due to the fact that the excitation of electrons are also accompanied by the constant vibratory and rotatory motion of the molecules. Since the energy levels of a molecule are quantized, the energy required to bring about the excitation is a fixed quantity. Thus, the electromagnetic radiation with only a particular value of frequency will be able to cause excitation.

In this experiment, the sorption capacity is determined by using Beer-Lambert's law. The Beer-Lambert's law states that 'the absorbance of the solution at a particular wavelength is directly proportional to the concentration of the solution into path length of the sample cell (cm)'. It can be represented below and a plot of absorbance (A) against concentration of the solution gives a straight line for constant path length (l).

$$A = \epsilon c l \qquad \text{---- (8)}$$

where, A=absorbance of the light absorbing solution.

c =molar concentration of the solute.

Є =molar extinction coefficient

l = path length of sample cell.

A spectrophotometer is a device which detects the percentage transmittance of light radiation when light of certain intensity and frequency range is passed through the sample. Thus, the instrument compares the intensity of the transmitted light with that of the incident light.

The modern ultra-violet-visible spectrometers consist of light source, monochromator, detector, amplifier and the recording devices. The most suitable sources of light are: Tungsten Filament Lamp and hydrogen-deuterium discharge lamp which is rich in red radiations. Most spectrophotometers are double beam instruments. The primary source of light is divided into two beams of equal intensity. Before dividing it into two beams, the incident radiation is dispersed with the help of a rotating prism and then selected by slits such that the rotation of the prism causes a series of continuously increasing wavelengths to pass through the slits for recording purposes. The selected beam is monochromatic which is then divided into two beams of equal intensity. Dispersion grating can also be employed to obtain monochromatic beam of light from the polychromatic radiation. As the dispersion of a single beam or grating is very small, it is not possible to isolate or collimate very narrow band widths. Thus, light from the first dispersion is passed through a slit and then sent to the second dispersion. After the second dispersion, light passes through the exit slit. The main advantage of the second dispersion is that the band width of the emersion light increases and the light passing through the exit slit is almost monochromatic. Almost the entire of the stray light is suppressed. In this experiment, UV-Visible Spectrophotometer (Thermo Electron Corporation, England; Model: UV1**)** was used to quantify the chromium(VI) concentration.

2.1.2. Atomic Absorption Spectroscopy

Atomic absorption spectroscopy (AAS) is a spectro – analytical procedure for the qualitative and quantitative determination of chemical elements employing the absorption of optical radiation (light) by free atoms in the gaseous state. In analytical chemistry the technique is used for determining the concentration of a particular element (the analyte) in a sample to be analyzed. AAS can be used to determine over 70 different elements in solution or directly in solid samples.

The technique makes use of absorption spectrometry to assess the concentration of an analyte in a sample. It requires standards with known analyte content to establish the relation between the measured absorbance and the analyte concentration and relies therefore on Beer-Lambert Law. In short, the electrons of the atoms in the atomizer can be promoted to higher orbitals (excited state) for a short period of time (nanoseconds) by absorbing a defined quantity of energy (radiation of a given wavelength). This amount of energy, i.e., wavelength, is specific to a particular electron transition in a particular element. In general, each wavelength corresponds to only one element, and the width of an absorption line is only of the order of a few picometers (pm), which gives the technique its elemental selectivity. The radiation flux without a sample and with a sample in the atomizer is measured using a detector, and the ratio between the two values (the absorbance) is converted to analyte concentration or mass using Beer-Lambert Law.

In order to analyze a sample for its atomic constituents, it has to be atomized. The atomizers most commonly used nowadays are flames and electro thermal (graphite tube) atomizers. The atoms should then be irradiated by optical radiation, and the radiation source could be an element-specific line radiation source or a continuum radiation source. The radiation then passes through a monochromator in order to separate the element-specific radiation from any other radiation emitted by the radiation source, which is finally measured by a detector.

The relatively small number of atomic absorption lines (compared to atomic emission lines) and their narrow width (a few pm) make spectral overlap rare; there are only very few examples known that an absorption line from one element will overlap with another. Molecular absorption, in contrast, is much broader, so that it is more likely that some molecular absorption band will overlap with an atomic line. This kind of absorption might be caused by un-dissociated molecules of concomitant elements of the sample or by flame gases. We have to distinguish between the spectra of di-atomic molecules, which exhibit a pronounced fine structure, and those of larger (usually tri-atomic) molecules that don’t show such fine structure. Another source of background absorption, particularly in ET AAS, is scattering of the primary radiation at particles that are generated in the atomization stage, when the matrix could not be removed sufficiently in the pyrolysis stage.

All these phenomena, molecular absorption and radiation scattering, can result in artificially high absorption and an improperly high (erroneous) calculation for the concentration or mass of the analyte in the sample. There are several techniques available to correct for background absorption, and they are significantly different for LS AAS and HR-

CS AAS (Walsh, 1955; Welz and Sperling, 1999). The AAS, model: Fast Sequential Atomic Absorption Spectrometer, AA240FS, Varian, USA was fully employed for the estimation of copper, lead, cadmium and arsenic.

2.2. METHODS

2.2 1. Preparation of Manganese and Iron coated sand (MCS / ICS) samples

Manganese and iron coated sand were prepared by taking 120 g of cleaned and dried sand (30 – 60 BSS Standard in size) and 100 mL of 0.05 mol/L manganese /or iron nitrate solutions at pH = 9.0 in a flask of rotary evaporator. The mixture was then constantly stirred at 60^0C temperature in a rotary evaporator with the slow speed of 30 rpm till the volume reduced to about 10 mL. The solution was kept in a drying oven at 90^0C till it dried out completely. The sample was further kept at 160^0C for *Ca.* 3 hours for complete drying and better coating stability of manganese /or iron onto the sand surface. It was then cooled to room temperature and again washed with distilled water for several times. It was dried in a drying oven at 70^0C overnight (Tiwari *et al.*, 2007b) and stored in the tapered polyethylene bottles. These dried MCS and ICS samples were used for the present investigation. Moreover, the amount of manganese and iron coated on the surface of sand was analyzed with the standard EPA method(US EPA method 3050B)

2.2.2. Characterization of solid sample

The solid sample was characterized by using the Scanning Electron Microscope (SEM) machine (FE-SEM-Model: SU-70, Hitachi, Japan) equipped with energy dispersive X-ray Spectroscopy (EDX) system. X-Ray Diffraction (XRD) data was collected using the XRD machine i.e., PANalytical, Netherland (vide model- X’Pert PRO MPD). The data was collected with the scan rate of 0.034 of 2Ə illumination and the applied voltage was 45 kV with the observed current 35 mA and using the Cu K_α radiation having wavelength 1.5418 Å (Tiwari *et al.*, 2011a). The BET specific surface area was obtained by using the BET specific surface area analyzer (Mountech, Japan model MacSorb HM model – 1200 Series).

2.2.3. Stability of solids

The manganese /or iron particles aggregated onto the sand surface were assessed for its stability against the pH effect by varying the solution pH from 2 to 11. To this effect, 0.5 g of solid was equilibrated with 100 mL of distilled water at different initial pH values and then kept in an automatic shaker at 25^0C for 24 hrs. The solutions were then filtered using the 0.45 µm syringe filter and the filtrates were subjected for its total manganese /or iron content using the Atomic Absorption Spectrometer (AAS; Fast Sequential Atomic Absorption Spectrometer Model AA240FS, Varian) (Tiwari *et al.*, 2011a)

2.2.4. pH_{PZC} determination of solid

The pH_{PZC} (point of zero charge) of manganese coated sand or iron coated sand was defined as the pH value at which the surface carries net zero charge. Consequently, to evaluate the pH_{PZC}, the acid and base titrations were carried out by taking 5 g of the solid sample into 500 mL of distilled water and titrated against the 0.1 mol/L of $HNO_3$and 0.1 mol/L of NaOH solutions, separately. The corresponding pH was recorded using a pH meter (HANNA pH-213, Microprocessor pH meter, USA). The titration data were further utilized to evaluate the pH_{PZC} (Tiwari *et al.*, 2011a).

2.2.5. Speciation Studies

Speciation of chromium(VI), cadmium(II), copper(II), lead(II), arsenic (III) and arsenic(V) were conducted separately using the MINEQL+ (Version 4.5) a geochemical computer simulation program. The input parameters were taken as initial concentration of

Cr(VI): 20mg/L, As(III) and As(V): 2mg/L, Cd(II): 10mg/L, Cu(II):20 mg/L; Pb(II): 40 mg/L at constant temperature: 25^0C (Lee *et al.*, 2010 b; Tiwari *et al.*, 2011a). The thermo-dynamic equilibrium constants used were given in Table: 1, 2, 3. 4. 5 and 6 respectively for the Cr(VI), As(III), As(V), Cd(II), Cu(II) and Pb(II). The species distribution of these metal ions as a function of pH is further obtained and represented in figures elsewhere (figures 11, 12, 13, 14, 15 and 16).

Table 1: Various equilibrium constants used for the speciation of Cr(VI) in aqueous solutions at 25 ^{0}C.

Equilibrium	Log K
$CrO_4^{2-} + H^+ \leftrightarrow Cr_2O_7^{2-} + H_2O$	14.560
$CrO_4^{2-} + H^+ \leftrightarrow HCrO_4^-$	6.510
$CrO_4^{2-} + 2H^+ \leftrightarrow H_2CrO_4$ (aq)	6.419

Table 2: Various equilibrium constants used for the speciation of As(III) in aqueous solutions at 25 ^{0}C.

Equilibrium	Log K
$AsO_3^{3-} + H^+ \leftrightarrow HAsO_3^{3-}$	13. 414
$AsO_3^{3-} + 3H^+ \leftrightarrow H_3AsO_3$	34.744
$AsO_3^{3-} + 2H^+ \leftrightarrow H_2AsO_3^-$	25.454
$AsO_3^{3-} + 4H^+ \leftrightarrow H_4AsO_3^+$	34.439

Table 3: Various equilibrium constants used for the speciation of As(V) in aqueous solutions at 25 ^{0}C.

Equilibrium	Log K
$AsO_4^{3-} + H^+ \leftrightarrow HAsO_4^{2-}$	11.500
$AsO_4^{3-} + 2H^+ \leftrightarrow H_2AsO_4^-$	18.460
$AsO_4^{3-} + 3H^+ \leftrightarrow H_3AsO_4$	20.700

Table 4: Various equilibrium constants used for the speciation of Cd(II) in aqueous solutions at 25 ^{0}C.

Equilibrium	Log K
$Cd^{2+} + 3H_2O \leftrightarrow Cd(OH)_3^- + 3H^+$	-32.505
$Cd^{2+} + 4H_2O \leftrightarrow Cd(OH)_4^{2-} + 4H^+$	- 47.288
$Cd^{2+} + H_2O \leftrightarrow Cd(OH)^+ + H^+$	- 10.097
$Cd^{2+} + 2H_2O \leftrightarrow Cd(OH)_2\ (aq) + 2H+$	- 20.294
$2Cd^{2+} + H_2O \leftrightarrow Cd_2(OH)^{3+} + H^+$	- 9.397

Table 5: Various equilibrium constants used for the speciation of Cu(II) in aqueous solutions at 25 ^{0}C.

Equilibrium	Log K
$2Cu^{2+} + 2H_2O \leftrightarrow Cu_2(OH)_2^{2+} + 2H^+$	-10.594
$Cu^{2+} + 3H_2O \leftrightarrow Cu(OH)_3^-$	-26.879
$Cu^{2+} + 4H_2O \leftrightarrow Cu(OH)_4^{2-} + 4H^+$	-39.980
$Cu^{2+} + H_2O \leftrightarrow Cu(OH)^+ + H^+$	-7.4970
$Cu^{2+} + 2H_2O \leftrightarrow Cu(OH)_2\ (aq.) + 2H^+$	-16.497

Table 6: Various equilibrium constants used for the speciation of Pb(II) in aqueous solutions at 25 ^{0}C.

Equilibrium	Log K
$Pb^{2+} + 2H_2O \leftrightarrow Pb(OH)_2\ (aq) + 2H^+$	-17.094
$Pb^{2+} + H_2O \leftrightarrow Pb(OH)^+ + H^+$	-7.597
$4Pb^{2+} + 4H_2O \leftrightarrow Pb_4(OH)_4^{4+} + 4H^+$	-19.988
$2Pb^{2+} + H_2O \leftrightarrow Pb_2(OH)_3^+ + H^+$	-6.397
$Pb^{2+} + 3H_2O \leftrightarrow Pb(OH)_3^- + 3H^+$	-28.091
$Pb^{2+} + 4H_2O \leftrightarrow Pb(OH)_4^{2-} + 4H^+$	-39.699
$3Pb^{2+} + 4H_2O \leftrightarrow Pb_3(OH)_4^{2+} + 4H^+$	-23.888

2.2.6. Effect of pH

Batch experiments were carried out to study the effect of pH on Cr(VI), Cd(II), Cu(II), Pb(II) As(III) and As(V) sorption by taking potassium dichromate, cadmium nitrate, copper sulphate, lead nitrate, sodium meta arsenite and sodium arsenate solutions respectively.

Chromium and cadmium solutions of 20 mg/L and 10 mg/L concentrations respectively were prepared at different pH of 2 to 10. The pH was adjusted by the addition of drops of conc. HNO_3 and conc. NaOH solutions. To 100 mL of each of these sorptive solutions, 0.5 g of MCS/ or ICS sample was added. The solutions were constantly shaken for about 24 hours in a rotary shaker at 25±2 ^{0}C. The solutions were filtered with 0.45 µm syringe filter and the pH was again checked and reported as the final pH. The filtrates were then subjected to UV- visible Spectrophotometer (Thermo Electron Corporation, England; Model: UV1) for Cr(VI estimation or Atomic Absorption Spectrophotometer for total heavy metal (As, Cd, Pb, Cu) concentrations (Lee *et al.*, 2010 b).

100 mL each solution of 10 mg/L Cu(II) and 20 mg/L Pb(II) concentrations respectively were taken into the polyethylene bottle at pH of 2.0 to 10.0. The pH was adjusted by the addition of drops of conc. $HNO_3$and conc. NaOH solutions. 0.5 g of solid i.e., MCS /or ICS was then added. The bottles were kept in the automatic shaker for 24 hrs at 25±2^{0}C in order to complete the sorption process and an apparent equilibrium may likely to be attained between the solid/solution interfaces. The samples were taken out from the shaker and filtered using a 0.45 µm syringe filter and the pH was again checked and reported as the final pH. The filtrates were then subjected for its bulk sorptive concentration measurements using the Atomic Absorption Spectrophotometer (Tiwari *et al.*, 2011a).

Arsenic (III) and Arsenic (V) solutions of 2 mg/L concentration each were prepared at different pH of 2.0 to 10.0. The pH was again adjusted by the addition of drops of conc. $HNO_3$and conc. NaOH solutions. To 100 mL of each of these sorptive solutions, 0.2 g of Manganese Coated Sand MCS/or Iron Coated Sand ICS sample was added. The solutions were constantly shaken for about 24 hours in a rotary shaker at 25±2 ^{0}C. The solutions were filtered with 0.45 µm syringe filter and the pH was again checked and reported as the final pH. The filtrates were then subjected to Atomic Absorption Spectrophotometer for total arsenic concentrations.

The percentage removal of the target metal ion was calculated using the equation

$$\%\ \text{Removal} = \frac{C_0 - C_e}{C_0} x\ 100 \qquad \ldots(9)$$

where C_0 and C_e are the initial and bulk sorptive concentrations, respectively.

2.2.7. Effect of sorptive concentration

The concentration dependence study was carried out varying the sorptive concentration from 5 mg/L to 100 mg/L for Cr(VI) and 1 mg/L to 20 mg/L for Cd(II), keeping constant pH 3.0 for Cr(VI) and 6.0 for Cd(II)). The 100mL sorptive solutions were equilibrated with 0.5 g of MCS /or ICS at 25±2 ^{0}C for 24 hrs in a rotary shaker. The solutions were filtered with 0.45 µm syringe filter and the filtrates were then subjected for the bulk sorptive concentrations using UV – visible Spectrophotometer for Cr(VI)(Thermo Electron Corporation, England; Model: UV1) and Atomic Absorption Spectrophotometer for total Cadmium concentration.

Similarly, the sorptive dependence data were collected taking the sorptive concentration from 1 mg/L to 20 mg/L for Cu(II) and from 1 to 40 mg/L for Lead Pb(II) at the constant pH 4.0 and temperature 25 ± 2^0C. Results obtained were then reported in terms of sorptive concentration and respective amount of Cu(II)/or Pb(II) removed with the help of Atomic Absorption Spectrophotometer. The As(III) and As(V) concentration dependence study was carried out varying the arsenic concentration from 1 mg/L to 20 mg/L at the constant pH 5.0 and temperature 25 ± 2^0C. The results obtained were reported in terms of sorptive concentration and the amount/or percent of total arsenic removal with the help of Atomic Absorption Spectrophotometer.

2.2.8. Ionic dependence study

The ionic dependence study for the adsorption of As(III), As(V), Cd(II), Cu(II), Pb(II), by the manganese coated sand (MCS) or iron coated sand (ICS) was conducted varying the background concentration of sorptive solutions using the different concentrations i.e., from 0.0001 to 0.1 mol/L of $NaNO_3$ solution. The sorptive pH (4.0) and temperature (25 ± 2^0C) was kept constant throughout the experiments. The remaining sorption procedure was followed as mentioned in the previous section. The results obtained were reported as percent removal as a function of the ionic strength.

2.2.9. Column Studies

The column experiments were performed using a glass column (1 cm inner diameter) packed with 1g of solid manganese coated sand (MCS) / or iron coated sand (ICS) sample (kept in the middle of column) and below and above to the MCS / or ICS, was filled with the 2 g of bare sand and finally packed with the glass beads. Sorptive solutions of As(III) and As(V) 2 mg/L, Cd(II), Cu(II) and Pb(II), 10 mg/L at constant pH 4.0 each was pumped upward from the bottom of the column using Acuflow Series II, High - pressure liquid chromatograph, at a constant flow rate of 1.2 mL/min. Effluent solution were then collected using Spectra/Chrom CF-1 fraction collector. These collected solutions were filtered using a 0.45 μm syringe filter and the total bulk sorptive concentrations were measured using Atomic Absorption Spectrophotometer (AAS).

The breakthrough data obtained were simulated for the removal capacity of Manganese Coated Sand (MCS) / or Iron Coated Sand (ICS) using the Thomas equation (4) (Thomas, 1944):

$$\frac{C_e}{C_0} = \frac{1}{1+ e^{\,[K_T\,(\,q_0\,m - C_0\,V)\,]/\,Q}} \qquad \text{--(10)}$$

Where C_e is the As(III), As(V), Cd(II), Cu(II) and Pb(II) concentration in the effluent (mg/L); C_o is the As(III), As(V), Cd(II), Cu(II) and Pb(II) concentration in the feed (mg/L); K_T the Thomas rate constant (L/min/mg); q_0 is the maximum amount of the As(III), As(V), Cd(II), Cu(II) and Pb(II) which can be loaded (mg/g) under the specified column conditions; $m$the mass of adsorbent loaded (g); V the throughput volume (L); and Q is the flow rate (L/min). A non-linear regression of the breakthrough data were performed for the least square fitting of the estimation of two unknown parameters i.e., K_T and q_o (Tiwari *et al.*, 2007b; Tiwari *et al.*, 2011a; Lee *et al.*, 2010 b).

REMOVAL BEHAVIOUR OF IRON COATED SAND (ICS) AND MANGANESE COATED SAND (MCS) FOR HEAVY METAL TOXIC IONS FROM AQUEOUS SOLUTIONS

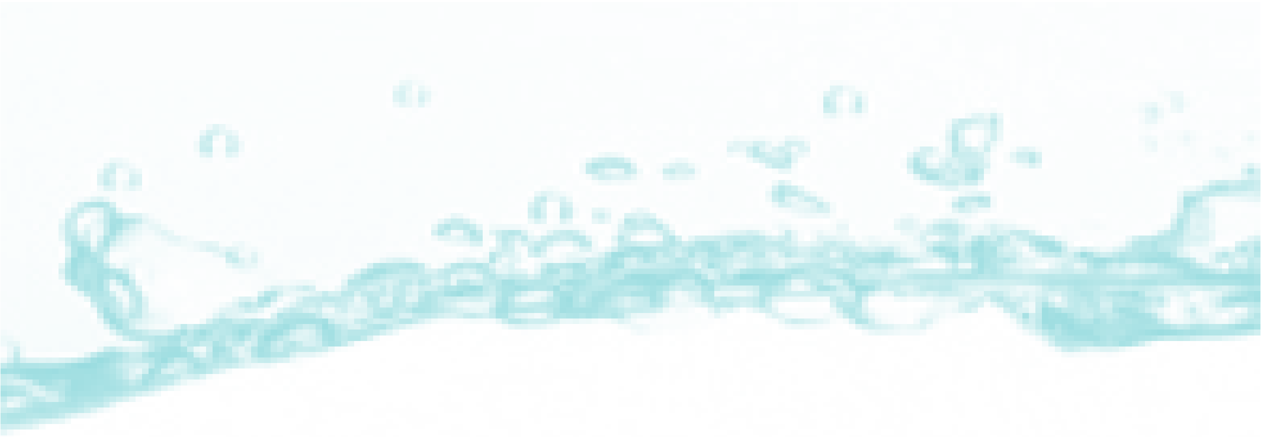

CHAPTER

3

Results and Discussions

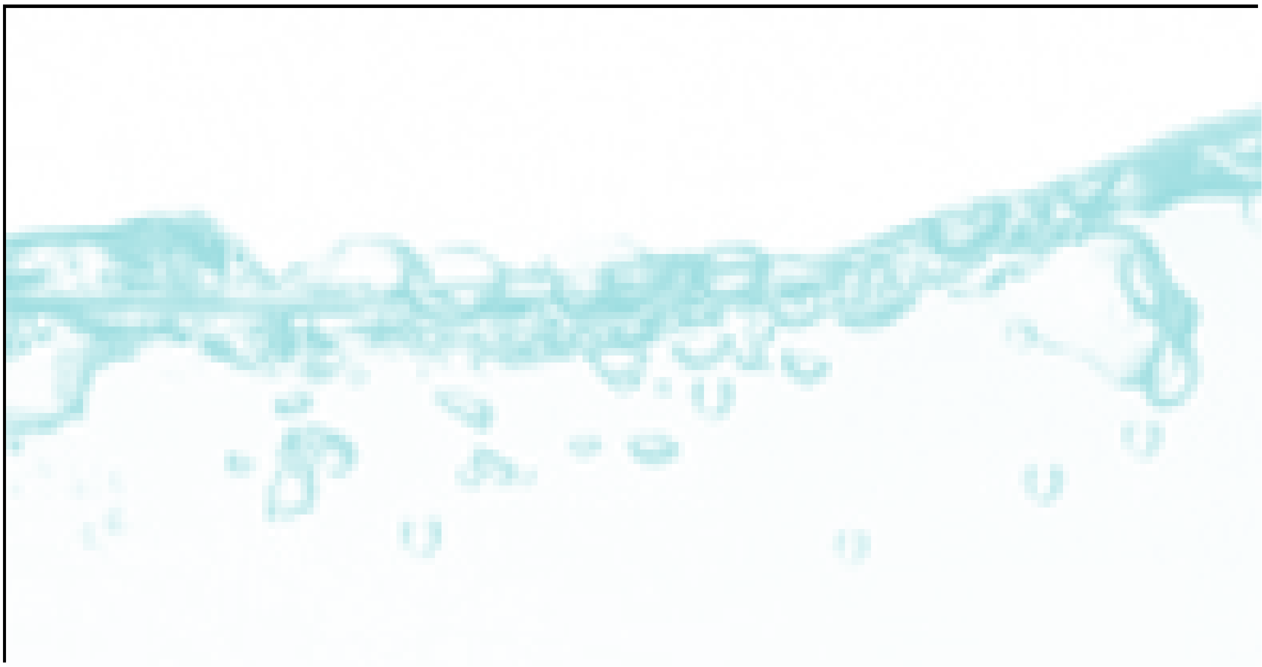

RESULTS AND DISCUSSIONS

3.1. CHARACTERIZATION OF MANGANESE COATED SAND (MCS) AND IRON COATED SAND (ICS)

3.1.1. Surface Morphology and Mineralogical Analysis of Manganese Coated Sand (MCS)

Figure 1(a), and 1(b) show the physical appearance of bare sand and manganese coated sand (MCS). The distinct colour change as shown in figure clearly indicated that manganese was aggregated significantly onto the surface of sand.

3.1.1.1. Scanning Electron Microscopic (SEM) Studies

The scanning electron microscopic (SEM) images of these two samples i.e., sand and manganese coated sand (MCS) were obtained and shown in figures 2(a) and 2(b) respectively for sand and manganese coated sand (MCS). However, the scanning electron microscopy (SEM) images (using FE-SEM-Model: SU-70, Hitachi, Japan) showed that the bare sand possessed very compact and disordered surface structure hardly found pores on its surface but contained several aggregated particles of silica. On the other hand the SEM images show that the manganese coated sand (MCS) sample was possessed with micro-pores hence likely to have higher specific surface area. Manganese is likely to be aggregated as in the form of manganese dioxide onto the sand surface. Manganese was very orderly clustered onto sand surface and the average particle size of manganese was estimated to be in the order of nano-meter range, *Ca*100 – 200nm. The low dose of manganese used (i.e., 0.05 mol/L) for the modification of activated sand samples likely to cause for less amount of manganese aggregated onto the sand surface. Other studies inferred that fine particles of manganese were

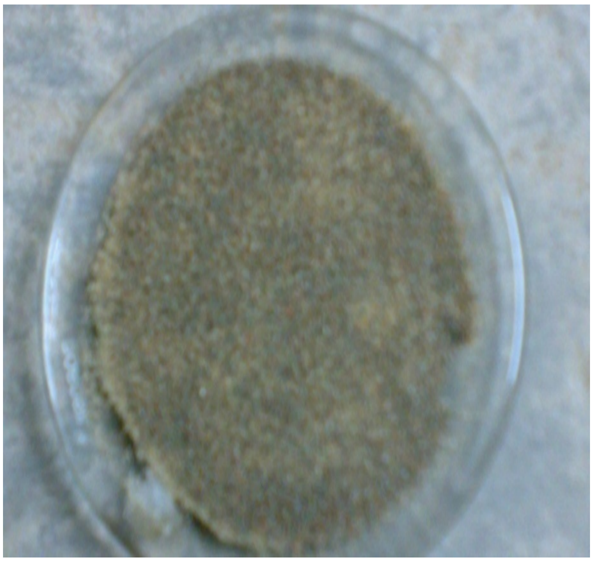

Figure 1(a): Bare sand

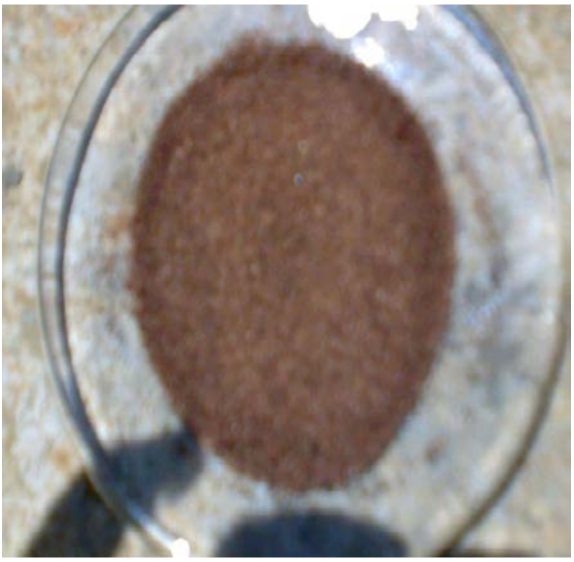

Figure 1(b): Manganese coated sand (MCS)

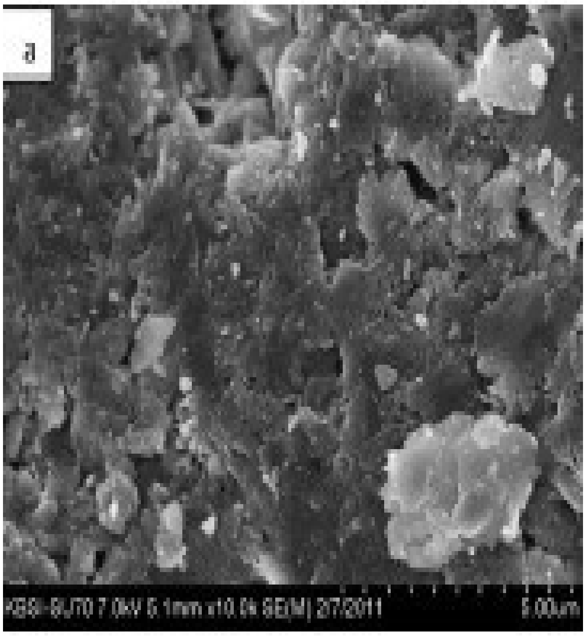

Figure 2(a): SEM image of bare sand

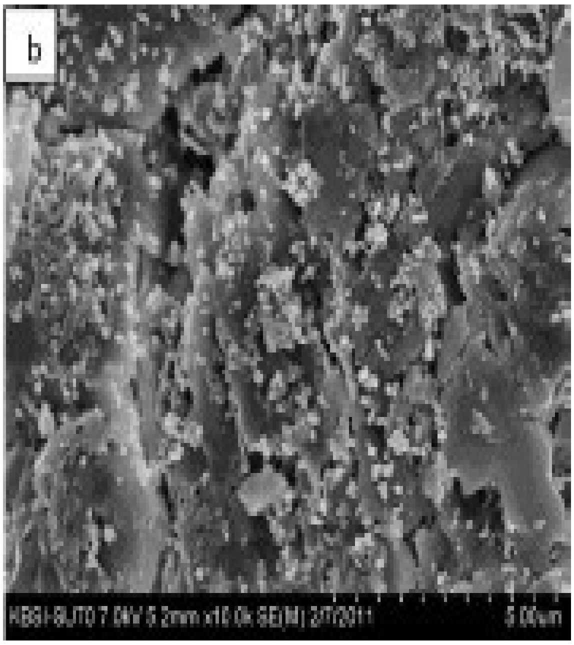

Figure 2(b): SEM image of manganese coated sand (MCS) orderly arranged onto the sand surface. Further, it was revealed that the manganese coated sand (MCS) surface was found to be porous and irregular surface with aggregated manganese oxide particles (Lee *et al.*, 2004). Moreover, manganese oxide coated sand (MOCS) was reported to possess a rough surface structure than bare sand and the coated sand surfaces were apparently occupied by newly born manganese dioxides, which were formed during the impregnation process (Han *et al.*, 2006).

3.1.1.2. Energy Dispersive X- Ray (EDX) Studies

The Energy Dispersive X – ray Spectrophotometric (EDX) analysis was performed and the results obtained were shown in Tables 7 and 8 along with Figures 3(a) and 3(b) respectively for the sand and manganese coated sand (MCS). Sand sample showed distinct peaks for the silica, iron, aluminium, magnesium etc. whereas the manganese coated sand (MCS) showed an additional peak for the manganese i.e., *Ca* 4.54 % (weight percent). These results again confirmed the low level aggregation of the manganese onto the surface of sand. Earlier, it was noted that significantly high manganese content was aggregated onto the sand surface making dense clustering onto the substrate which was prepared by the different preparative route (Hu *et al.*, 2004; Han *et al.*, 2006). Moreover, total manganese coated onto sand was reported to be relatively high.

The manganese content aggregated onto the surface of sand was also obtained by using the United States Environmental Protection Agency (US EPA) standard method 3050B. The amount of manganese aggregated was found to be 1446 mg/Kg of sand which is slightly higher than the result obtained by the similar works reported by the same group using different sand surfaces where the amount of manganese aggregated onto manganese coated sand was found to be 1045.7 mg/Kg (Lee *et al.*, 2010a).

3.1.1.3. *pH$_{PZC}$ Determination of Manganese Coated Sand (MCS)*

The pH$_{PZC}$ (point of zero charge) of the solid was obtained by the usual acid/base titrations and it was found to be 6.28. This value is somewhat higher than the pH$_{PZC}$ of the manganese dioxide as reported to be 5.5 (Koulouris, 1995) and 6.0 (Lee *et al.*, 2009). This may be because of the mixed effect of sand and manganese content possibly in the form of manganese dioxide.

3.1.1.4. X – Ray Diffraction (XRD) studies

The X– ray diffraction (XRD) data were obtained for the sand and manganese coated sand (MCS) and results were shown in Figure 4. The spectra clearly possessed with distinct diffraction peaks at the two theta value of 21.04, 26.76, 36.64, 39.58, 42.62, 50.24, 55.44, 60.04, 68.42, 81.57 etc. because of the reflections because of the presence of silica in both the samples. The d-spacings along with the relative intensities obtained for these reflections were then reported in Table 9. The data published by the Joint Committee on Powder Diffraction standards (JCPDS) were used to identify the crystalline phases of silica (SiO_2) in sand. Further, it was noted that the introduction of manganese caused for a slight shift in d-values, as mentioned in Table 8. This indicated that the interlayer of sand structure was prop up slightly. Moreover, due to the very low content of manganese onto the surface of sand, it could possibly not provide very sharp reflections of the mineral phases of manganese. These results were in accordance to the previous reports in which the pyrolusite was coated onto the clay surface using very low loading of pyrolusite. The pyrolusite was not detected by the XRD analysis because of the reasons that there may be inhibition of oxide crystallization or that the oxide nucleated as nano – meter particles which were not detected by XRD

Element	Wt %	At %
O K	45.47	62.54
MnL	00.00	00.00
NaK	01.87	01.79
MgK	01.18	01.07
AlK	10.31	08.41
SiK	24.52	19.21
K K	02.46	01.38
FeK	14.19	05.59

Table 7: EDX Data for sand

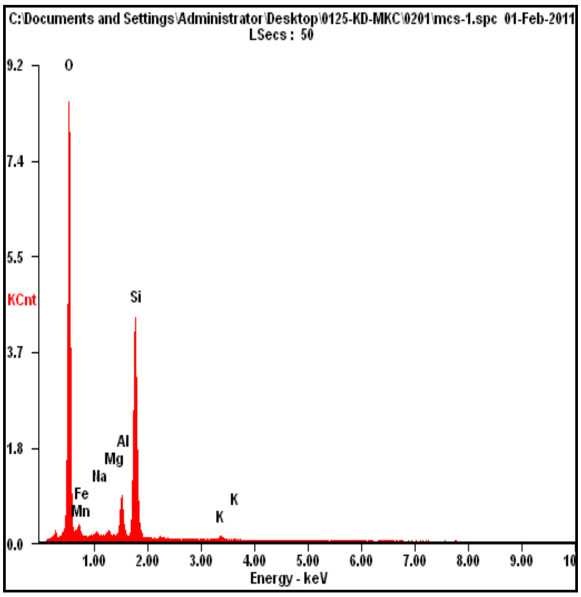

Figure 3(a): EDX spectra for sand

Element	Wt %	At %
O K	48.16	65.28
MnL	04.54	01.79
FeL	09.54	03.70
NaK	00.61	00.58
MgK	00.68	00.61
AlK	05.24	04.21
SiK	29.93	23.11
K K	01.30	00.72

Table 8: EDX Data for the manganese coated sand (MCS)

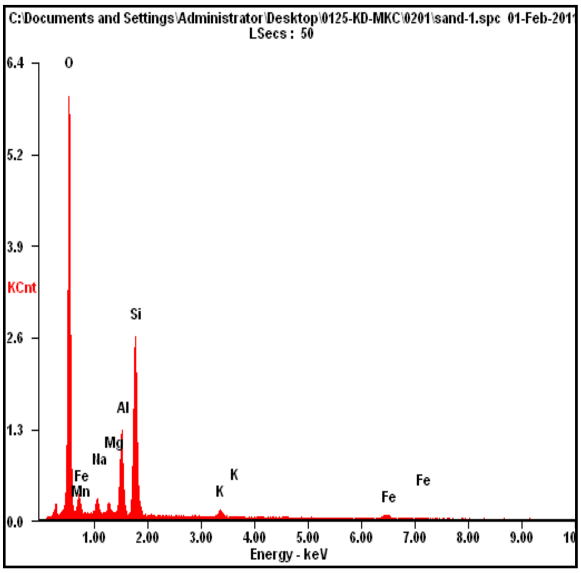

Figure 3(b): EDX spectra for manganese coated sand (MCS)

Table 9: The d-values and relative intensities for sand and manganese coated sand (MCS) using the XRD analysis

Sand			**MCS**			**difference with d-value**
2θ	**d-value**	**I/I_0x100**	**2θ**	**d-value**	**I/I_0x100**	
21.0441	4.2215	34.59	20.9141	4.2474	16.02	0.0259
26.7641	3.3308	100.00	26.7121	3.3372	100.00	0.0064
36.6441	2.4523	14.61	36.5920	2.4557	7.88	0.0034
39.5821	2.2768	10.29	39.5301	2.2797	8.99	0.0029
42.6241	2.1211	8.88	42.4941	2.1273	4.09	0.0062
50.2421	1.8159	11.35	50.1641	1.8185	14.58	0.0026
55.4421	1.6573	4.90	55.3641	1.6594	2.38	0.0021
60.0441	1.5408	9.34	59.9921	1.5420	5.94	0.0012
68.4161	1.3712	8.84	68.3381	1.3726	5.61	0.0014
81.5721	1.1801	4.16	81.4941	1.1810	2.31	0.0009

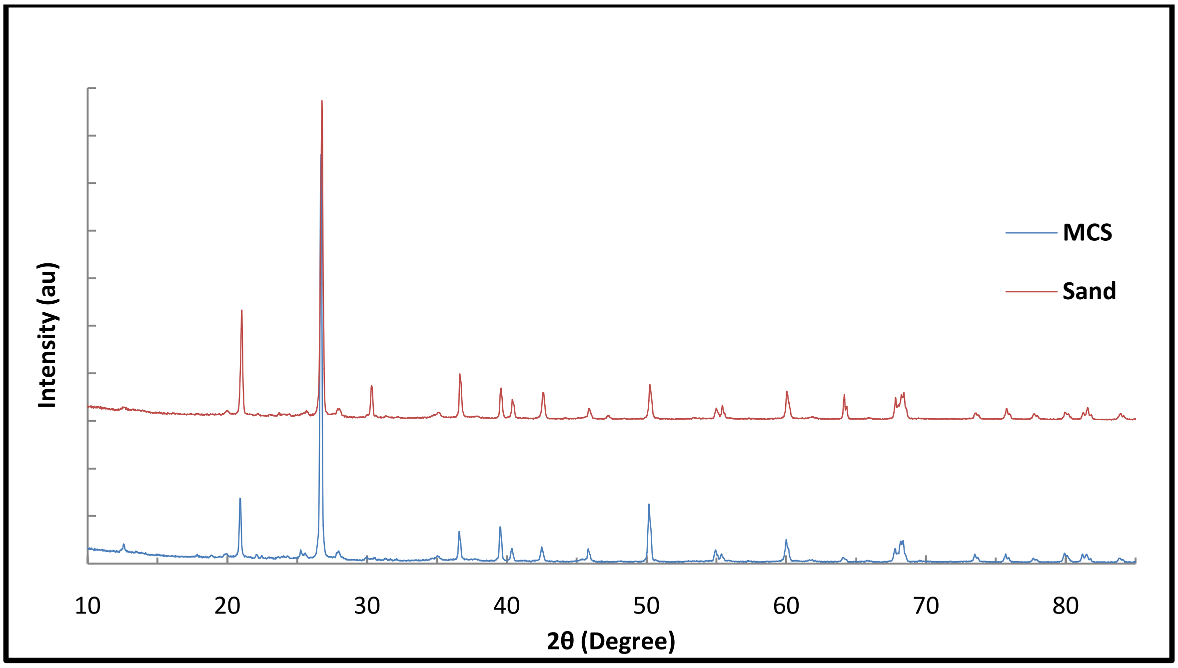

Figure 4: XRD spectra for sand and manganese coated sand

(Boonfueng *et al.*, 2005). This observation is also in accordance to the poorly crystalline lepidocrocite – coated montmorillonite (Green – Pederson *et al.*, 2000). However, the other reports indicated that it mainly contained with the pyrolusite (δ-MnO_2) (Chang *et al.*, 2008). Moreover, Hu *et al.*, (2004) reported that the manganese was aggregated onto sand as randomly stacked pyrolusite (MnO_2), γ-$Mn_2O_3$and $Mn(OH)_4$.

3.1.2. Surface Morphology and Mineralogical Analysis of Iron Coated Sand (ICS)

Fig. 5(a) and 5(b) show the physical appearance of sand and iron coated sand (ICS). The distinct colour change as shown in figure 5(b) clearly indicated that iron was coated onto the surface of sand.

3.1.2.1. Scanning Electron Microscopic (SEM) Studies

Figure 6(a) and 6(b) show the SEM images of the bare sand and iron coated sand (ICS) respectively. The image of sand indicated that the surface of sand is very compact and disordered which hardly possessed with micro- or meso-pores on its surface. On the other hand the SEM images showed that the iron coated sand (ICS) samples had more micro-pores hence possessed higher specific surface area, owing to attachment of iron likely in the form of ferric oxide on sand surface. No cracks were visible, except for the crystalline iron oxides found on the surface, similar to the observations reported by other workers (Lai *et al.*, 2000; Kitis *et al.*, 2007). They were very orderly clustered onto sand surface and the average size of these particles was estimated to be *Ca*<200-300 nm. The low dose of iron used (i.e., 0.05 mol/L) for the modification of activated sand samples likely to cause for less amount of iron aggregated/impregnated onto the sand surface.

Figure 5(a): Bare sand

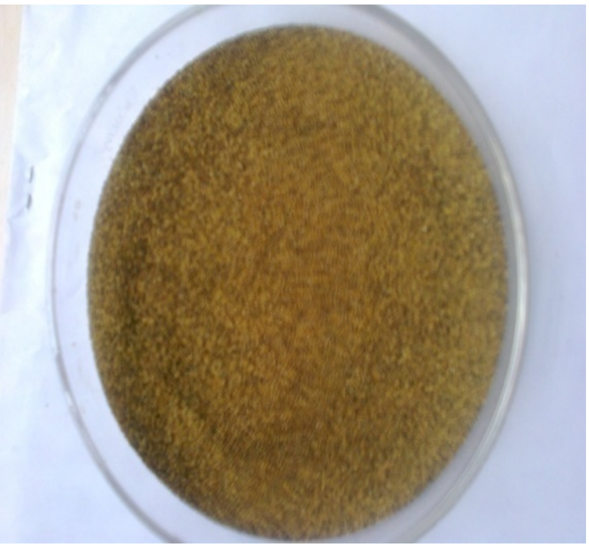

Figure 5(b): Iron coated sand (ICS)

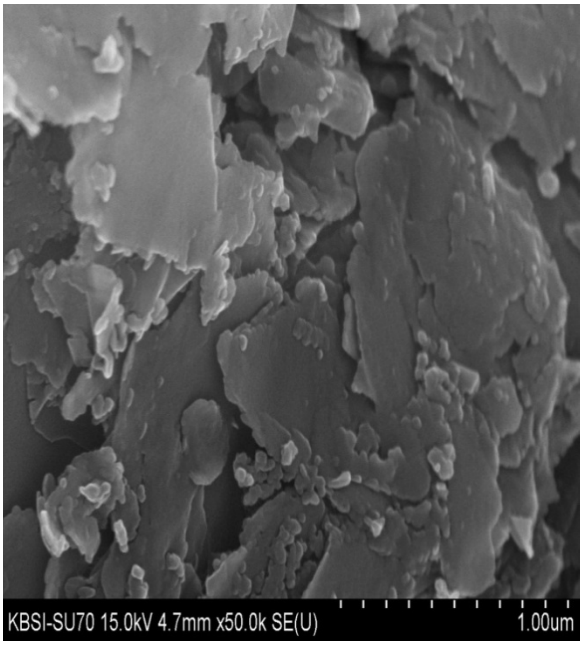

Figure 6(a): SEM image of bare sand

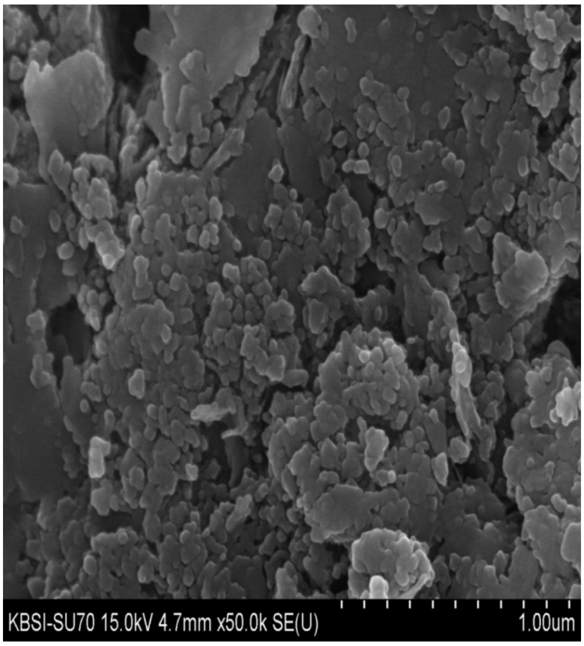

Figure 6(b): SEM image of iron coated sand (ICS)

3.1.2.2. Energy Dispersive X – Ray (EDX) studies

The Energy Dispersive X – ray Spectrophotometry (EDX) analysis was performed and the results obtained were shown in figures 7(a) and 7(b) respectively for the sand and iron coated sand (ICS) samples. Sand showed distinct peaks for the silica, iron, aluminium, magnesium, etc. The content of iron was found to be *Ca*. 6.82% (weight percent). But on the other hand the iron coated sand (ICS) sample showed an enhance intensity for the iron and quantitatively it is *Ca* 15.54 % (weight percent). These results again confirmed the low level aggregation of the iron onto the surface of sand. The other studies showed that significantly high iron content was aggregated onto the sand surface making dense clustering onto the substrate (Han *et al.*, 2006), which was prepared by the different preparative route. Moreover, total iron coated onto sand was reported to be relatively much higher. The elemental mapping obtained by the EDX data showed previously that the iron is mostly concentrating in the rough areas, and the relative distribution of Fe and Si indicated a non-uniform coating on the silica surface (Xu *et al.*, 2005; Edwards *et al.*, 1989; Scheidegger *et al.*, 1993).

The iron oxide content aggregated onto the surface of sand was also obtained by using the United States Environmental Protection Agency (US EPA) standard method 3050B. The amount of iron oxide aggregated effectively was found to be 5700 ± 0.3 mg/Kg of sand. Similar observations were also reported by other worker (Lai *et al.*, 2000) as well.

3.1.2.3. pH_{PZC} Determination of Iron Coated Sand (ICS)

The pH_{PZC} of the solid was obtained by the usual acid/base titrations and it was found to be 6.23 which, was very close to the reported pH_{PZC} of ferric hydroxide 6.28 (Koulouris, 1995). The other studies showed that the pH_{PZC} of reclaimed iron oxide coated sand (IOCS) was found to be 7.0±0.4 (Hsu *et al.*, 2008) and 6.5 to 8.5 (Cornell and Schwertmann, 1996).

Element	**Wt %**	**At %**
C K	15.29	24.00
O K	41.72	49.18
NaK	01.97	01.62
MgK	00.70	00.54
AlK	07.35	05.14
SiK	24.37	16.36
K K	01.77	00.86
FeK	06.82	02.30

Table 10: EDX data for sand

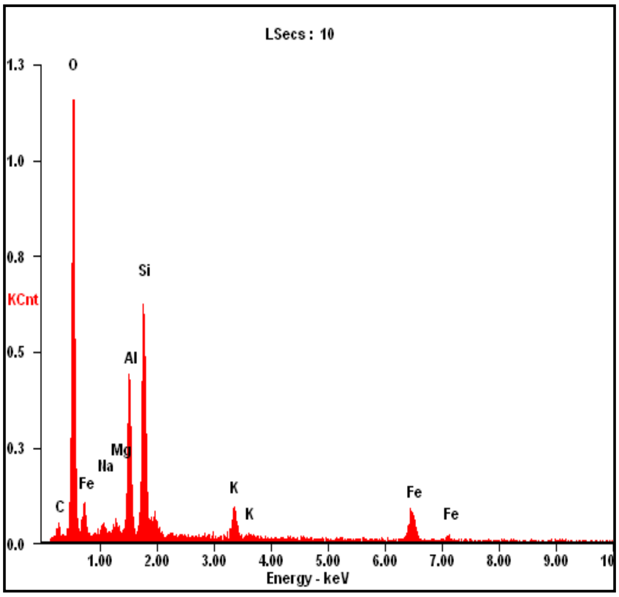

Figure 7(a): EDX spectra of sand

Element	**Wt %**	**At %**
C K	07.30	12.59
O K	42.65	55.19
NaK	01.10	00.99
MgK	01.42	01.21
AlK	08.53	06.54
SiK	23.57	17.37
K K	02.46	01.30
FeK	12.96	04.81

Table 11: EDX data for iron coated sand (ICS)

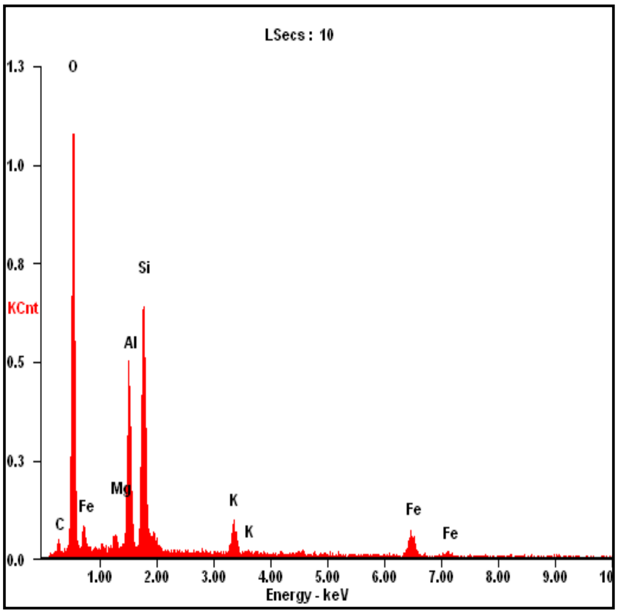

Figure 7(b): EDX spectra of iron coated sand (ICS)

This may be because of the mixed effect of sand and iron content possibly in the form of ferric oxide.

3.1.2.4. X –Ray Diffraction (XRD) studies

The X – ray diffraction (XRD) data obtained for the sand and iron coated sand (ICS) were shown in Figure 8. Figure clearly indicated that INS and sand samples possessed with very characteristics and distinct diffraction peaks occurred at the 2θ values of 20.88, 26.68, 28.00, 36.58, 39.50, 40.33, 42.46, 50.18, 59.96, 67.73, 68.31 etc. The d-values along with the relative intensities obtained for these reflections were then reported in Table 12. These reflections were because of the presence of silica as compared with the standards mentioned by the Joint Committee on Powder Diffraction Standards (JCPDSs). Moreover, the difference in d-values was insignificant for these two solids inferred that iron oxide was hardly to prop-up the silicate layers hence, mostly it was aggregated onto the surface or within the accessible pores of the sand. Moreover, it was noted that iron coated sand hardly showed any sharp or additional reflections because of the particular mineral phase of iron present onto the sand surface. This was perhaps due to the very low content of iron aggregated onto the surface of sand (Xu *et al.,* 2005; Tiwari *et al.,* 2011a). These results were in accordance to the previous reports in which the pyrolusite was coated onto the clay surface using very low loading of pyrolusite. The pyrolusite was not detected by the XRD analysis because of the reasons that there may be inhibition of oxide crystallization or that the oxide nucleated as nanometer particles which were not detected by XRD (Boonfueng *et al.*, 2005). This observation was also in accordance to the poorly crystalline lepidocrocite-coated montmorillonite (Green-Pederson *et al.*, 2000). Other studies mentioned that anamorphous iron oxide was coated onto sand surface which was converted to goethite and hematite at 150 ^{0}C and hematite above 300^{0}C (Lo *et al.*, 1997). Similarly, γ-Fe_2O_3 was occurred at 400 ^{0}C while iron was coated onto alumina (Zhong *et al.*, 1999). The mixture of hematite and goethite were observed by Chang *et al.*, (2008) as they obtained iron and manganese coated sand materials which was further used to pack the columns to remove As(III) under dynamic conditions.

3.2. STABILITY OF MANGANESE AND IRON COATED SAND

The stability of manganese and iron coated sand at different pH were conducted and the stability results are included in Tables 13 &14 and Figures 9 &10 respectively for MCS and ICS. The results clearly showed that the manganese /or iron strongly occupied the surface within the pH region 3 to 10 since no significant amount of manganese /or iron was desorbed into the bulk solution. Whereas, it was slightly unstable at pH 2 since total of *Ca*0.5 mg/L of manganese or 0.60 mg/L of iron was desorbed respectively from MCS and ICS samples. These results suggested that manganese/or iron occupied the surface of sand firmly and likely to have some strong chemical binding with the substrate. Moreover, these solids are useful to employ in water purification purposes over the wide pH range. The similar experiment studies carried out for manganese coated activated carbon by Tiwari *et al.*, (2011b) emphasized that the manganese coating is relatively stable within pH 3.0 to 11.0.

The specific surface area of the solids is obtained by using a Brunauer-Emmett-Teller (BET) specific surface area analyzer (Mountech, Japan model MacSorb HM model-1200 Series). The BET multipoint surface area was found to be respectively, 8.51, 11.03, 11.12 m^2/g for sand, MCS and ICS respectively. This clearly showed that the manganese coated or iron coated sand possessed with significantly higher specific surface area compared to the bare sand sample.

Table 12: The d-values and relative intensities for sand and iron coated sand (ICS) using the XRD analysis

Sand			**ICS**			**difference with d- value**
2θ	**I/I_0x100**	**d – value**	**2θ**	**I/I_0x100**	**d – value**	
20.8811	18.12	4.25074	21.1151	16.05	4.20150	0.04924
26.6791	100.00	3.33867	26.8351	100.00	3.31959	0.01908
28.0051	3.11	3.18351	28.1091	1.40	3.17197	0.01154
36.5851	15.19	2.45420	36.7411	9.83	2.44414	0.01006
39.4971	11.71	2.27971	39.6791	5.54	2.26967	0.01004
40.3291	3.95	2.23458	40.5111	2.25	2.22496	0.00962
42.4611	3.59	2.12718	42.6691	4.41	2.11729	0.00989
50.1831	8.48	1.81646	50.3391	10.98	1.81120	0.00526
59.9591	6.33	1.54155	60.1411	7.21	1.53732	0.00423
67.7331	5.16	1.38230	67.9151	4.96	1.37903	0.00327
68.3051	6.29	1.37211	68.3311	5.64	1.37165	0.00046

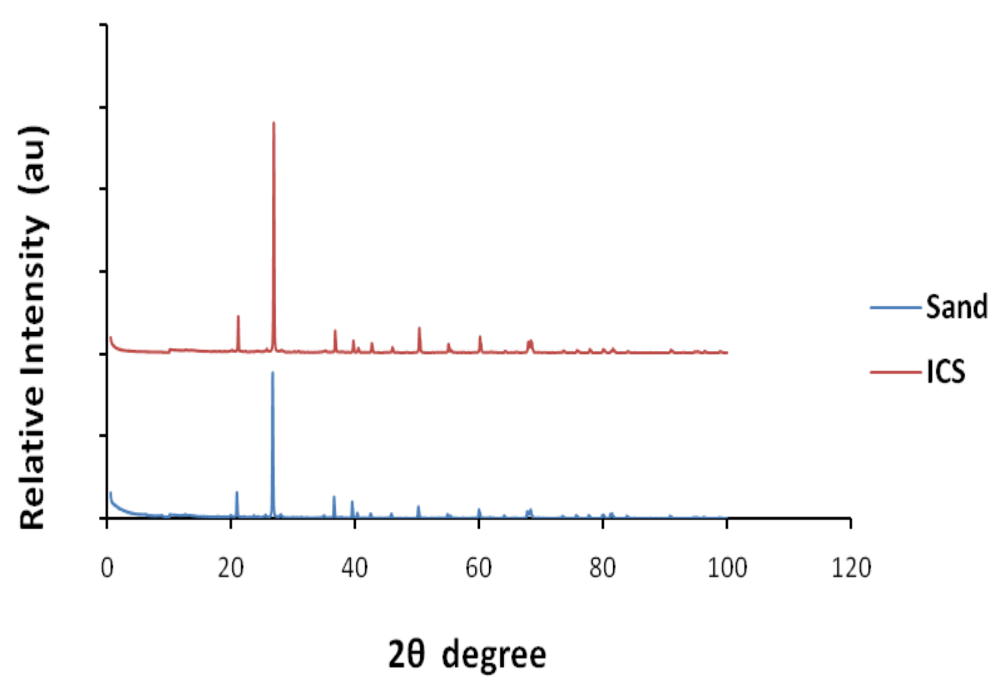

Figure 8: XRD spectra for sand and iron coated sand (ICS) samples

pH	Bulk manganese conc.(mg/L)
2.02	0.5000
3.05	0.0100
4.01	0.0040
4.97	0.0020
6.01	0.0010
7.04	0.0010
7.96	0.0004
8.89	0.0004
10.03	0.0002

Table 13: Stability data for manganese coated sand (MCS)

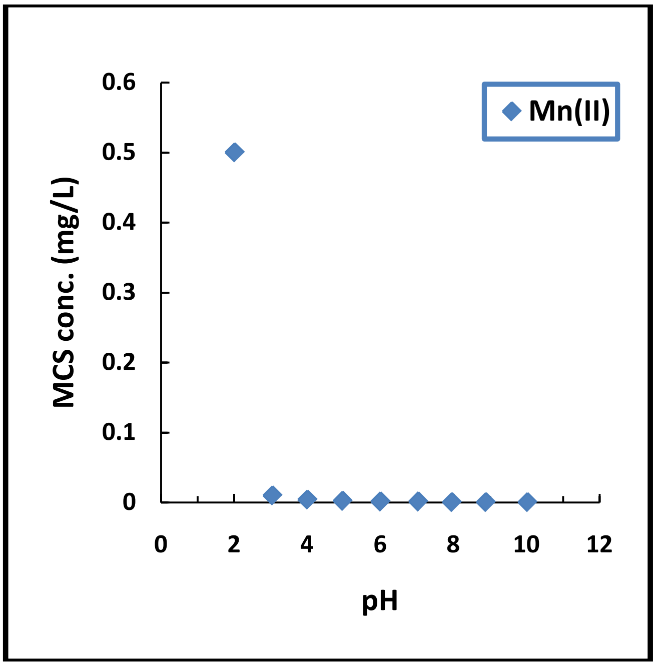

Figure 9: The stability curve for manganese coated sand (MCS)

pH	Bulk iron conc. (mg/L)
1.95	0.6000
3.01	0.0400
3.96	0.0060
4.99	0.0040
6.04	0.0020
7.12	0.0010
7.98	0.0005
9.02	0.0006
10.01	0.0003

Table 14: Stability data for iron coated sand (ICS)

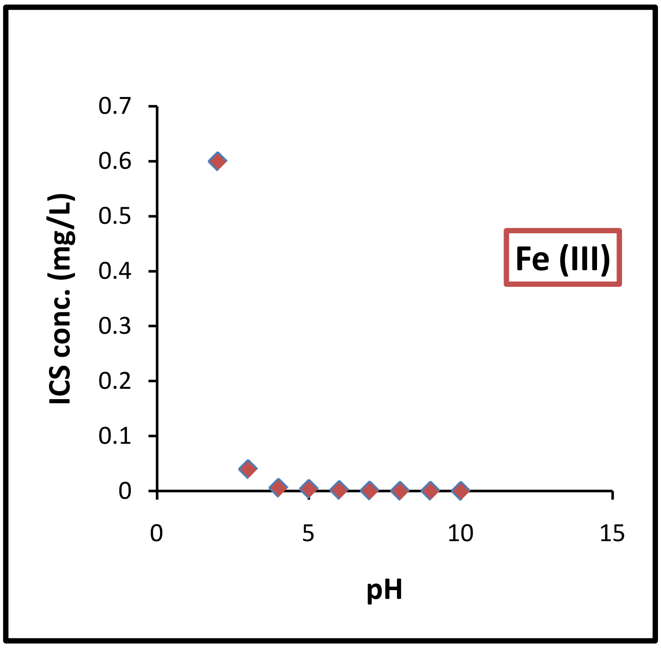

Figure 10: Stability curve for iron coated sand (ICS)

3.3. SPECIATION STUDY OF Cr(VI), Cd(II), Cu(II), Pb(II), As(III) AND As(V)

The speciation of chromium(VI) (20 mg/L), arsenic(III), arsenic(V) (2 mg/L), cadmium(II) (10 mg/L), copper(II) (10 mg/L) and lead(II) (20 mg/L)species as a function of pH were obtained using a MINEQL geochemical simulation program keeping the ionic strength 0.01 mol/L and at constant temperature 25 ^{0}C. The speciation studies were important to elucidate the mechanism involved at solid solution interface. Moreover, it intended to describe, under the specified conditions that the sorptive ions were distributed in aqueous solutions with what specific species at the varied pH region i.e., pH 2 – 11. Further, the outcome of these studies were shown respectively in Figure 11, 12, 13, 14, 15 and 16 for Cr(VI), As(III), As(V), Cd(II), Cu(II) and Pb(II).

3.3.1. Speciation Study of Chromium(VI)

The speciation results of Cr(VI) were shown in Figure 11. The equilibrium constants used were already given in Table 1. The figure clearly indicated that Chromium Cr(VI) mostly exists as the soluble anionic species of CrO_4^{2-}, $HCrO_4^-$ or $Cr_2O_7^{2-}$ throughout the pH range of 2 – 10. However, it was observed that up to the pH of 5.5, the major species was $HCrO_4^-$. Beyond this pH, Cr(VI) was existed mainly as anionic CrO_4^{2-} species. Similar observations had also cited by Sonia *et al.*, (1999).

3.3.2. Speciation Study of As(III)

Depending on pH, different forms of As(III) *viz.*, H_3AsO_3, $H_2AsO_3^-$, $HAsO_3^{2-}$, and AsO_3^{3-} were occurred.The speciation analysis results of As(III) was represented in Figure 12.

The input data introduced was stated in Table 1. It was observed that the species H_3AsO_3wasdominated below the pH = 8and above pH = 8 the anionic species was $H_2AsO_3^-$ dominated. The relative distribution of all the species of Arsenic(III) with respect to pH was also appended elsewhere (Edwards, 1994; Ferguson *et al.*, 1972).

3.3.3. Speciation Study of Arsenic(V)

The different species of arsenic(V) i.e., H_3AsO_4, $H_2AsO_4^-$, $HAsO_4^{2-}$, and AsO_4^{3-} were existed in aqueous solutions depending upon the solution pH. The speciation studies of As(V) which was represented in Figure 13 had revealed that at lower pH till pH 6.8, $H_3AsO_4$and $H_2AsO_4^-$species dominated whereas above pH = 7, $HAsO_4^{2-}$anionic species dominated**.** Similar observations were mentioned by Zouboulis *et al.,* (1993) for As(V) speciation.

3.3.4. Speciation Study of Cadmium(II)

The speciation studies for cadmium(II) showed in Figure 14 that even up to pH 8.5 the cadmium was exited as Cd^{2+}soluble cationic species. Beyond the pH 8.5 the cadmium was turned into insoluble $Cd(OH)_2$ species and at pH 10 and beyond it was occurred with 100%. In between these two species at pH 9.2 a maximum of *Ca.* 2 % of Cd(II) existed as $Cd(OH)^+$species. Similar observation was reported previously in our research papers (Lee *et al.*, 2010b; Tiwari *et al.*, 2011b). Ma *et al.,* (2003) reported that at pH 4, Cd(II) existed as cationic Cd^{2+}species with 97 – 99.9 % abundance.

3.3.5. Speciation Study of Copper(II)

The speciation studies obtained by the MINEQL geochemical program for Copper Cu(II) were shown in Figure 15. Figure 13 showed that Copper was existed to its bionic form i.e., Cu^{2+}upto the pH region ~5.8. But beyond that it was started precipitating as the Cu(II) converted to tenorite. It was observed that around pH 7.0 a complete precipitation of the Cu(II) occurred. Similar observation were also reported elsewhere (Davis *et al.*, 2000; Tiwari *et al.*, 2006; Tiwari *et al.*, 2007a; Tiwari and Lee, 2011)

3.3.6. Speciation Study of Lead(II)

Figure 16 projected the speciation studies performed for Pb(II). It was observed that lead existed to its ionic form i.e., Pb^{2+} up to the pH region ~5.8. However, beyond this pH, lead was precipitated to $Pb(OH)_2$(s) and around pH 7.0, the ion was completely precipitated. The data was already published elsewhere (Tiwari *et al.*, 2006; Tiwari *et al.*, 2007b; Tiwari and Lee, 2011). Other studies showed that at higher pH values a substantive hydrolysis of lead could take place to give $Pb(OH)_2$ (Kovacˇevic´ *et al.*, 2000).

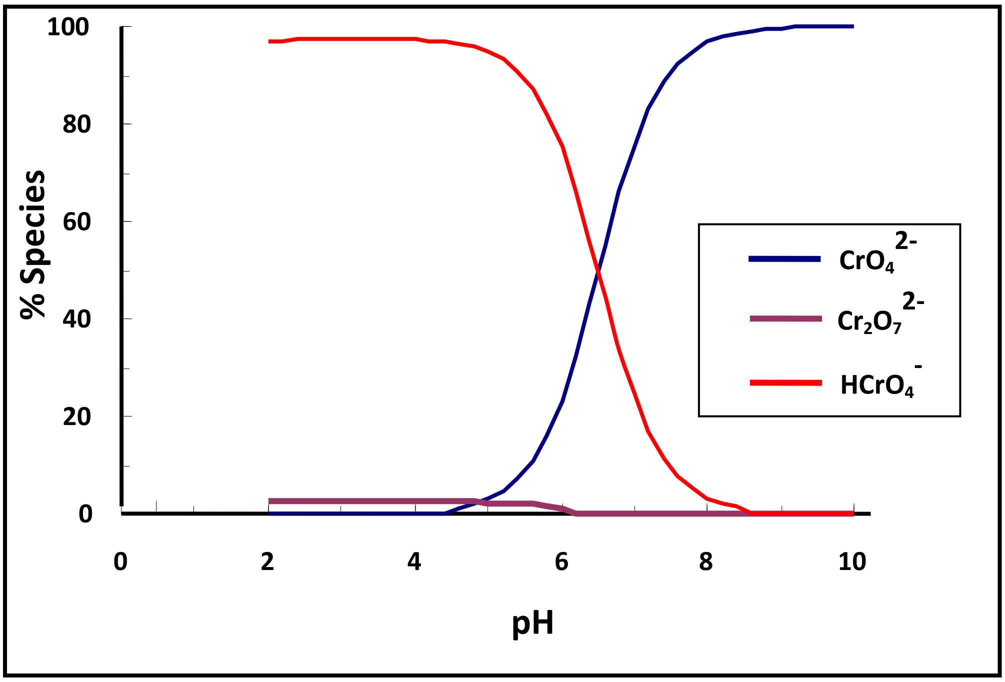

Figure 11: Speciation of Cr(VI): 20 mg/L as a function of pH.

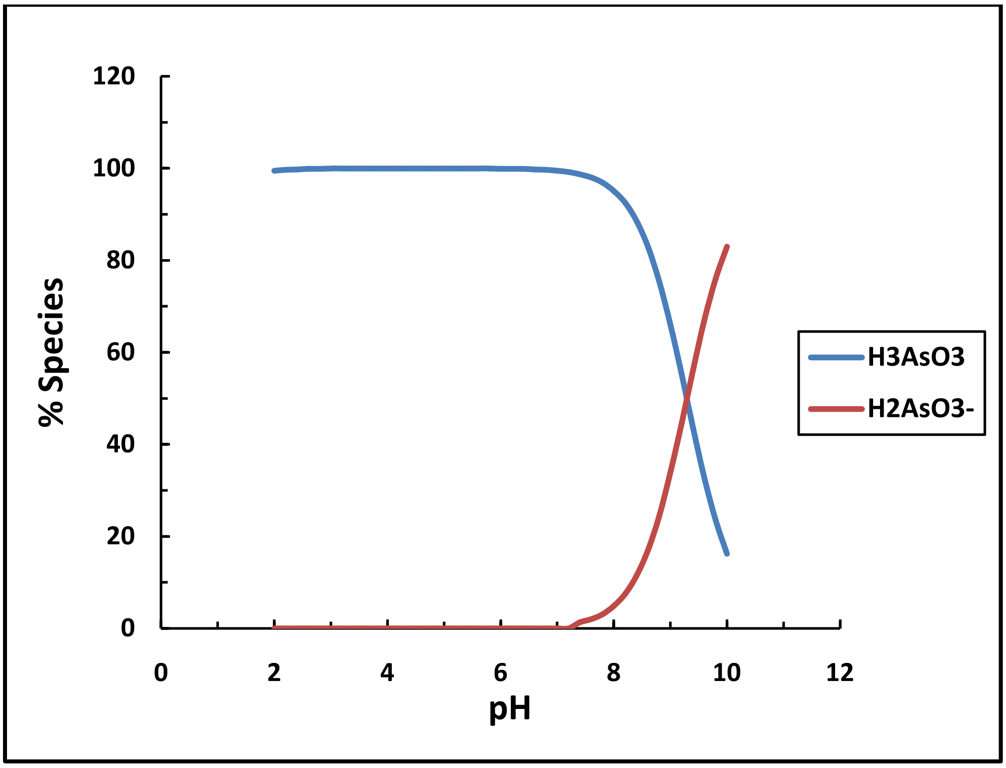

Figure 12: Speciation of As(III): 2 mg/L as a function of pH.

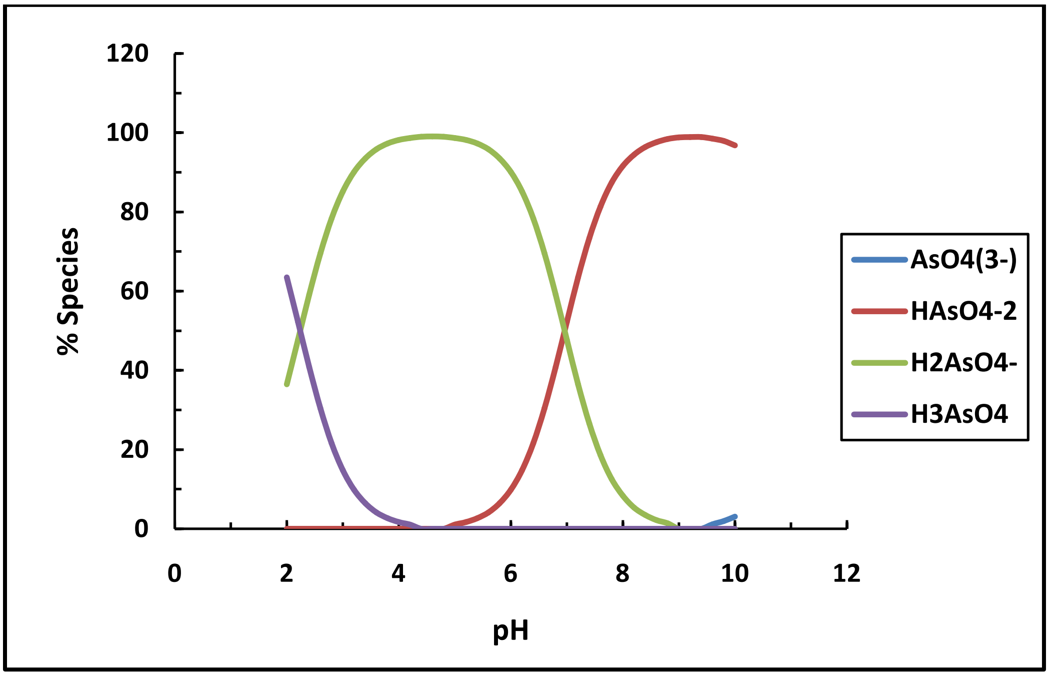

Figure 13: Speciation of As(V): 2 mg/L as a function of pH.

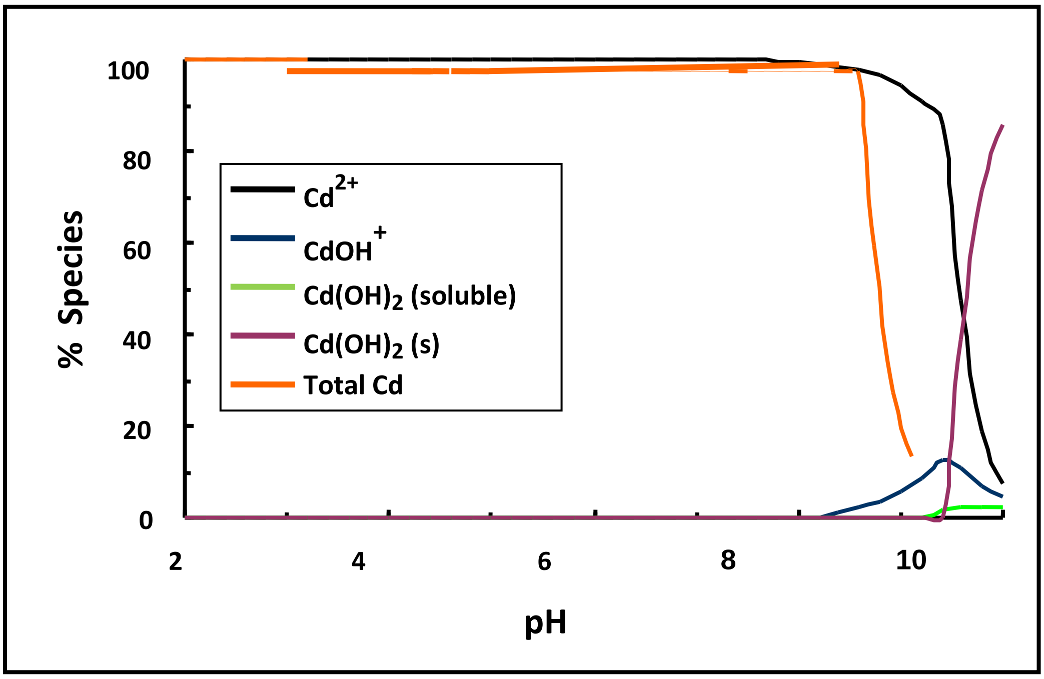

Figure 14: Speciation of Cd(II): 10 mg/L as a function of pH.

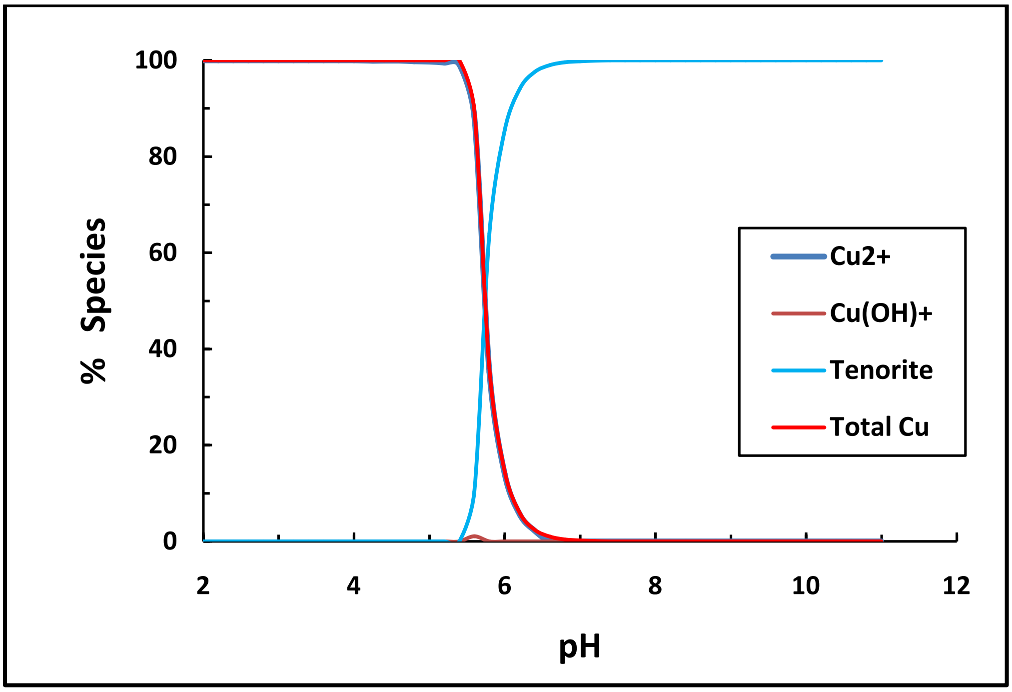

Figure 15: Speciation of Cu(II): 10 mg/L as a function of pH.

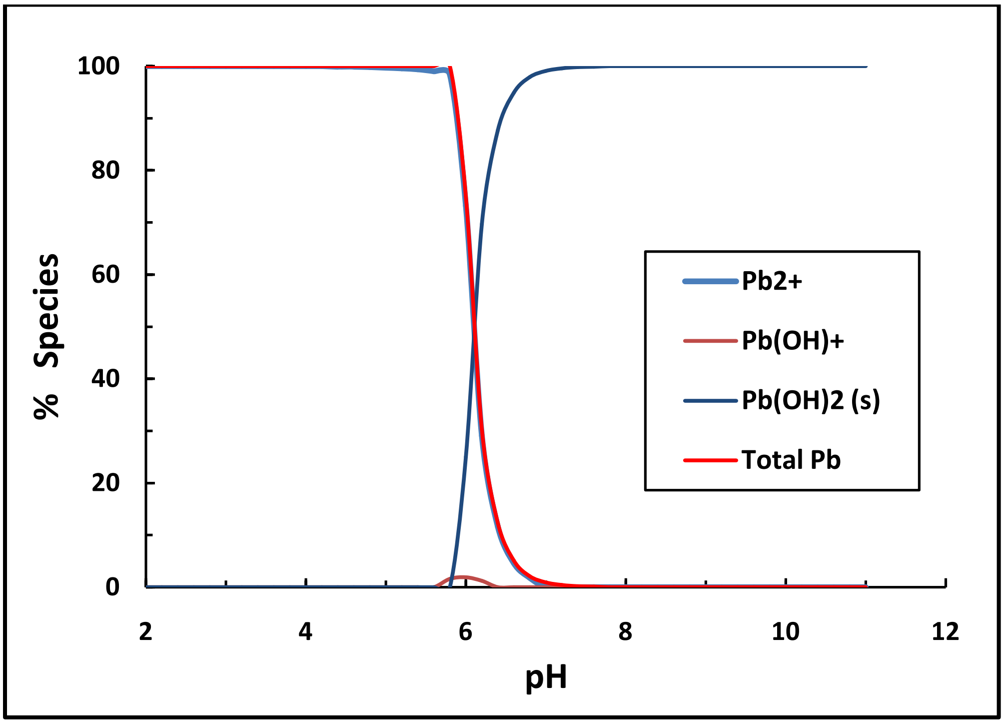

Figure 16: Speciation of Pb(II): 20 mg/L as a function of pH.

3.4. REMOVAL BEHAVIOR OF MANGANESE COATED SAND (MCS) AND IRON COATED SAND (ICS)

3.4.1. Effect of pH

The pH dependence data is an important parameter enabling the mechanism involved at solid/solution interface. Moreover, it greatly affects the sorption capacity of sorbing species onto the solid surface (Ho and McKay, 2003).As demonstrated earlier, the solution pH affects, among others, the speciation of the metal ions in aqueous solutions (Katsoyiannis *et al.*, 2002; Schmuhl *et al.*, 2001). Similarly, the pH of an aqueous solution is a variable which controls the adsorption process of metal ions at the surface of solids. This phenomenon helps in the removal of toxic metal ions from the aqueous medium. The presence of H^+ and OH^- ions greatly influence the adsorption of ions from the aqueous solutions. Generally low pH favours the adsorption of anions due to protonated surface of the adsorbent which at the higher pH leads to deprotonation of the adsorbent and favours the adsorption of the cations.

The adsorption of trace cations was very small in strongly acidic solutions, which increases with the increase in pH (Tamura and Nagayama, 1984, Tamura *et al.*, 1986, Sanders 1987, Singh *et al.*, 1992, Viraraghavan *et al.*, 1990). Sometimes even a little increase in the pH may cause an abrupt change in the amount adsorbed (Tewari *et al.*, 1972; Music *et al.*, 1988**.** This could be due to the increase in the negative charge of the adsorbent surface and decrease of the competitions of H_3O^+ ions for ion exchange or hydrolysis of trace cations. The strength of adsorption bonds is generally much greater for heavy metal cations. Herczynska (1961a; 1961b; 1965) suggested the formation of two adsorption maxima for trace ions, one in the neutral and the other in the alkaline pH regions for cations or one in the acidic region and the other in the neutral region for anions. The existence of the first adsorption peak in the medium pH region is attributed to the primary exchange with already adsorbed H^+ or OH^- ions while the other peak is explained by ion exchange in the outer part of the electrical double layer.

A number of studies were reported the effect of pH on the uptake of arsenic species onto the zero valent iron (ZVI) systems where it was observed that the increase in pH had decreased the uptake of arsenic species (Bang *et al.*, 2005a; Bang *et al.*, 2005b; Sun *et al.*, 2006; Su and Pulis, 2001a). In addition, the pH effect on the removal of arsenic species by iron oxides and iron hydroxides was well established (Su and Pulis, 2001b; Meng *et al.*, 2000; Jia *et al.*, 2006). It was reported that decrease in removal of As(V) by $FeCl_3$ at acidic pH values had observed by other researchers (Behrang *et al.*, 2011; Baskan *et al.*, 2009; Wang *et al.*, 2003).

Murray *et al.* (1968) observed the adsorption of alkali and alkaline earth metal cations on magnetite in aqueous solution was strongly pH dependent at low sorptive concentrations. However, at higher sorptive concentrations, it became independent of pH. Therefore keeping in view the previous studies and information already gathered, it was considered that the pH dependence studies would highly be useful to study the mechanism of adsorption.

3.4.1.1. Chromium(VI)

The pH dependence data for the removal behaviour of Cr(VI) by manganese coated sand and iron coated sand were obtained and listed in Tables 15 and 16 and presented graphically in Figures 17 and 18, respectively. It was noted that the per cent removal of Cr(VI) by MCS was decreased from 84.74% to 72.11% with the increase in pH i.e., from 2.04 to 10.10 (*cf* Figure 17). Consequently, the amount adsorbed decreases from 8.521 to 7.251 mg/g with the increase in pH from 2.04 to 10.10. The pH dependence data obtained by

MCS could be explained with the help of surface properties of MCS as well the properties of the adsorbing species present in the solution. Since MCS solid contained with manganese dioxide layer on its surface and the pH_{PZC} for manganese dioxide was reported to be 5.5 for (Koulouris, 1995). However, the pH_{PZC} obtained for MCS was 6.28. Hence, the surface supposed to be positively charged below pH 6.2 and beyond that it became negatively charged (*cf* equation 12).

$$\equiv SH_2^+ \leftrightarrow \underset{pH_{PZC}}{\equiv SH^0} \leftrightarrow \equiv S^- \qquad \ldots.(12)$$

The higher uptake of Cr(VI) at very low pH may be explicable because of the anionic species of Cr(VI) present ($HCrO_4^-$, CrO_4^{2-}, $Cr_2O_7^{2-}$; *cf* Figure 11) which preferred the positively charged solid surface. However, with the increase in pH beyond 6.2 the MCS surface became negatively charged which apparently caused for relative decrease in adsorption of Cr(VI) species. However, the decrease in adsorption at higher pH values was because of competitiveness of the oxy-anions of chromium and OH^- ions present in the bulk solutions. In this region perhaps the repulsion of negatively charged surface to Cr(VI) anion also reduced the adsorption of Cr(VI) at higher pH values. Similar pH dependent results were also been reported for Cr(VI) on various sorbents (Pehlivan *et al.,*2008; Gode *et al.,* 2008; Bhattacharya *et al.,* 2008).

On the other hand, the percentage removal of the Cr(VI) by ICS was more or less unaffected with the increase in pH of the solution, i.e., 73.73% to 78.98% with the increase in pH from 2.14 to 9.49. At the same time the amount adsorbed also remains more or less constant within the range of 2.955 to 3.166 mg/g. The results obtained clearly demonstrated the strong affinity of the sorbing species towards the sorbent. The similar data was also obtained for the sorption of Cs(I), Zn(II) and Cd(II) by sodium titanate (Mishra *et al.*, 1997a; Mishra *et al.*, 2004).

It was reported by other workers that depending on the solution pH the adsorbent can be utilized to adsorb cations or anions. The removal of Cr(VI) by ICS resulted in better than 99% consistently. The pH of the regenerant solution determined the kinetics and efficiency of the regeneration process (Bailey *et al.*, 1992).

3.4.1.2. Arsenic(III)

The pH dependence studies for the removal of As(III) onto the MCS and ICS surface was carried out at 25^0C with the initial sorptive concentration 2 mg/L. The results obtained were listed in Tables 17 and 18 respectively for MCS and ICS. Similarly, Figures 19 and 20 show the graphical representation of MCS and ICS, respectively. The results showed that increase in pH apparently caused for decrease in uptake of As(III). Quantitatively, increase in pH from 1.96 to 9.34 caused for decrease in per cent removal of As(III) from 69.23% to 37.02%, respectively and a decrease in amount adsorbed from 0.288 to 0.154 mg/g whereas the increase in pH from 1.61 to 7.37 caused for decrease in As(III) uptake from 64.59% to 41.15%, respectively with the decrease in amount adsorbed from 0.270 to 0.172 mg/g by ICS solid. The results obtained can be explained on the basis of the speciation studies of the metal ions against the change in pH of the solution along with the surface properties of MCS and ICS. The speciation studies revealed that at all pH range, As(III) exists as negatively charged complex ions. Thus the surface charge of MCS and ICS i.e., positive charge below pH_{PZC} favoured the uptake of these two ions due to electrostatic attraction at lower pH. Similarly, electrostatic attraction was reported for the sorption of As(III) by hybrid materials, or soil samples etc. (Arai *et al.,* 2001; Xu *et al.,* 2009; Mandal *et al.,* 2011). However the negative charge surface beyond the pH_{PZC} hindered the removal of As(III) at higher pH due to

Table 15: Effect of pH on the sorption of Cr(VI) onto the surface of MCS (MCS dose = 2g/L).

pH	Initial Cr(VI) conc.(mg/L)	Final Cr(VI) conc.(mg/L)	Amount adsorbed (mg/L)	Amount adsorbed (mg/g)	% Removal
2.04	20.11	3.07	17.04	8.521	84.74
2.97	20.11	3.21	16.90	8.451	84.05
4.10	20.11	3.85	16.26	8.128	80.84
4.96	20.11	4.39	15.72	7.858	78.16
6.12	20.11	5.03	15.08	7.541	75.00
6.99	20.11	5.04	15.07	7.536	74.95
8.02	20.11	5.05	15.06	7.530	74.89
9.30	20.11	5.11	14.99	7.499	74.58
10.10	20.11	5.61	14.50	7.251	72.11

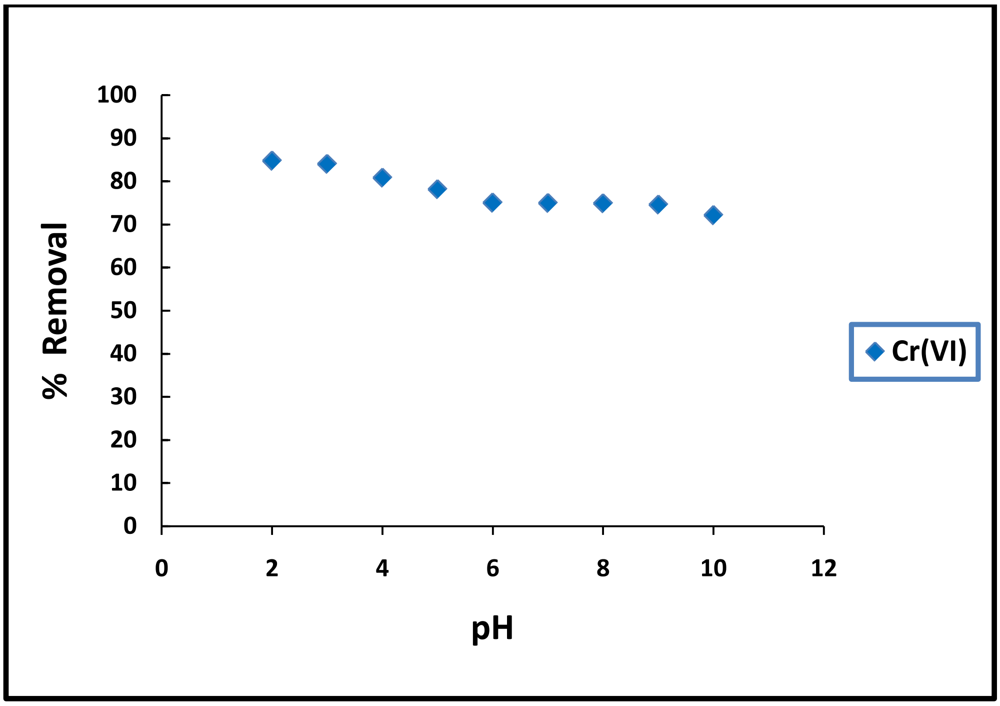

Figure 17: Effect of pH on the sorption of Cr(VI) onto the surface of MCS (Initial concentration of Cr(VI): 20.11 mg/L).

Table 16: Effect of pH on the sorption of Cr(VI) onto the surface of ICS (ICS dose = 5g/L).

pH	Initial Cr(VI) conc. mg/L	Final Cr(VI) conc. mg/L	Amount adsorbed mg/L	Amount adsorbed (mg/g)	% Removal
2.14	20.04	5.26	14.78	2.955	73.73
3.20	20.04	5.47	14.57	2.914	72.71
4.70	20.04	5.72	14.32	2.865	71.47
5.40	20.04	6.09	13.94	2.789	69.58
6.15	20.04	1.49	18.55	3.709	92.54
6.45	20.04	3.28	16.76	3.351	83.62
6.82	20.04	3.67	16.37	3.274	81.69
7.02	20.04	4.01	16.03	3.205	79.97
9.49	20.04	4.21	15.83	3.166	78.98

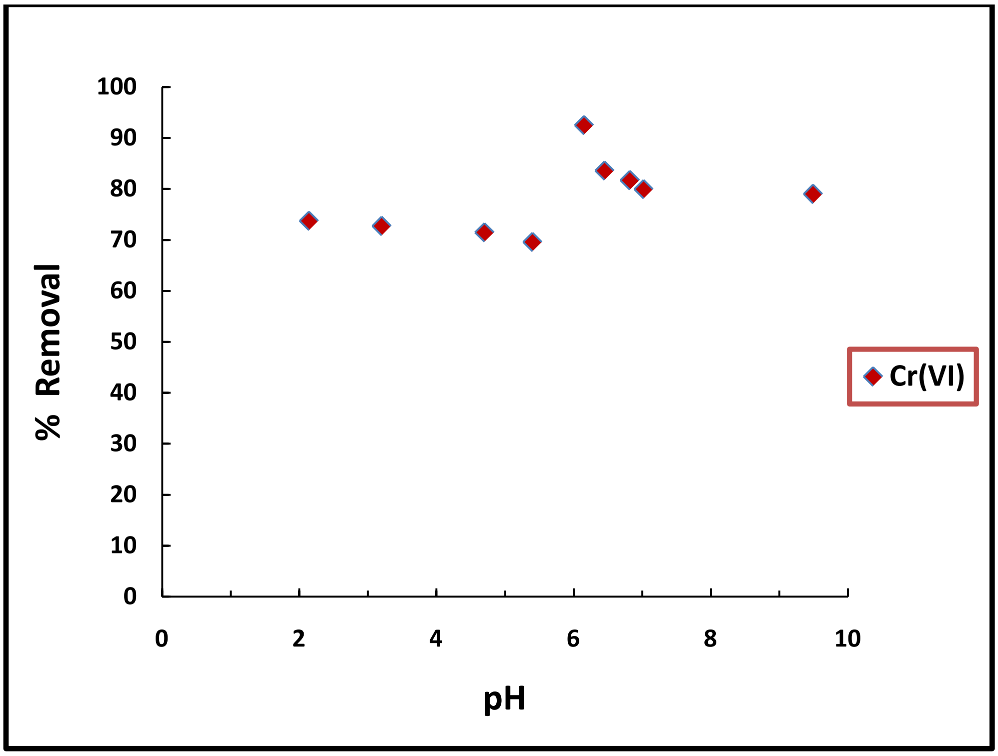

Figure 18: Effect of pH on the sorption of Cr(VI) onto the surface of ICS (Initial concentration of Cr(VI): 20.04mg/L).

electrostatic repulsive force (Hsu *et al.*, 2008). Thus a decrease in removal of As(III) was observed at higher pH values. Similarly the competition between the OH^- and the As(III) ions towards the solid surface has been cited in the case of organo modified sericite material (Li *et al.,* 2000). Besides, the uptake of AsO_3^{3-} species by iron coated sand was reported to be due to the vander Waals attraction (Vaishya and Gupta, 2002).

3.4.1.3. Arsenic(V)

The pH dependence studies in the uptake of As(V) by MCS and ICS had been carried out at 25^0C with the sorptive concentrations 2.05 mg/L. The results obtained were listed in Tables 19 and 20 respectively for MCS and ICS. Figures 21 and 22 correspond to the graphical representation of them respectively. The results obtained had revealed that as the pH increases, there is a decrease in uptake of these ions from 80.00% to 33.66% for MCS and 71.63 % to 50.00 % for ICS sorbents. Simultaneously, a decrease in the amount adsorbed by these adsorbents had been observed from 0.328 to 0.138 mg/g in the case of MCS and 0.298 to 0.208 mg/g for ICS. It could be explicable from the speciation studies of the metal ions with respect to the change in pH of the solution which showed that at all pH range, As(V) exists as negative complex ions (Gupta and Chen, 1978). Thus the surface charge of MCS and ICS possessing positive charge below pH_{PZC} favours the uptake of As(V) ions at lower pH and the negative charge surface beyond the pH_{PZC} held up the removal of these ions due to electrostatic repulsive force. Thus a distinct decrease in removal percent has been observed at higher pH. However, similar studies on organo-sericite reveals that with the increase of pH, the speciation studies (Chang *et al.*, 2009) showed that in the intermediate region of pH i.e., pH 5.0-6.5 both these anion species i.e., $H_2AsO_4^-$ and $HAsO_4^{2-}$contribute to total arsenic species, which greatly facilitated in the attraction by the solid surface followed by the ‘ion-exchange' or even the inner sphere complexation of the arsenic species with the silicate or aluminate hydroxyl group lying at the apices of the interlayer space. The probable mechanism was proposed as specific arsenic sorption and OH^- release from the surface. However, beyond pH 6.5 there was strong competition between the OH^- ions and the anion As(V) species which greatly rendered in decrease of As(V) sorption by the surface (Li *et al.,* 2000).

Table 17: Effect of pH on the sorption of As(III) onto the surface of MCS (MCS dose = 5g/L).

pH	Initial As(III) conc.(mg/L)	Final As(III) conc.(mg/L)	Amount adsorbed (mg/L)	Amount adsorbed (mg/g)	% Removal
1.96	2.08	0.64	1.44	0.288	69.23
3.10	2.08	0.7	1.38	0.276	66.35
4.69	2.08	0.68	1.40	0.280	67.31
5.90	2.08	0.93	1.15	0.230	55.29
6.22	2.08	0.98	1.10	0.220	52.88
6.55	2.08	1.03	1.05	0.210	50.48
6.63	2.08	1.05	1.03	0.206	49.52
7.01	2.08	1.13	0.95	0.190	45.67
9.34	2.08	1.31	0.77	0.154	37.02

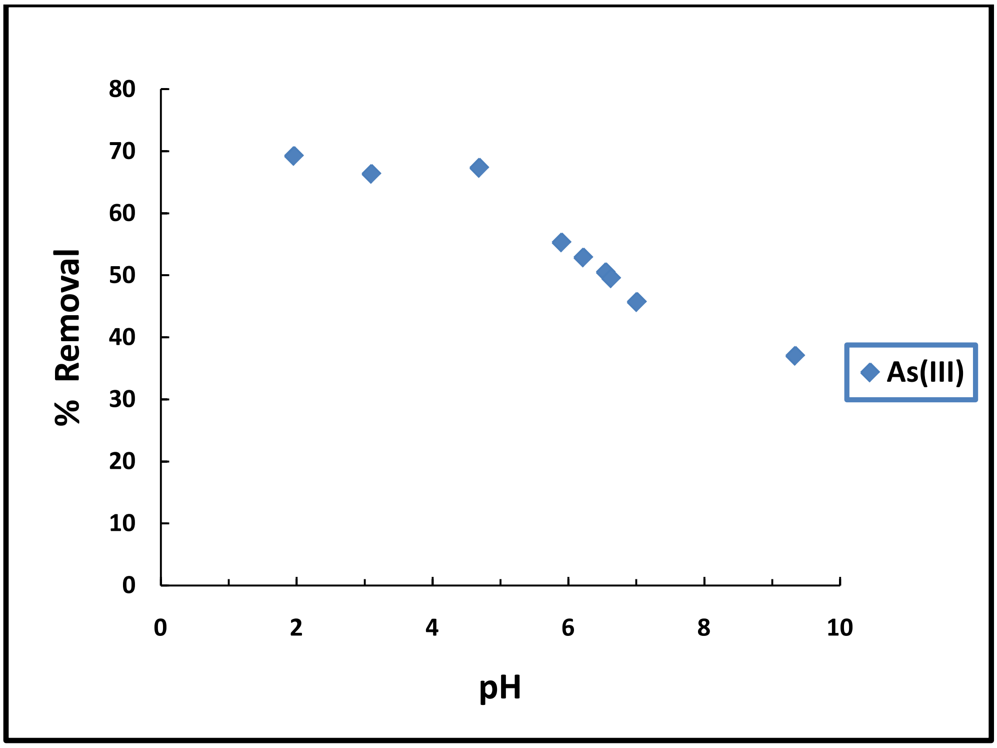

Figure 19: Effect of pH on the sorption of As(III) onto the surface of MCS (Initial concentration of As(III): 2.08 mg/L).

Table 18: Effect of pH on the sorption of As(III) onto the surface of ICS (ICS dose = 5g/L).

pH	Initial As(III) conc.(mg/L)	Final As(III) conc.(mg/L)	Amount adsorbed (mg/L)	Amount adsorbed (mg/g)	% Removal
1.61	2.09	0.74	1.35	0.270	64.59
2.65	2.09	0.77	1.32	0.264	63.16
3.52	2.09	0.59	1.50	0.300	71.77
4.06	2.09	0.55	1.54	0.308	73.68
4.75	2.09	0.79	1.30	0.260	62.20
4.82	2.09	0.77	1.32	0.264	63.16
5.89	2.09	0.90	1.19	0.238	56.94
5.97	2.09	1.09	1.00	0.200	47.85
7.37	2.09	1.23	0.86	0.172	41.15

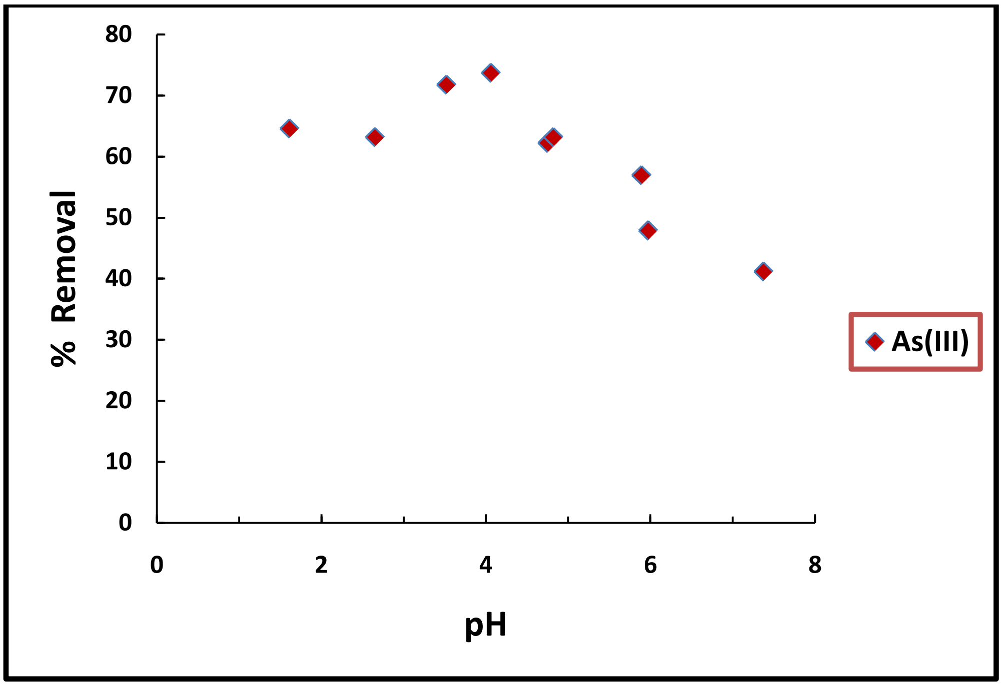

Figure 20: Effect of pH on the sorption of As(III) onto the surface of ICS (Initial concentration of As(III): 2.09 mg/L).

Table 19: Effect of pH on the sorption of As(V) onto the surface of MCS (MCS dose = 5g/L).

pH	**Initial As(V) conc.(mg/L)**	**Final As(V) conc.(mg/L)**	**Amount adsorbed (mg/L)**	**Amount adsorbed (mg/g)**	**% Removal**
2.08	2.05	0.41	1.64	0.328	80.00
3.14	2.05	0.53	1.52	0.304	74.15
4.70	2.05	0.54	1.51	0.302	73.66
6.11	2.05	0.61	1.44	0.288	70.24
6.26	2.05	0.91	1.14	0.228	55.61
6.67	2.05	1.11	0.94	0.188	45.85
7.13	2.05	1.26	0.79	0.158	38.54
7.16	2.05	1.48	0.57	0.114	27.80
9.39	2.05	1.36	0.69	0.138	33.66

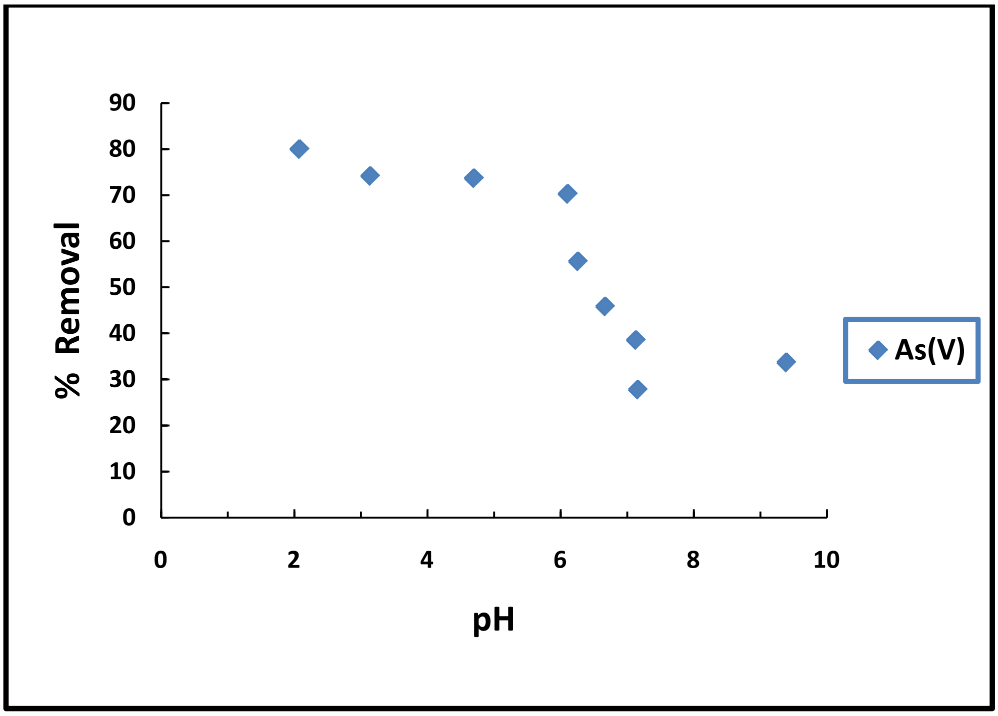

Figure 21: Effect of pH on the sorption of As(V) onto the surface of MCS (Initial concentration of As(V): 2.05 mg/L).

Table 20: Effect of pH on the sorption of As(V) onto the surface of ICS (ICS dose = 5g/L).

pH	Initial As(III) conc.(mg/L)	Final As(III) conc.(mg/L)	Amount adsorbed (mg/L)	Amount adsorbed (mg/g)	% Removal
1.86	2.08	0.59	1.49	0.298	71.63
2.61	2.08	0.51	1.57	0.314	75.48
3.74	2.08	0.69	1.39	0.278	66.83
4.40	2.08	0.72	1.36	0.272	65.38
5.02	2.08	0.74	1.34	0.268	64.42
5.84	2.08	0.79	1.29	0.258	62.02
6.51	2.08	0.85	1.23	0.246	59.13
6.43	2.08	0.91	1.17	0.234	56.25
7.35	2.08	1.04	1.04	0.208	50.00

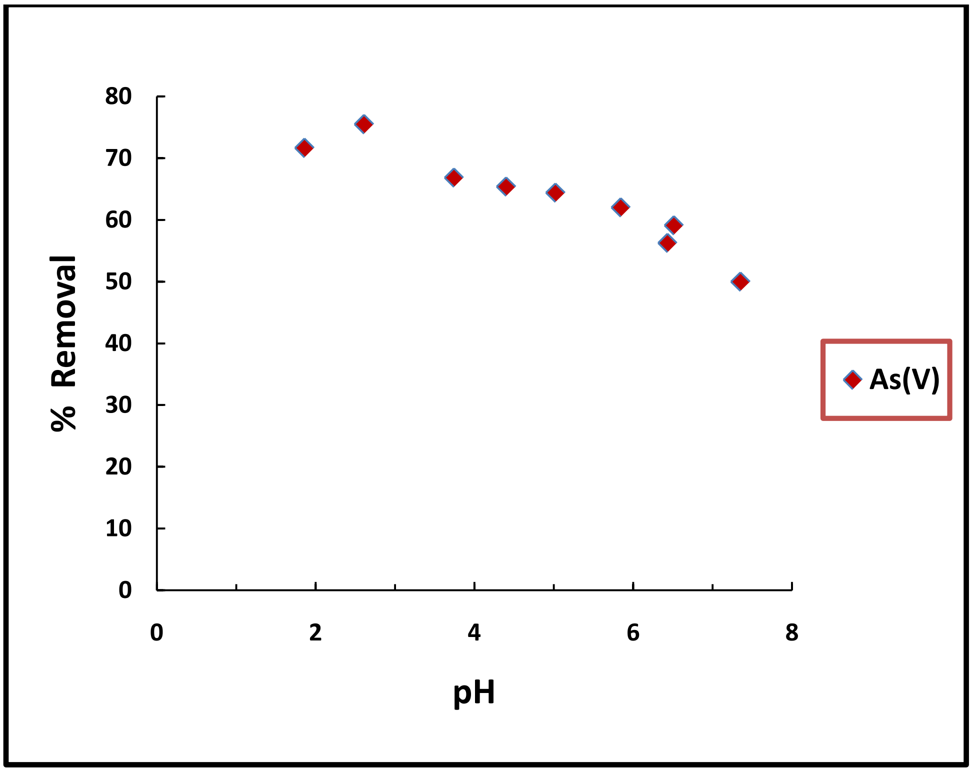

Figure 22: Effect of pH on the sorption of As(V) onto the surface of ICS (Initial concentration of As(V): 2.08 mg/L).

3.4.1.4. Cadmium(II)

The pH dependence studies for cadmium(II) with MCS were carried out with the initial sorptive concentration of 10.01mg/L and at 25°C. Table 21 and Figure 23 show the experimental results obtained which revealed that increasing the pH from 2.34 to 9.33 the removal percentage of Cd(II) was increased from 13.94 % to 99.26 %. Subsequently, the amount adsorbed by MCS has increased from 0.619 to 4.963 mg/g. The result obtained could be explicable with the help of speciation studies where cadmium mostly existed as cationic form in the pH range 2.0 to 9.0 (*cf* Figure 14) hence a sharp increase in adsorption was occurred after pH 5.5 since the surface apparently became negatively charged and the further increase in pH beyond the pH 9.0 almost 100% Cd(II) removal perhaps due to the mixed effect of adsorption and formation of insoluble species of cadmium i.e., $Cd(OH)_2$ (*cf* figure 14). Moreover, below the pH 5.5 the removal of Cd(II) was greatly hindered since the surface itself was positively charged. In general the specific surface reactions may be occurred as follows (Pretorious and Peter, 2001; Han *et al.*, 2006):

$$\equiv MnOH + Cd^{2+} \rightarrow \equiv MnO\text{-}Cd^{+} + H^{+} \quad ...\ (13)$$

$$\equiv MnO^{-} + Cd^{2+} \rightarrow \equiv MnO\text{-}Cd^{+} \quad ...\ (14)$$

$$2(\equiv MnOH) + Cd^{2+} \rightarrow (\equiv MnO^{-})_2Cd^{2+} + 2H^{+} \quad ...\ (15)$$

$$2(\equiv MnO^{-}) + Cd^{2+} \rightarrow (\equiv MnO^{-})_2Cd^{2+} \quad ...(16)$$

On the other hand, the pH dependence change in percent uptake of Cd(II) by ICS could be explained on the surface properties of ICS as well the nature of sorbing species in solutions. It was noted that the nano – particles of iron oxide mostly covered the surface of sand hence, the bulk sand properties was changed markedly in presence of impregnated iron oxide. The removal behaviour of ICS upon the Cd(II) ions was given in Table 22 and Figure 24. It was noted that the increase in pH from 2.34 – 9.33 caused for increase in

Cd(II) removal from 2.87 % to 97.28 %. Moreover, a significant increase in amount adsorbed has been observed from 0.054 to 1.842 mg/g within the observed pH range. This could be attributed to the fact that beyond the pH_{PZC}= 6.23, the surface of the ICS was negatively charged (Koulouris, 1995). At the same time, speciation studies revealed that cadmium mostly existed as cationic form in the pH range 2.0 to 9.0. Consequently, a sharp increase in adsorption was occurred beyond pH_{PZC} since the surface of ICS, in fact, became negatively charged. Further increase in pH i.e., beyond 9.0 results in the increase in removal to nearly 100% . This could be explicable from the speciation of Cd(II) that reveals that it existed as insoluble species of cadmium i.e., $Cd(OH)_2$ (*cf* figure 14), thereby beyond the pH 9.0 may be because of the mixed effect of sorption along with the co-precipitation or even coagulation of the metal ions (Hui *et al.*2005; Tiwari *et al.*, 2007(a); Lee *et al.*, 2009). Besides, below the pH 6.28 the removal of Cd(II) was greatly held up as the surface itself was positively charged. Similar metal uptake mechanism was proposed for the sorption of Cd(II) onto the goethite coated sand (Lai *et al.*, 2002), iron-oxide coated sand (Benjamin *et al.*, 1996) or metal oxide surfaces (Hayes and Leckie, 1987). Similar observations have been made such that the increase in uptake of Cd(II) below pH_{PZC} had been attributed to the chemical interaction with enough energy to overcome repulsive forces between the positively charged goethite-coated sand surface and cadmium ions. As pH increases to the range 6.0 – 7.5, where Cd^{2+}, $Cd(OH)^+$ and $Cd(OH)_2^0$ species are present in the solution, the goethite surface starts to acquire a net negative charge, creating a situation electrostatically favourable for higher adsorption of cadmium ions. Thus, at a solution $pH > pH_{PZC}$, the goethite-coated sand surface becomes negatively charged and the cadmium is present mainly as Cd^{2+}, $Cd(OH)^+$. In such cases, adsorption occurs by electrostatic attraction (Lai *et al.*, 2002).

Table 21: Effect of pH on the sorption of Cd(II) onto the surface of MCS (MCS dose = 2g/L).

pH final	Initial Cd(II) conc.(mg/L)	Final Cd(II) conc.(mg/L)	Amount adsorbed (mg/L)	Amount adsorbed (mg/g)	(%) Removal
2.34	10.01	8.76	1.24	0.619	13.94
4.53	10.01	6.74	3.26	1.630	33.79
5.78	10.01	3.60	6.40	3.200	6464
6.02	10.01	3.08	6.92	3.461	69.76
6.60	10.01	3.18	6.82	3.411	68.78
6.90	10.01	2.35	7.65	3.823	76.88
6.99	10.01	2.34	7.65	3.826	76.93
7.02	10.01	2.62	7.38	3.692	74.31
7.13	10.01	1.47	8.53	4.264	85.54
9.33	10.01	0.08	9.93	4.963	99.26

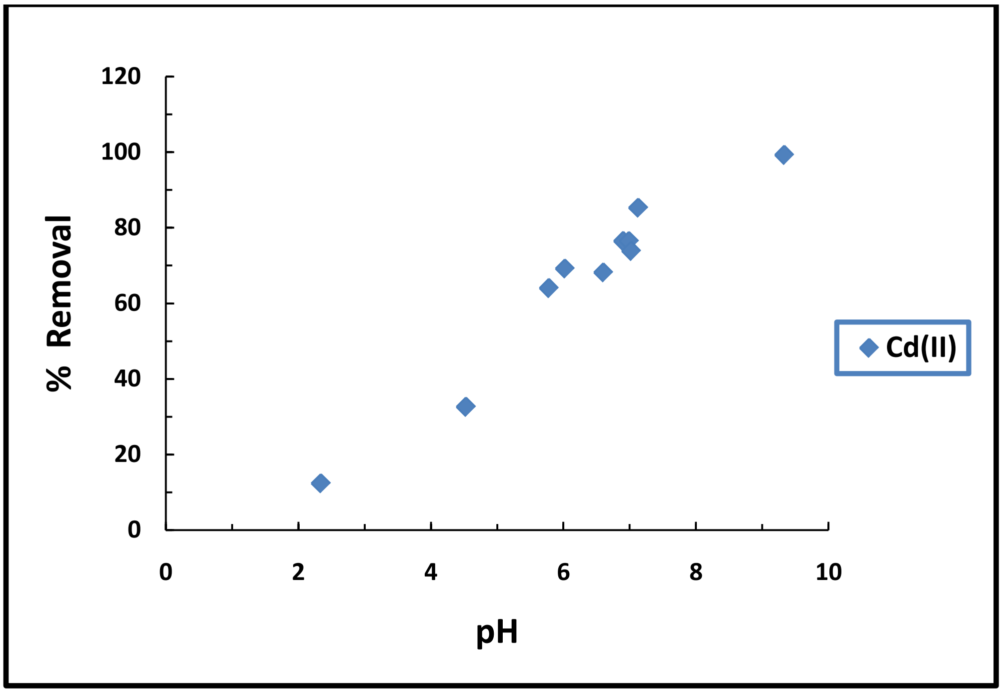

Figure 23: Effect of pH on the sorption of Cd(II) onto the surface of MCS (Initial concentration of Cd(II): 10.01mg/L).

Table 22: Effect of pH on the sorption of Cd(II) onto the surface of ICS (ICS dose = 5g/L).

pH	**Initial Cd(II) conc.(mg/L)**	**Final Cd(II) conc.(mg/L)**	**Amount adsorbed (mg/L)**	**Amount adsorbed (mg/g)**	**(%) Removal**
2.37	9.47	9.19	0.27	0.054	2.87
3.41	9.47	8.87	0.59	0.119	6.30
4.25	9.47	6.99	2.47	0.495	26.11
5.54	9.47	6.58	2.89	0.578	30.50
5.89	9.47	6.20	3.27	0.654	34.52
6.27	9.47	4.74	4.73	0.946	49.94
7.36	9.47	3.59	5.88	1.176	62.10
8.82	9.47	1.15	8.32	1.665	87.90
9.12	9.47	0.26	9.21	1.842	97.28

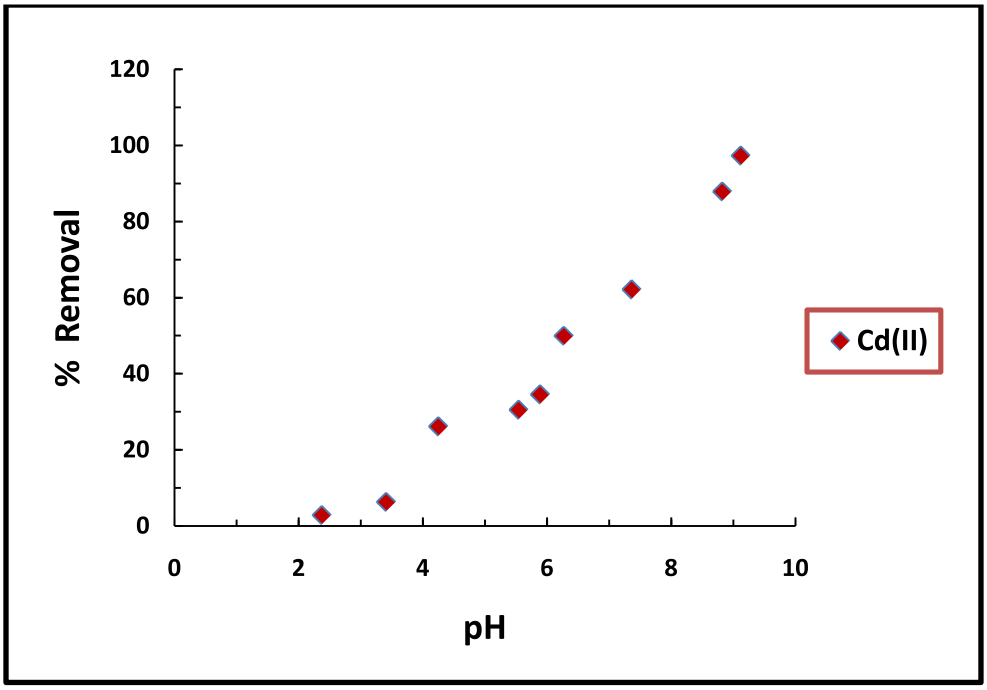

Figure 24: Effect of pH on the sorption of Cd(II) onto the surface of ICS (Initial concentration of Cd(II): 9.47 mg/L).

3.4.1.5. Copper(II)

The effect of pH on the sorption of Cu(II)was conducted with 10.14 mg/L sorptive solution at constant temperature (25^{0}C) with both MCS and ICS sorbent. The results obtained in terms of percent adsorption were shown in Tables 23 and 24 along with the graphical representation in Figures 25 and 26 for MCS and ICS samples respectively. These results indicated that a sharp initial increase of removal attained a maximum of almost 100%removal beyond pH 6.38 for MCS sample. More quantitatively, increasing the pH from 3.30to 6.87 the respective increase in Cu(II) removal was occurred from 10.25% to almost 100%. At the same time an increase in the amount adsorbed by MCS has been observed from 0.216 to 1.980 mg/g with the same pH range. Similarly, for ICS s ample, a sharp increase was occurred from 1.87 % to 61.24% with the increase in pH from 1.76 to 6.15, beyond which the removal percent was reached almost to 100% at the pH 8.18. Again, the amount adsorbed by the ICS within this pH range had increased from 0.038 to 1.992 mg/g.

The increase of percent removal using MCS and ICS mainly depends largely upon the mixed effect of sorbing species and the surface properties of solids**.** The earlier observation showed that the manganese coated sand which has pH$_{PZC}$ value of 6.28 against the manganese dioxide reported pH$_{PZC}$ value of 5.5 (Koulouris, 1995). Hence, it was expected that the manganese fine particles are aggregated as manganese dioxide on the surface of sand. Similarly, in iron coated sand, the surface of sand was likely to be aggregated with ferric oxide. Hence, the surface properties of MCS and ICS were mostly dependent to the manganese dioxide and ferric oxide, respectively.

The surface of MCS become negatively charged beyond the pH 6.28 and below this it could possess the positive charge. Below pH 6.28, the dominant species of Cu(II) was the cationic species *viz*., Cu^{2+} etc. Hence, increasing the pH above 6.28, surface of MCS favoured greatly the positively charged cations, however, the pH below 6.28 hindered significantly uptake of positively charged cations. Hence, based on these facts, it was assumed that relatively low uptake was occurred at very low pH values i.e., around pH 3.0 (Lee *et al.*, 2010a). Moreover, relatively very high uptake of Cu(II) occurred even at lower region of pH i.e., in between 3.0 to 6.0 may be explained with the possible specific chemisorption of these cations to the manganese coated surfaces Equations (17-21) (Han *et al.*, 2006, Lee *et al.*, 2004, Aksu, 2002, Lee *et al.*, 2010b):

$$\equiv MnOH + M^{2+} \rightarrow \equiv Mn\text{-}O\text{-}M^{+} + H^{+} \quad \ldots (17)$$

$$\equiv Mn\text{-}O^{-} + M^{2+} \rightarrow \equiv Mn\text{-}O\text{-}M^{+} \quad \ldots (18)$$

$$2(\equiv Mn\text{-}OH) + M^{2+} \rightarrow (\equiv Mn\text{-}O^{-})_2M^{2+} + 2H^{+} \quad \ldots (19)$$

$$2(\equiv Mn\text{-}O^{-}) + M^{2+} \rightarrow (\equiv Mn\text{-}O^{-})_2M^{2+} \quad \ldots (20)$$

$$\equiv Mn\text{-}OH + M^{2+} + H_2O \rightarrow \equiv Mn\text{-}O\text{-}M\text{-}OH + 2H^{+} \quad \ldots (21)$$

where M denoted to Cu. Hence, the reactions (17,19 and 21) were supposed to be predominant below the pH 6.28. The chemisorption of these cations were further investigated using the background electrolytes i.e., the effect of ionic strength using the $NaNO_3$ solutions. Moreover, further increase in pH i.e., beyond pH 6.28, Cu(II) ion exist as insoluble derivative compound of tenorite. Therefore, there might be a mixed effect of adsorption and co-precipitation of metal ions on the surface of solids. Hence, apparently, it caused for very high uptake of metal ions in this pH region(Hui *et al.*, 2005; Tiwari *et al.*, 2007(a); Lee *et al.*, 2009). Han *et al.*, (2006) made similar observations that the increase in adsorption with the decrease in H^+ ion concentration (high pH) indicated that ion exchange was one of the major adsorption process. Above pH 6.0, insoluble copper or lead hydroxide started precipitating from the solution, making true sorption studies impossible. Therefore, at these pH values, both adsorption and precipitation were the effective mechanisms involved in the removal of Cu(II) and Pb(II) from aqueous solution. At higher pH values, Cu(II) and Pb(II) tend to form different hydrolysis products.

On the other hand, the pH_{PZC} for ICS was obtained as 6.23. Hence, the surface of ICS was positively charged below this pH value and became negatively charged beyond pH 6.23. At extreme low pH region i.e., pH between 2.0 to 4.0 both solid surface of ICS and sorbing species were possessed with enhanced positive charge which ultimately caused for strong electrostatic repulsion. Therefore, apparently it caused a significantly low uptake of the metal cations. However, on further increase in pH beyond 4.0 there could be partial acidic dissociation of solid ICS surface causing some electrostatic attraction of the metal cations resulted in a gradual increase in metal uptake. However, the only electrostatic attraction could not be attributed to explain the sorption of these cations since the surface carries net negatively charged beyond pH 6.23 (pH_{PZC} of ICS). Hence, in addition to partial electrostatic attraction, the surface complexation of these metal cations through ion-exchange process could also be postulated for enhanced uptake within the pH region 4.0 to 6.0 as suggested with equations (22 & 23):

$$M^{2+} + \equiv SH_2^{+} \leftrightarrow \equiv S\text{-}OM^{+} + 2H^{+} \qquad \ldots(22)$$

$$M(OH)^{+} + \equiv SH_2^{+} \leftrightarrow \equiv S\text{-}OM(OH)^{0} + 2H^{+} \qquad \ldots(23)$$

The retention of copper by ICS was attributed to the chemisorption of the Cu(II) on to the solid surface. The chemisorption process resulted by the inner-sphere bonding of the Cu to the surface-OH group available with ferric oxides. Benjamin and Leckie (1981) postulated the Cu adsorption onto iron oxide surfaces to be a combination of ion exchange and inner-sphere complexation with edge –OH groups. The studies have been made by other workers where similar observations were reported (Lai *et al.*, 2001) and reported that Cu(II) ions can

Table 23: Effect of pH on the sorption of Cu(II) onto the surface of MCS (MCS dose = 5g/L).

pH	**Initial Cu(II) conc.(mg/L)**	**Final Cu(II) conc. (mg/L)**	**Amount absorbed (mg/L)**	**Amount absorbed (mg/g)**	**% Removal**
1.99	10.01	8.92	1.09	0.218	10.88
3.30	10.01	8.97	1.04	0.207	10.34
4.06	10.01	6.17	3.84	0.768	38.36
4.89	10.01	3.30	6.71	1.342	67.03
5.03	10.01	2.12	7.89	1.577	78.79
5.05	10.01	1.00	9.01	1.802	89.99
6.17	10.01	0.33	9.68	1.936	96.71
6.38	10.01	0.23	9.78	1.955	97.66
6.41	10.01	0.13	9.88	1.976	98.72
6.87	10.01	0.09	9.91	1.982	99.02
8.00	10.01	***BDL***	-	-	-
9.00	10.01	***BDL***	-	-	-

Note: BDL = below detection limit

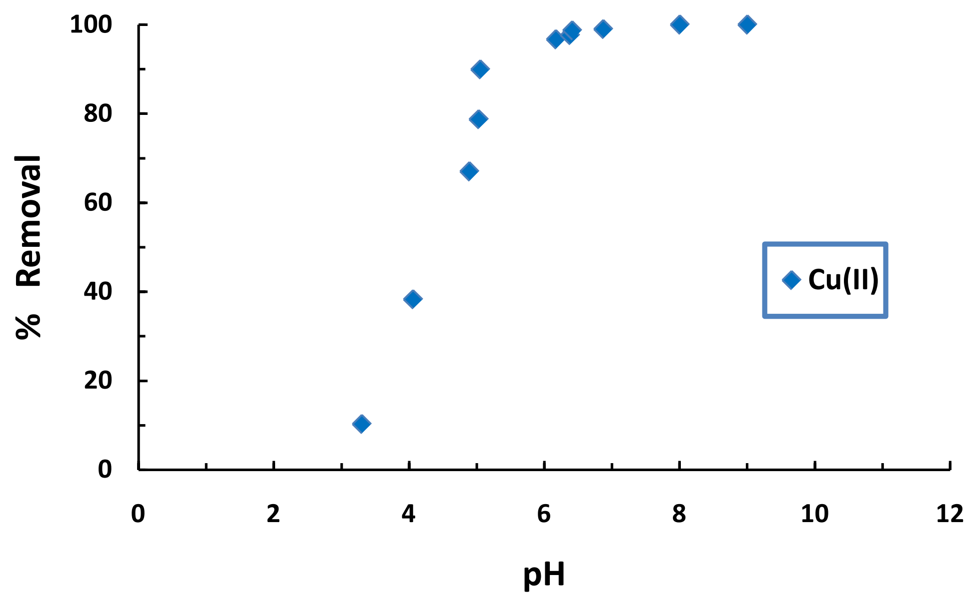

Figure 25: Effect of pH on the sorption of Cu(II) onto the surface of MCS (Initial concentration of Cu(II): 10.01 mg/L).

Table 24: Effect of pH on the sorption of Cu(II) onto the surface of ICS (ICS dose = 5g/L).

pH	Initial Cu(II) conc.(mg/L)	Final Cu(II) conc.(mg/L)	Amount adsorbed (mg/L)	Amount adsorbed (mg/g)	% Removal
1.76	10.14	9.95	0.19	0.038	1.87
2.74	10.14	9.73	0.41	0.082	4.04
3.53	10.14	9.12	1.02	0.204	10.06
4.48	10.14	7.34	2.80	0.560	27.61
6.15	10.14	3.93	6.21	1.242	61.24
6.44	10.14	1.86	8.28	1.656	81.65
6.62	10.14	0.87	9.27	1.854	91.42
7.09	10.14	0.61	9.53	1.906	93.98
8.18	10.14	0.18	9.96	1.992	98.26

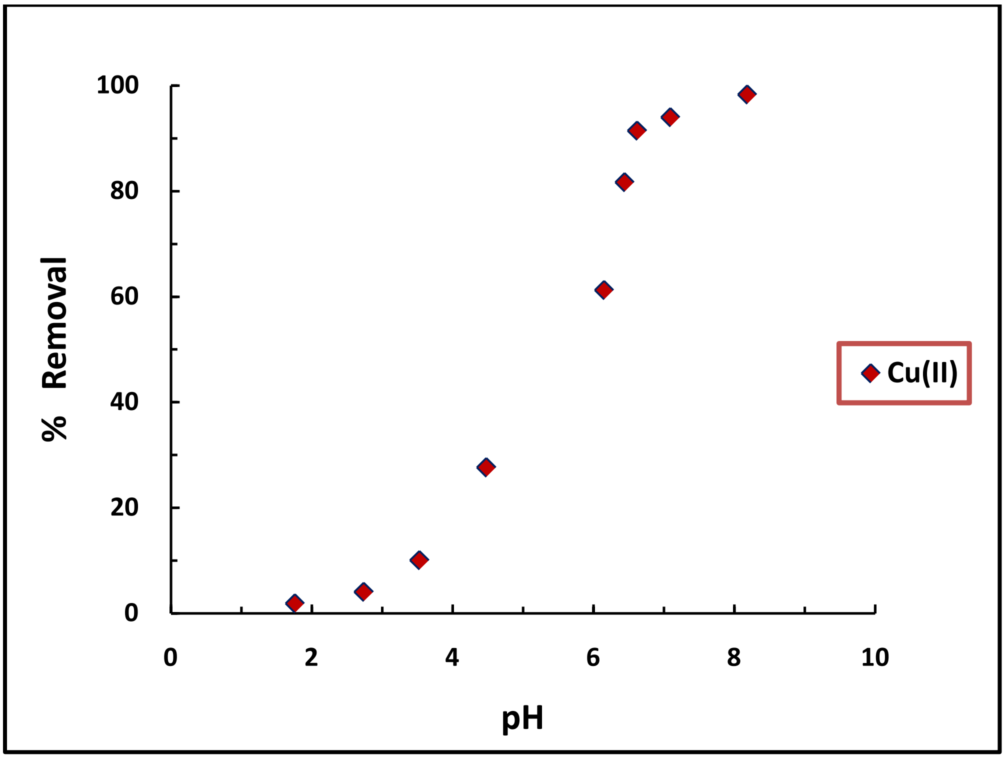

Figure 26: Effect of pH on the sorption of Cu(II) onto the surface of ICS (Initial concentration of Cu(II): 10.14 mg/L).

firmly adsorb to the interface of water/ICS. The interface of water/ICS can provide sufficient adsorption sites for metal ions and the adsorption of copper increases with increasing solution pH or high surface loading of iron (Lai *et al.*, 2000).

3.4.1.6. Lead(II)

The removal behaviour of Pb(II) as a function of pH by MCS and ICS was presented in Tables 25 and 26 and graphically represented in Figures 27 and 28, respectively for MCS and ICS. It was noted that quantitatively, increasing the pH from 2.39 to 6.48 the uptake of Pb(II) ions increased from 55.39 % to 99 % by MCS and the amount adsorbed by the adsorbent has been obtained as 2.217 to 3.963 mg/g. On the other hand increasing the pH from 2.09 to 5.84 the Pb(II) was removed from 2.05 % to 62.82% by ICS and beyond this pH i.e., 6.0 it was increased to *Ca*.95 % at pH 10. At the same time an increase in amount adsorbed by ICS has been found to be 0.042 to 1.940 mg/g. The increase of percent removal using MCS and ICS mainly depended upon the mixed effect of sorbing species and the surface properties of solids.

The earlier observation showed that the manganese coated natural sand has pH_{PZC} value of 6.28 against the manganese dioxide reported pH_{PZC} value of 5.5 (Koulouris, 1995). Hence, it was expected that the manganese fine particles are aggregated as manganese dioxide on the surface of sand. Hence, the surface properties of MCS were dependent on the manganese dioxide. The surface of MCS becomes negatively charged beyond the pH 6.2 and below this it could possess the positive charge (*cf* Eq. (12).

On the other hand, below pH 6.2, the dominant species of Pb (II) were the cationic species viz., Pb^{2+} or insignificant $Pb(OH)^{+}$ etc. Hence, increasing the pH above 6.2, surface of MCS favoured to attract the positively charged cations. However, the pH below 6.2 hindered the attraction of positively charged cations. Hence, based on these observations, it was assumed that relatively low uptake occurred at the lower pH values (Lee *et al.,* 2010 b). Additionally, relatively very high uptake of Pb(II) occurred even at lower pH values may be explained with the possible specific chemisorption of these cations to the manganese-modified surfaces Eqs. (17–21) (Han *et al.*, 2006; Lee *et al.*, 2010 b; Aksu, 2002; Lee *et al.*, 2004). Hence, the equations (17, 19 and 21) were supposed to be predominant below pH 6.2. Moreover, the significant decrease in pH after adsorption as observed for these ions particularly for the Pb(II) (Table 25) indicated the occurrence of equations (17, 19 and 21). The chemisorption of these cations were further investigated using the background electrolytes i.e., the effect of ionic strength using the $NaNO_3$ solutions.

Moreover, further increase in pH i.e., beyond pH 6.2, there might be a mixed effect of adsorption and co-precipitation of metal ions on the surface of solids. Hence, apparently, it caused for very high uptake of metal ions in this pH region.

The pH dependence data obtained for these metals ions using ICS was explained by the surface properties of ICS as well the nature of sorbing species present in solution. The nano-particles of iron oxide mostly covered the surface of sand hence, the bulk sand properties was changed markedly in presence of impregnated iron oxide. Moreover, the pH_{PZC} of ICS sample was found to be 6.23 which, was very close to the reported pH_{PZC} of ferric hydroxide 6.28 (Koulouris, 1995). The other studies indicated the pH_{PZC} of reclaimed IOCS was found to be 7.0 ± 0.4 (Hsu *et al.*, 2008)and 6.5–8.5 (Cornell and Schwertmann, 1996) Similarly, Stenkamp and Benjamin (1994),found the pH_{PZC} close to 7.5 for iron oxide-coated sand. Hence, our values of pH_{PZC} for ICS were slightly different from the previously reported values. The surface of ICS was carried with positive charge below pH 6.23 and became negatively charged beyond this (*cf* equation 12).

On the other hand up to the pH 5.8 both Pb(II) dominantly existed as positively charged species of Pb^{2+} (MINEQL studies). At extreme low pH region i.e., pH between 2 and 4 both solid surface of ICS and sorbing species were possessed with enhanced positive charge which ultimately caused for strong electrostatic repulsion. Therefore, seemingly it caused for significantly low uptake of these metal cations. However, the further increase in pH i.e., beyond 4.0 the partial acidic dissociation of solid ICS surface may perhaps cause for some electrostatic attraction of these metal cations which showed a gradual increase in metal uptake. The similar results were occurred for different metal cations uptake by the manganese coated sand (Tiwari *et al.,* 2007b; Lee *et al.,* 2009; Lee *et al.*, 2010b). However, the only electrostatic attraction could not be explain the sorption of these metal cations since surface carries a net negative charge beyond pH 6.23 (pH_{PZC} of ICS) hence, in addition to partial electrostatic attraction, the surface complexation through ion-exchange process was also postulated for enhanced uptake of the metal cations Pb(II)) within the pH region 4.0 –6.0 (Lai *et al* ., 2002; Benjamin *et al.*, 1996) and this was suggested with Eqs. (22) and (23). Similar ion exchange mechanism was suggested for the uptake of cadmium by goethite coated sand (Lai *et al.*, 2002), iron-oxide coated sand (Benjamin *et al.*, 1996) or even metal oxide surfaces (Hayes and Leckie, 1987). Further, increase in pH, i.e., beyond pH 6.0, there could be a mixed effect of sorption with co-precipitation or even coagulation of the metal cations (Lee *et al.*, 2009; Hui *et al.*, 2005; Tiwari *et al.*, 2007a) which caused for almost 100% removal of these studied metal cations. These results were in conformity to the speciation studies conducted for these cations previously (*cf* Figure 16).

Table 25: Effect of pH on the sorption of Pb(II) onto the surface of MCS (MCS dose = 5g/L).

pH	Initial Pb(II) conc.(mg/L)	Final Pb(II) conc.(mg/L)	Amount absorbed (mg/L)	Amount absorbed (mg/g)	% Removal
2.39	20.02	8.93	11.08	2.217	55.39
3.01	20.02	8.98	11.03	2.207	55.12
4.12	20.02	2.62	17.39	3.479	86.90
4.85	20.02	0.34	19.67	3.935	98.30
5.03	20.02	0.32	19.69	3.939	98.40
5.14	20.02	0.13	19.88	3.977	99.35
5.37	20.02	0.19	19.82	3.965	99.05
5.35	20.02	0.21	19.81	3.961	98.95
5.76	20.02	0.19	19.82	3.965	99.05
6.48	20.02	0.20	19.82	3.963	99.00

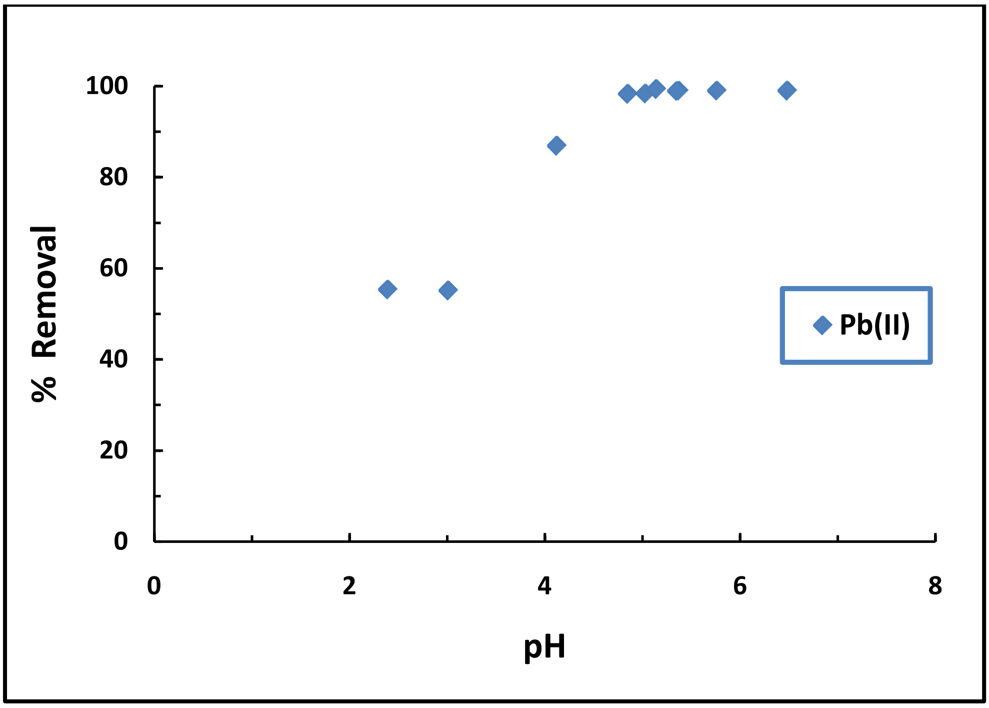

Figure 27: Effect of pH on the sorption of Pb(II) onto the surface of MCS (Initial concentration of Pb(II): 20.02 mg/L).

Table 26: Effect of pH on the sorption of Pb(II) onto the surface of ICS (ICS dose = 5g/L).

pH	Initial Pb(II) conc.(mg/L)	Final Pb(II) conc.(mg/L)	Amount absorbed (mg/L)	Amount absorbed (mg/g)	% Removal
2.09	10.22	10.01	0.21	0.042	2.05
2.99	10.22	9.01	1.21	0.242	11.84
4.03	10.22	6.62	3.60	0.720	35.23
4.65	10.22	4.83	5.39	1.078	52.74
5.84	10.22	3.80	6.42	1.284	62.82
6.43	10.22	1.16	9.06	1.812	88.65
6.62	10.22	1.17	9.05	1.810	88.55
6.97	10.22	1.22	9.00	1.800	88.06
7.62	10.22	0.52	9.70	1.940	94.91

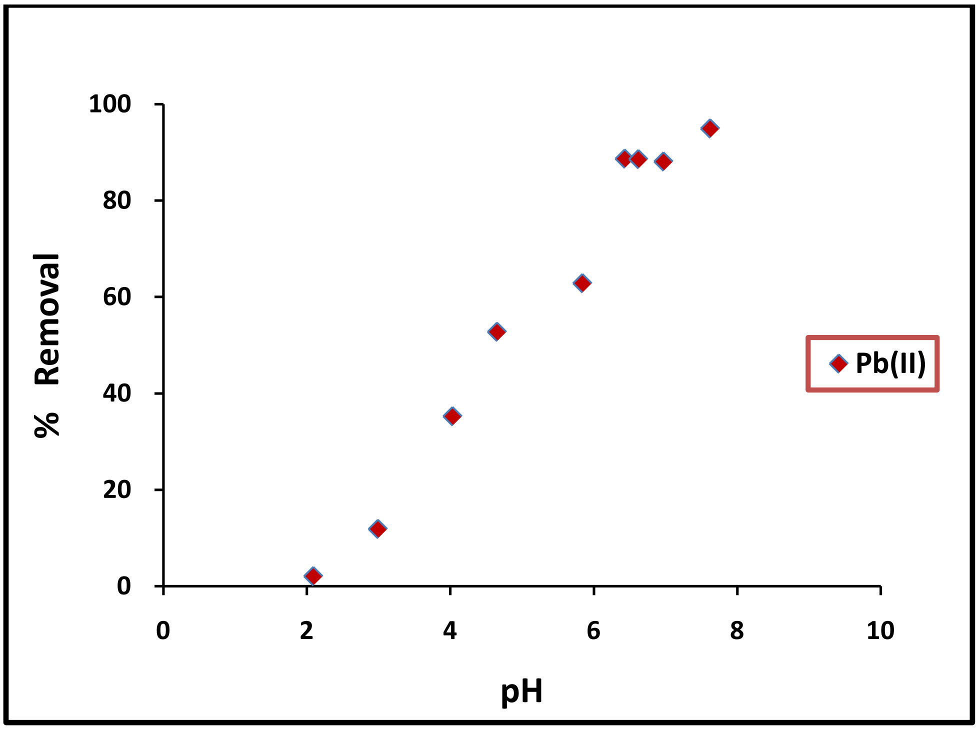

Figure 28: Effect of pH on the sorption of Pb(II) onto the surface of ICS (Initial concentration of Pb(II): 10.22 mg/L)

3.4.1.7. Summary

The experimental results revealed that the removal of Cr(VI), As(III) and As(V) were greatly hindered at higher pH values however, it greatly favoured at low pH values. However, the very high uptake of Cr(VI) by ICS was almost unaffected with the change of pH. Perhaps an electrostatic attraction is likely to be the main mechanistic pathway demonstrated in the removal process since at low pH values i.e., below pH 6.28 for MCS and 6.23 for ICS, both they carry net positive charge which may cause for electrostatic attraction of these anions. However, the uptake of Cr(V) onto the surface of ICS was assumed to be associated with some chemisorption via ion-exchange process since very strong affinity was observed between adsorbate and solid surface. On the other hand, the cations *viz.*, Cd(II), Cu(II) and Pb(II) were showed very high uptake at higher pH values whereas it was very low uptake at low pH values i.e., around pH 3 – 4 which was gradually increased increasing the pH of the solution. Therefore, it was assumed that in addition to the electrostatic attraction apparently a chemisorptive uptake could take place via ion-exchange process or a complexation reaction could place between these cations and solid surfaces. Hence, an inner sphere bonding of metal cations could possibly take place with surface -OH group available with the MCS or ICS. Further, at very high pH values i.e., around 8 – 10 , very high uptake of these cations occurred which is because of the simultaneous process of adsorption and co-precipitation of metal ions on to the surface of solids. Therefore, very high uptake of metal ions in this pH region was observed.

3.4.2. Effect of Sorptive Concentrations

It was reported that the initial concentration of a metal ion provided an important driving force to overcome all mass transfer resistances of the metal ions between aqueous and solid phase (Malkoc, 2006). Several studies on the dependence of cation adsorption to the sorptive concentration were carried out to understand the different molecular interactions between the adsorbed species and the adsorbent surface. Mahoney and Langmuir (1991) deduced that an increase in the outer layer surface charge cause a decrease in the adsorption of strontium on kaolinite, illite and montmorillonite on increasing bulk ionic strength. It was also reported that the adsorption of micro amounts of mercury on manganese dioxide decreased with the increase in the electrolyte concentrations (Hassany and Chaudhary, 1985; Tamura *et al.*, 1986).

The distribution coefficient (K_D) for adsorption of cadmium and mercury ions on lateritic soil was increased greatly with a decrease in the initial concentration of the metal ion and followed the Freundlich adsorption isotherm (Del Debbio, 1991). The distribution coefficient for the adsorption of cesium on manganese dioxide was increased with the decrease in cesium concentration (Hassany and Chaudhary, 1984). Mikhail and Misak (1988) reported that the distribution coefficients for adsorption of cesium and cobalt on manganese dioxide remain same upto the sorptive concentration of *Ca.*5 x 10^{-5}M for cesium and *Ca*. 5 x 10^{-6} mol/L for cobalt. However, further increase in the sorptive concentration decreased the K_D values for these cations. The deviation from Freundlich isotherm at higher concentrations (> 10^{-2}mol/L) occurred owing to the approach of saturation on manganese oxide surface by the adsorbate species. Increasing the initial sorptive concentration in case of manganese, arsenic, mercury, chromium, cadmium, copper and lead enhanced the amount adsorbed by the solid surface of adsorbent (Lee *et al.*, 2010(a); Kim and Chung, 2002; Tiwari *et al.*, 1999; Lee *et al.*, 2010(b), Tiwari *et al.*, 2011). However, the percent removal of these ions with respect to the MCS and ICS was normally decreased as the sorptive concentration was increased. On the other hand the increase in percent adsorption with decreasing the sorptive concentration was perhaps explicable on the basis that at higher dilution relatively smaller number of adsorptive species was available for deposition on the equal number of adsorptive surface sites (Mishra *et al.*, 1996). Keeping in view the study was extended by varying the sorptive concentration for constant solid dose and the sorption of these metal cations/anions onto the surface of MCS and ICS was obtained and discussed. These studies were also enabled to learn the concentration barrier effect in the sorption process.

3.4.2.1. Chromium(VI)

The effect of sorptive concentration on the removal behaviour of MCS for Chromium Cr(VI) was obtained varying the sorptive concentration from 5.00 to 100.00 mg/L at pH 3.0 and at 25^{o}C temperature with the constant solid dose of MCS i.e., 5g/L. The results obtained were shown in Table 27 and Figure 29. It is clearly indicated that increasing the concentration from 5.00 to 100.00 mg/L of Cr(VI) caused for an increase in percent removal of Cr(VI) from 38.20% to 69.50 %. The amount adsorbed by MCS with the increase in sorptive concentrations also increase from 0.382 to 13.900 mg/g. The result was explained such that at pH 3.0, the surface of MCS carried a net positive charge. The speciation studies of Cr(VI) were revealed that at this pH, Cr(VI) mostly exists as the soluble anionic species of CrO_4^{2-}, $HCrO_4^-$ or $Cr_2O_7^{2-}$. Hence, the positively charged surface of MCS would greatly attract these anionic species of Cr(VI) and therefore the removal of these ions would likely to be increased with the increase in sorptive concentrations. Similar observations were reported by some authors (Mishra *et al.*, 2004; Tiwari *et al.*, 2007(a); Pehlivan *et al.*, 2008; Gode *et al.*, 2008).

Table 27: Effect of sorptive concentration on the sorption of Cr(VI) onto the surface of MCS. (MCS dose = 5g/L; pH= 3.0).

Initial Cr(VI) conc. (mg/L)	Final Cr(VI) conc. (mg/L)	Amount adsorbed (mg/L)	Amount adsorbed (mg/g)	% Removal
5.00	3.09	1.91	0.382	38.20
10.00	4.79	5.21	1.042	52.10
20.00	11.05	8.95	1.790	44.75
30.00	16.19	13.81	2.762	46.03
40.00	20.00	20.00	4.000	50.00
50.00	30.00	20.00	4.000	40.00
70.00	36.00	34.00	6.800	48.57
100.00	30.50	69.50	13.900	69.50

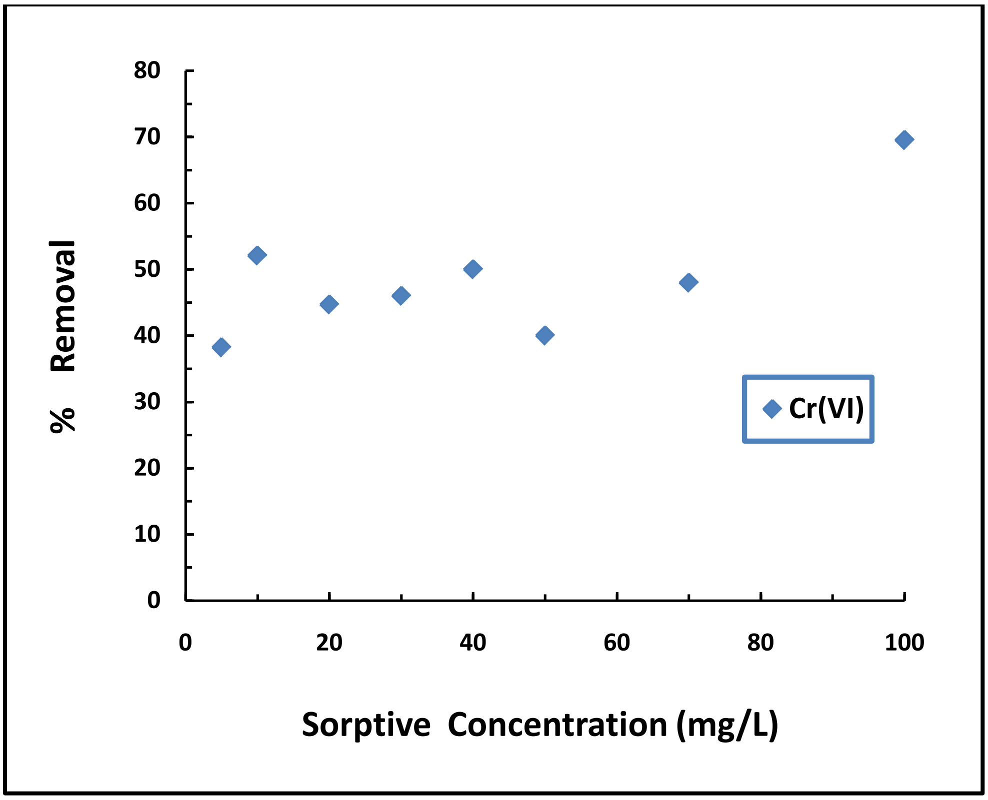

Figure 29: Effect of sorptive concentration on the sorption of Cr(VI)

onto the surface of MCS.

Table 28: Effect of sorptive concentration on the sorption of Cr(VI) onto the surface of ICS. (ICS dose = 5g/L; pH = 3.0).

Initial Cr(VI)conc. mg/L	**Final Cr(VI) conc. mg/L**	**Amount adsorbed mg/L**	**Amount adsorbed mg/g**	**% Removal**
5.00	3.27	1.74	0.347	34.70
50.00	48.27	1.74	0.347	34.70
80.00	64.88	15.12	3.025	18.90
90.00	69.89	20.10	4.021	22.34
100.00	76.22	23.78	4.755	23.77

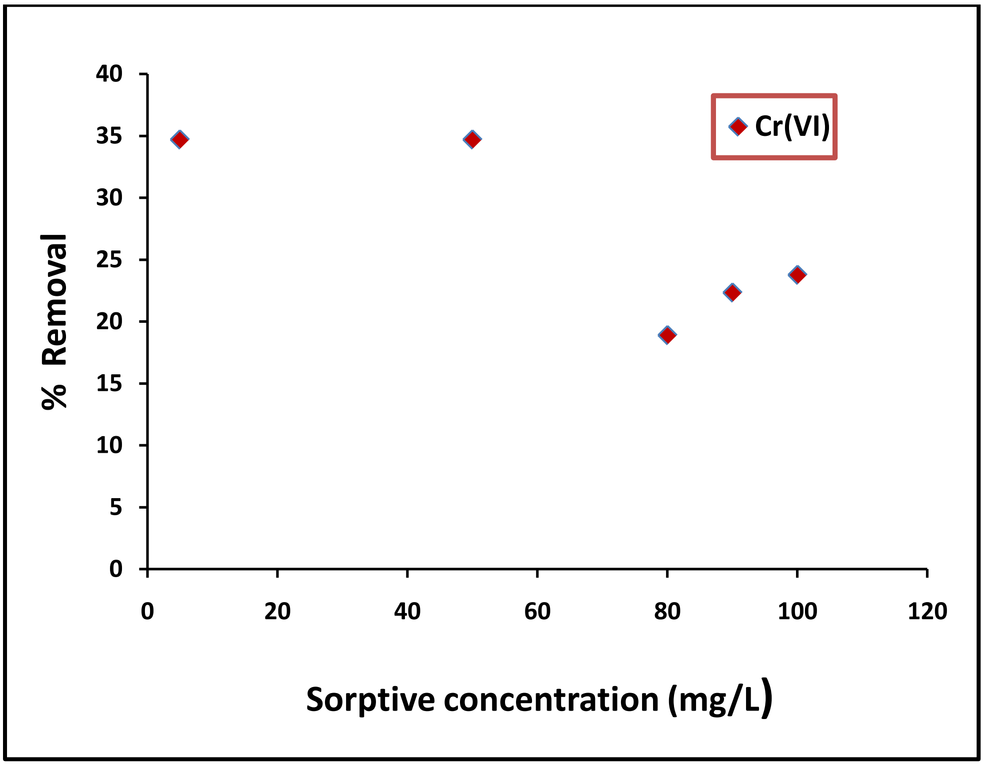

Figure 30: Effect of sorptive concentration on the sorption of Cr(VI)

onto the surface of ICS.

Similarly, the effect of sorptive concentration on the removal behaviour of ICS for Cr(VI) was obtained by varying concentrations from 5.00 to 100.00 mg/L at $25^{o}C$ and at pH 3.0 with the ICS dose of 5g/L. The results obtained were shown in Table 28 and the graphically represented in Figure 30. The results indicated an apparent decrease in percent removal from *Ca.*35 to20. In other words increasing the dilutions enhanced the percent uptake of Cr(VI) from aqueous solutions. However, a significant increase in the amount adsorbed with the increase in sorptive concentrations has been observed from 0.347 to 4.755 mg/g. The decrease in percent uptake could be explained on the basis of the fact that more and more active sites were available for a similar number of sorbing ions at higher dilutions (Hassany and Chaudhary, 1986; Ma *et al.*, 1992).

3.4.2.2. Arsenic(III)

The concentration dependence studies for Arsenic As(III) for manganese coated sand and iron coated sand were carried out at $25^{o}C$ at pH=3.0 for MCS and at pH = 6.0 for ICS. The data obtained were shown in Tables 29 and 30 respectively for MCS and ICS. Similarly, the data represented graphically in the Figures 31 and 32 respectively, for MCS and ICS. The figures clearly indicated that increasing the concentration from 1.00 to 25.00 mg/L of As(III) caused for a decrease for percent removal respectively from 62.75 %to 4.03 % for MCS. At the same time, the amount adsorbed by MCS has been observed with apparently negligible increase from 0.124 to 0.180 mg/g as compared to the extent of increase in sorptive concentration.

Similarly, an increase in sorptive concentration from 1.05 to 10.19 mg/L apparently caused for a decrease of percent removal of As(III) from 68.57 to 27.97 % by ICS with a small increase in amount adsorbed from 0.144 to 0.570 mg/g. The possible reason for the decrease in percent removal of As(III) at higher concentrations was because of the fact that

Table 29: Effect of sorptive concentration on the sorption of As(III) onto the surface of MCS. (MCS dose = 5g/L; pH = 3.0).

Initial As(III) conc. (mg/L)	Final As(III) conc. (mg/L)	Amount adsorbed (mg/L)	Amount adsorbed (mg/g)	% Removal
1.03	0.38	0.62	0.124	62.75
4.01	3.02	0.98	0.196	25.43
6.95	5.84	1.16	0.232	16.69
10.01	8.91	1.09	0.218	11.87
12.03	11.03	0.97	0.194	8.39
15.02	14.15	0.85	0.170	5.48
19.98	19.10	0.90	0.180	5.07
25.02	24.07	0.93	0.186	4.03

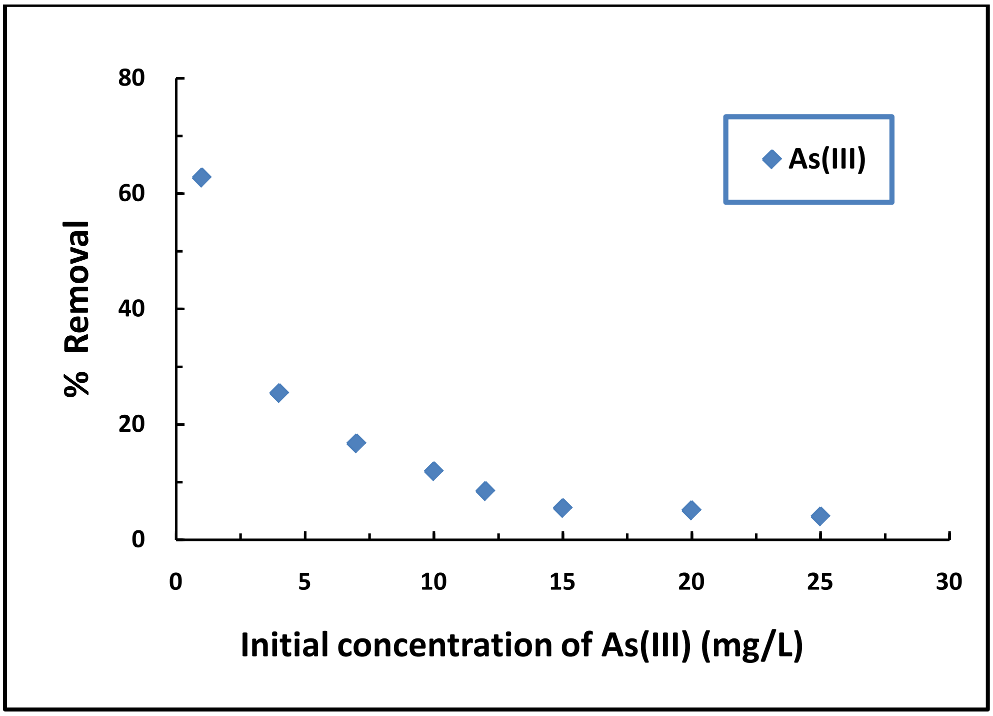

Figure 31: Effect of sorptive concentration of on the sorption of As(III) onto the surface of MCS.

Table 30: Effect of sorptive concentration on the sorption of As(III) onto the surface of ICS. (ICS dose = 5g/L; pH ~ 6.0).

Initial As(III) conc.(mg/L)	Final As(III) conc.(mg/L)	Amount adsorbed (mg/L)	Amount adsorbed (mg/g)	% Removal
1.05	0.33	0.72	0.144	68.57
2.10	1.15	0.95	0.190	45.24
5.09	3.26	1.83	0.366	35.95
10.19	7.34	2.85	0.570	27.97

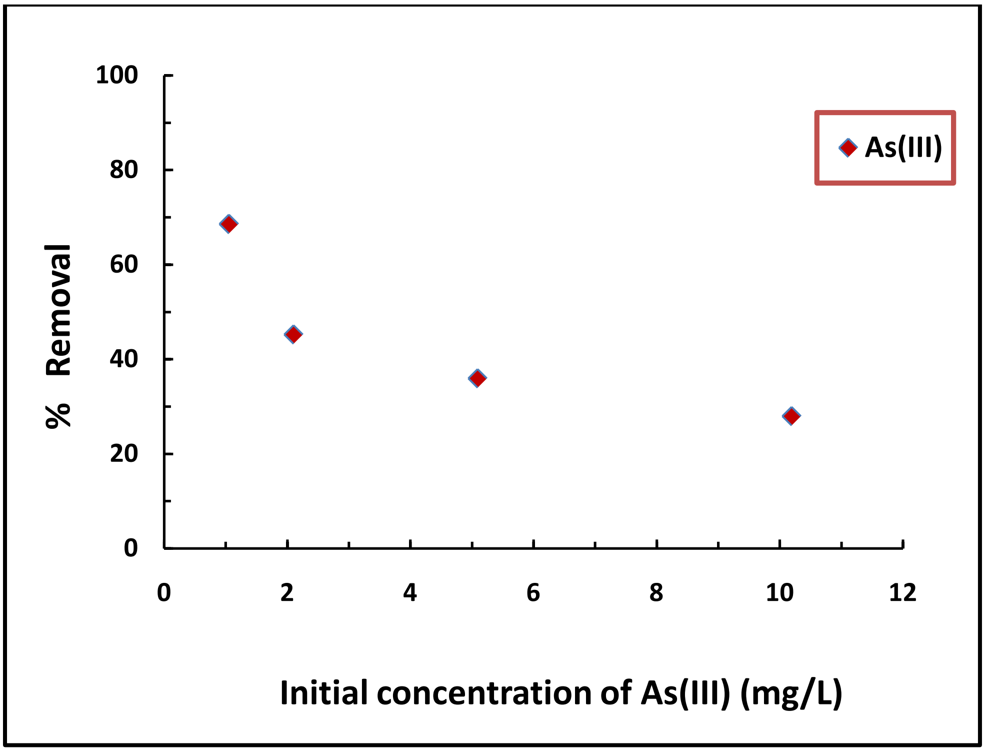

Figure 32: Effect of sorptive concentration on the sorption of As(III)

onto the surface of ICS.

more active sites were available for relatively smaller number of sorbing species. However, at higher concentration of the sorptive ions, reasonably, lesser number of active sites was available for larger number of sorbing ions (Tiwari *et al.,* 2007a; Tiwari *et al.,* 2011a).

3.4.2.3. Arsenic(V)

The removal behaviour of MCS and ICS for As(V) were studied varying the sorptive concentration from 1.00 to 25.00 mg/L for MCS and 1.10 to 10.46 mg/L for ICS at pH ~ 6.0 at 25°C respectively. The results obtained were shown in Tables 31 and 32 which were represented graphically in Figures 33 and 34 respectively for MCS and ICS. A decrease in percent uptake was observed from 70.48 to 3.22% for MCS and 74.55 to 29.06 for ICS with the increase in sorptive concentration respectively, from 1.00 to 25.00 mg/L (for MCS) and 1.10 to 10.46 mg/L (for ICS). However, the amount adsorbed by the adsorbent increases from 0.138 to 0.316 mg/L in the case of MCS and 0.164 to 0.618 mg/L for ICS. This could be explicable with the fact that at low arsenic concentrations more and more active sites were available for relatively smaller number of sorbing species. However, at higher sorptive concentration comparably lesser number of active site was available for very large number of sorbing ions (Tiwari *et al.*, 2007a; Tiwari *et al.*, 2011a).

Table 31: Effect of sorptive concentration on the sorption of As(V) onto the surface of MCS. (MCS dose = 5g/L; pH ~6.0).

Initial As(V) conc. mg/L	**Final As(V) conc. (mg/L)**	**Amount adsorbed (mg/L)**	**Amount adsorbed (mg/g)**	**% Removal**
1.00	0.31	0.69	0.138	69.00
4.01	2.58	1.43	0.286	35.66
6.99	5.67	1.32	0.264	18.88
10.01	8.57	1.44	0.288	14.39
12.01	10.55	1.46	0.292	12.16
14.99	14.04	0.95	0.190	6.34
20.00	19.21	0.79	0.158	3.95
25.01	23.42	1.59	0.318	6.36

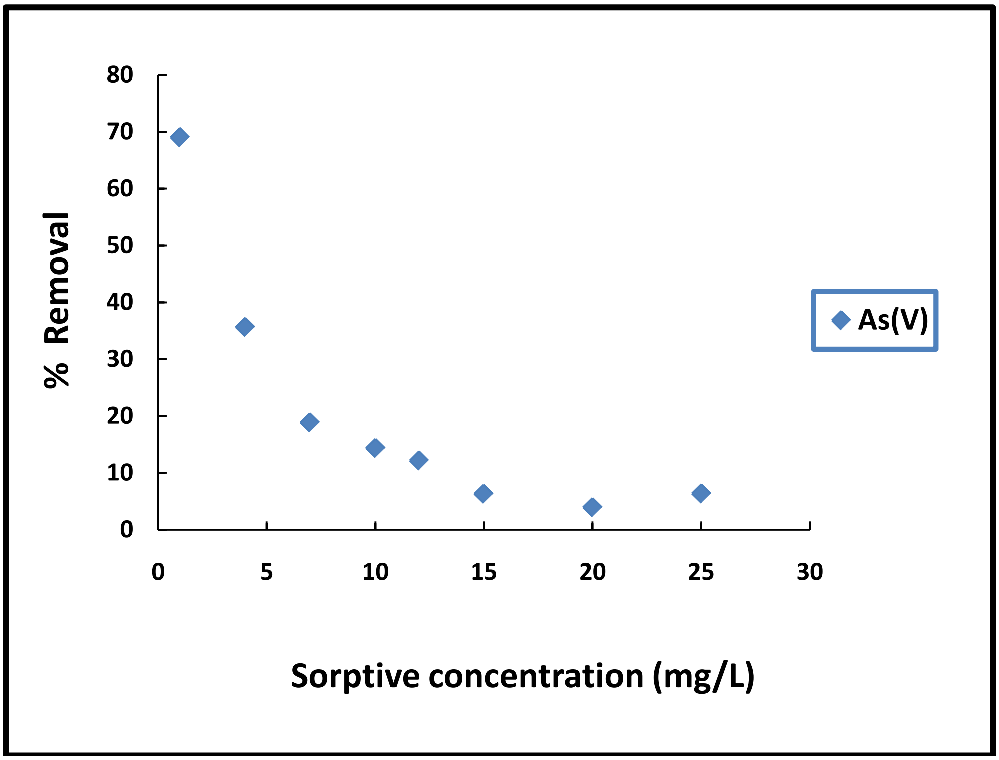

Figure 33: Effect of sorptive concentration on the sorption of As(V) onto the surface of MCS.

Table 32: Effect of sorptive concentration on the sorption of As(V) onto the surface of ICS. (ICS dose = 5g/L; pH ~6.0).

Initial As(V) conc.(mg/L)	**Final As(V) conc.(mg/L)**	**Amount adsorbed (mg/L)**	**Amount adsorbed (mg/g)**	**% Removal**
1.10	0.28	0.82	0.164	74.55
2.26	1.32	0.94	0.188	41.59
3.54	2.43	1.11	0.222	31.35
10.46	7.42	3.04	0.608	29.06

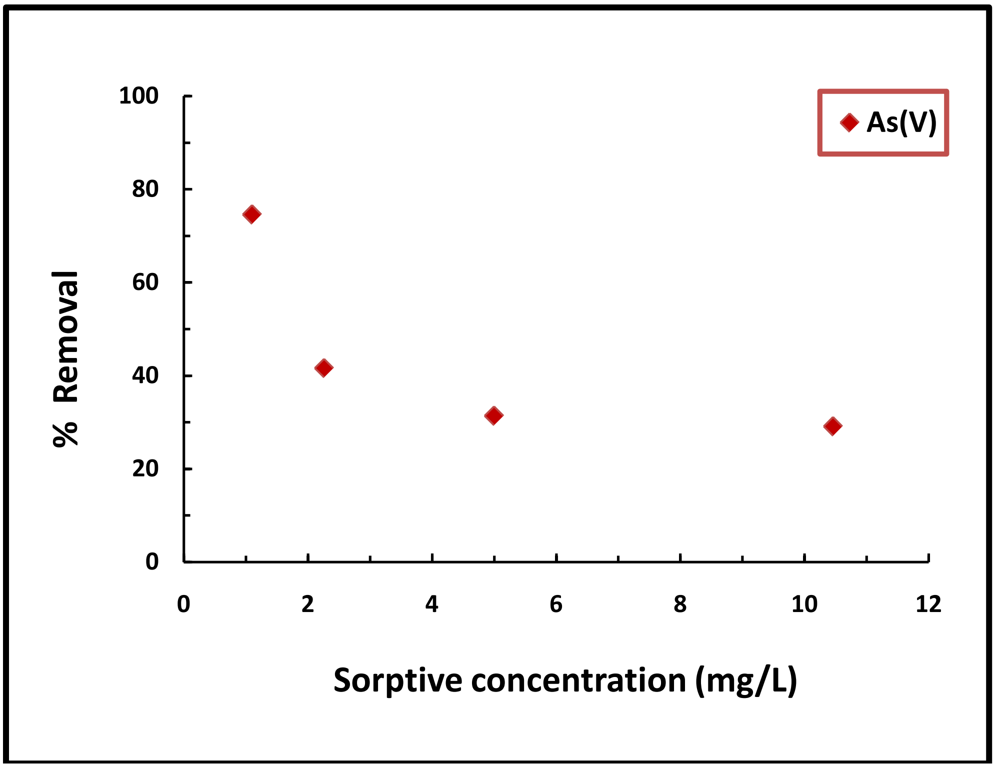

Figure 34: Effect of sorptive concentration on the sorption of As(V) onto the surface of ICS.

3.4.2.4. Cadmium(II)

The concentration dependence studies for Cd(II) ions with MCS were carried out at 25°C and pH 6.0 with MCS dose 5g/L. The results obtained were shown in Tables 33 and 34 along with the graphical representation in Figures 35 and 36 respectively for MCS and ICS. It was clearly observed that increasing the concentration from 0.82 to 21.23 mg/L of Cd(II) caused for decrease in percent removed of Cd(II) from 88.30% to 65.75 % by MCS.However, an increase in amount removed had been observed from 0.145 to 2.792 mg/g with the same increase in sorptive concentrations. Similarly, for the similar increase in Cd(II) concentration i.e., from 1.00 to 20.00 mg/L (at 25°C; pH 4.5 and ICS dose of 5g/L), was caused for an apparent decrease of percent of Cd(II) removal respectively from 52.81to 12.16 % by ICS (*cf* Table 34 and Figure 36). At the same time, an increase in amount adsorbed by the ICS with respect to the increase in sorptive concentrations had been obtained from 0.088 to 0.482 mg/g. These results can be explained such that at pH 6.0, the surface of MCS is likely to be negative charge. The gradual decrease in removal percent with the increase in sorptive concentrations could be explained with the fact that the gradual saturation of the active sites occurred on the adsorbent surface such that more active sites are available at higher dilution or lesser number of sorbing ions (Mishra and Singh, 1987a).

Table 33: Effect of sorptive concentration on the sorption of Cd(II) onto the surface of MCS. (MCS dose = 5g/L; pH~ 6.0).

Initial Cd(II) conc.(mg/L)	**Final Cd(II) conc.(mg/L)**	**Amount adsorbed (mg/L)**	**Amount adsorbed (mg/g)**	**% Removal**
0.82	0.09	0.73	0.145	88.30
3.25	0.45	2.80	0.560	86.16
6.20	1.46	4.75	0.949	76.48
9.22	2.70	6.52	1.304	70.69
10.20	3.87	6.33	1.266	62.05
14.72	5.72	8.99	1.799	61.15

21.23	7.27	13.96	2.792	65.75

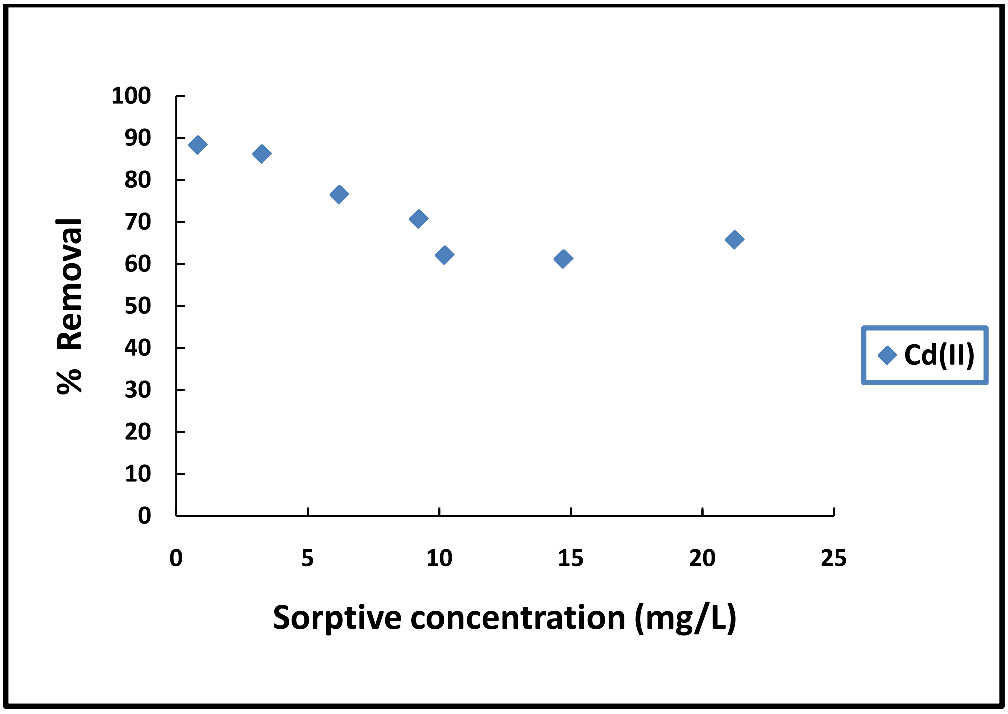

Figure 35: Effect of sorptive concentration on sorption of Cd(II) onto the surface of MCS.

Table 34: Effect of sorptive concentration on the sorption of Cd(II) onto the surface of ICS. (ICS dose = 5g/L; pH = 4.5).

Initial Cd(II) conc. (mg/L)	Final Cd(II) conc. (mg/L)	Amount adsorbed (mg/L)	Amount Adsorbed (mg/g)	(%) Removal
1.00	0.56	0.44	0.088	52.81
5.00	2.67	2.34	0.467	44.54
10.00	6.79	3.20	0.640	27.39
20.00	17.59	2.41	0.482	12.16

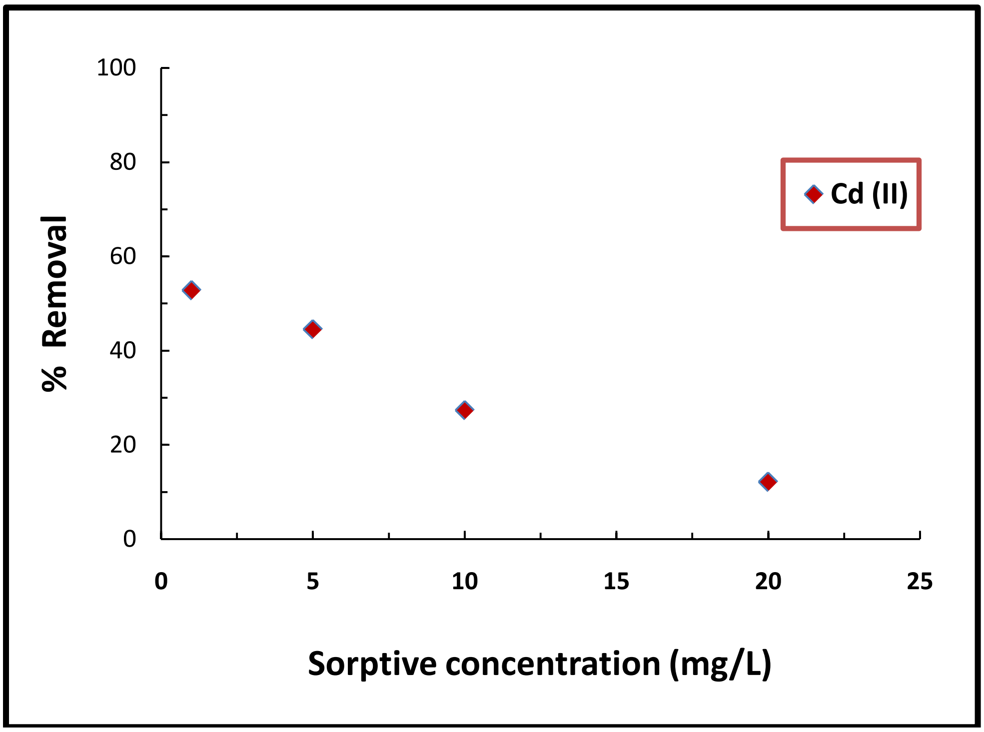

Figure 36: Effect of sorptive concentration on sorption of Cd(II) onto the surface of ICS.

3.4.2.5. Copper(II)

The concentration dependence data in the removal of Cu(II) by MCS was obtained, increasing the Cu(II) concentration from 1 to 20 mg/L for Cu(II) and keeping the constant solution pH 4.0 and temperature 25 ^{0}C. Results obtained were presented in Table 35 and graphically represented as a function of percent removal in Figure 37. The results clearly indicated that increasing the concentration from 1.00 to 20.00 mg/L caused to a decrease in percent removed of Cu(II) from 81.65% to 54.04 %. Similarly, the concentration dependence data for ICS was obtained and given in Table 36 and graphically represented in Figure 38. It was observed that increasing the Cu(II) concentration from 1.02 mg/L to 20.2 mg/L resulted in a decrease of percent uptake from 91.18 to 27.92. However, as we increase the concentration of Cu(II) ions in aqueous solutions from 1.00 mg/L to 20.00 mg/L, the amount adsorbed by the adsorbent i.e. MCS increases to a significant amount from 0.151 to 2.498 mg/g for MCS. Similarly, ICS shows an increase in the amount adsorbed from 0.186 to 1.128 mg/g as sorptive concentration increases from 1.02 mg/L to 20.2 mg/L.This decrease in percent uptake of metal cations was explicable on the basis that less number of active sites was available at the solid surface at higher concentration of sorbing ions (Kim *et al.*, 2002; Tiwari *et al.*, 1999; Mishra *et al.*, 1996).

Table 35: Effect of sorptive concentration on the sorption of Cu(II) onto the surface of MCS. (MCS dose = 5g/L; pH = 4.0).

Initial Cu(II) conc.(mg/L)	**Final Cu(II) conc. (mg/L)**	**Amount adsorbed (mg/L)**	**Amount adsorbed (mg/g)**	**% Removal**
1.00	0.24	0.76	0.151	81.65
3.00	0.92	2.08	0.417	69.60
5.00	1.47	3.53	0.706	62.35
8.00	2.86	5.14	1.029	58.90
10.00	3.25	6.75	1.351	58.96
12.00	4.31	7.69	1.539	58.11
15.00	6.48	8.52	1.705	54.66
20.00	7.51	12.49	2.498	54.05

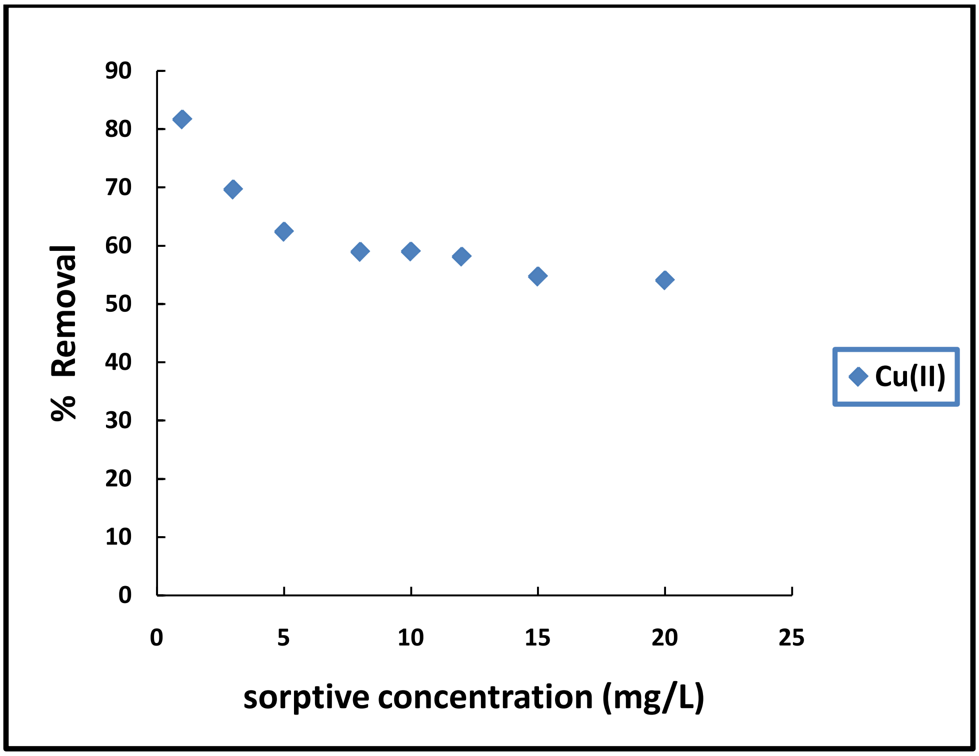

Figure 37: Effect of sorptive concentration of on the sorption of Cu(II) onto the surface of MCS.

Table 36: Effect of sorptive concentration on the sorption of Cu(II) onto the surface of ICS. (ICS dose = 5g/L; pH =4.5).

Initial Cu(II) conc. (mg/L)	**Final Cu(II) conc. (mg/L)**	**Amount adsorbed (mg/L)**	**Amount adsorbed (mg/g)**	**% Removal**
1.02	0.09	0.93	0.186	91.18
2.15	0.47	1.68	0.336	78.14
5.10	2.01	3.09	0.618	60.59
10.08	4.67	5.41	1.082	53.67
15.14	8.43	6.71	1.342	44.32
20.20	14.56	5.64	1.128	27.92

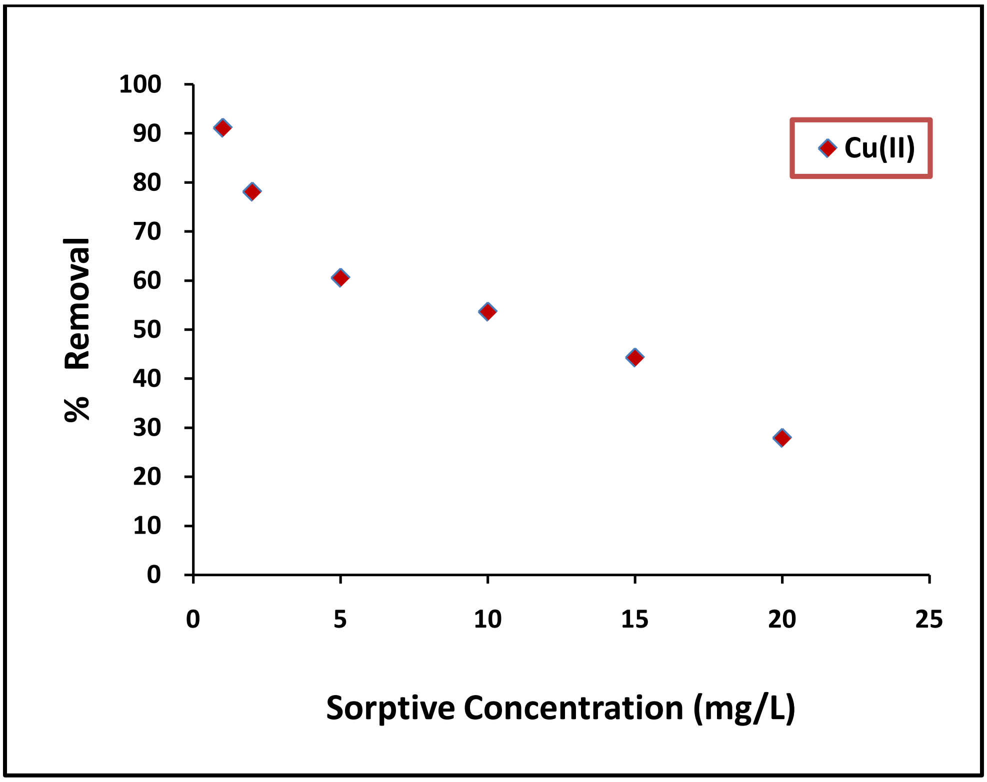

Figure 38: Effect of sorptive concentration on the sorption of Cu(II) onto the surface of ICS.

3.4.2.6. Lead(II)

The concentration dependence data for Pb(II) with MCS was obtained keeping the solution pH 4.0 and temperature 25^{0}C as constant. Results obtained were presented in Table 37 and graphically represented as a function of percent removed in Figure 39. The results obtained clearly indicated that the increase in sorptive concentration from the 1.00 to 40.00 mg/L, corresponds to a decrease in the removal percent of Pb(II) from 99.00 to 75.02%, respectively. Similarly, the effect of sorptive concentration in the removal of Pb(II) by ICS was also studied at 25^{0}C at pH 4.5, which were shown in Table 38 and graphically represented in Figure 40. The percent removal of Pb(II) was decreased from 95.45 to 20.03% with the increase of Pb(II) concentrations from 1.10 mg/L to 50.23 mg/L. Nevertheless, an increase in the amount adsorbed by the sorbents with the increase in sorptive concentrations had been obtained from 0.138 to 4.30 mg/g for MCS and for ICS, an increase from 0.21 to 2.012 mg/g had been shown with the change in observed sorptive concentrations.This decrease in percent uptake of Pb(II)at higher concentrations was explained because of increase in active sites for a smaller number of sorbing ions at higher dilutions which consequently enhances the relative increase in the sorption of the metal ions at higher dilution i.e., lower concentration. Similar observations had been reported in the removal of Ba(II) by hydrous manganese oxide (Mishra and Tiwary, 1993), removal of cadmium ions from aqueous solutions by hydrous ceric oxide (Mishra and Singh, 1995), removal of Zn(II) ions using rice husk (Mishra *et al.*, (1997a), a radiotracer study for biosorptive behaviour of mango and neem bark for Hg(II), Cr(III) and Cd(II) (Tiwari *et al.*, 1999) and removal of copper(II) ion by kaolin in aqueous solutions (Kim *et al.*, 2002).

Table 37: Effect of sorptive concentration on the sorption of Pb(II) onto the surface of MCS. (MCS dose = 5g/L; pH = 4.0).

Initial Pb(II) conc. (mg/L)	Final Pb(II) conc. (mg/L)	Amount adsorbed (mg/L)	Amount adsorbed (mg/g)	% Removal
1.00	0.31	0.69	0.138	99.00
5.00	3.11	1.89	0.378	89.80
10.00	5.69	4.31	0.862	96.80
15.00	8.19	6.81	1.362	84.13
20.00	10.28	9.72	1.944	79.75
25.00	12.95	12.05	2.410	80.96
30.00	15.36	14.64	2.928	80.13
40.00	18.50	21.50	4.300	75.02

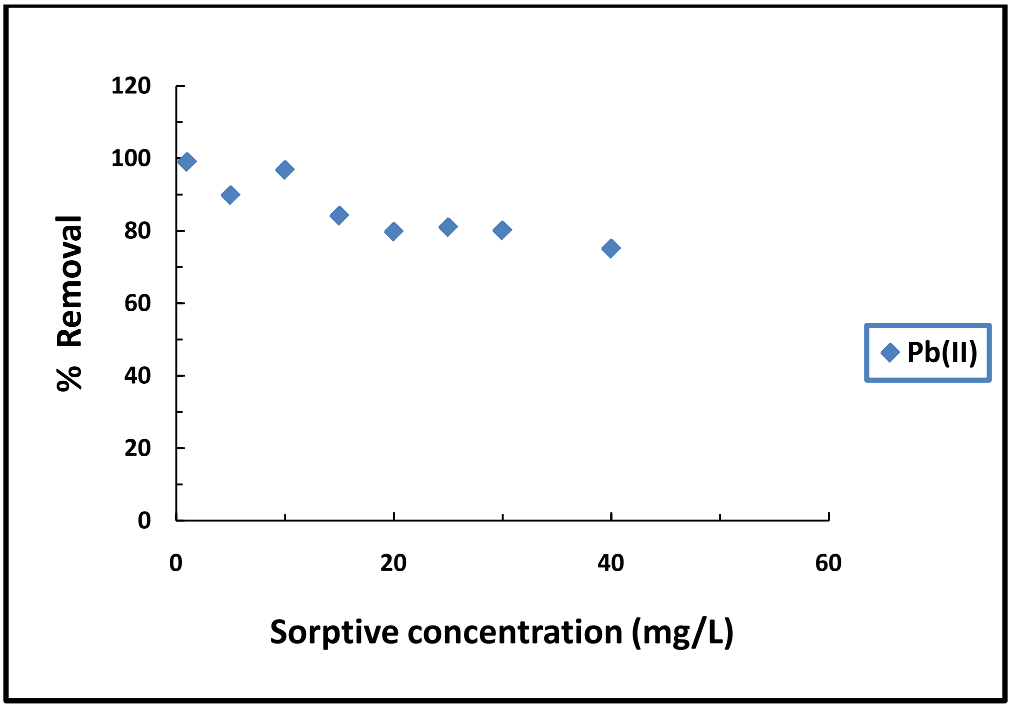

Figure 39: Effect of concentration of on the sorption of Pb(II) onto the surface of MCS.

Table 38: Effect of sorptive concentration on the sorption of Pb(II) onto the surface of ICS. (ICS dose = 5 g/L, pH ~4.5).

Initial Pb(II) conc.(mg/L)	Final Pb(II) conc.(mg/L)	Amount adsorbed (mg/L)	Amount adsorbed (mg/g)	% Removal
1.10	0.05	1.05	0.21	95.45
5.09	0.56	4.53	0.906	89.00
10.15	3.14	7.01	1.402	69.06
20.18	11.38	8.80	1.760	43.61
30.11	18.43	11.68	2.336	38.79
50.23	40.17	10.06	2.012	20.03

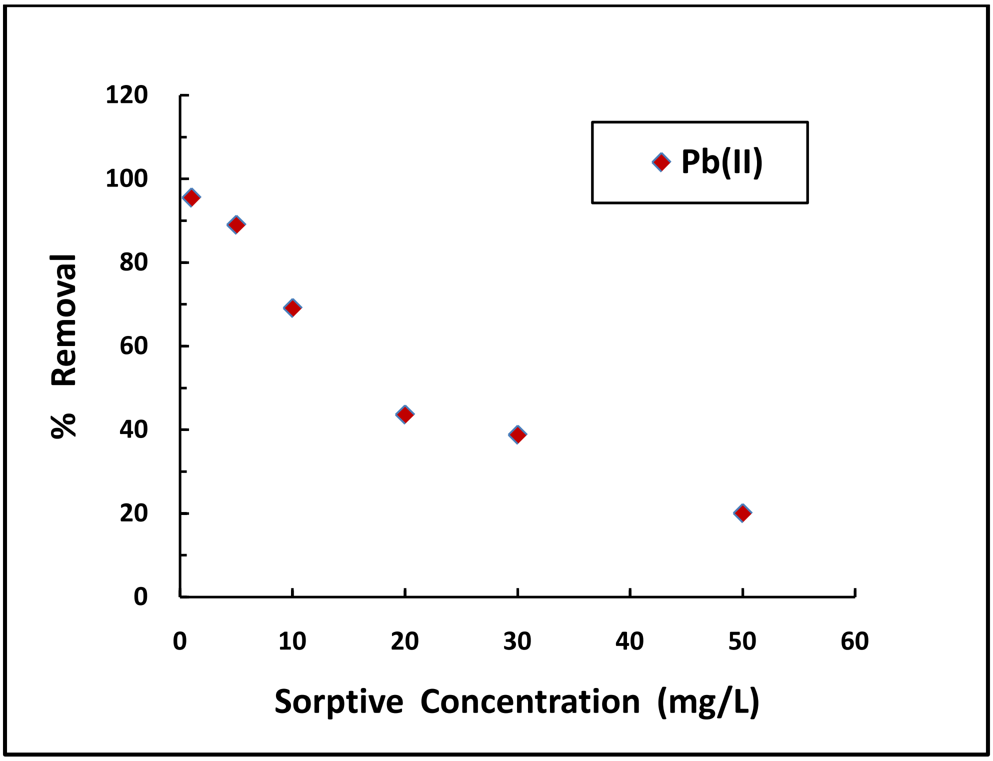

Figure 40: Effect of sorptive concentration on the sorption of Pb(II) onto the surface of ICS

3.4.2.7. Summary

The concentration dependence data obtained for these systems showed that increasing the sorptive concentration enabled to increase in amount removed; however, the increase in dilution favoured the percent uptake of metal removal by these two solids i.e., MCS and ICS employed. This increase in percent uptake by increasing the sorptive dilution was explained because of the fact that more and more active sites were available for a lesser number of sorbing ions at higher dilutions, which consequently enhanced the relative increase in the sorption of these metal ions at higher dilutions.

3.4.3. Equilibrium Modelling

The concentration dependence data was further utilized to model it towards the known Freundlich adsorption isotherm (Equation (2). The Freundlich model assumed with the assumption that the sorption occurs on an energetically heterogeneous surface on which the sorbed molecules interact laterally. Tables 39, 40, 41, 42, 43 and 44 show the values of the bulk concentrations (C_e) and the amount adsorbed in mg/g (a_e) of Cr(VI), As(III), As(V), Cd(II), Cu(II) and Pb(II), ions and the corresponding values of Log C_e and Log a_e of these ions for MCS. Similarly, the values obtained for the Cr(VI), As(III), As(V), Cd(II), Cu(II) and Pb(II) for ICS were included in the Tables 45, 46, 47, 48, 49 and 50, respectively. The Figures 41, 42, 43, 44, 45 and 46 represented the plots drawn between Log C_e *vs* Log a_e for the metal ions Cr(VI), As(III), As(V), Cd(II), Cu(II) and Pb(II) using MCS. Moreover, the similar plots for these ions Cr(VI), As(III), As(V), Cd(II), Cu(II) and Pb(II) for ICS were returned in the Figures 47, 48, 49, 50, 51 and 52 respectively. Reasonably a good straight line was obtained while fitting the data for linear line (*cf*. Figures 41-52). Further, using the fitting equation, the Freundlich constants i.e., *1/n* and K_f along with R^2 values were evaluated for these metal ions studied. The Freundlich constants along with R^2 values for the two solids i.e., MCS and ICS were again returned in Tables 51 and 52, respectively.

The closure scrutiny of the Freundlich constants and the R^2 values (*cf* tables 51 and 52), it was observed that the data is fitted well for the linearized Freundlich model since reasonably a high R^2 values obtained for these systems. Further, the fractional values of 1/n ($0<1/n<1$) obtained for all the systems (except Cr(VI) onto MCS) referred to the heterogeneous nature of the solid surface along with the exponential distribution of energy of the adsorption sites (Benes and Majer, 1980; Mishra *et al.*, 1998). In the case of Cr(VI) onto the MCS the 1/n value was close to the 1.0 hence, it was assumed that the surface likely to behave as homogeneous in nature. However, the only Freundlich model hardly could infer it to draw a final conclusion. Further, relatively higher value sorption capacity (K_f) obtained for these systems were inferred a strong attraction and affinity of the solid surfaces towards these cations/anions. Comparatively, the Pb(II) the capacity is maximum for Pb(II) onto these two solids. MCS showed reasonably high capacity for As(III) or As(V). In general, comparing these two solids, MCS possessed higher removal capacity than ICS at least for the studied ions. Moreover, the applicability of Freundlich adsorption isotherm again points it towards the chemisorptive type of sorption taking place at the solid/solution interface. The similar results were obtained for the sorption of other cations using different sorbents (Tiwari *et al.*, 1999; Agarwal *et al.*, 2006; Mesquita *et al.*, 2002).

Table 39: Table for Freundlich adsorption isotherm for the sorption of Cr(VI) on MCS

Initial Cr(VI) (mg/L) C_e	**Final Cr(VI) (mg/L)**	**Amount adsorbed (mg/L)**	**Amount Adsorbed (mg/g) a_e**	**Log C_e**	**Log a_e**
5.00	3.09	1.91	0.382	0.6989	-0.4179
10.00	4.78	5.21	1.042	1.0000	0.0179
20.00	11.05	8.95	1.790	1.3010	0.2529
30.00	16.19	13.81	2.762	1.4771	0.4412
40.00	20.00	20.00	4.000	1.6020	0.6020
50.00	30.00	20.00	4.000	1.6989	0.6021
70.00	36.00	34.00	6.800	1.8451	0.8325
100.00	30.50	69.50	13.900	2.0000	1.1430

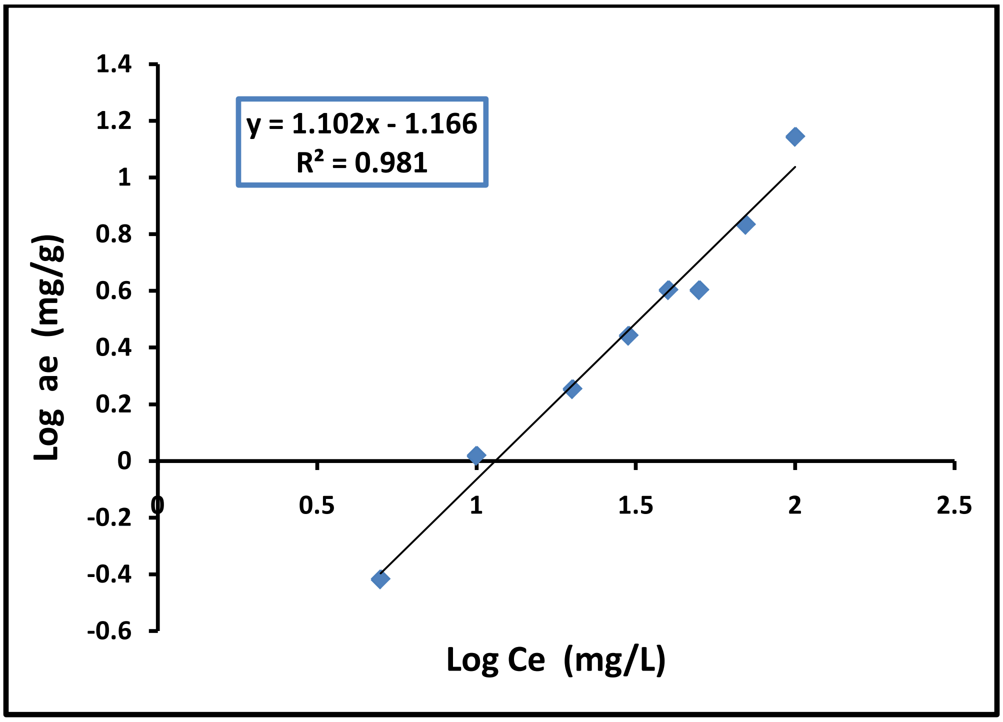

Figure 41: Freundlich adsorption isotherm for the sorption of Cr(VI)on MCS.

Table 40: Table for Freundlich adsorption isotherm for the sorption of As(III) on MCS.

Initial As(III) conc. (mg/L)	**Final As(III) conc.(mg/L) C_e**	**Amount adsorbed (mg/L)**	**Amount adsorbed (mg/g) a_e**	**Log C_e**	**Log a_e**
1.00	0.38	0.62	1.24	-0.4202	0.0934
12.00	11.03	0.97	1.94	1.0426	0.2878
15.00	14.15	0.85	1.70	1.1508	0.2305
20.00	19.10	0.90	1.80	1.2810	0.2553
25.00	24.07	0.93	1.86	1.3815	0.2695

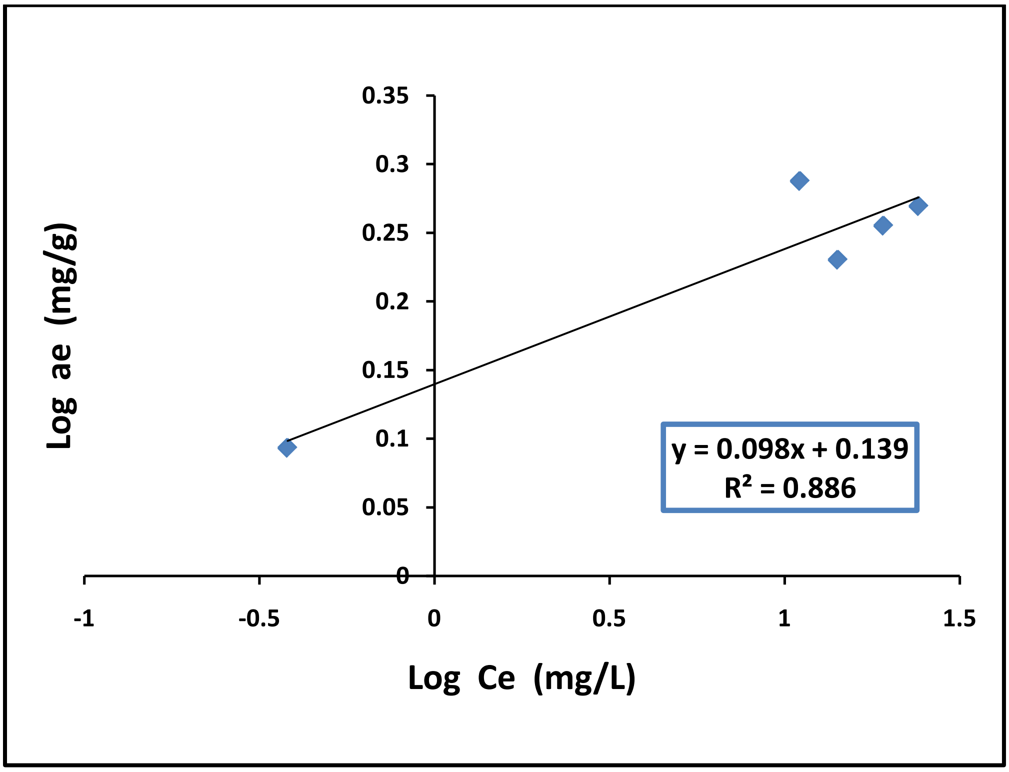

Figure 42: Freundlich adsorption isotherm for the sorption of As(III) on MCS.

Table 41: Table for Freundlich adsorption isotherm for the sorption of As(V) on MCS.

Initial As(V) conc. (mg/L)	**Final As(V) conc. (mg/L) C_e**	**Amount adsorbed (mg/L)**	**Amount adsorbed (mg/g) a_e**	**Log C_e**	**Log a_e**
1.00	0.31	0.69	1.38	-0.5086	0.1399
4.00	2.58	1.42	2.84	0.4116	0.4533
7.00	5.67	1.33	2.66	0.7536	0.4249
10.00	8.57	1.43	2.86	0.9330	0.4564
12.00	10.55	1.45	2.9	1.0233	0.4624
25.00	23.42	1.58	3.16	1.3696	0.4997

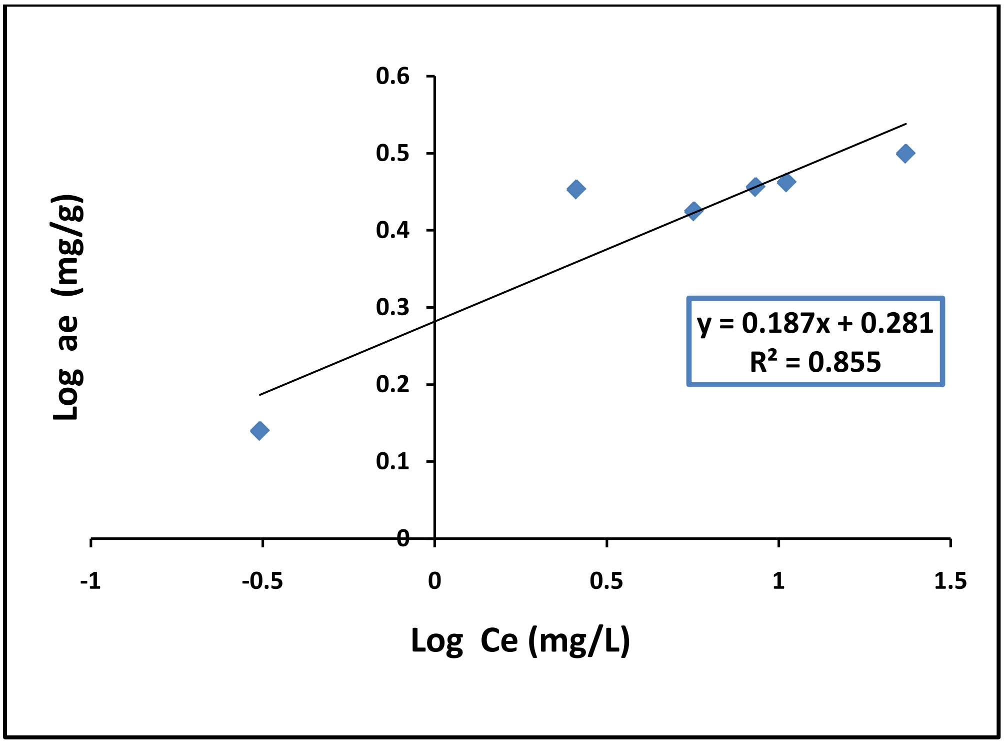

Figure 43: Freundlich adsorption isotherm for the sorption of As(V) on MCS.

Table 42: Table for Freundlich adsorption isotherm for the sorption of Cd(II) on MCS.

Initial Cd(II) conc.(mg/L)	Final Cd(II) conc. (mg/L) C_e	Amount adsorbed (mg/L)	Amount adsorbed (mg/g) a_e	log C_e	log a_e
0.82	0.09	0.73	0.146	-0.0875	-0.8368
3.24	0.45	2.79	0.558	0.5101	-0.2536
6.18	1.46	4.73	0.945	0.7912	-0.0244
9.18	2.69	6.50	1.300	0.9630	0.1137
10.17	3.85	6.32	1.260	1.0073	0.1015
14.66	5.70	8.96	1.790	1.1662	0.2533
21.15	7.25	1.39	2.780	1.3252	0.4440

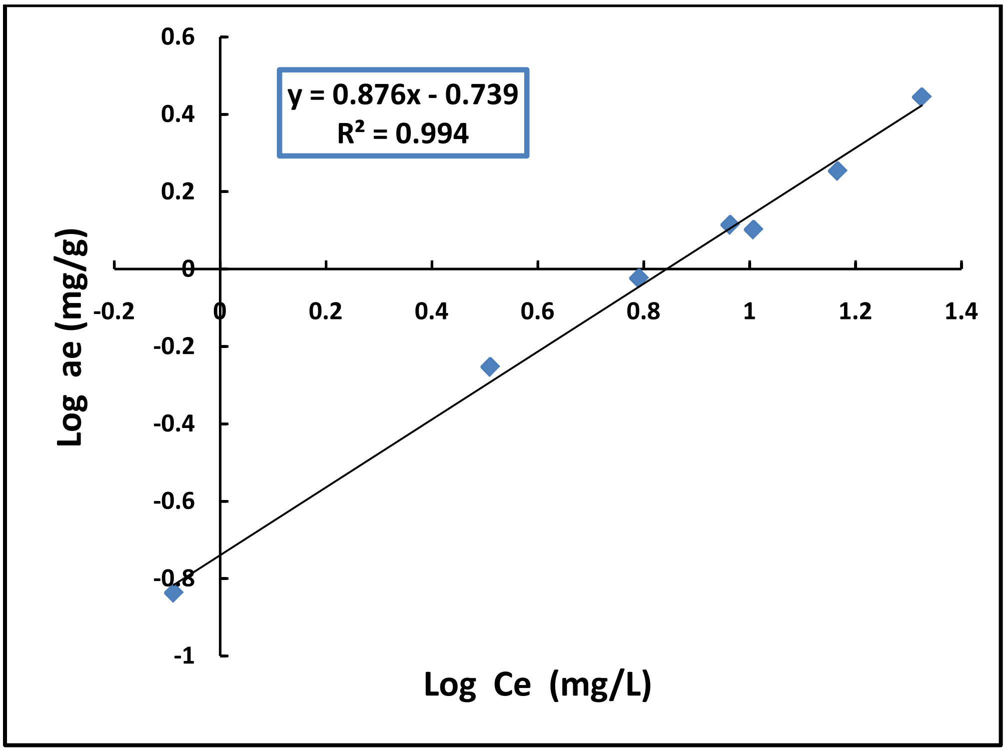

Figure 44: Freundlich adsorption isotherm for the sorption of Cd(II) on MCS.

Table 43: Table for Freundlich adsorption isotherm for the sorption of Cu(II) on MCS.

Initial Cu(II) conc.(mg/L)	**Final Cu(II) conc.(mg/L) C_e**	**Amount adsorbed (mg/L)**	**Amount adsorbed (mg/g) a_e**	**Log C_e**	**Log a_e**
1.32	0.24	1.08	0.216	-0.6143	-0.6651
3.02	0.92	2.10	0.419	-0.0376	-0.3769
3.90	1.47	2.43	0.487	0.1673	-0.3127
6.94	2.86	4.09	0.818	0.4558	-0.0875
7.91	3.27	4.67	0.933	0.5115	-0.0301
10.28	4.30	5.97	1.195	0.6342	0.0774
14.28	6.48	7.81	1.562	0.8113	0.1936
16.35	7.51	8.84	1.767	0.8757	0.2472

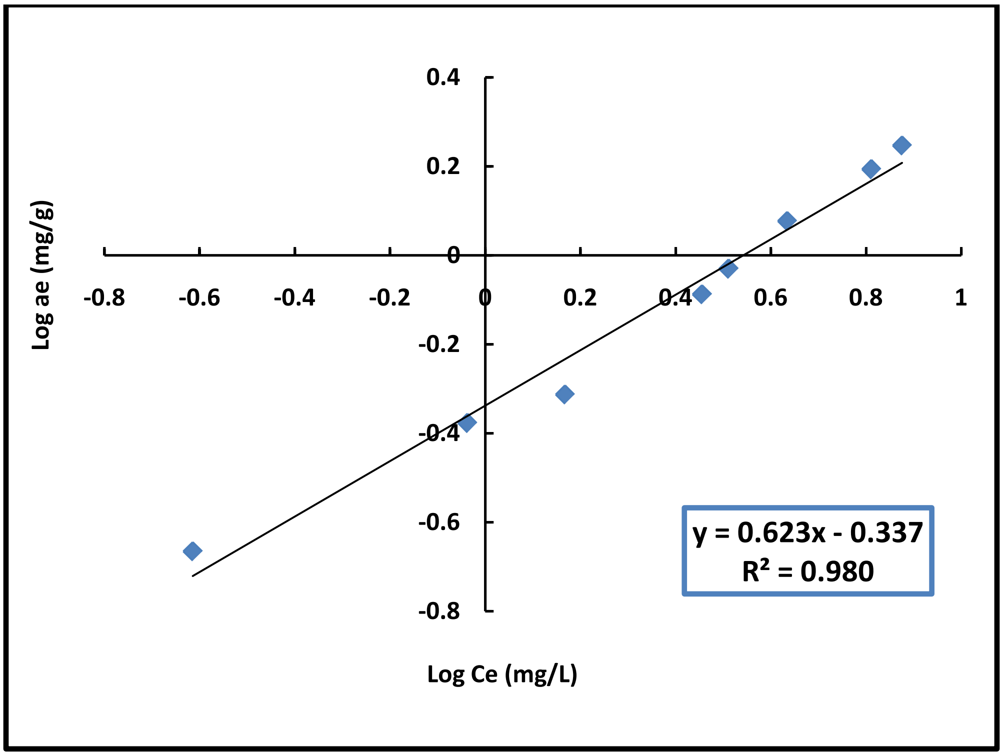

Figure 45 : Freundlich adsorption isotherm for the sorption of Cu(II) on MCS

Table 44: Table for Freundlich adsorption isotherm for the sorption of Pb(II) on MCS.

Initial Pb(II) conc.(mg/L)	**Final Pb(II) conc.(mg/L) C_e**	**Amount adsorbed (mg/L)**	**Amount adsorbed (mg/g) a_e**	**Log C_e**	**Log a_e**
1.00	0.01	0.99	0.198	-2.0000	-0.0467
5.00	0.51	4.49	0.898	-0.2924	0.2869
10.00	0.32	9.68	1.936	-0.4949	0.4021
15.00	2.38	12.62	2.524	0.3766	0.5038
20.00	4.05	15.95	3.190	0.6075	0.6072
25.00	4.76	20.24	4.048	0.6776	0.6819
30.00	5.96	24.04	4.808	0.7752	0.7783

40.00	9.99	30.01	6.002	0.9996	0.7783

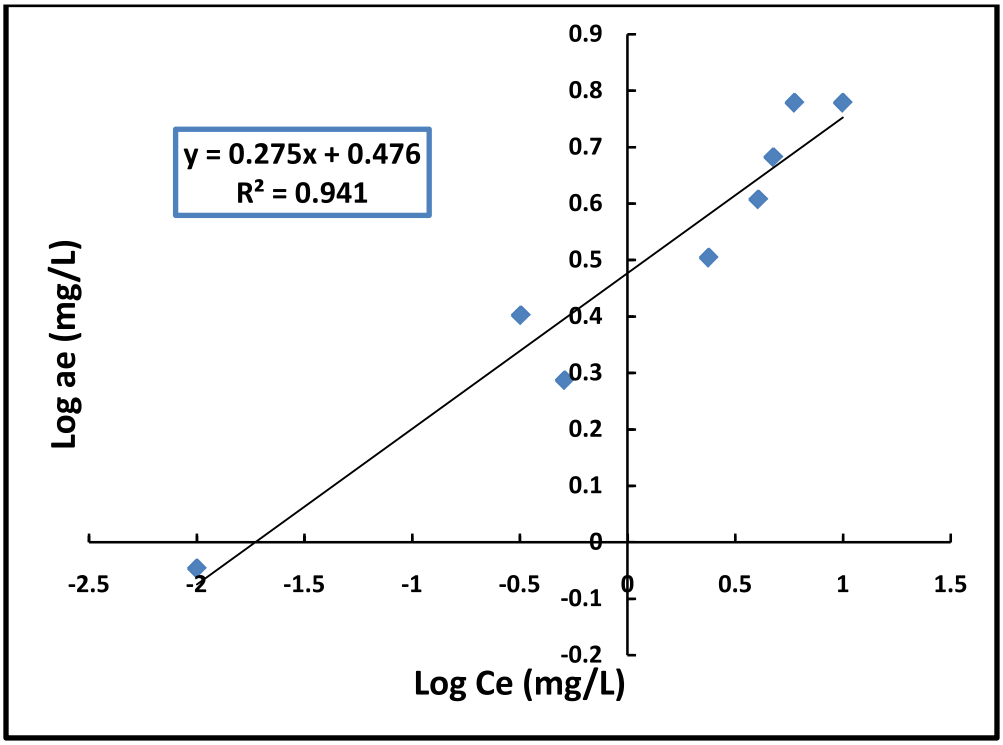

Figure 46: Freundlich adsorption isotherm for the sorption of Pb (II) on MCS.

Table 45: Table for Freundlich adsorption isotherm for the sorption of Cr(VI) on ICS.

Initial Cr(VI) conc.(mg/L)	**Final Cr(VI) conc.(mg/L) C_e**	**Amount adsorbed (mg/L)**	**Amount adsorbed (mg/g) a_e**	**Log C_e**	**Log a_e**
5.00	3.265	1.735	0.347	0.514	-0.460
80.00	64.877	15.123	3.025	1.812	0.481
90.00	69.897	20.103	4.021	1.844	0.604
100.00	76.224	23.776	4.755	1.882	0.677

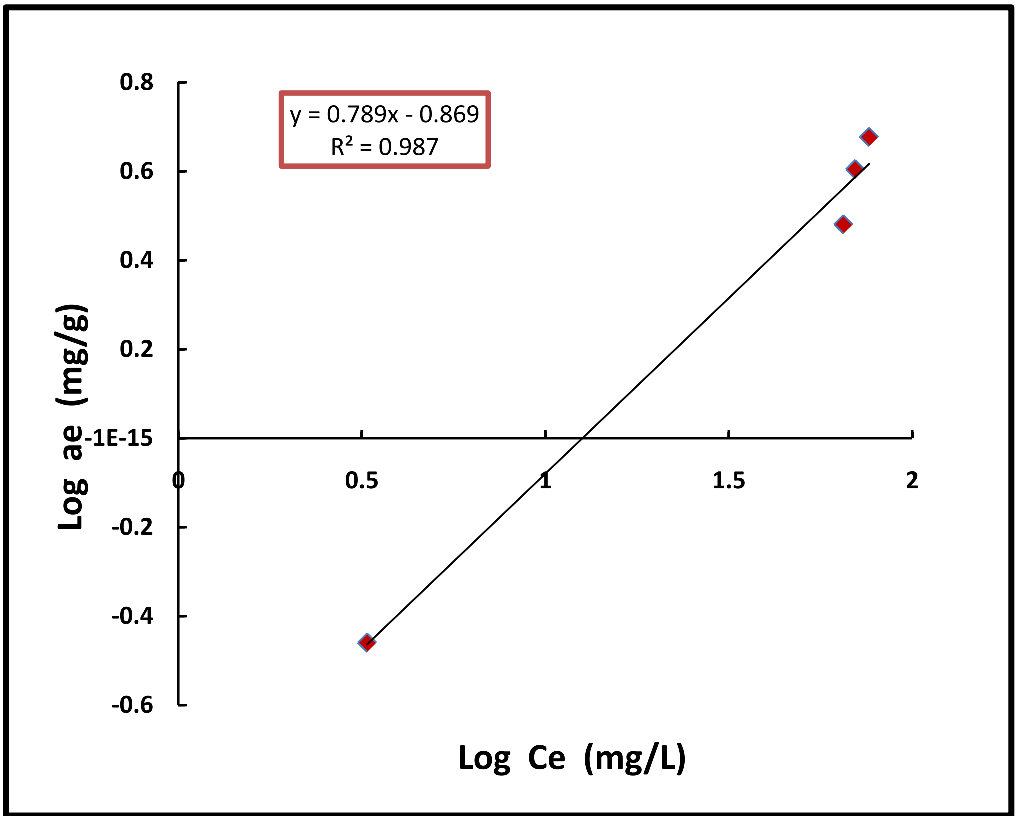

Figure 47: Freundlich adsorption isotherm for the sorption of Cr(VI) on ICS.

Table 46: Table for Freundlich adsorption isotherm for the sorption of As(III) on ICS.

Initial As(III) conc. (mg/L)	**Final As(III) conc. (mg/L) C_e**	**Amount adsorbed (mg/L)**	**Amount adsorbed (mg/g) a_e**	**Log Ce**	**Log a_e**
1.05	0.33	0.72	0.144	-0.96297	-0.84164
2.10	1.15	0.95	0.190	0.121396	-0.72125
5.09	3.26	1.83	0.366	1.026435	-0.43652
10.19	7.34	2.85	0.570	1.731392	-0.24413

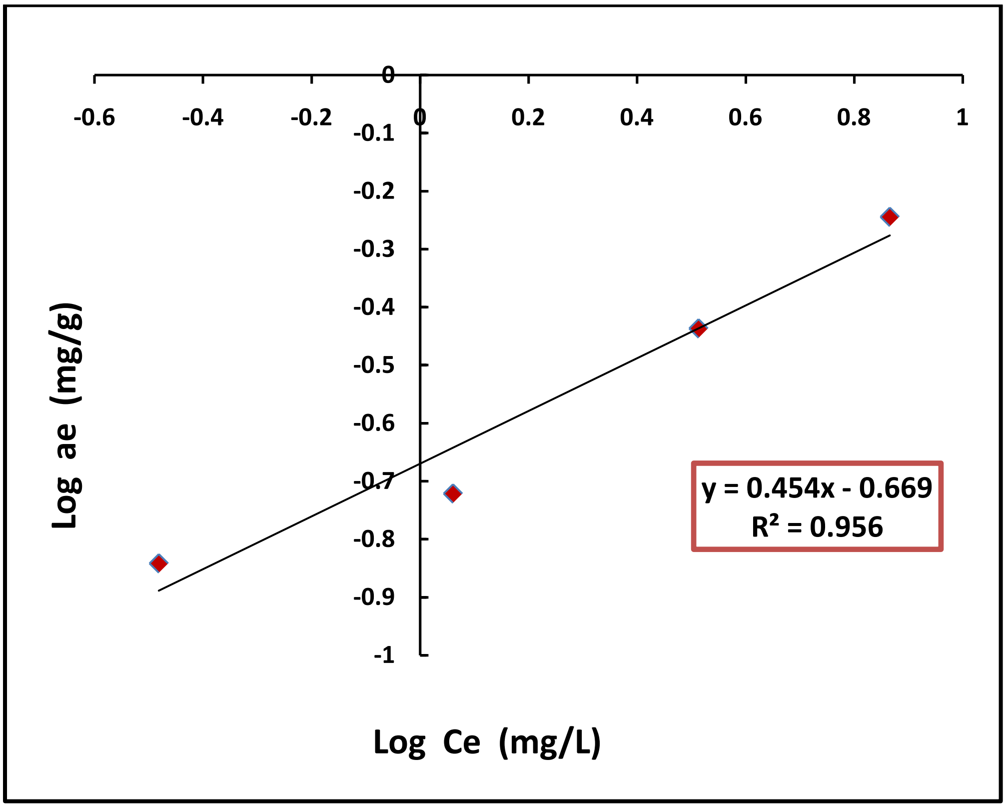

Figure 48: Freundlich adsorption isotherm for the sorption of As(III) on ICS.

Table 47: Table for Freundlich adsorption isotherm for the sorption of As(V) on ICS.

Initial As(III) conc. (mg/L)	**Final As(III) conc. (mg/L) C_e**	**Amount adsorbed (mg/L)**	**Amount adsorbed (mg/g) a_e**	**Log Ce**	**Log a_e**
1.10	0.28	0.82	0.164	-0.5528	-0.7851
2.26	1.32	0.94	0.188	0.1205	-0.7258
5.00	3.46	1.54	0.308	0.5390	-0.5114
10.46	7.42	3.04	0.608	0.870	-0.2161

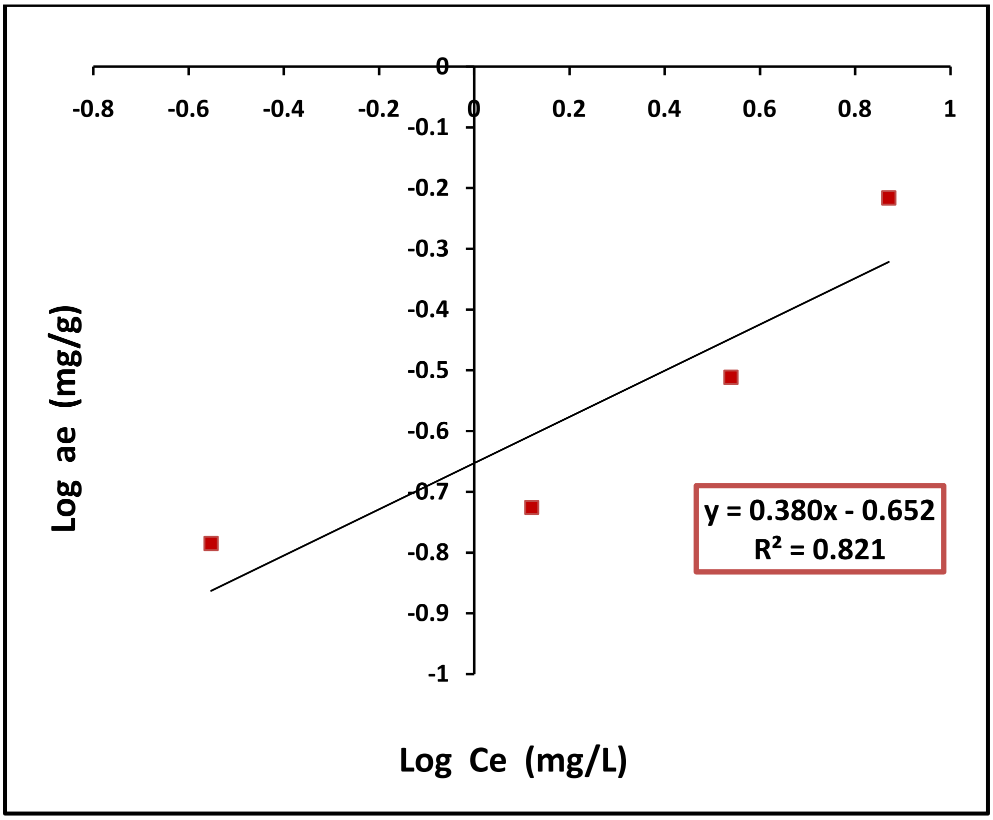

Figure 49: Freundlich adsorption isotherm for the sorption of As(V) on ICS.

Table 48: Table for Freundlich adsorption isotherm for the sorption of Cd(II) on ICS.

Initial Cd(II) conc. (mg/L)	Final Cd(II) conc.(mg/L) C_e	Amount adsorbed (mg/L)	Amount adsorbed (mg/g) a_e	Log C_e	Log a_e
1.00	0.558	0.442	0.0884	-0.2533	-1.0535
5.00	2.663	2.337	0.4674	0.4253	-0.3303
10.00	6.799	3.201	0.6402	0.8324	-0.1937
20.00	17.592	4.088	0.4816	1.2453	-0.3173

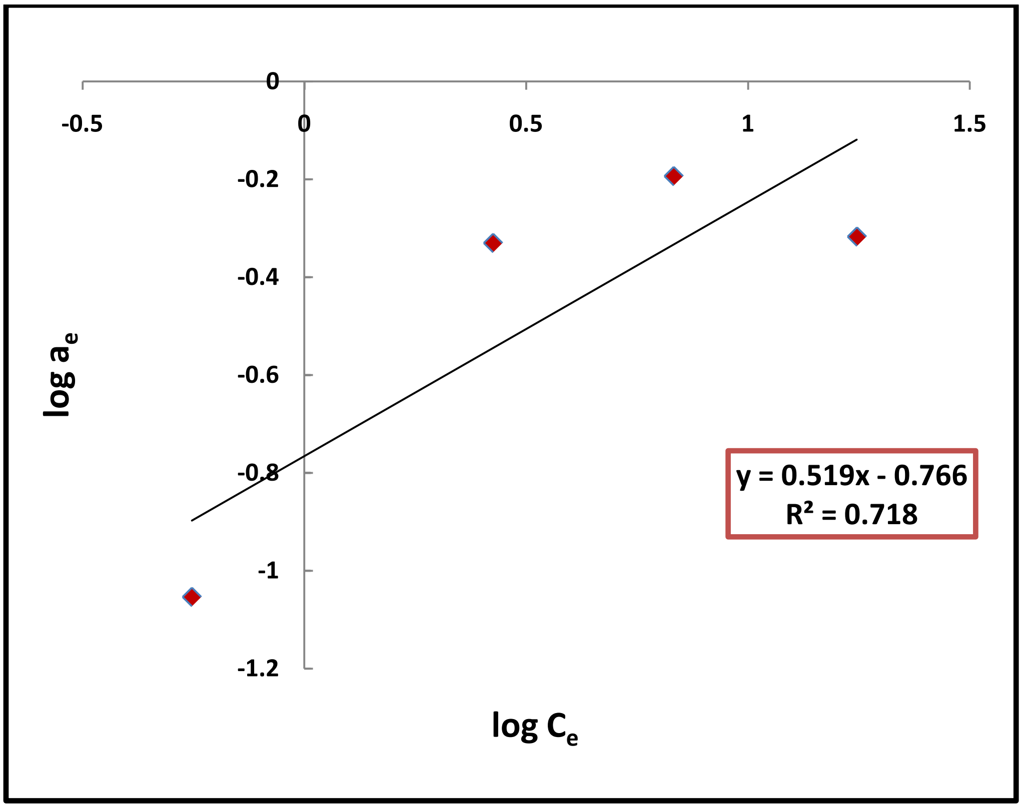

Figure 50: Freundlich adsorption isotherm for the sorption of Cd(II) on ICS.

Table 49: Table for Freundlich adsorption isotherm for the sorption of Cu(II) on ICS.

Initial Cu(II) (mg/L)	**Final Cu(II) (mg/L) C_e**	**Amount adsorbed (mg/L)**	**Amount adsorbed (mg/g) a_e**	**Log C_e**	**Log a_e**
1.02	0.09	0.93	0.186	-1.0458	-0.7305
2.15	0.47	1.68	0.336	-0.3279	-0.4737
5.10	2.01	3.09	0.618	0.3032	-0.2090
10.08	4.67	5.41	1.082	0.6693	0.0342
15.14	8.43	6.71	1.342	0.9258	0.1277
20.20	14.56	5.64	1.128	1.1631	0.0523

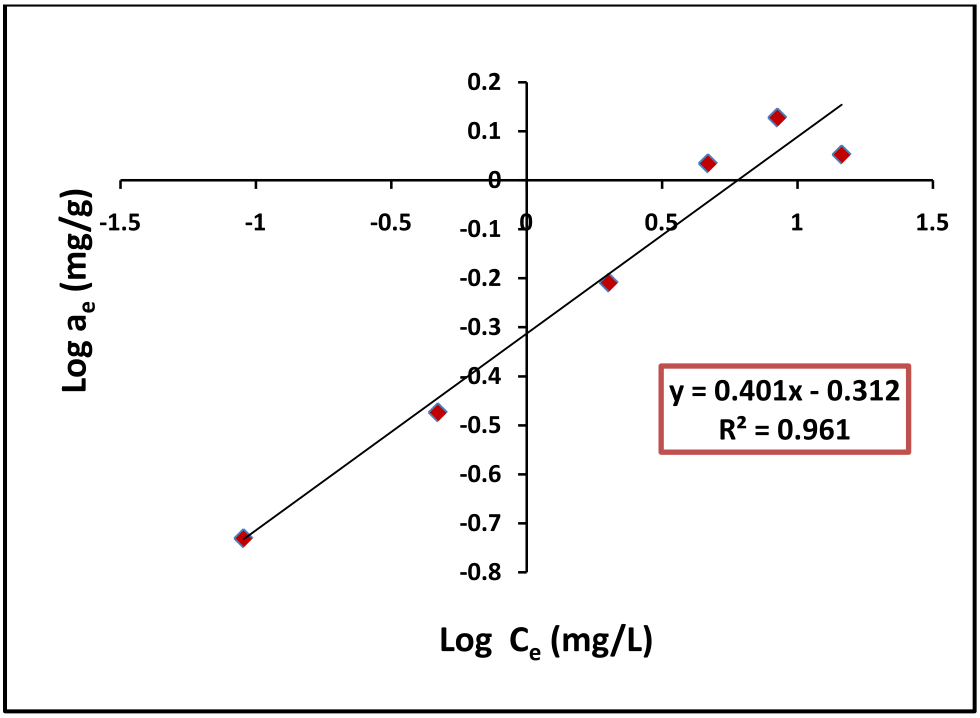

Figure 51: Freundlich adsorption isotherm for the sorption of Cu(II) on ICS.

Table 50: Table for Freundlich adsorption isotherm for the sorption of Pb(II) on ICS.

Initial Pb(II) (mg/L)	**Final Pb(II) (mg/L) C_e**	**Amount adsorbed (mg/L)**	**Amount adsorbed (mg/g) a_e**	**Log C_e**	**Log a_e**
1.10	0.05	1.05	0.210	-1.3010	-0.6780
5.09	0.56	4.53	0.906	-0.2520	-0.0430
10.15	3.14	7.01	1.402	0.4969	0.1467
20.18	11.38	8.80	1.760	1.0561	0.2455
30.11	18.43	11.68	2.336	1.2655	0.3685
50.23	40.17	10.06	2.012	1.6039	0.3036

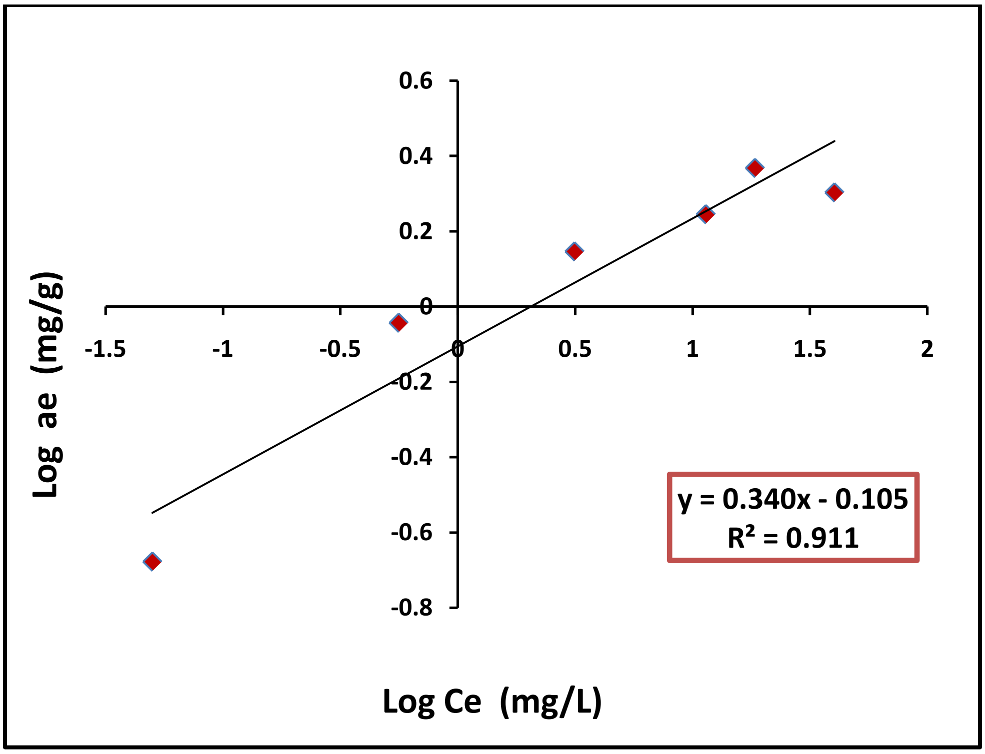

Figure 52: Freundlich adsorption isotherm for the sorption of Pb(II) on ICS.

Table 51: Freundlich constants obtained for the Cr(VI), Cd(II), Cu(II), Pb(II), As(III) and As(V) adsorption onto the surface of MCS.

Sample	***1/n***	***K_f (mg/g)***	***R^2***
Cr(VI)	1.04	0.022	0.981
As(III)	0.098	1.377	0.886
As(V)	0.187	1.909	0.855
Cd(II)	0.876	0.182	0.994

Cu(II)	0.623	0.460	0.980
Pb(II)	0.275	2.992	0.941

Table52: Freundlich constants obtained for the Cr(VI), Cd(II), Cu(II), Pb(II), As(III) and As(V) adsorption onto the surface of ICS.

Sample	***1/n***	**K_f *(mg/g)***	**R^2**
Cr(VI)	0.789	0.135	0.987
As(III)	0.454	0.214	0.956
As(V)	0.380	0.223	0.821
Cd(II)	0.519	0.171	0.718
Cu(II)	0.401	0.486	0.961
Pb(II)	0.340	0.785	0.911

3.4.3.1. Summary

All these systems studied showed reasonably a good applicability of linearized Freundlich adsorption isotherm model which indicated that these polluting ions sorbed onto the surface of MCS or ICS mainly by the chemisorption process. This conclusion was again tried to reaffirm with the ionic strength studies presented in the next sections. Moreover, MCS showed relatively higher removal capacity than the ICS. Further, both these solids showed maximum removal capacity for lead. The fractional values of Freundlich constants 1/n obtained for all these systems studied (except Cr(VI) onto MCS) showed to the heterogeneous nature of the solid surface along with the exponential distribution of energy of the adsorption sites

3.4.4. Effect of ionic strength

The change of ionic strength is one of the important parameter which determines the nature of binding of the sorptive ions onto the surface of solids. The ionic strength dependence data by soil minerals is usually used to distinguish between non-specific and specific adsorption (Hayes *et al.*, (1988).The specific adsorption is unaffected by the change in ionic strength, whereas the non – specific adsorption is likely to be influenced by the change in ionic strength because of the competitive adsorption with counteractions. It was observed that a characteristic pH usually observed above which the adsorption of phosphate by goethite and soils increased with the increase in ionic strength and below which a reverse-engineering trend was observed (Barrow *et al.*, 1980; Bolan *et al.*, 1986). Outer sphere complexes involved with only electrostatic interaction and were strongly affected by the ionic strength of the aqueous phase, whereas inner sphere complexes involved much stronger covalent or ionic binding and were only weakly affected by the ionic strengths (Sparks 1995; Tiwari *et al.*, 2007b). A model was developed by Bowden *et al.*, (1980) to describe the adsorption of phosphate, selenite and citrate on goethite. This model was applied to explain the effects of ionic strength and pH on the adsorption of phosphate on goethite and soil (Barrow *et al.*, 1980; Bolan *et al.*, 1986). According to this model, the effect of ionic strength on the adsorption was operated through its effect on electrostatic potential in the plane of adsorption, rather than through its effect on surface charge (Barrow *et al.*, 1980). However such complex model applications were generally not subject to direct experimental confirmation due to several employed fitting parameters which cannot be analytically measured (McBride 1997). Hence, keeping in view the present studies were extended to obtain the ionic strength dependence data in order to observe the sorption behaviour of studied metal ions onto the surface of MCS or ICS.

3.4.4.1. Arsenic(III)

The studies on the effect of ionic strength in the removal process of As(III) by MCS and ICS were shown in Tables 53 and 54 and graphically represented in Figures 53 and 54, respectively. It was clearly observed that a change in ionic strength of background electrolyte $NaNO_3$from 0.0001 mol/L to 0.1 mol/L (1000 times increase) resulting in an insignificant decrease in the removal percent of As(III). Quantitatively, increasing the background electrolyte concentration from 0.0001 to 0.1 mol/L $NaNO_3$ caused for the respective decrease of percent uptake of As(III) was found to be from 49.5 to 56.0% (total decrease by 6.5%) by MCS and from 39.65to 33.75 % (total decrease by 5.9%) by ICS. The results clearly depicted that the uptake of the metal ions by these sorbents were hardly affected by the concentration of the background electrolyte. Hence, these results clearly emphasize that the sorbing ion (As(III) was firmly bound by the strong forces and forming an inner sphere complexes onto the surface of MCS and ICS. It was explained that the ionic strength of the aqueous phase strongly affected the outer sphere complexes which involves only electrostatic interaction

Table 53: Ionic strength dependence data for As(III) adsorption onto the surface of MCS (pH~5.0).

Ionic strength ($NaNO_3$) (mol/L)	**Initial As(III) conc. (mg/L)**	**Final As(III) conc. (mg/L)**	**Amount adsorbed (mg/L)**	**% Removal**
0.0001	2.04	1.01	1.03	50.49
0.0005	2.04	0.97	1.07	52.45
0.0010	2.04	1.03	1.01	49.51
0.0050	2.04	0.88	1.16	56.86

0.0100	2.04	0.87	1.17	57.35
0.0500	2.04	0.98	1.06	51.96
0.1000	2.04	0.89	1.15	56.37

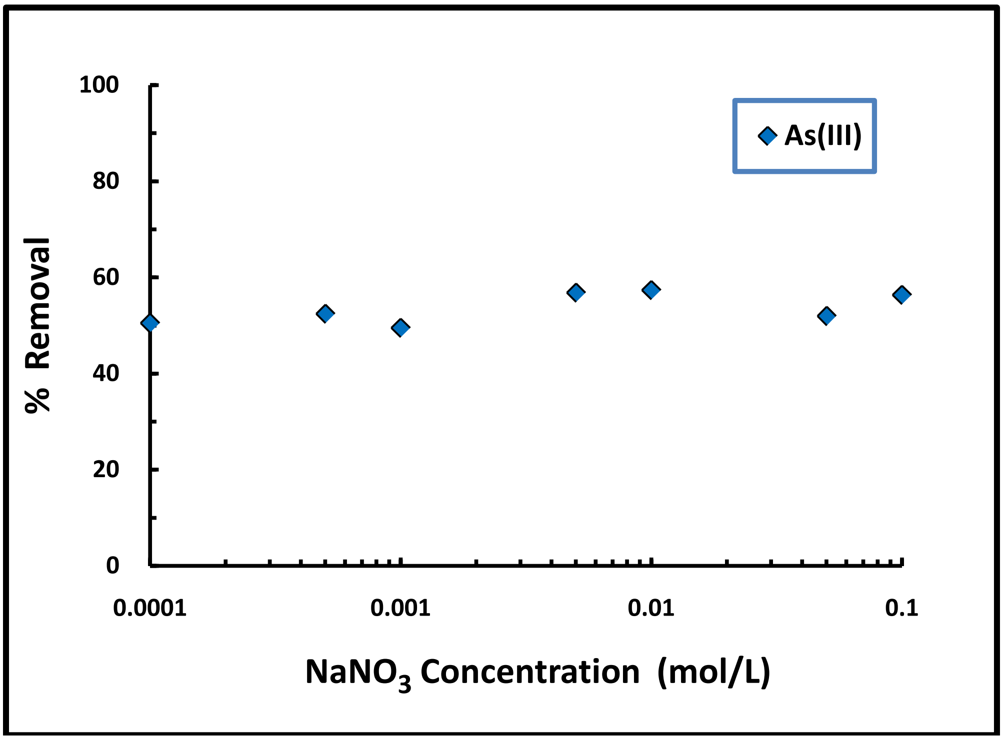

Figure 53: Ionic strength dependence for As(III) adsorption on MCS.

Table 54: Ionic strength dependence data for As(III) adsorption onto the surface of ICS (pH ~5).

Ionic strength ($NaNO_3$)	**Initial As(III) conc. (mg/L)**	**Final As(III) conc. (mg/L)**	**Amount adsorbed (mg/L)**	**% Removal**
0.001	9.76	6.24	3.52	39.65

0.010	9.76	6.43	3.33	37.81
0.100	9.76	6.38	3.38	38.29
1.000	9.76	6.85	2.91	33.75

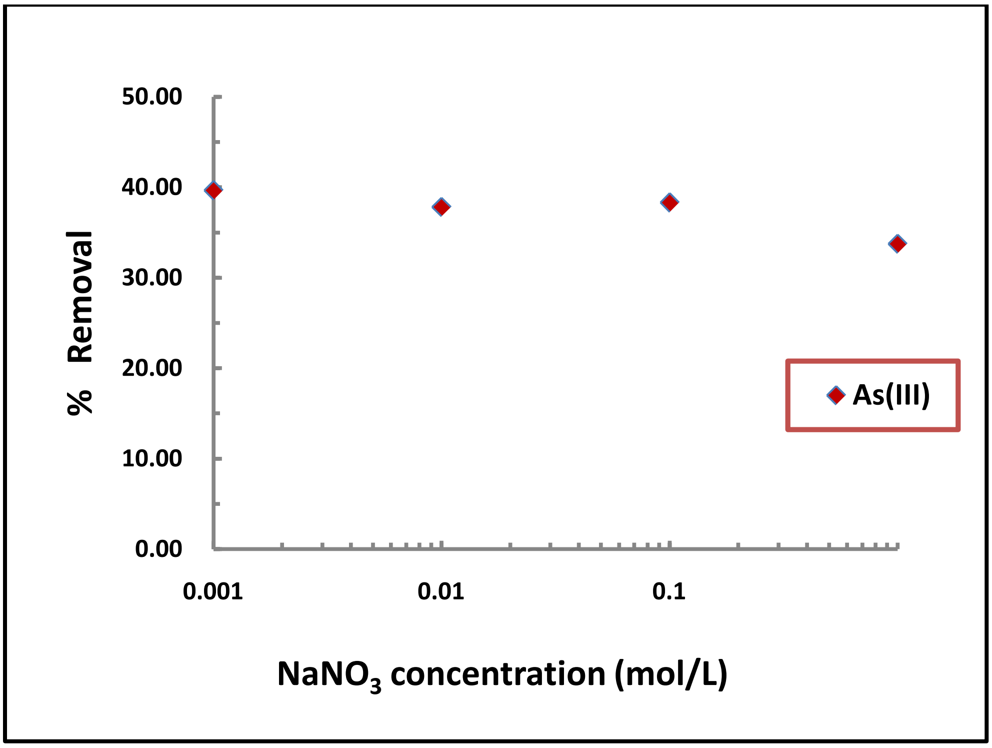

Figure 54: Ionic strength dependence for As(III) on ICS.

whereas inner sphere complexes involve stronger covalent or ionic binding and were weakly affected by the ionic strength (Sparks 1995, Tiwari *et al.*, 2007a).

3.4.4.2. Arsenic(V)

The effect of ionic strength in the removal behaviour of MCS and ICS for As(V) was carried out wherein the background electrolyte i.e., NaNO$_3$ was increased from 0.001 to 1 mol/L and keeping the initial sorptive concentration for these ions at 10 mg/L each and temperature 25^{0}C and pH~5.0. The results obtained were presented in table 55 and 56 along with the graphical representation in figures55 and 56 respectively for MCS and ICS. It can be seen that the increase in ionic strength i.e., from 0.001 to 1 mol/L of $NaNO_3$ caused for decrease in percent removal of As(V) from 57.5 % to 60.0 % (total decrease by 2.5%; for MCS) and 45.07 % to 31.89 % (total decrease by 13.18%;for ICS), respectively. The results show that the 1000 times increase in ionic strength cause an eligible decrease in percent removal of the metal ions. These results clearly inferred that the sorbing ions were firmly bound by the strong forces and forming the inner sphere complexes onto the surface of MCS and ICS. It was reported that outer sphere complexes involve only electrostatic interaction and are strongly affected by ionic strength of the aqueous phase while inner sphere complexes involve stronger covalent or ionic binding and are weakly affected by the ionic strength (Sparks, 1995). The similar results also obtained for the removal of Cu(II) and Pb(II) by sericite (Tiwari *et al.*, 2007a); Ni(II) and Cd(II) by rice straw (El-Sayed *et al.*, 2010).

Table 55: Ionic strength dependence data for As(V) adsorption onto the surface of MCS (pH ~ 5).

Ionic strength $NaNO_3$ (mol/L)	**Initial As(V) conc. (mg/L)**	**Final As(V) conc. (mg/L)**	**Amount adsorbed (mg/L)**	**% Removal**
0.0001	1.98	0.85	1.13	57.07
0.0005	1.98	0.97	1.01	51.01
0.0010	1.98	0.79	1.19	60.10
0.0050	1.98	0.84	1.14	57.58
0.0100	1.98	0.77	1.21	61.11
0.0500	1.98	0.81	1.17	59.09

0.1000	1.98	0.80	1.18	59.60

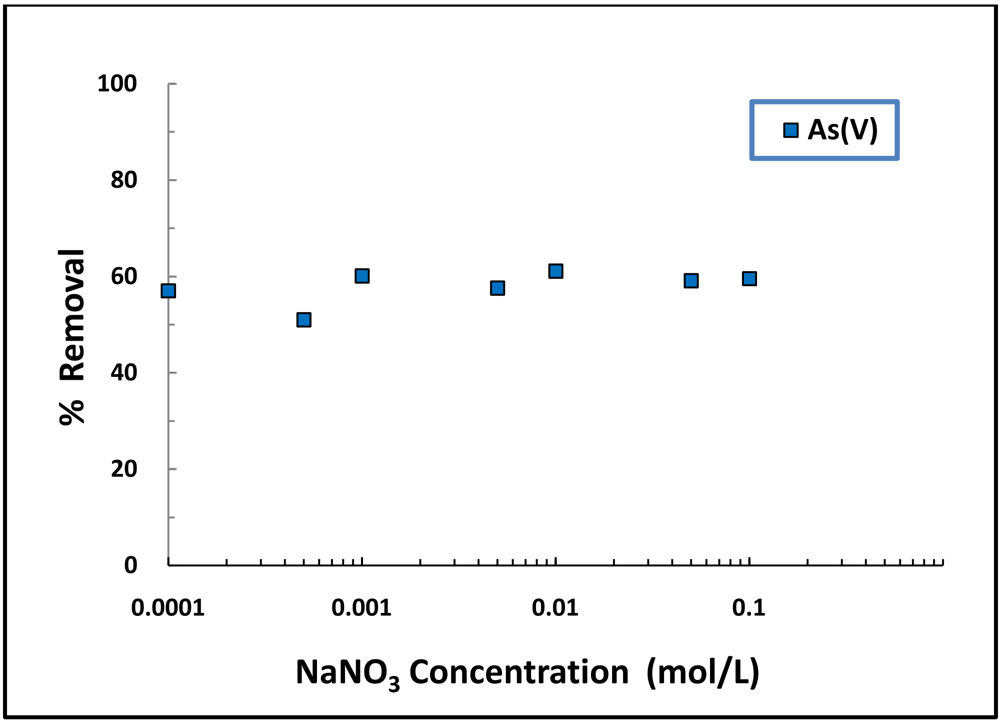

Figure 55: Ionic strength dependence for As(V) adsorption on MCS.

Table 56: Ionic strength dependence data for As(V) adsorption onto the surface of ICS (pH ~ 5.0)

Ionic strength ($NaNO_3$)	**Initial As(V) conc. (mg/L)**	**Final As(V) conc. (mg/L)**	**Amount adsorbed (mg/L)**	**% Removal**
0.001	10.04	5.49	4.55	45.29
0.010	10.04	6.02	4.02	40.09
0.100	10.04	6.13	3.91	38.92

1.000	10.04	6.81	3.23	32.16

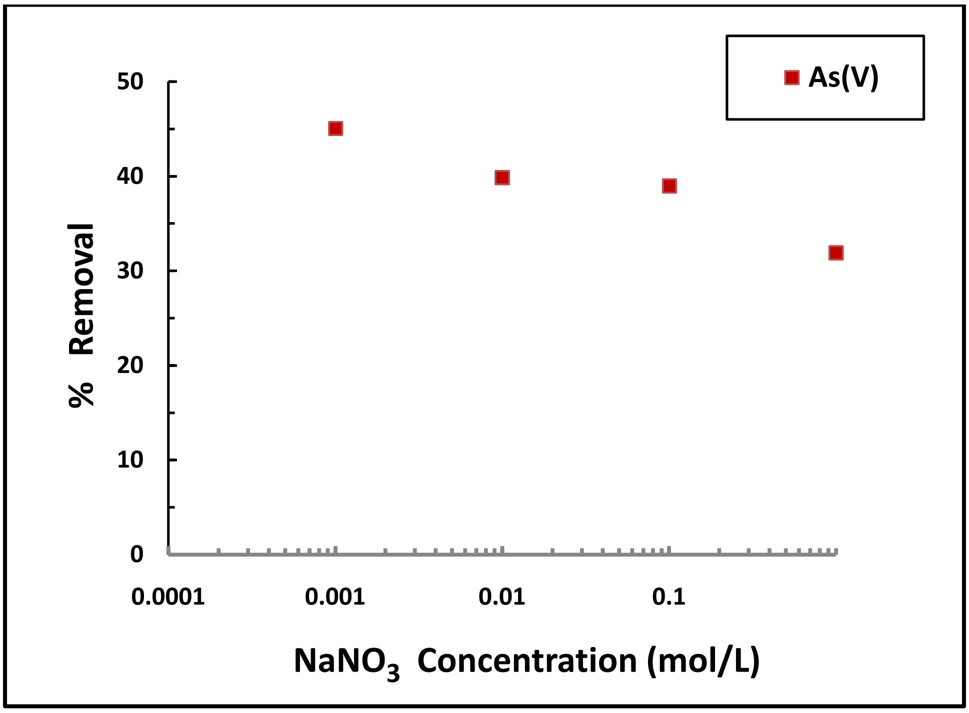

Figure 56: Ionic strength dependence for As(V) on ICS.

3.4.4.3. Cadmium(II)

The ionic strength dependence study was carried out by increasing the background electrolyte from 0.001 to 1.0mol/L NaNO$_3$ and the removal of Cd(II) ions by MCS and ICS was studied keeping the initial sorptive concentration of ~9 mg/L at constant temperature 25^{0}C with constant pH~6.0 (for MCS) and 5.0 (for ICS). The results obtained were shown in Table 57 and 58 which then represented graphically in Figures57 and 58 for MCS and ICS, respectively. It was clearly demonstrated that the increase in ionic strength i.e., from 0.001 to 1.0mol/L of NaNO$_3$ caused for decrease in percent removal from 42.8% to 6.9 % (total decrease by 35.9%; for MCS) and from 45.83 % – 11.69 % (decrease by 34.14%; for ICS), respectively. These results clearly indicated that the increase in ionic strength caused for some decrease in the removal percent. Hence, the sorption of Cd(II) by these solids is associated with some electrostatic attraction partly with chemisorption. The electrostatic adsorption took place by sorbing ion onto the solid surface virtually forming an outer sphere complex, which is affected by ionic strength of the aqueous phase. Similar observations had been reported for ionic strength dependence in sorption of Cd(II) by manganese coated activated carbon (MCAC) where a mixture of inner-sphere and outer-sphere complexation took place in the sorption of Cd(II) by MCAC (Tiwari and Lee, 2011b). A significantly decrease in cadmium sorption on wheat barn with the increase in ionic strength has been reported by Nouri *et al.*, (2007).

Table 57: Ionic strength dependence data for Cd(II) adsorption onto the surface of MCS (pH ~6.0)

Ionic strength ($NaNO_3$) (mol/L)	**Initial Cd(II) conc.(mg/L)**	**Final Cd(II) conc.(mg/L)**	**Amount adsorbed (mg/L)**	**% Removal**
0.001	9.47	5.42	4.053	42.80
0.005	9.42	5.55	3.870	41.10
0.010	9.27	6.77	2.495	26.92
0.050	9.01	7.38	1.635	18.15

0.100	9.50	7.22	2.282	24.02
0.500	9.43	8.64	0.788	8.36
1.000	9.48	8.83	0.647	6.83

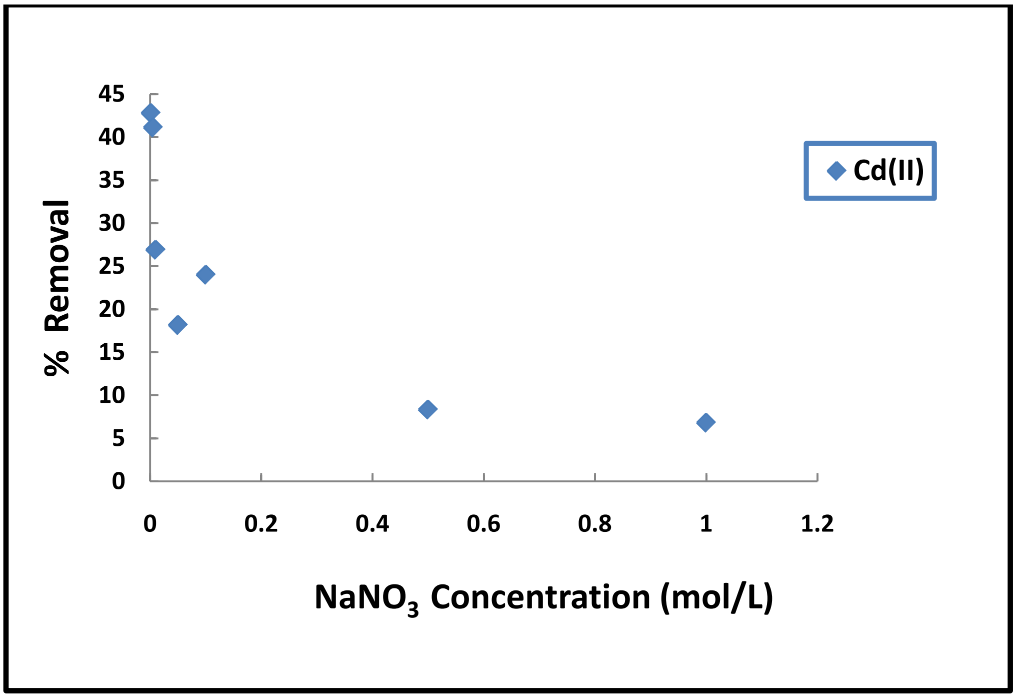

Figure 57: Ionic strength dependence for Cd(II) adsorption on MCS.

Table 58: Ionic strength dependence data for Cd(II) adsorption onto the surface of ICS (pH~5.0)

Ionic strength ($NaNO_3$) (mol/L)	**Initial Cd(II) conc. (mg/L)**	**Final Cd(II) conc. (mg/L)**	**Amount adsorbed (mg/L)**	**% Removal**
0.001	9.56	5.17	4.38	45.83
0.005	9.87	5.47	4.39	44.55
0.010	10.03	6.79	3.23	32.27

0.050	10.23	7.54	2.68	26.25
0.100	10.31	7.44	2.86	27.82
0.500	10.42	9.00	1.41	13.60
1.000	10.10	8.91	1.18	11.69

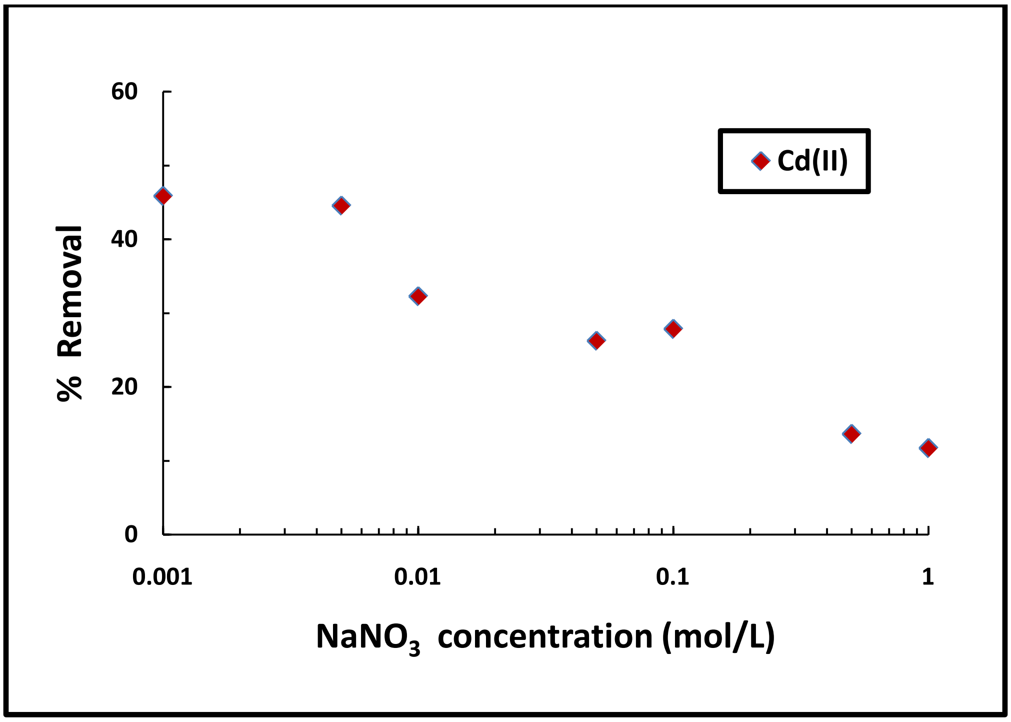

Figure 58: Ionic strength dependence for Cd(II) adsorption on ICS.

3.4.4.4. Copper(II)

Similarly, the ionic strength dependence data was collected for the sorption of Cu(II) by MCS and ICS varying the background electrolyte concentration from 0.0001 to 0.10 mol/L $NaNO_3$. The initial Cu(II) concentration was kept constant as 10.00 mg/L and at temperature 25^0C and pH 4.0. The results obtained from these experiments were given in Tables 59 and 60 for MCS and ICS, respectively. The graphical representations of the result obtained were shown in Figures 59 and 60, for MCS and ICS, respectively. The result clearly revealed that the increase in the ionic strength from 0.0001 to 0.1 mol/L $NaNO_3$ caused for decrease in Cu(II) removal from 50.36 to 34.97% (for MCS; decrease by 15.39) and from 53.5% to 43.51 % (for ICS; decrease by 9.99%), respectively. Results showed that 1000 times increase in background electrolyte concentration caused insignificantly the uptake of Cu(II) by MCS or ICS which inferred that sorbing ions were forming strong bonds and form the inner sphere complexes with the surface of solids along with the ion exchange process (Benjamin and Leckie, 1981; Tiwari *et al.*, 2011b). Likewise, sorption of Cu(II) onto the GMZ betonite was affected by ionic strength only at less than pH 6.5 (Li *et al.*, 2009).

3.4.4.5. Lead(II)

Ionic strength dependence data collected for the sorption of Pb(II) onto the surface of MCS and ICS was carried out varying the background electrolyte concentration from 0.0001 to 0.1 mol/L $NaNO_3$. The initial Pb(II) concentration was kept constant as 10 mg/L, temperature 25^0C and pH ~4.0. Further, the results obtained were shown in Tables 61 and 62 and also represented graphically in Figures 61 and 62, respectively MCS and ICS. The results clearly revealed that the increase in the ionic strength from 0.0001 to 0.1 mol/L caused only for decrease in Pb(II) uptake from 87.94 to 69.81 % (for MCS; total decrease by 18.13%) and from 65.7 % to 22.6 % (for ICS; decrease by 43.1%), respectively. These results clearly indicated that the 1000 times increase in background electrolyte concentration caused for substantial decrease in percent removal of Pb(II) as observed for the solids MCS and ICS. The results supported the mechanism suggested previously (vide reactions 17 – 21) or even the applicability of the Freundlich sorption isotherm. Similar observations have been made by Tiwari *et al.*, (2007b) and El-Sayed *et al.*, (2010). It may be emphasized that Pb(II) was sorbed partly by electrostatic attraction along with the ion exchange process. Eren and Gumus, (2011) reported that the uptake of Pb(II) by Iron oxide coated sepiolite was significantly affected with a decrease while increasing the background electrolyte concentrations which were in line with the present experimental observations.

Table 59: Ionic strength dependence data for Cu(II) adsorption onto the surface of MCS (pH = 4.0)

Ionic strength ($NaNO_3$) (mol/L)	**Initial Cu(II) conc.(mg/L)**	**Final Cu(II) conc.(mg/L)**	**Amount adsorbed (mg/L)**	**% Removal**
0.0001	10.01	4.96	5.04	50.36
0.0005	10.04	5.72	4.31	42.96
0.0010	9.98	5.85	4.12	41.34

0.0050	10.12	6.53	3.58	35.39
0.0100	10.41	7.27	3.13	30.07
0.0500	9.87	7.03	2.83	28.76
0.1000	10.03	6.52	3.50	34.97

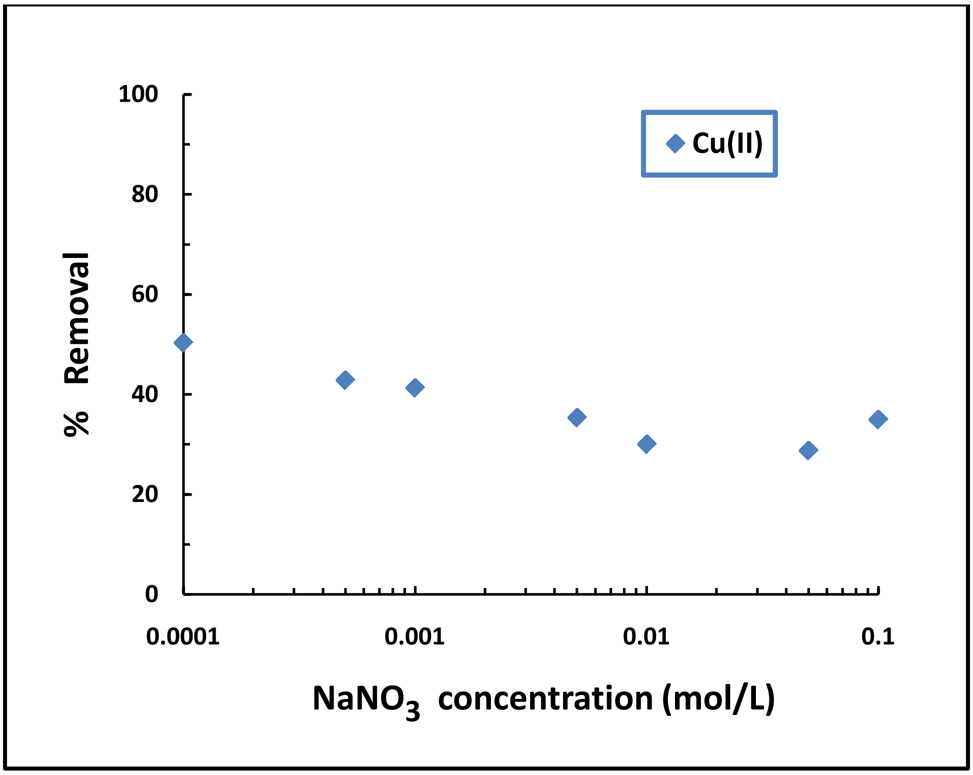

Figure 59: Ionic strength dependence for Cu(II) adsorption on MCS.

Table 60: Ionic strength dependence data for Cu(II) adsorption onto the surface of ICS (pH ~ 5.0)

Ionic strength ($NaNO_3$) (mol/L)	**Initial Cu(II) conc. (mg/L)**	**Final Cu(II) conc.(mg/L)**	**Amount adsorbed (mg/L)**	**% Removal**
0.001	9.885	4.65	5.35	52.96
0.010	10.08	5.04	4.96	50.03

0.100	10.30	5.06	4.94	50.90
1.000	10.21	5.15	4.85	49.56

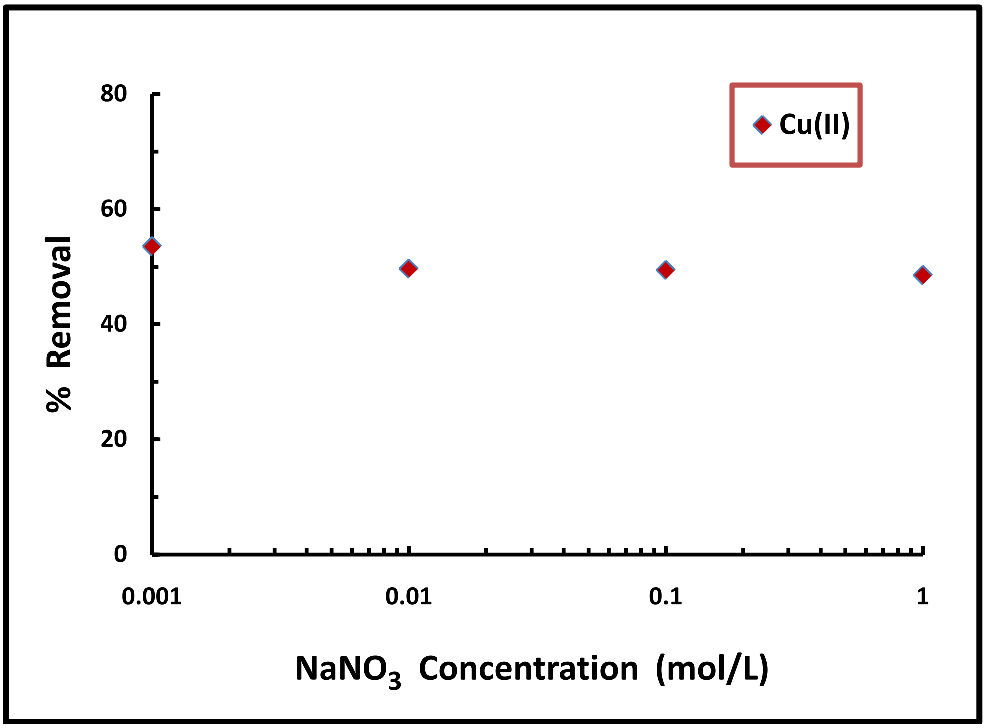

Figure 60: Ionic strength dependence for Cu(II) adsorption on ICS.

Table 61: Ionic strength dependence data for Pb(II) adsorption onto the surface of MCS (pH = 4.0).

Ionic strength ($NaNO_3$) (mol/L)	**Initial Pb(II) conc. (mg/L)**	**Final Pb(II) conc.(mg/L)**	**Amount adsorbed (mg/L)**	**% Removal**
0.0001	19.89	2.39	17.49	87.94
0.0005	20.02	2.99	17.02	85.03
0.0010	20.13	3.75	16.37	81.37

0.0050	20.21	4.42	15.78	78.12
0.0100	20.33	5.33	14.99	73.74
0.0500	20.42	6.82	13.59	66.56
0.1000	20.25	6.11	14.13	69.81

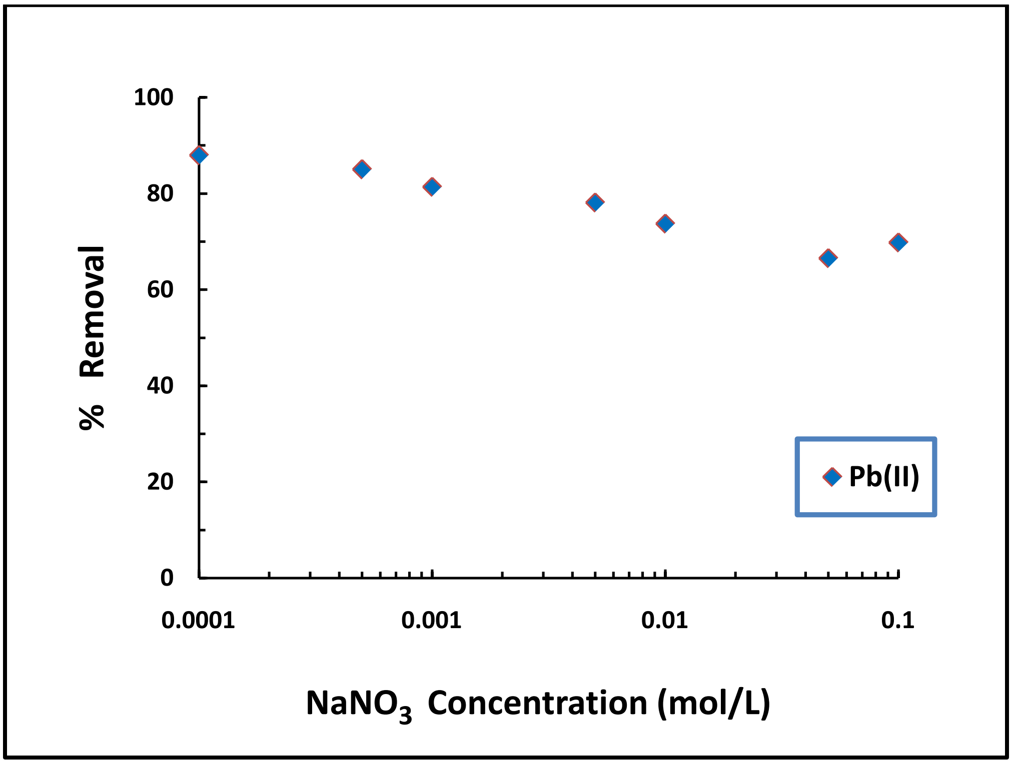

Figure 61: Ionic strength dependence for Pb(II) adsorption on MCS.

Table 62: Ionic strength dependence data for Pb(II) adsorption onto the surface of ICS(pH ~ 4.0).

Ionic strength ($NaNO_3$) (mol/L)	**Initial Pb(II) conc.(mg/L)**	**Final Pb(II) conc.(mg/L)**	**Amount adsorbed (mg/L)**	**% Removal**
0.001	9.16	3.43	5.73	62.55
0.010	10.33	5.69	4.64	44.92

0.100	10.45	7.68	2.77	26.51
1.000	10.36	7.74	2.62	25.29

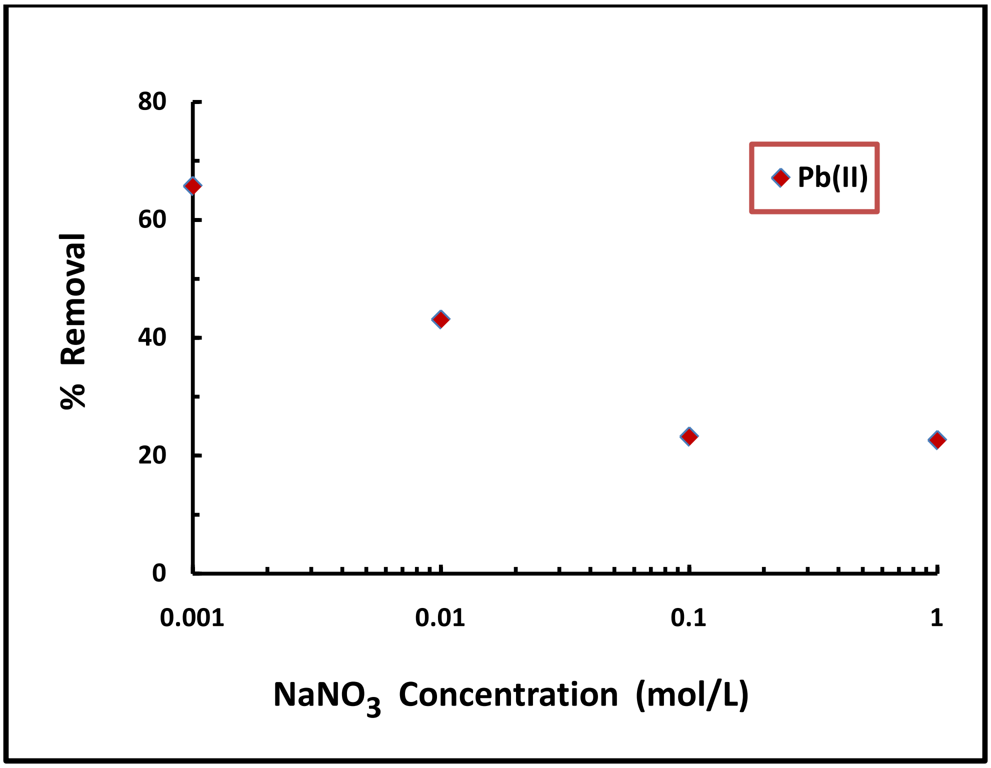

Figure 62: Ionic strength dependence for Pb(II) adsorption on ICS.

3.4.4.6. Summary

The sorption of these metal anions/cations i.e., As(III), As(V), Cd(II), Cu(II) and Pb(II) onto the surface of MCS and ICS was studied by increasing 1000 times the background electrolyte concentration using the $NaNO_3$ solution. The results obtained showed that As(III), As(V) and Cu(II) was insignificantly affected with this 1000 times increase in background electrolyte concentration indicated that these ions were sorbed specifically and forming strong chemical bonds onto the surface of solids MCS and ICS. Hence, the sorption process of these ions mainly governed by the ‘chemisorption’. However, the sorption of Cd(II) and Pb(II) was decreased upto some significant extent by the MCS and ICS indicated that the sorption process not proceeded only with chemisorption but also involved with the electrostatic attraction and partly forming outer sphere complexes onto the surface.

3.4.5. Column experiments

The applicability of fluidized bed reactor (FBR) technique was extensively employed as an alternative method for removal of various water toxins including heavy metal toxic ions (Harns *et al.*, 1992; Aktor 1994; Nielson *et al.*, 1997; Scholler *et al.*, 1987; Wilms *et al.*, 1992). The process of crystallizing $CaCO_3$ in an FBR was applied in softening of drinking water (Harns *et al.*, 1992). The FBR technique was tested at coal-fired power station with wastewater from a flue gas desulphurisation unit in the removal of heavy metals from waste water (Nielson *et al.*, 1997). The adsorptive granules of either FeOOH (ferric oxo-hydroxide) or manganese dioxide were utilized for coating the carrier surface. Furthermore, the removal of heavy metals using FBR by means of crystallization of carbonates was utilized to reduce the disposal of hydroxide sludge and to reduce the cost of metals involved (Scholler *et al.*, 1987; Scholler *et al.*, 1991; Wilms *et al.*, 1992). Therefore, the applicability of the manganese coated sand (MCS) and iron coated sand (ICS) were assessed under the dynamic conditions for the removal of As(III), As(V), Cd(II), Cu(II) and Pb(II)from aqueous solution using the column studies. The breakthrough curves obtained were further analysed using Thomas equation (Thomas 1944).

3.4.5.1. Arsenic(III)

The removal of Arsenic As(III) by MCS and ICS were studied using specified column parameters. The column parameters for MCS was maintained as the influent flow rate: 1.0

mL/min, As(III): 10 mg/L; MCS: 1.0 g and sand 4 g; pH~4.5, whereas in case of ICS the column was packed with 0.5g IC + 2 g of sand; influent flow rate: 1.2 mL/L; As(III):10 mg/L; pH~4.0. The breakthrough curves obtained were shown in Figure 63 and 64 respectively for MCS and ICS.

These figures clearly demonstrated that a gradual increase of C_e/C_0 was obtained with the increase in throughput volume and a complete breakthrough occurred with the throughput volume of 0.6 and 0.4 L respectively for MCS and ICS. The high value of breakthrough volume indicated that MCS or ICS could possess higher removal capacity for the As(III) under the dynamics conditions and showed the potential and promising materials for the removal of As(III). The observations made by Singh *et al.,* (2012) and Yan and Viraraghavan, (2011) using biosorbents revealed that our system is in line with these observations. The observations made by Mandal *et al.,*(2011) have shown that the removal percent was gone upto 98% with low concentration of arsenic(III) in water samples. The arsenic removal using zero valent iron reveals that the removal of arsenic goes even below the detectable level (<1ppb) after 18 months of continuous monitoring (Nikolaidis *et al.,* 2003).

3.4.5.2. Arsenic(V)

The removal of Arsenic As(V) by MCS and ICS were studied using column experiments. The column conditions were maintained as the influent flow rate: 1.0 mL/min, As(III): 10 mg/L; MCS: 1.0 g and sand 4 g; pH~4.5 for MCS, whereas in case of ICS the column was packed with 0.5g ICS+ 2 g of sand; influent flow rate: 1.2 mL/L; As(III):10 mg/L; pH~4.0. The breakthrough curves obtained were shown in Figure 65 and 66 respectively for MCS and ICS. These figures clearly demonstrated that a gradual increase of

C_e/C_0 was obtained with the increase in throughput volume and a complete breakthrough occurred with the throughput volume of 0.7 and 0.4 L respectively for MCS and ICS. Relatively, the high value of breakthrough volume indicated that MCS or ICS could possess higher removal capacity for the As(III) under the dynamics conditions and showed the potential and promising materials for the removal of As(III). Xu *et al.*, (2002) observed a similar high value of breakthrough in the removal of As(V) using aluminium-loaded Shirasu-zeolite (Al-SZP_1).

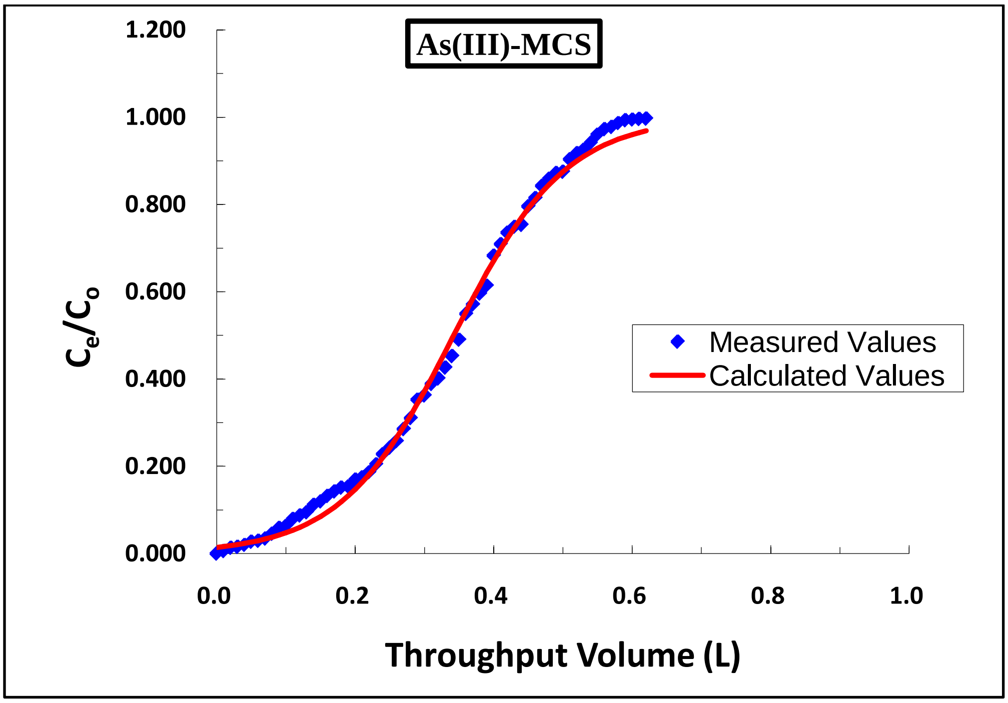

Figure 63: Breakthrough curve for As(III) using MCS packed column.

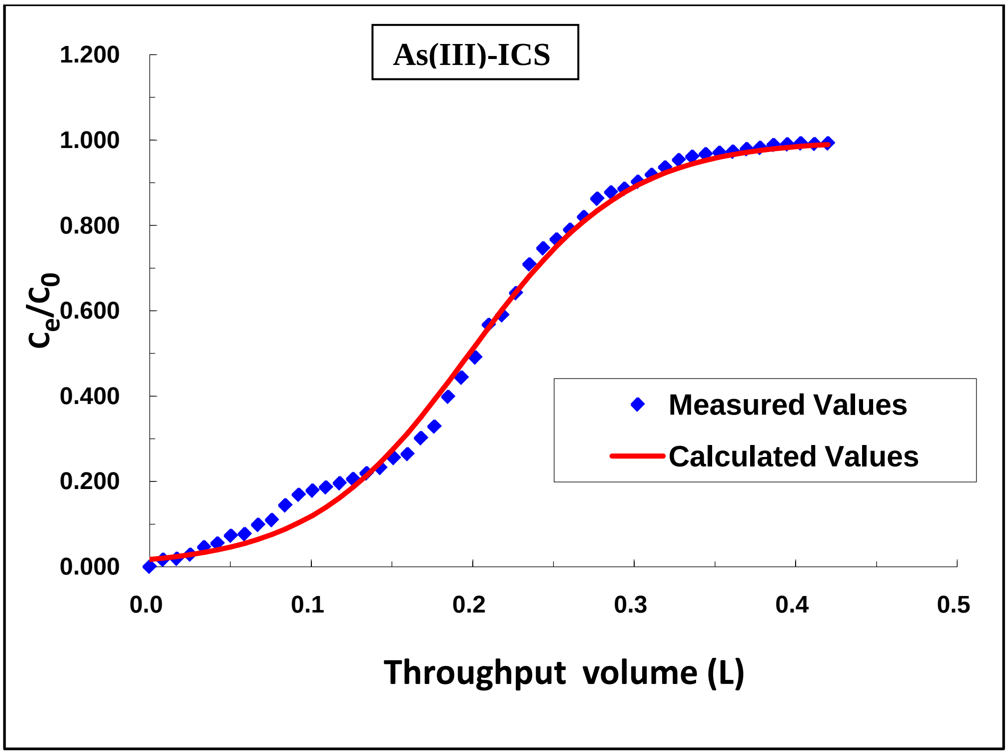

Figure 64: Breakthrough curve for As(III) using ICS packed column.

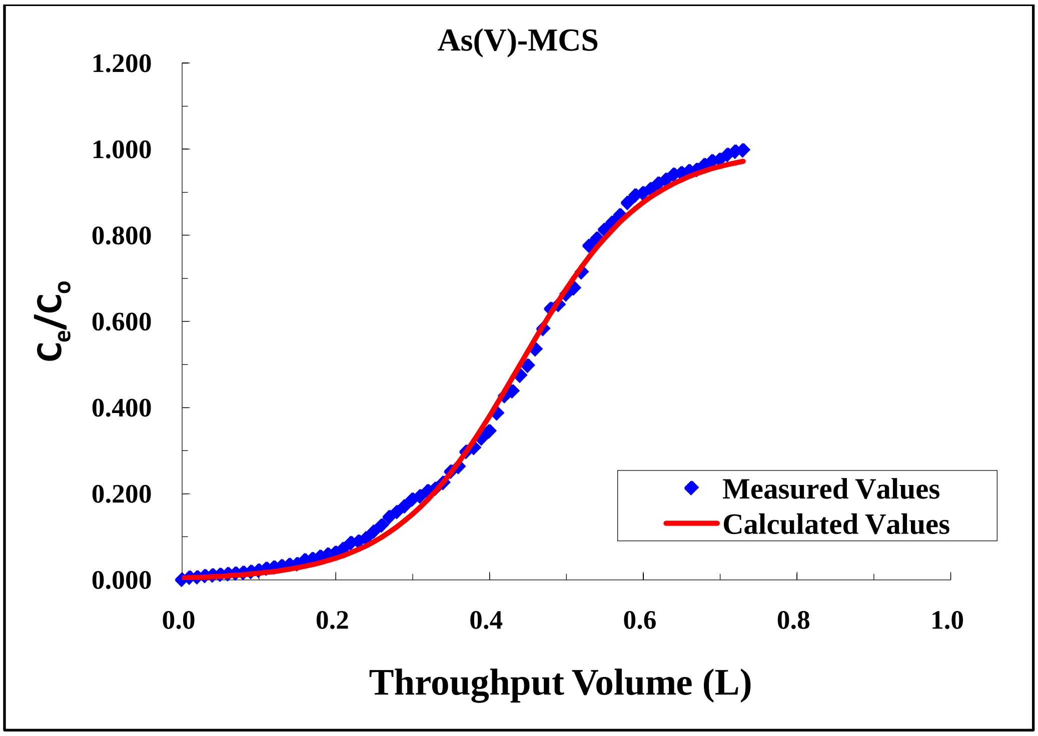

Table 65: Breakthrough curve for As(V) using MCS packed column.

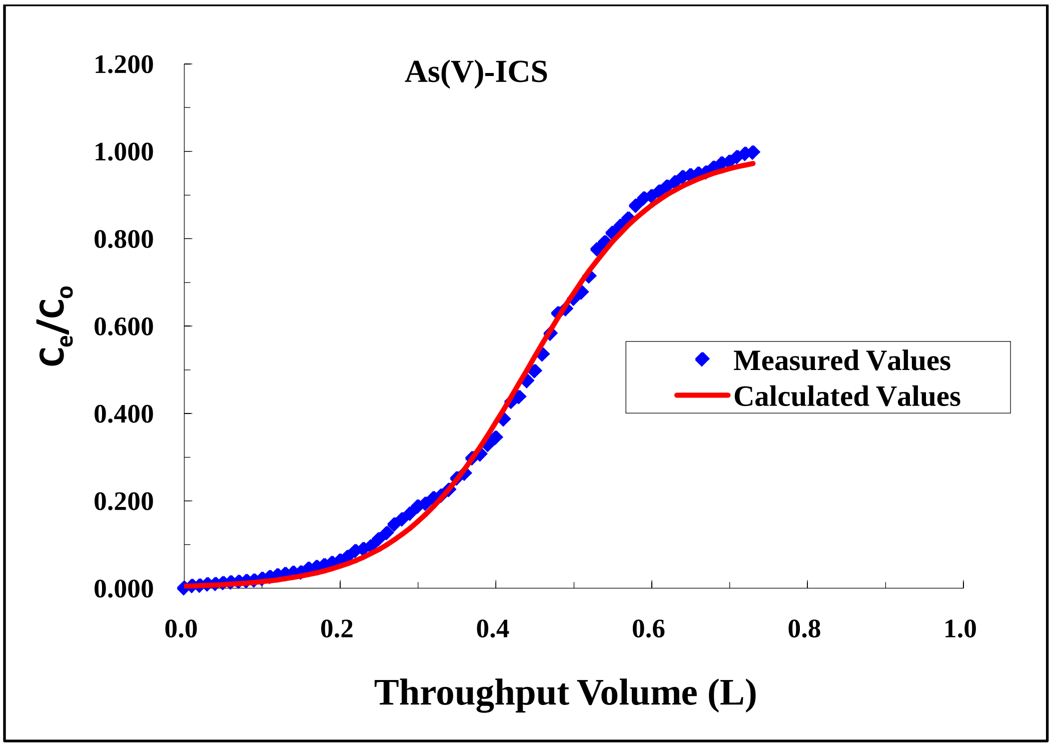

Figures 66: Breakthrough curve for As(V) using ICS packed column.

3.4.5.3. Cadmium(II)

The cadmium(II) removal under the dynamic conditions in the column experiments was performed using MCS and ICS solids. The column conditions were maintained as the influent flow rate: 1.0 mL/min, Cd(II): 10 mg/L; MCS: 1.0 g and sand 4 g; pH~4.5 for MCS, whereas in case of ICS the column was packed with 0.5g ICS+ 2 g of sand; influent flow rate: 1.2 mL/L; Cd(II):10 mg/L; pH~4.0. The breakthrough curves obtained were shown in Figure 67 and 68 respectively for MCS and ICS. These figures clearly demonstrated that a breakthrough starts at 0.12 and 0.18 L, respectively for MCS and ICS. Further, a gradual increase of C_e/C_0 was obtained and almost complete breakthrough was occurred at the throughput volume of 0.85 and 0.64 L respectively for MCS and ICS packed columns. These results indicated that MCS or ICS could possess higher removal capacity for the Cd(II) under the dynamics conditions and showed the potential and promising materials for the removal of Cd(II). Similarly, removal of Cd(II) from the waste of electroplating industry at pH~4.5 using *Spirogyra* biomass packed column (Singh *et al.*,2012).

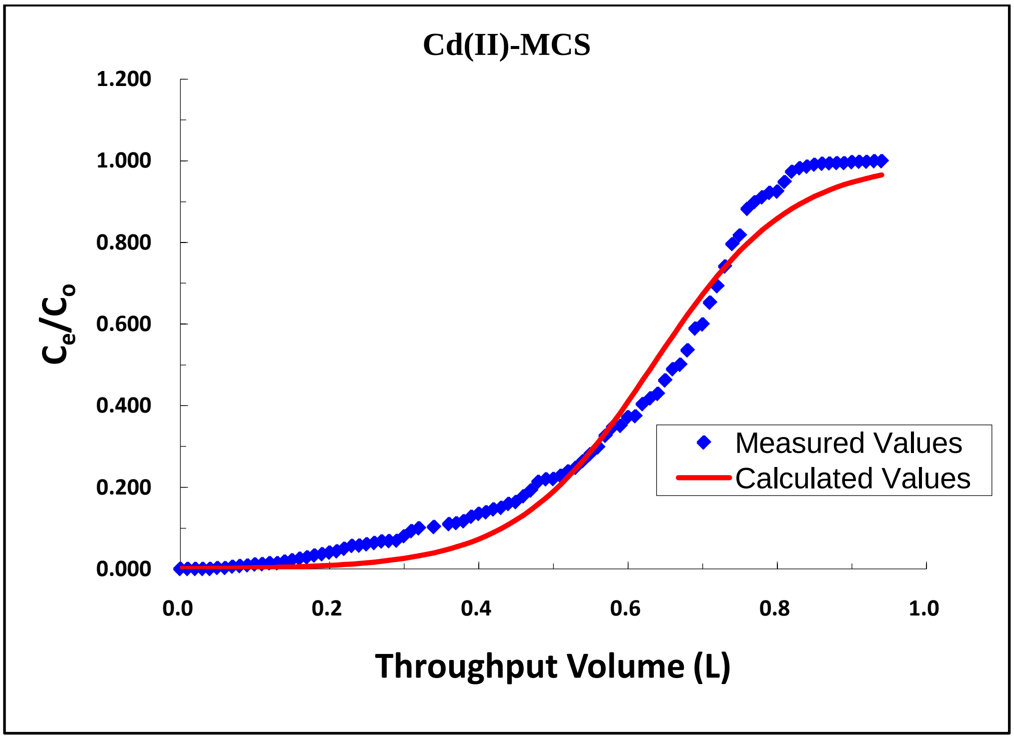

Figure 67: Breakthrough curve for Cd(II) using MCS packed column.

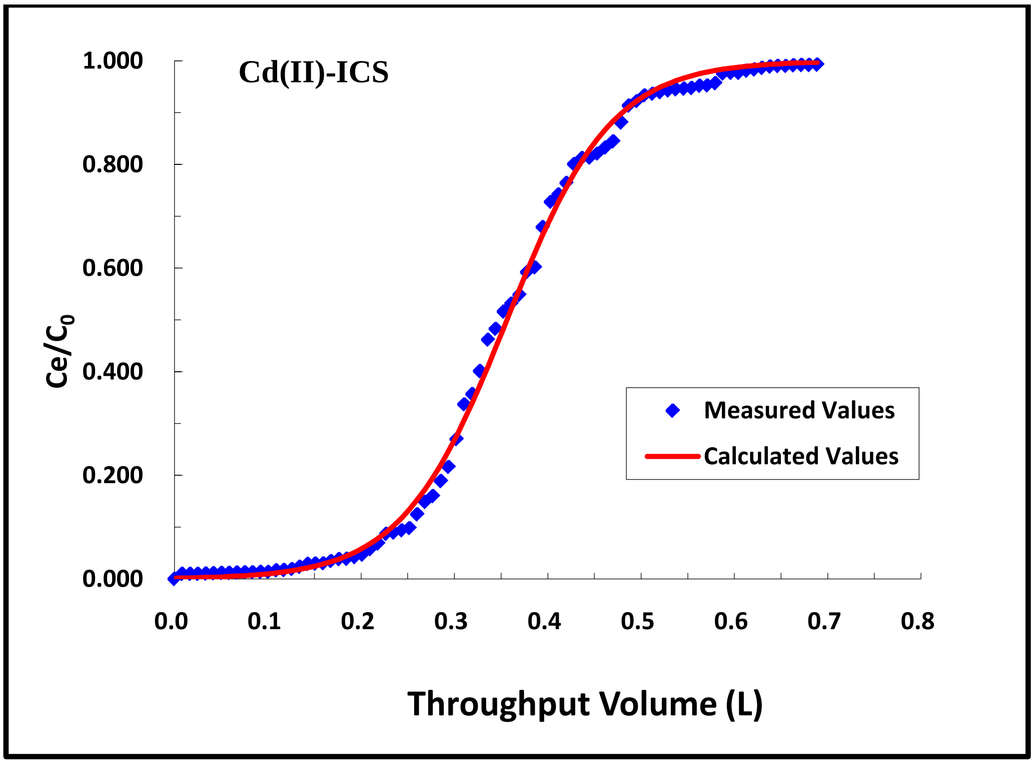

Figure 68: Breakthrough curve for Cd(II) usingICS packed column.

3.4.5.4. Copper(II)

The removal of copper(II) was investigated under the dynamic conditions in the column experiments using the MCS or ICS packed columns. The column conditions were maintained as the influent flow rate: 1.25 mL/min, Cu(II): 10 mg/L; MCS: 0.5 g and sand 2 g; pH~4.5 for MCS, whereas in case of ICS the column was packed with 0.5g ICS+ 2 g of sand; influent flow rate: 1.2 mL/L; Cu(II):10 mg/L; pH~4.0. The breakthrough curves obtained were shown in Figure 69 and 70 respectively for MCS and ICS. These figures clearly demonstrated that a breakthrough started at 0.025 and 0.176 L, respectively for MCS and ICS. Further, a gradual increase of C_e/C_0 was obtained and almost complete breakthrough was occurred at the throughput volume of 0.145 and 0.437 L respectively for MCS and ICS packed columns. These results indicated that MCS or ICS could possess fair affinity towards the Cu(II) even under dynamic conditions. The similar observations were observed by Singh *et al.*, (2012) showed that at pH~ 4.5 a significant removal of metals ions occurred using the biosorbents. However, a significant decrease in the removal was observed pH below 4.0 (Mehta and Gaur, 2005; Singh *et al.*, 2007; Kumar and Gaur, 2011).

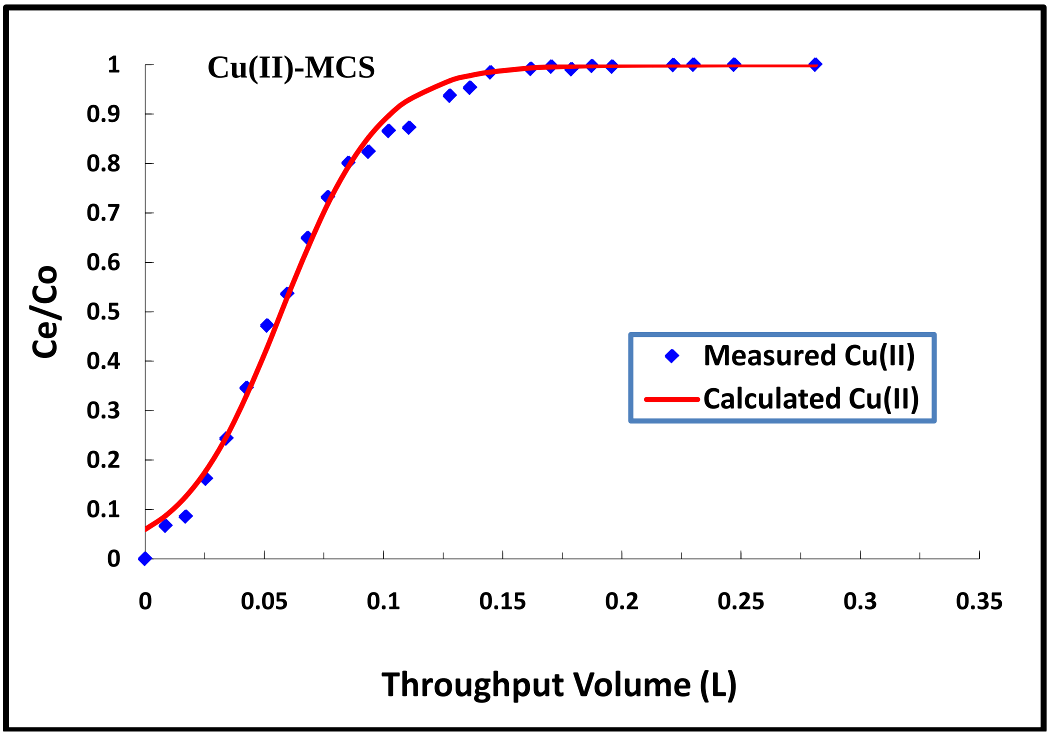

Figure 69: Breakthrough curve for Cu(II) using MCS packed column.

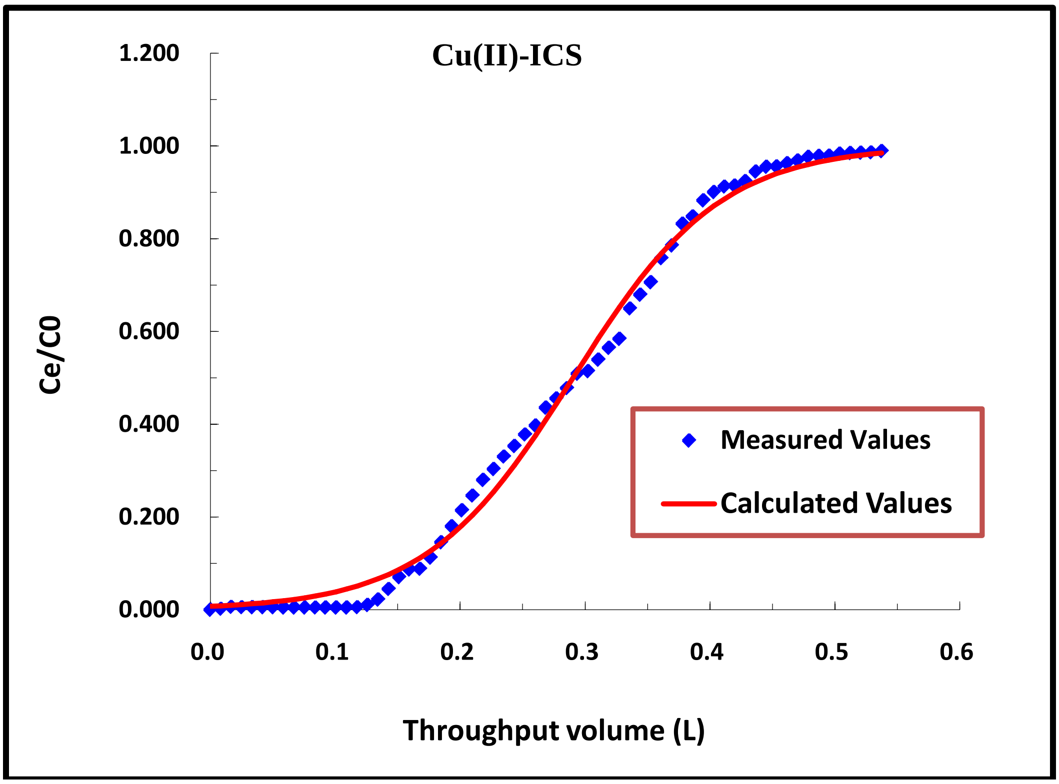

Figure 70: Breakthrough curve for Cu(II) using ICS packed column.

3.4.5.5. Lead Pb(II)

The removal of lead(II) was studied under the dynamic conditions in the column experiments using the MCS or ICS packed column.The column conditions were maintained as the influent flow rate: 1.25 mL/min, Pb(II): 10 mg/L; MCS: 0.5 g and sand 2 g; pH~4.5 for MCS, whereas in case of ICS the column was packed with 0.5g ICS+ 2 g of sand; influent flow rate: 1.2 mL/L; Pb(II):10 mg/L; pH~4.0. The breakthrough curves obtained were shown in Figure 71 and 72 respectively for MCS and ICS. These figures clearly demonstrated that a breakthrough started at 0.137 and 0.428 L, respectively for MCS and ICS. Further, a gradual increase of C_e/C_0 was obtained and almost complete breakthrough was occurred at the throughput volume of 0.225 and 0.806 L respectively for MCS and ICS packed columns. These results indicated that MCS or ICS could possess high affinity towards the Pb(II) even under dynamic conditions which showed potential of these solids towards the Pb(II) removal.

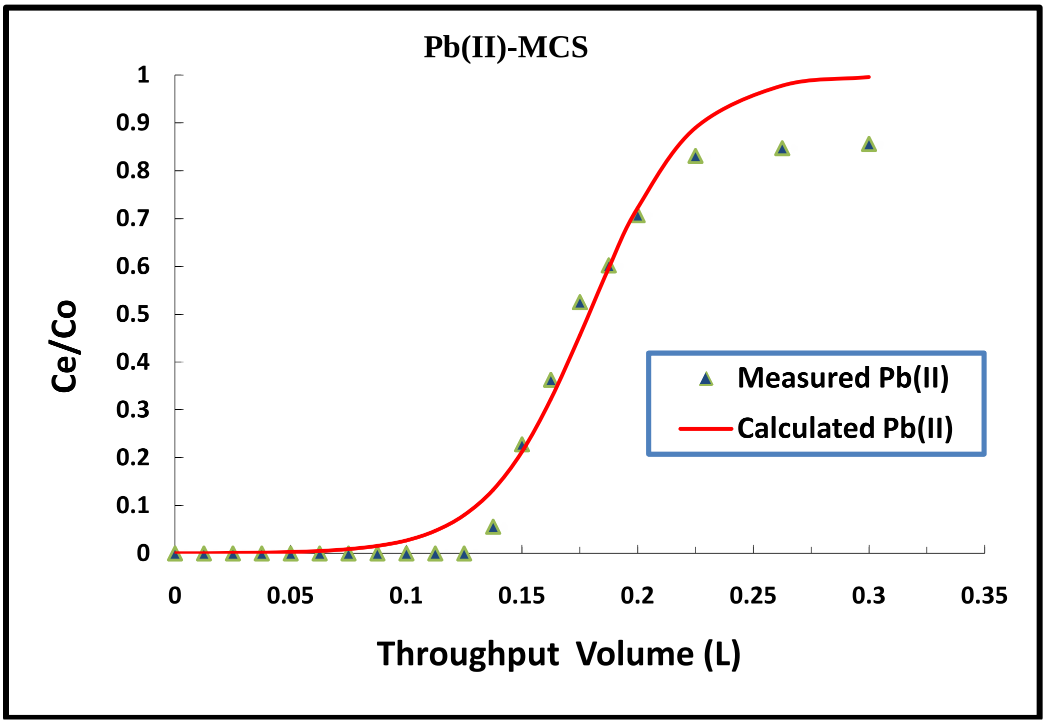

Figure 71: Breakthrough curve for Pb(II) using MCS packed column.

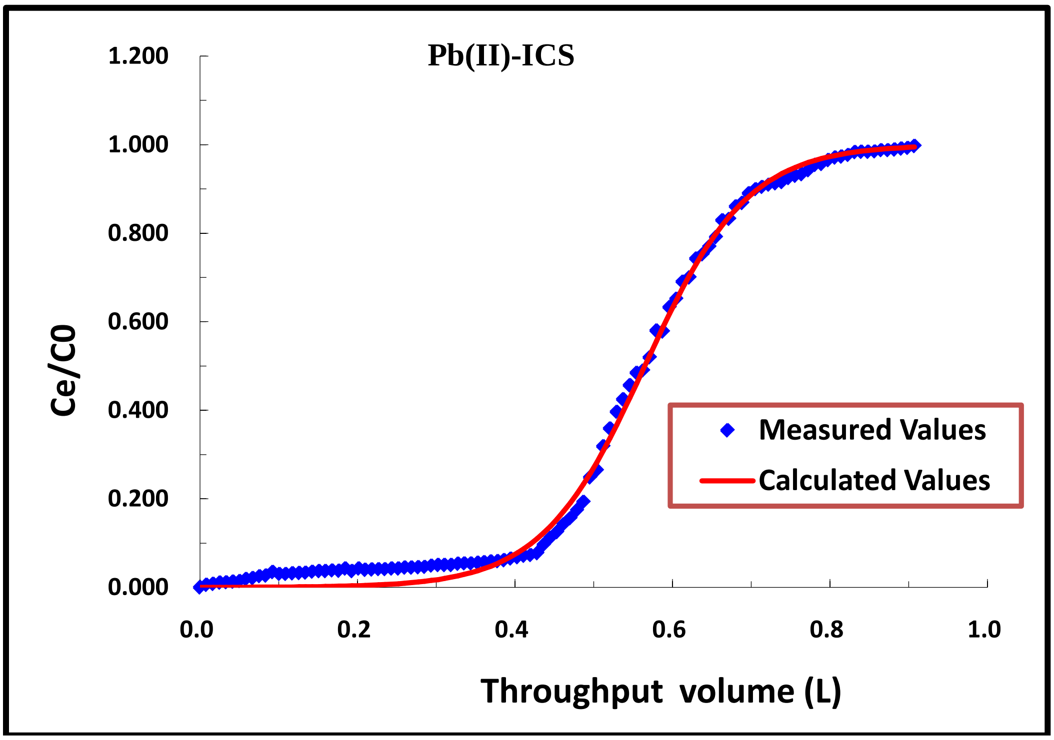

Figure 72 : Breakthrough curve for Pb(II) using ICS packed column.

3.4.6. Thomas Simulation

The breakthrough data obtained for the studied systems i.e., As(III), As(V), Cd(II), Cu(II) and Pb(II) using MCS and ICS solids were further utilized to the non-linear fitting of Thomas equation (11). The least square fitting was conducted, independently for these systems, as to estimate the two unknown parameters i.e., q_0 and K_T which referred respectively to maximum amount of metal ions to be loaded under the specified column conditions and Thomas rate constant. Further, the fitting curves were shown as calculated values in the figures shown above. These curves showed that reasonably a good fitting was obtained for these systems, since the least square sums obtained in the range of 10^{-2} to 10^{-3}. Similar results were also reported previously for the biosorbents or manganese coated sands etc. (Tiwari *et al.*, 2011; Singh *et al.*, 2012; Yan and Viraraghavan, 2011). The estimated values of the Thomas constants i.e., the q_0 and K_T were obtained and returned in Tables 63 and 64 respectively for MCS and ICS solids. The solids showed fairly strong affinity towards these metal ions since relatively high removal capacity was obtained for these metal ions. It was observed that MCS and ICS showed almost identical removal capacity at least for the As(III), As(V) and Cd(II). However, ICS possessed very high loading capacity for the Cu(II) and Pb(II). This may be because of the influent pH used for MCS, which was low comparing to influent pH employed for ICS. Moreover, the batch data inferred that decreasing the pH caused for significant decrease in the removal of these cations. In general the loading capacity observed for MCS was found to be Cd(II)>As(V)>As(III)>Pb(II)>Cu(II).

Table 63: Thomas constants for the removal of As(III), As(V), Cd(II), Cu(II) and Pb(II) by MCS

Metal ions	**q_0 (mg/g)**	**K_T (L/min/mg)x10^{-3}**
As(III)	3.37	1.25
As(V)	4.38	1.23
Cd(II)	6.29	1.09
Cu(II)	0.19	1.42
Pb(II)	0.89	5.67

Table 64: Thomas constants for the removal of As(III), As(V), Cd(II), Cu(II) and Pb(II) by ICS

Metal ions	**q_0 (mg/g)**	**K_T (L/min/mg)x10^{-3}**
As(III)	3.96	2.46
As(V)	4.29	2.93
Cd(II)	7.13	2.14
Cu(II)	5.81	2.03
Pb(II)	11.3	1.83

Similarly, the trend obtained for ICS was found to be Pb(II) > Cd(II) > Cu(II) > As(V) >As(III). Previous studies showed that the biomass *Spirogyra*-packed column possessed the removal capacity of 18.87 and 29.50 mg/g respectively for the Cu(II) and Pb(II) at relatively low flow rate of 0.6 mL/min (Singh *et al.*, 2012). On the other hand the biomass *Macrophthalmusrouxii* showed the removal capacity of 4.06 (at the flow rate 2.28 mL/min) and 1.25 mg/g (at the flow rate 2.60 mL/min), respectively for the Pb(II) and Cd(II) (Yan and Viraraghavan, 2011). In fact, very low value of Thomas rate constant i.e., in the order of 10^{-3}(L/min/mg) is an indicative of efficient and higher affinity of these solids towards the employed pollutants.

3.4.6.1. Summary

The removal capacity of MCS and ICS were investigated under the dynamic conditions as to assess the practical removal capacity of these solids for the metal ions studied. It was revealed that a high value of throughput volume required for the complete breakthrough for these cations/or anions hence could be a potential and promising solids for such applications. Moreover, the breakthrough data was fitted well to the Thomas equation. The column loading capacity was estimated by the least square fitting non-linear Thomas equation. Very high loading capacity obtained for these metal ions studied using MCS or ICS inferred that these two materials are found to be efficient and perhaps alternative materials, which could show promising and efficient for the treatment of waste/effluent waters contaminated with these pollutants.

REMOVAL BEHAVIOUR OF IRON COATED SAND (ICS) AND MANGANESE COATED SAND (MCS) FOR HEAVY METAL TOXIC IONS FROM AQUEOUS SOLUTIONS

CHAPTER

4

Conclusions

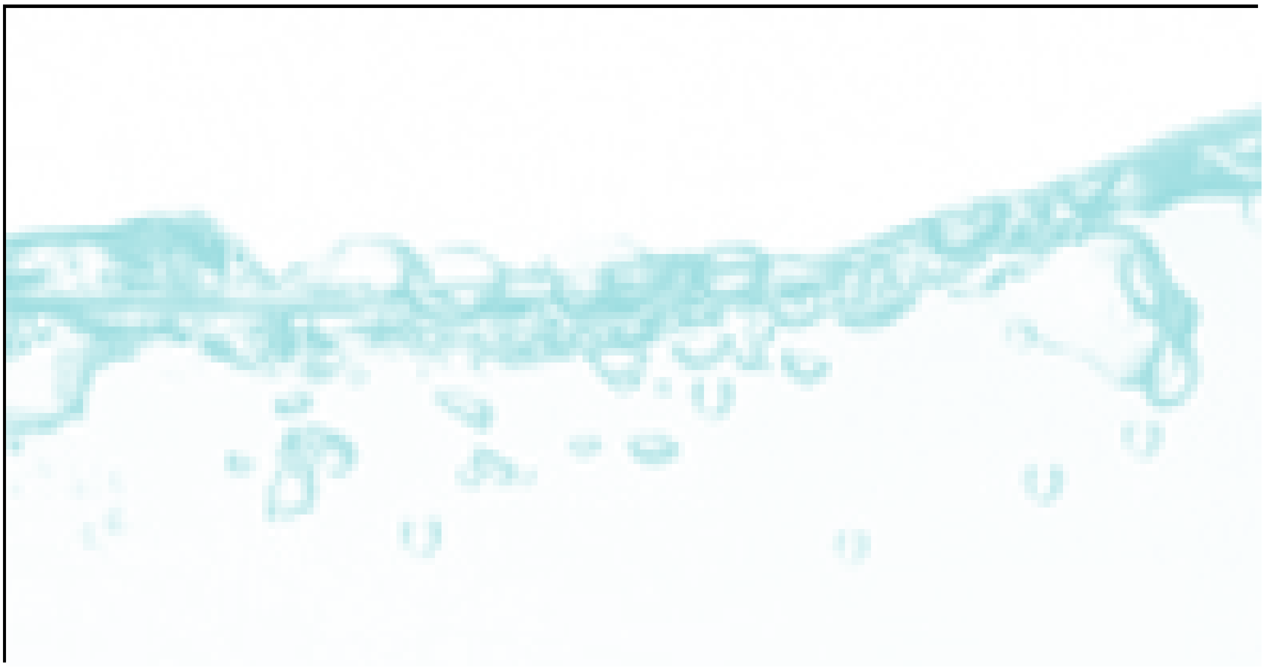

CONCLUSIONS

The natural sand was fully exploited in order to obtain the manganese coated and iron coated sand materials. The impregnation of manganese and iron was carried out by using the cleaned and activated surface of sand in the laboratory. It was observed that manganese and iron oxides were aggregated onto the surface of sand forming very ordered small sized or even nano-sized particles which were evenly distributed onto the surface of sand. The size of these particles was estimated to be 200–300 nm. The materials were morphologically characterized by the SEM/EDX and XRD analyses. The characteristic diffraction peaks of silica were observed with XRD data. Moreover, the low content of iron or manganese onto the sand surface was perhaps caused for distinct diffraction peaks. However, the EDX analytical data showed the presence of manganese and iron onto MCS and ICS samples. Further, the stability of these impregnated solids was assessed towards the stability tests at wide range of pH (pH 2 to 10) studies and it was observed that the coating is fairly stable within the pH region 2.5 to 10.0. The amount of manganese or iron coated onto the surface of sand was obtained by the standard US EPA method 3050B and it was found to be 1446 mg/Kg for manganese onto MCS; whereas 5700 mg/Kg for iron onto ICS sample. The BET specific surface area analysis showed that MCS and ICS possessed with significantly higher surface area comparing to the bare sand samples. The observed specific surface area was found to be 8.51, 11.03, 11.12 m^2/g respectively for sand, MCS and ICS samples. The acid and base titrations studies were carried out in order to obtain the pH_{ZPC} (point of zero charge) and it was found to be 6.28 and 6.23 respectively for MCS and ICS.

The MINEQL geochemical computer simulation program were conducted using the known thermodynamic data to observe the speciation of the metal ions studied i.e., Cr(VI), As(III), As(V), Cd(II), Cu(II) and Pb(II). The speciation results were further introduced, deducing the mechanism involved at solid/solution interface in the adsorption studies.

Further, these solids i.e., MCS and ICS were assessed for the low level removal of several heavy metal toxic ions *viz.*, Cr(VI), As(III), As(V), Cd(II), Cu(II) and Pb(II) from aqueous solutions under batch reactor operations. The column reactor operation was however, conducted for the metal ions As(III), As(V), Cd(II), Cu(II) and Pb(II) using the MCS or ICS packed columns. The batch experiments were performed for various parametric studies *viz.*, effect of sorptive pH, concentration and ionic strength. The sorptive dependence equilibrium data was further modelled to the Feundlich adsorption isotherm and the Freundlich constants were evaluated for these systems.

Batch studies implied that manganese coated sand and iron coated sand was found to be suitable materials for the low level removal of Cr(VI), Cd(II), Cu(II),Pb(II), As(III) and As(V) ions from aqueous solutions. The pH dependence data, which enabled to deduce the mechanism involved at solid/solution interface, was shown that the uptake of these pollutant ions greatly dependent to the solution pH.The results showed that the lower pH range favoured the uptake of anions i.e., Cr(VI), As(III) and As(V) by these solids. However, the high uptake of Cr(VI) onto ICS was almost unaffected with pH. On the other hand, the uptake of cations viz., Cd(II), Cu(II) and Pb(II) were favoured at higher pH regions. Moreover, the pH_{PZC} of these two solids (MCS and ICS) was greatly affected the uptake of these cations. Above the pH_{ZPC} a greater extent of these cations were removed. Therefore, it was assumed that in addition to the electrostatic attraction, apparently a chemisorptive uptake could take place via ‘ion-exchange’ process or a complexation reaction could place between these cations and solid surfaces. Hence, an inner sphere bonding of metal cations could possibly take place with surface -OH group available with the MCS or ICS. Further, at very high pH values i.e., around 8-10, very high uptake of these cations occurred which could perhaps the simultaneous occurrence of adsorption and co-precipitation of metal ions on to the surface of solids.

The concentration dependence data obtained varying the sorptive concentration at constant pH and temperature. The results obtained in general showed that with the increase in concentration, the amount uptake of these ions i.e., Cr(VI), As(III), As(V), Cd(II), Cu(II) and Pb(II) was apparently increased using MCS or ICS samples. However, the similar increase in sorptive concentration caused for a gradual decrease in percent uptake of these ions. Further, the equilibrium state concentration dependence data was employed to model it for the linearized the Freundlich adsorption isotherm equation. It was found that these systems follow well the Feundlich adsorption isotherm since a good fitting of data was obtained for the systems studied. The applicability of Freundlich equation pointed it again for the chemisorptive type adsorption of metal ions onto the surface of solids. Moreover, the sorbed ions were perhaps interacting laterally. Moreover, MCS showed relatively higher removal capacity than the ICS. Further, both these solids showed maximum removal capacity for Pb(II). The fractional values of Freundlich constants '1/n' obtained for all these systems studied (except Cr(VI) onto MCS) showed to the heterogeneous nature of the solid surface along with the exponential distribution of energy of the adsorption sites.

The sorption of these metal anions/cations i.e., As(III), As(V), Cd(II), Cu(II) and Pb(II) onto the surface of MCS and ICS was studied by increasing 1000 times the background electrolyte concentration using the $NaNO_3$ solution. The results obtained showed that As(III), As(V) and Cu(II) was insignificantly affected with this 1000 times increase in background electrolyte concentration indicated that these ions were sorbed specifically and forming strong chemical bonds onto the surface of solids MCS and ICS. Hence, the sorption process of these ions mainly governed by the 'chemisorption'. However, the sorption of Cd(II) and Pb(II) was decreased up to some significant extent by the MCS and ICS indicated that the sorption process not proceeded only with chemisorption but also involved with the electrostatic attraction and partly forming an outer sphere complexes onto the surface of solids.

The column experiments carried out for As(III), As(V), Cd(II), Cu(II) and Pb(II) with MCS and ICS solids. Hence, the dynamic experiments under experiments enabled to obtain the breakthrough. The breakthrough curves therefore, showed a significant breakthrough volume required for these metal ions indicated a strong affinity of these solids for the removal of these cations/anions. Moreover, the breakthrough data was fitted well to the Thomas equation. The column loading capacity was estimated by the least square fitting of non-linear Thomas equation. Very high loading capacity obtained for these metal ions studied using MCS or ICS inferred that these two materials are found to be efficient and perhaps alternative materials in the effective treatment of waste/effluent waters contaminated with these pollutants.

From the present investigations carried out, it can be concluded that the manganese coated sand (MCS) and iron coated sand (ICS) were proved to be the effective materials for purification of waste waters contaminated with these heavy metal toxic ions even up to low level concentrations.

REMOVAL BEHAVIOUR OF IRON COATED SAND (ICS) AND MANGANESE COATED SAND (MCS) FOR HEAVY METAL TOXIC IONS FROM AQUEOUS SOLUTIONS

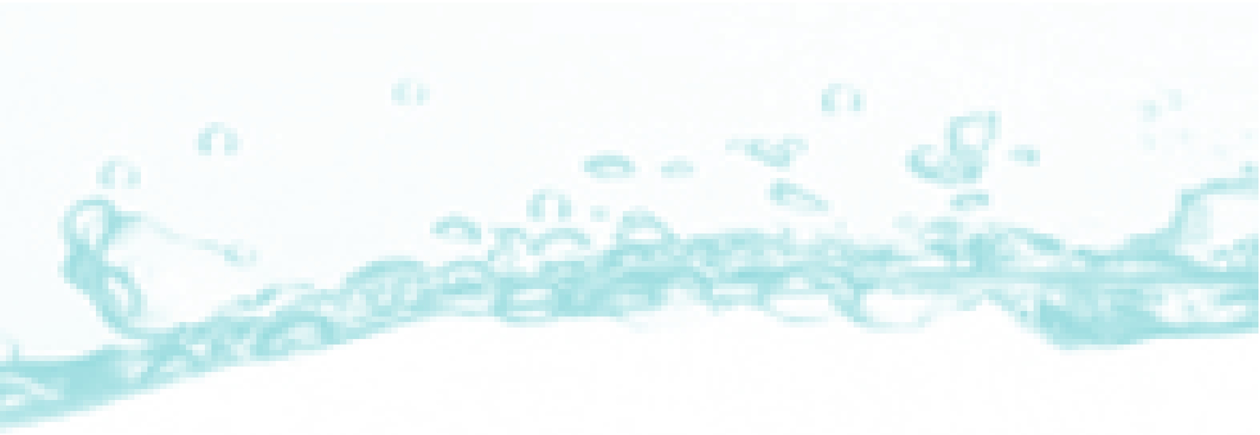

References

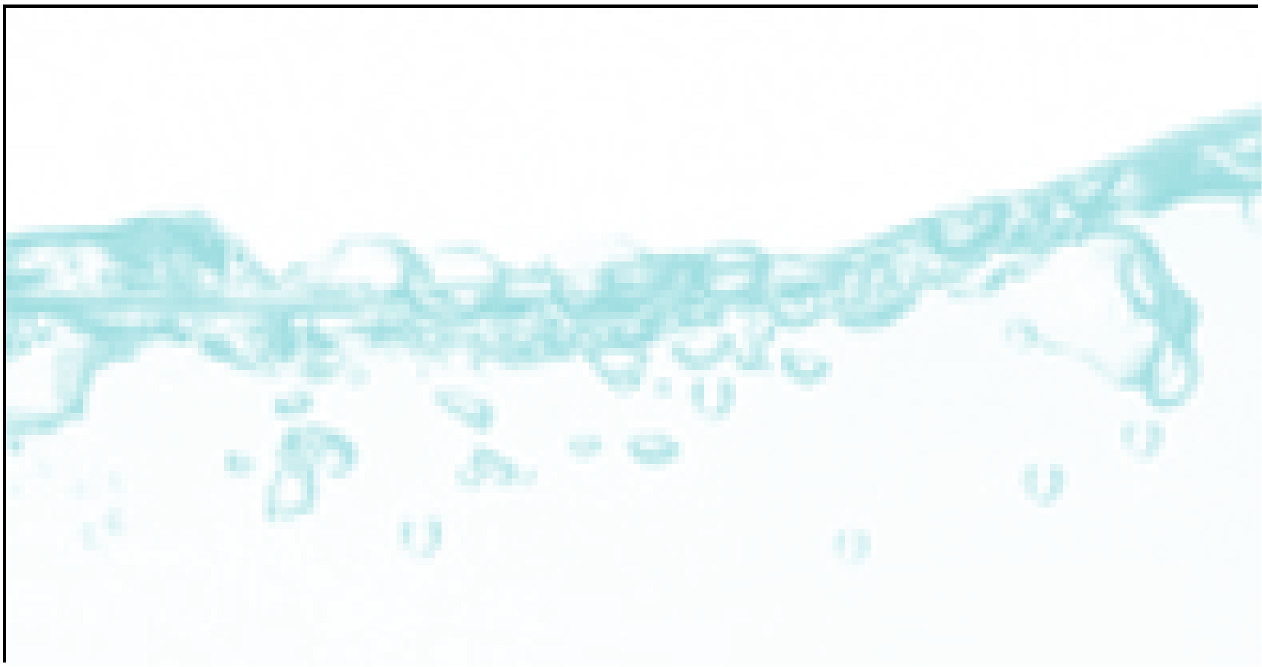

REFERENCES

Absorption Chemistry, 2010. Memidex (WordNet) Dictionary/Thesaurus.

Adria-Cerezo, D.M., Llobat – Estelles, M., Mauri – Aucejo, A.R., 2000. Pre-concentration and speciation of Cr in waters using solid – phase extraction and atomic absorption spectrometry, ***Talanta*, 51:** 531 – 536.

Agarwal, A., Sahu, K. K., 2006. Kinetic and isotherm studies of cadmium adsorption on manganese nodule residue**.** ***J. Haz. Mat.*, B137:** 915 – 924.

Ahluwalia, S.S., Goyal, D., 2007. Microbial and plant derived biomass for removal of heavy metals from wastewater, ***Bioresour. Technol.*,98:** 2243 – 2257.

Ahmad, S.M., 1969. Studies of the double layer at oxide – solutions interface. ***J. Phys. Chem.*, 73(11):** 3546 – 3555.

Aigrain, P., Dugas, C., 1952. ***Z. Electrochem.*, 56:** 363.

Ajmal, M., Khan, A.H., Ahamad, S., Ahmad, A., 1998. Role of saw dust in the removal of Copper(II) from industrial Wastes. ***Water Res.*, 32(10):** 3085 – 3091.

Aksoyoglu, S., 1989. ***J. Radional. Nucl. Chem.*, 134:** 392.

Aksu, Z., 2002. Determination of the equilibrium, kinetic and thermodynamic parameters of the batch biosorption of lead(II) ions onto *Chlorella vulgaris*, ***Process Biochem.*, 38**: 89 – 99.

Aktor, 1994. Continous high rate removal of chromate in a fluidized bed without sludge generation, ***Wat. Sci. Technol.*, 30(7):** 31 – 40.

Alfarra, A., Frackowiak, Bui, F., 2004. Application of the HSAB concept to the adsorption of metal ions on activated carbons, ***Appl. Surface Sci.*, 228**: 84–92.

Al-Degs, Y., Khraisheh, M.A.M., 2000 The feasibility of using diatomite and Mn – diatomite for remediation of Pb^{2+}, Cu^{2+} and Cd^{2+} from water, ***Sep. Sci. Technol.*,**

35:2299 – 2310.

Alley, E.R., 2000 & 2002, Water Quality Control Handbook, Mc Graw Hill Publication.

Amdur, M. O., Doull, J., Klaasen, C., 1991. Casarett and Doull’s Toxicology, the Basic science of poisons. Pergamon press, New York PP.639 – 643.

An, B. R., Steinwinder, T. R, Zhao, D. Y., 2005. Selective removal of arsenate from drinking water using a polymeric ligand exchanger, ***Wat. Res.,*** **39:** 4993 – 5004.

An, H.K., Park, B.Y., Kim, D.S., 2001. Crab shell for the removal of heavy metals from aqueous solution, ***Water Res.,*** **35:** 3551 – 3556.

Aoshima, K., Fan, J., Cai, Y., Katoh, T., Teranishi, H., Kasuya. M., 2003. Assessment of bone metabolism in cadmium-induced renal tubular dysfunction by measurements of biochemical markers, ***Tox. Lett.,*** **136:** 183 – 192.

Arai, Y., Elzinga, E.J., Sparks, D.L., 2001. X - ray adsorption spectroscopic investigation of arsenite and arsenate adsorption at the aluminum oxide-water interface, ***J. Colloid Interface Sci.,*** **235:** 80 – 88 .

Bailey, R.P., Bennett, T., Benjamin, M.M., 1992. Sorption onto and recovery of Cr(VI) using iron oxide-coated sand***, Wat. Sci. Technol.,*** **26:**1239 – 1244.

Balasubramanian, S., Pugalenthi, V., 1999. Determination of total Cr in tannery wastewater by inductively coupled plasma–atomic emission spectrometry, flame atomic absorption spectrometry and UV – visible spectrometric methods, ***Talanta,*** **50:** 45 –467.

Bamsforth, Manning, D.A.C., Singleton, L., Younger, P.L., Johnson, K.L., 2006. Manganese removal from mine waters; investigating the occurrence and importance of manganese carbonates, ***Appl. Geochem,*** **21:** 1274 – 1287.

Bang, S., Korfiatis, G.P., Meng,X., 2005 (a). Removal of arsenic from water by zero-valent iron***, J. Hazard. Mater.,*** **121:** 61–67.

Bang, S., Johnson, M.D., Korfiatis, G.P., Meng, X., 2005 (b). Chemical reactions between arsenic and zero-valent iron in water, ***Wat. Res.,*** **39:** 763–770.

Baral, A.., Engelken, R.D. 2002 . Chromium - based regulations and greening in metal finishing industries in the USA, ***Environ. Sci. Policy,*** **5:**121 – 133.

Barbee, J.Y.J., Prince, T. S., 1999. Acute respiratory distress syndrome in a welder exposed to metal fumes, ***South Med. J.,*** **92(5):** 510 – 512.

Barrow, N.J., Bowden, J.W., Posner, A.M., Quirk, J.P., 1980. Describing the effects of electrolyte on adsorption of phosphate by a variable charge surface, ***Australian J. Soil Res.,*** **18:** 395 – 404.

Baskan, M.B., Pala, A., 2009. Determination of arsenic removal efficiency by ferric ions using response surface methodology, ***J. Hazard. Mater.,*** **166:** 796–801.

Benaissa, H., Elouchdi, M.A., 2007. Removal of Copper ions from Aqueous Solutions by Dried Sunflower Leaves. ***Chem. Eng. Process.,*** **46(7):** 614 – 622.

Benjamin, M. M., Leckie, J. O., 1981(a). Multiple –site adsorption of Cd, Cu, Zn and Pb on amorphous iron oxyhydroxide***. J. Colloid Interface Sci.,*** **79:** 209–236.

Benjamin, M. M., Leckie, J. O., 1981(b). Competitive adsorption of Cd, Cu, Zn, and Pb on amorphous iron oxyhydroxide. ***J. Colloid Interface Sci.,*** **83**: 410 – 419.

Benjamin, M. M., Leckie, J. O., 1982. Effects of complexation by Cl, SO_4, S_2O_3 on adsorption behavior of Cd on oxide surfaces, ***Environ. Sci. Technol.,*** **16:** 162 – 170.

Benjamin, M.M., Sletten, R.S., Bailey, R.P., Bennett, T., 1996. Sorption and filtration of metals using iron-oxide-coated sand. ***Water Res.,*** **30:** 2609 –2620.

Benes, P., Paulenova, M., 1971. ***Kolloidz. Polym.,*** **25:** 766.

Benes, P., Kucerra, J., 1972. ***J. Collect. Czech. Chem. Commun.,*** **37:** 523.

Benes, P., Vidova, E., 1972. ***Collect. Czech. Chem. Commun.,*** **37:** 2864.

Benes, P., Majer, V., 1980. Trace Chemistry of Aqueous Solutions, ***Elsevier***, Amsterdam. pp 207

Berenyi, L., 1920. ***Z. Phys. Chem.,*** **94:** 628.

Bhattacharya, A. K., Naiya, T. K., Mandal, S. N., Das, S. K. 2008. Adsorption, kinetics and equilibrium studies on removal of Cr(VI) from aqueous solutions using different low-cost adsorbents, ***Chem. Eng. J.,*** **137:** 529– 541.

Bhumbla, D.K., Keefer, R.F., 1994. Arsenic mobilization and bioavailability in soils, in: J.O. Nriagu (Ed.), Arsenic in the Environment. Part I. Cycling and Characterization, John Wiley & Sons, New York,

Bissen, M., Frimmel, F. H., 2003. Arsenic – a review. Part II: Oxidation of arsenic and its removal in water treatment, ***Acta Hydrochimica et Hydrobiologica,*** **31(2)**: 97 – 107.

Bodek, I., Lyman, W.J., Reehl, W.F., Rosenblatt, D.H., 1998. *Environmental Inorganic Chemistry: Properties, Processes and Estimation methods,* Pergamon Press, USA,

Bolan, N.S., Syers, J.K., Tillman, R.W., 1986. Ionic strength effects on surface charge and adsorption of phosphate and sulphate by soils. ***J. Soil Science,*** **37:** 379 – 388.

Bond, G. C., 1984. *Heterogeneous catalysis, Principles and Applications*, Oxford University Press, Cambridge.

Boonfueng, T., Axe, L., Xu, Y., 2005. Properties and structure of manganese oxide – coated Clay, ***J. Colloid Interface Sci.***, **281:** 80 – 92.

Borum, D. R., Abernathy, C. O., Chappel, W. R., Abernathy, C. O., Cothern, C. R., 1994 Eds., “ In Arsenic Exposure and Health Effects”, *Science and Technology Lett.,* Northwood: U.K., pp. 21-29, Bowden, J.W., Nagarajah, S., Barrow, N.J., Posner, A.M., Qurirk, J.P., 1980. Describing the adsorption of phosphate, citrate and selenite on a variable – charge mineral surface. ***Australian J. Soil Res.,*18:** 49 - 60

Bradly, R. S., 1936. ***J. Chem. Soc.,*** 1467.

Brandao, M., Galembeck, F., 1990. Copper, lead and zinc adsorption on MnO_2 impregnated cellulose acetate. ***Colloids Surf.,* 48**: 351 – 362.

Brunauer, S., Emmett, P. H., Teller, E., 1938. ***J. Am. Chem. Soc.,* 60:** 309.

Burclova, J., Prasilova, J., Bene, P.S., 1973. ***J. Inorg. Nucl. Chem.,* 35:** 909.

Burkel, R.S., Stoll, R.C., 1999. Naturally occurring arsenic in sandstone aquifer water supply wells of North eastern Wisconsin. ***Ground Water Monitoring and Remediation,* 19(2):** 114–121.

Cassel, H., 1931. ***Z. Elektrochem.,* 37:** 642.

Cebrian, M.E., Albores, A., Aguilar, M., Blakely, E., 1983. Chronic arsenic poisoning in the North of Mexico, ***Human Toxicol.,* 2:** 121–133.

Chakravarti, A.K., Chowdhury, S.B., Chakrabarty, S., Chakrabarty, T., Mukherjee, D.C., 1995. Liquid membrane multiple emulsion process of chromium(VI) separation from waste waters, ***Coll. Surf. A: Physicochem. Eng. Aspects,* 103:** 59 – 71.

Chakravarty, S., Dureja, V., Bhattacharyya, G., 2002. Removal of arsenic from groundwater using low cost ferruginous manganese ore, ***Wat. Res.,* 36(3):** 625–632.

Chang, Y.Y., Song, K.H., Yang, J.K., 2008. Removal of As(III) in a column reactor packed with iron-coated sand and manganese-coated sand**. *J. Hazard. Mater.,* 150:** 565–572.

Chang, Y.Y., Lee, S.M., Yang, J.K., 2009. Removal of As(III) and As(V) by natural and synthetic metal oxides. Colloids and Surfaces A: ***Physicochem. Eng. Aspects,* 346:** 202-207.

Chatterjee, A., Das D, Mandal B.K, Chowdhury T.R, Samanta G, Chakraborti, D. 1995. Arsenic in ground water in six districts of West Bengal, India: the biggest arsenic calamity in the world. Part 1. Arsenic species in drinking water and urine of the affected people, ***Analyst Royal Soc. Chem. UK,*** **120:** 643–50.

Chen, C. J., Lin, L. J., 1994. Human carcinogenicity and atherogenicity induced by chronic exposure to inorganic arsenic. In: Nriagu J O, ed. *Arsenic in the Environment, Part II: Human Health and Ecosystem Effects.* New York: John Wiley & Sons, Inc. 27: 109–131

Chiron, N., Guilet, R., Deydier, E., 2003. Adsorption of Cu(II) and Pb(II) onto a grafted silica: isothermal and kinetic models, ***Wat. Res.,*** **37:** 3079-3086.

Chwastowska, J., Skwara, W., Sterlinska, E., Pszonicki, L., 2005. Speciation of Cr in mineral waters and salinas by solid – phase extraction and graphite furnace atomic absorption Spectrometry, ***Talanta,*** **66:** 1345 – 1349.

Cimino, G., Caristi, C., 1990. Acute toxicity of heavy metals to aerobic digestion of waste cheese whey, ***Biol. Wastes,*** **33:** 201 – 210.

Clark, A., 1970. The Theory of Adsorption and Catalysis, Academic Press, New York, p 54.

Corapcioglu, M. O., Huang, C. P., 1987. The surface acidity and characterization of some commercial activated carbons, ***Carbon,*** **25:** 569 – 578.

Cornell, R.M., Schwertmann, 1996. The Iron Oxides: Structure, Properties, Reactions, Occurrence and Use, Wiley-VCM, New York.

Costa, M., Klein, C.B. 2006. Toxicity and carcinogenicity of chromium compounds in Humans, ***Crit. Rev. Toxicol.,*** **36:** 155–163.

Coston, J.A., Fuller, C.C., Davis, J.A., 1995. $Pb^{2+}$and Zn^{2+} adsorption by a Natural aluminum and iron–bearing surface coating on an aquifer sand, ***Geochim. et Cosmochim. Acta,*** **59**: 3535 – 3547.

Dabrowski, A., Hubicki, Z., Podkoscielny, P., Robens, E., 2004. Selective removal of the heavy metal ions from waters and industrial wastewaters by ion – exchange method, ***Chemosphere,*** **56:** 91 – 106.

Daniel, P. H., 2006. "Investing in Tomorrow's Liquid Gold," http://finance.yahoo.com / columnist /article/trenddesk/pp 3748.

Das D, Chatterjee A, Mandal B, Samanta G, Chanda B, Chakraborti D. 1995. Arsenic in ground water in six districts of West Bengal, India: the biggest arsenic calamity in the world. Part 2. Arsenic concentration in drinking water, hair, nails, urine, skin-scale and liver tissue (biopsy) of the affected people, ***Analyst, Royal Soc. Chem. UK***, **120:** 917–24.

Davis, J. A., Leckie, J. O., 1978. Effect of adsorbed complexing ligands on trace metal uptake by hydrous oxides, ***Environ. Sci. Technol.,*** **12**: 1309 – 1315.

Davis A. P., Bhatnagar V., 1995. Adsorption of cadmium and humic acid onto hematite, ***Chemosphere,*** **30**: 243 – 256.

Davis, T. A., Volesky, B. and Vieira, R. H. S. F. , 2000. Sargassum Seaweed as biosorbent for heavy metals, ***Wat. Res.,*** **34(17) :** 4270 – 4278.

Dean, J. A., 1985. *Lange's Handbook of Chemistry*, McGraw-Hill: New York, pp 5 – 33.

de Boer, J.H., Zwikker, C., 1929. ***Z. Phys. Chem.,*** **B3:** 407

Del Debbio, 1991. ***Radiochem. Acta.,*** **52 – 53:** 181.

Deng , S., Bai, R., 2004. Removal of trivalent and hexavalent Cr with aminated polyacrylonitrile fibers: performance and mechanisms, ***Wat. Res.,*** **38(9):** 2424 – 2432.

Desesso, J. M., Jacobson, C.F., Scialli, A.R., Farr, C.H., Holson, J. F., 1998. An assessment of the developmental toxicity of inorganic arsenic, ***Reproductive Toxicol.,*** **12(4):** 385-433.

Desjonqueres, M.C., Spanjaard, D., 1993. *Concepts in surface physics*. Springer-Verlag, Dhar, R.K., Biswas, B.K., Samanta, G., 1997. Groundwater arsenic calamity in Bangladesh ***Current Sci.,*** **73(1):** 48–59.

Donais, M.K., Henry, R., Rettberg, T., 1999. Cr speciation using an automated liquid handling system with inductively coupled plasma mass spectrometric detection, ***Talanta,*** **49 (5):** 1045–1050.

Donald , G. Barceloux, Donald Barceloux, 1999. Copper, ***J. Toxicol.: Clinical Toxicol.,*** **37(2):** 217 – 230.

Duker, A. A., Carranza, E. J. M., Hale, M., 2005**.** Arsenic geochemistry and health. ***Environ. Inter.,*** **31(5):** 631 – 641.

Dyck, W., 1968**.** Adsorption of silver on borosilicate glass. ***Anal. Chem.,*** **40:** 454 – 455.

Edwards, C. P., Benjamin, M. M., 1989. Adsorptive filtration using coated sand, a new approach for treatment metal – bearing wastes. ***J. Wat. Pollut. Contr. Fed.,*** **61(9):** 1523 - 1533.

Edwards, M., 1994. Chemistry of arsenic removal during coagulation and Fe–Mn oxidation. ***J. Am. Water Works Assoc.,*** **76:** 64–78.

Elliot, H.A., Huang, C.P., 1980. Adsorption of some copper(II) - amino acid complexes at the solid - solution interface. Effect of ligand and surface hydrophobicity, ***Environ. Sci. Technol.,*** **14:** 87 – 93.

Elliott, H. A., Huang, C. P., 1984. Factors affecting the Adsorption of complexed heavy metals on hydrous Al_2O_3, ***Wat. Sci. Technol.,*** **17:** 1017 – 1028.

El-Sayed, G.O., Dessouki, H.A., Ibrahim, S.S., 2010. Biosorption of Ni(II) and Cd(II) ions from aqueous solutions onto rice straw, ***Chem. Sci. J.,*** **9:** 1 – 11.

Engell, H. J., Hauffe, K., 1953. ***Z. Electrochem.,*** **57:** 762.

Environmental health criteria 165, 1995. *Inorganic Lead*. Jointly publish by U.N. Environmental programme, WHO and International labour organization, Geneva, pp 26 – 33 and 232 – 233.

Eren, E., Gumus, H., 2011. Characterization of the structural properties and Pb(II) adsorption behaviour of iron oxide coated sepiolite, ***Desal.*, 273:** 276–284.

EPA, 2000. Arsenic removal from drinking water by ion exchange and activated alumina plants. Cincinnati, OH: Office of Research and Development. EPA/600/R–00/088

Fan, H. J., Anderson, P. R., 2005. Copper and cadmium removal by Mn oxide-coated granular activated carbon, ***Sep. Purf. Technol.*, 45**: 61 – 67.

Ferguson, J. F., Gavis, J. 1972. A review of arsenic cycle in natural waters, ***Wat. Res.*, 6:** 1259 – 74.

Ferrari, L., Kaufmann, J., Winnefeld, F., Plank, J., 2010. Interaction of cement model systems with superplasticizers investigated by atomic force microscopy, zeta potential, and adsorption measurements, ***J. Colloid Interface Sci.***, **347(1):** 15–24.

Förstner, U.; Wittmann, T. W., 1981. Metal Pollution in the Aquatic Environment, ***Springer-Verlag: Berlin,***113.

Foster, A. G., 1932. ***Trans. Faraday Soc.*, 28:** 645.

Friberg, L., Nordberg, G. F. and Vouk, B., 1979. Handbook on the toxicology of metals, ***Elsevier***, North-Holland, *Biomedical press***,** Amsterdam.

Fridrikhsberg, D. A., 1986. *A Course in Colloid Chemistry*. Mir Publishers, Moscow, p. 167.

Fristoe, B. R., Nelson, P. O. 1983. Equilibrium chemical modeling of heavy metals in activated sludge, ***Wat. Res.*, 17:** 771 – 778.

Fuller, C.C., Davis, J.A., Coston, J.A., Dixon, E., 1996. Characterization of metal adsorption variability in a sand and gravel aquifer, Cape Cod, Massachusetts, USA, ***J. Contaminant Hydrol.,*** **22**: 165–187.

Gardea-Torresdey. J. L., Tang. L, Salvador. J.M., 1996. Copper adsorption by esterified and unesterified fractions of Sphagnum peat moss and its different humic substances, ***J. Hazard. Mater***., **48**: 191–206.

Garner, W.E., Stone, F. S., Tiley, P. F., 1952. ***Proc. Roy. Soc. (London) Ser.,*****A211:** 472.

Glossary, 2009. The Brownfields and Land Revitalization Technology Support Center.

Gode, F., Pehlivan, E., 2005. Removal of Cr(VI) from aqueous solution by two Lewatit-anion exchange resins, ***J. Hazard. Mater.,*** **119:** 175–182.

Gode, F.; Atalay, E. D.; Pehlivan, E., 2008. Removal of Cr(VI) from aqueous solutions using modified red pine sawdust, ***J. Hazard. Mater.,*** **152:** 1201– 1207.

Goel. J., Kadirvelu, K., Rajagopal. C., Garg. V.K., 2005. Removal of lead(II) by adsorption using treated granular activated carbon: batch and column studies. ***J. Hazard. Mater.,*** **B125**: 211–220.

Gopi Krishna, P., Mary Gladis, J., Rambabu, U., Prasada Rao, T., Naidu, G.R.K., 2004. Pre-concentrative separation of Cr(VI) species from Cr(III) by co-precipitation of its ethyl xanthate complex onto naphthalene, ***Talanta,*** **63 (3):** 541 – 546.

Gosset, T., Trancart, J. L., Thevenot, D. R., 1986. Batch metal removal by peat, ***Wat. Res.,*** **20:** 21 – 26.

Gode, F., Pehlivan, E., 2006. Removal of chromium(III) from aqueous solutions using Lewatit S 100: the effect of pH, time, metal concentration and temperature, ***J. Hazard. Mater.,*** **B 136:** 330 – 337.

Gode, F., Atalay, E.D., Pehlivan, E., 2008. Removal of Cr(VI) from aqueous solutions using modified red pine sawdust, ***J. Hazard. Mater.,*** **152:** 1201 – 1207.

Green, M., Kofalas, J.A., Robinson, P.H., 1957. *Semiconductor Surface Physics*, Univ. of Pennsylvania Press, Philadelphia, p. 349.

Green – Pedersen , H., Pind, N., 2000. Preparation, characterization and sorption properties for Ni(II) of iron oxyhydroxide – montmorillonite, ***Colloids Surf. A: Physicochem. Eng. Aspects,*** **168**: 133–145.

Groffman, A.; Peterson, S., Brookins, D., 1992. Removing lead from wastewater using zeolites, ***Wat. Environ. Technol.,*** **4(5):** 54–59.

Grebenshesikova, V.I., Davydov, P.Y., Pershin, A.S., 1972. ***Radiokhimiya,*** **14:** 511.

Guha, H., Saiers, J. E., Brooks, S., Jardine, P., Jayachandran, K., 2001. Chromium transport, oxidation and adsorption in manganese – coated sand, ***J. Contam. Hydrol.,*** **49:** 311 – 334.

Gupta, S.K., Chen, K.Y., 1978. Arsenic removal by adsorption***. J. Wat. Pollut. Con. F.,*** **50:** 493–506.

Gutsanu, V.L., Gaffichuk, V.A., 1990. ***Khim. Teknol. Vody.,*** **11(7):** 584.

Haber, F., 1914. ***Z. Electrochem.,*** **20:** 521.

Hajialigol, S., Taher, M.A., Malekpour, A. 2006. A new method for the selective removal of cadmium and zinc ions from aqueous solution by modified clinoptilolite, adsorption, ***Sci. Technol.,*** **24:** 487 – 496.

Han, R, Zou, W., Zhang, Z., Shi, Z., Yang, J., 2006. Removal of copper(II) and lead(II) from aqueous solution of manganese oxide coated sand: I. Characterization and kinetic study, ***J. Hazard. Mater.,*** **137(1):** 384 – 395.

Hans Luth, 1993. *Surfaces and interfaces of solids*. Springer-Verlag,.

Hamilton, J.W., Wetterhahn, K.E., 1988. Chromium. In: Seiler, H.G. and H. Sigel, Eds. *Handbook on Toxicity of Inorganic Compounds*. Marcel Dekker, Inc., New York, pp. 239 – 250.

Harns, W.D., Robinson, R.B., 1992. Softening by fluidized-bed crystallizers, ***J. Environ. Eng. Div., (Am. Soc. Civ. Eng.),*** **118:** 513 – 529.

Hasany, S.M., Chaudhary, H., 1984. ***J. Radional. Nucl. Chem.,*** **84/2:** 247.

Hasany, S.M., Chaudhary, M.H., 1985. ***J. Radional. Nucl. Chem.,*****100:** 353.

Hasany, S.M., Chaudhary, M. H., 1986. Investigation of adsorption behaviour of mercury in micro amounts on manganese dioxide from aqueous solutions, ***J. Radional. Nucl. Chem.,*** **100:** 307 – 315.

Hauffe, K., Engell, H., 1952. ***Z. Electrochem.,*** **56:** 366.

Hayes, R.B. 1982. Carcinogenic effects of chromium. In: Langard, S., Ed. *Biological and Environmental Aspects of Chromium.* Elsevier Biomedical Press, Amsterdam, pp. 221 – 247.

Hayes, K.F., Leckie, J.O., 1987. Modeling ionic strength effects on cation adsorption at hydrous oxide solution interfaces, ***J. Colloid Interface Sci.,*** **115:** 564 – 572.

Hayes, K.F., Papelis, C., Leckie, J.O., 1988. Modeling ionic strength effects on anion adsorption at hydrous oxide/solution interfaces. ***J.Colloid interface Sci.,*** **125:** 717 – 726.

HDR Engineering Inc, (2001). *Hand Book of Public water Systems*, 2nd edition, New York, John wiley and Sons, pp. 39.

Helfferich, F., 1962. Ion exchange, McGraw Hill Publishing Company, New York.

Herezynska, E., 1961a. ***Z. Phys. Chem.,*** **217:** 139.

Herezynska, E., 1961 b. ***Nucleonika-Tom-VI Nr.,*** **10:** 659.

Herezynska, E., 1965. ***Nucleonika-Tom-X Nr.,*** **2:** 95.

Ho, Y.S., Porter, J.F., Mckay, G., 2002. Equilibrium isotherm studies for the sorption of divalent metal ions onto peat: copper, nickel and lead single component systems, ***Water, air, and soil pollution***, **141**: 1 – 33.

Ho, Y.S., McKay, G., 2003. Sorption of dyes and copper ions onto biosorbents, ***Process Biochem.,*** **38 (7):** 1047–1061.

Ho, Y.S., Chiu, W.T., Wang, C. C., 2005. Regression analysis for the sorption isotherms of basic dyes on sugarcane dust, ***Bioresour. Technol.,*** **96 :** 1285 – 1291.

Higgins, I. R., 1973. ***Environ. Sci. Technol.,*** **7:** 1110.

Hsu, J.C., Lin, C.J., Liao, C.H., Chen, S.T., 2008. Removal of As(V) and As(III) by reclaimed iron-oxide coated sands, ***J. Hazard. Mater.,*** **153:** 817 – 826.

Huang, C. P., Wu, M. H., 1975. Chromium removal by carbon absorption, ***J. Wat. Pollut. Control Fed.,*** **47:** 2437.

Huang, C. P., Bowers, A. R., 1978. The use of activated carbons for chromium(Vl) removal, ***Prog. Wat. Tech.,*** **10:** 45.

Huang, C. P., Wu M. H., 1977. The removal of chromium (VI) from dilute aqueous solution by activated carbons, ***Wat. Res.,*** **l l :** 673.

Huang, C. P., Van, L. M., 1989. Enhancing As(V) removal by Fe(II) -Treated Activated Carbon. ***J. WPCF,*** **61(9):** 1596 – 1603.

Huang, C., Huang, C. P., Morehart, A. L. 1990. The removal of Cu(II) from dilute aqueous solutions by S. Cerevisiae, ***Wat., Res.,*** **24:** 433 – 439.

Huang, C., Huang, C. P., Morehart, A. L. 1991. Proton competition in Cu(II) adsorption by fungal mycelia, ***Wat., Res.,*** **25:** 1365 – 1375.

Huang, J. G., Liu, J. C., 1997. Enhanced removal of As(V) from water with iron-coated spent catalyst, ***Sep. Sci. Technol.,*** **32:** 1557 – 1569.

Hui, K. S., Chao, C.Y.H., Kot, S.C., 2005. Removal of mixed heavy metal ions in waste water by zeolite 4A and residual products from recycled coal fly ash, ***J. Hazard Mater.,*** **B127:** 89 – 101.

Hu, P.Y., Hsieh, Y.H., Chen, J.C., Chang, C.Y., 2004. Characteristics of manganese coated sand using SEM and EDAX analysis, ***J. Colloid Interface Sci.,*** **272:** 308 – 313.

Hutton, M. 1983. Sources of cadmium in the environment, ***Ecotox. Env. Safety.,*** **7(1):** 9 – 24.

IARC 1982. IARC Monographs on the evolution of the carcinogenetic risk of chemical to humans, Supplement 4.

Imre, L., 1934. ***Z. Phys. Chem.,*****171:** 239.

Iqbal, M., Edyvean, R. G. J., 2005. Loofa sponge immobilized fungal biosorbent: A robust system for cadmium and the dissolved metal removal from aqueous solution ***Chemosphere,*** **61:** 510 – 518.

Iqbal, M., Saeed, A., Zafar, S.I., 2007. Hybrid biosorbent: An innovative matrix to enhance the biosorption of Cd(II) from aqueous solution, ***J. Hazard. Mater.,*** **148:** 47 – 55.

Inglezakis, V.J., Loizidou, M.M., Grigoropoulou, H.P., 2004. Ion exchange studies on natural and modified zeolites and the concept of exchange site accessibility, ***J. Colloid Interface Sci.,*** **275:** 570 – 576.

]Inglezakis, V. J., Zorpas, A. A., Loizidou, M. D., Grigoropoulou, H. P., 2005. The effect of competitive cations and anions on ion exchange of heavy metals**,** ***Sep. Purif. Technol.,*** **46(3):** 202 – 207.

I.S.I., 1982. Tolerance limits for industrial effluents prescribed by Indian Standards Institution, ***IS: 2490 (Part II),*** New Delhi, India.

Jain, C . K., Ali, I., 2000. Arsenic: occurrence, toxicity and speciation techniques, ***Wat. Res.,*** **34(17):** 4304–4312.

Jarup, L., 1998. Health effects of cadmium exposure – a review of the literature and a risk estimate, ***Scandinavian J. Work, Environ. Health,*** **24:** 11–51.

Jia, Y., Xu, L., Fang, Z., Demopoulos, G.P., 2006. Observation of surface precipitation of arsenate on ferrihydrite, ***Environ. Sci. Technol..,*** **40:** 3248 – 3253.

Jin, T., Nordberg, M., Frech, W., Dumont, X., Bernard, A., Ye, T.T., Kong, Q., Wang, Z., Li, P., Lundstrom, N.G., Li, Y., Nordberg, G.F., 2002. Cadmium bio monitoring and renal dys-function among a population environmentally exposed to cadmium from smelting in China (China Cad), ***Biometals*, 15(4):** 397 – 410.

Joshi, A., Chaudhuri, M., 1996. Removal of arsenic from groundwater by iron–oxide coated sand, ***J. Environ. Eng.*, 122:** 796 – 800.

Juang, R.S., Shiau, R.C., 2000. Metal removal from aqueous solutions using chitosan-enhanced membrane filtration, ***J. Membr. Sci.*, 165:** 159 – 167.

Kadirvelu, K., Namasivayam, C., 2003. Activated carbon from coconut coirfith as metal adsorbents: adsorption of Cd(II) from aqueous solution, ***Adv. Environ. Res.*, 7:** 471 – 478.

Karim, M. M., 2000. Arsenic in ground water and health problems in Bangladesh. ***Wat. Res.*, 34(1):** 304 – 310.

Kasuya, M., 2000. Recent epidemiological studies on itai – itai disease as a chronic cadmium poisoning in Japan, ***Wat. Sci. Technol.*, 42 (7-8):** 147 – 154.

Kato, C., Kuroda, K., Yoshihara, T., Wada, H., 1981. ***Waseda Daigaku Rikogaku Kenkyusho, Hokaku*, 94:** 25

Katsoyiannis, I., Zouboulis, A., Althoff, H., Bartel, H., 2002 . As(III) removal from ground waters using fixed-bed upflow bioreactors, ***Chemosphere*, 47:** 325 – 332.

Kenta, O., Taka, K., Shunsaku, K., Kazuhiko, S., 1984. ***Nippon Kagaku Kaishi*, 4:** 534.

Khaodhiar, S., Azizian, M.F., Osathaphan, K., Nelson, P.E., 2000. Copper, chromium and arsenic adsorption and equilibrium modeling in an iron oxide – coated sand, background electrolyte system, ***Water Air soil Pollut.*, 119:** 105 – 120.

Kiffs, R.J., 1987. General inorganic effluents, in: D. Barnes, C.F.Forster, S.E. Hrudey (Eds.), surveys in Industrial Wastewater Treatment - Manufacturing and Chemical Industries, vol. 3, Longman, New York, NY. (Chapter 1).

Kikuchi, M., Ga, K., Funabashi, K., Yusa, H., Uchida, S., Fujita, K., 1979. Removal of radioactive Cobalt ion in High Temperature Water using Titanium Oxide, ***Nucl. Eng. Des.*,** **53:** 387.

Kim, M. S., Chung, J. G., 2002. Removal of copper(II) ion by kaolin in aqueous solutions, ***Environ. Eng. Res.*,** **7:** 49 – 57.

Kim, M. J., Nriagu, J., Haack, S., 2002. Arsenic species and chemistry in groundwater of southeast Michigan**,** ***Environ. Pollut.*,** **120**: 379 – 390.

Kim, W.G., Kim, S.J., Lee, S.M., Tiwari, D., 2009. Removal characteristics of manganese coated solid samples for Mn(II), ***Desal. Wat. Treatment,*** **4:** 218 – 223.

King, G.L., Rodriquez, J.M., Wai, C.M., 1974. Losses of Trace concentrations of Cadmium from aqueous – solution during storage in Glass containers, ***Anal. Chem.*,** **46:** 771 – 773.

Kiping, M. D. 1997. *Arsenic, the Chemical Environment, Environment and Man,* **6**, eds J. Lenihan and W. W.Fletcher. pp. 93–110, Glasgow.

Kitis, M., Kaplan, S.S., Karakaya, E., Yigit, N.O., Civelekoglu, G., 2007. Adsorption of natural organic matter from waters by Iron coated pumice, ***Chemosphere,*** **66(1):** 130–138.

Kolpin, D.W., Skopec, M., Meyer, M.T., Furlong, E.T., Zaugg, S.D., 2004. Urban contribution of pharmaceuticals and other organic waste water contaminants to stream during differing flow condition, ***Sci. Total Environ.*,** **328:** 119 – 130.

Kononova, O. N., Kholmogorov, A. G., Danilenko, N. V. and Kachin, S. V., 2005. Sorption of old and silver on carbon adsorbents from thiocyanate solutions, ***Carbon,*** **43:** 17 – 22.

Korngold, E., Belayev, N., Aronov, L., 2003. Removal of chromates from drinking water by anion exchangers. ***Sep. Purif. Technol.,*** **33:** 179 – 187.

Koulouris, G., 1995. Dynamic studies on sorption characteristics of ^{226}Ra on Manganese dioxide, ***J. Radioanal. Nucl. Chem.,*** **193:** 269 – 279.

Kovacˇevic´, D., Pohlmeier, A., zbas¸ G. O., Narres, H.D., Kallay, M.J.N., 2000. The adsorption of lead species on goethite, ***Colloids Surf. A: Physicochem. Eng. Aspects,*** **166 (1–3) :**225.

Kuan, W.H., Lo, S.L., Wang, M.K., Lin, C.F., 1998. Removal of Se(IV) and Se(VI) from water by aluminium – oxide – coated sand, ***Wat. Res.,*** **32:** 915 – 923.

Kumar, D., Gaur, J.P., 2011. Metal biosorption by two cyanobacterial mats in relations to pH, biomass concentration, pretreatment and reuse, ***Bioresour. Technol.,*** **102:** 2529 – 2535.

Kurbatov, M.H., 1948. Target Chemistry of Cesium; Isolation of Ba$^{133, 134}$, ***J. Chem. Phys.,*** **16:** 87

Lacour, S., Bollinger, J.C., Serpaud, B., Chantron, P., Arcos, R., 2001. Removal of heavy metals in industrial wastewaters by ion – exchanger grafted textiles, ***Anal. Chim. Acta,*** **428:** 121–132.

Lai, C. H., Lo, S. L., Lin, C. F., 1994. Evaluating an iron-coated sand for removing copper from water, ***Wat. Sci. Technol.,*** **30(9):** 175 – 182.

Lai, C. H., Lo, S. L., Chiang, H.L., 2000. Adsorption / desorption properties of copper ions on the surface of iron coated sand using BET and EDAX analyses, ***Chemosphere,*** **41(8):** 1249 – 1255.

Lai, C.H. Chen, C.Y., 2001. Removal of metal ions and humic acid from water by iron coated filter media, ***Chemosphere,*** **44(5):** 1177 – 1184.

Lai, C.H., Chen, C.Y., Wei, B.L., Yeh, S.H., 2002. Cadmium adsorption on goethite-coated sand in the presence of humic acid**,** ***Wat. Res.,*** **36(20):** 4943 – 4950.

Lakatos, J., Brown, S.D., Snape, C.E. 2002. Coals as sorbents for the removal and reduction of hexavalent Cr from aqueous waste streams, ***Fuel*, 81:** 691 – 698.

Langard, S., Vigander, T., 1983. Occurence of lung cancer in workers producing chromium Pigments, ***British J. of Industrial Medicine,* 40**: 71 – 74.

Langmuir, I., 1918. ***Am. J. Chem. Soc.,* 40:** 1361.

Larry, W.,2006. World Water Day: A Billion People Worldwide Lack Safe Drinking Water, *About.com Guide Q & A with Gary White of Water Partners International*.

Laws, B.V., Dickenson, E.R.V., Johnson, T.A., Synder, S.A., Drewes, J.E., 2011. Attenuation of contaminants of emerging concern during surface-spreading, ***Sci. Total Environ.,* 409:** 1087 – 1094.

Lee, S. M., Davis, A. P., 2001. Removal of Cu(II) and Cd(II) from Aqueous solution by seafood processing waste sludge, ***Wat. Res.,* 35:** 534-540.

Lee, C.I., Yang, W. F., Hsieh, C. I., 2004. Removal of copper (II) by manganese-coated sand in a liquid fluidized-bed reactor, ***J. Hazard. Mat.,* 114(1 – 3):** 45–51

Lee, S. M., Tiwari, D., Choi, K. M., Yang, J. K., Chang, Y. Y., Lee, H. D., 2009. Removal of Mn(II) from aqueous solutions using manganese coated sand samples, ***J. Chem. Eng. Data,* 54**: 1823 – 1828.

Lee, S. M, Kim, W.G, Yang, J.K., Tiwari, D., 2010 (a). Sorption behaviour of manganese coated calcined–starfish and manganese coated sand for Mn(II), ***Environ. Technol.,* 31(4):** 445 – 453.

Lee, S. M, Kim, W.G, Laldawngliana, C., Tiwari, D., 2010 (b). Removal behavior of surface modified sand for Cd(II) and Cr(VI) from aqueous solutions, ***J. Chem. Eng. Data,* 55:** 3089 – 3094.

Leinonen, H., Lehto, J., 2000. Ion – exchange of nickel by iminodiacetic acid chelating resin Chelex 100, ***React. Funct. Polym.,* 43**: 1 – 6.

Leonard, A., Lauwerys, R. R., 1980. Carcinogenicity and mutagenicity of chromium, ***Mutation Research*, 76**: 227 – 239.

Liang, P., Shi, T., Lu, H., Jiang, Z., Hu, B., 2003. Speciation of Cr(III) and Cr(VI) by nanometer titanium dioxide micro – column and inductively coupled plasma atomic emission spectrometry, ***Spectrochimica Acta*, B58:** 1709 – 1714.

Li, Z., Burt, T., Bowman, R.S., 2000. Sorption of ionisable organic solutes by surfactant-modified zeolite, ***Environ. Sci. Technol.*, 34:** 3756 – 3760.

Li, Y.H., Wang, S.G., Wei, J.Q., Zhang, X.F., Xu, C.L., Luan, Z.K., Wu, D.H., Wei, B.Q., 2002. Lead adsorption on carbon nanotubes, ***Chem. Phys. Lett.*, 357:** 263 – 266.

Li, J., Hu, J., Sheng, G., Huang, Q., 2009. Effect of pH, ionic strength, foreign ions and temperature on the adsorption of Cu(II) from aqueous solutions to GMZ betonite, ***Colloids Surf.*, *A*, 349(1-3):** 195 – 201.

Liu, D., Teng, Z., Cartledge, F. K., Sansalone, J. J., 2001. Surface characteristics of sorptive – filtration storm water media. I. Low - density ($\rho < 1.0$) oxide coated buoyant media. ***J. Environ. Eng.*, 27:** 866 – 878.

Lo, S. L., Jeng, H. T., Lin, C. F., Lee, D. Y., 1994(a). Adsorption of heavy metals by the iron-coated filter medium, ***J. Chinese Inst. Of Civil & Hydraulic Engr*., 6(l):** 101 – 110.

Lo, S. L., Shiu, S. H., Lin, C. F., Lee, D. Y., 1994(b). Adsorption of Metals on oxides formed from $Fe(N0_3)_3$, $FeC1_3$ and Fe(ClO) solutions, ***Env. Geochem. Health.*,**

16: 89 – 99.

Lo, S. L., Chen, T. Y., 1997(a). Adsorption of Se(IV) and Se(VI) on an iron coated sand from water, ***Chemosphere*, 35:** 919 – 930.

Lo, S. L., Chen, T. Y., 1997(b). A growth inhibition test with sewage bacteria-results of an international ring test, ***Chemosphere,*** **35:** 919 – 930.

Lo, S. L., Jeng, H. T., Lai. C. H., 1997. Characteristics and adsorption properties of iron-coated sand, ***Wat. Sci. Technol.,*** **35:** 63 – 70.

Lo, W., Chua, H., Lam, K.H., Bi, S.H. 1999. A comparative investigation on the bio-sorption of lead by filamentous fungal biomass, ***Chemosphere,*** **39(15):** 2723 – 2736.

Low, K.S., Lee, C.K., Ng, A.Y., 1999. Column study on the sorption of Cr(VI) using quaternized rice hulls, ***Bioresour. Technol.,*** **68:** 205 – 208.

Lum Max., Orti, D., Poindexter, P., 1994. Lead – Toxicity. Agency for Toxic substances and Disease registry. Biological Sciences Division Academic computing, University of Chicago.

Ma, W., Tobin, J.M., 2003. Development of multimetal binding model and application to binary metal biosorption onto peat biomass, ***Wat. Res.,*** **37(16):** 3967–3977.

Ma. X., Subramanian, K.S., Chakrabarti, C.L., Guo, R., Cheng, J., Lu, Y., Pickering, W.F., 1992. ***J. Environ. Sci. Health,*** **A 27:** 1389

Madoni, P., Davoli, D., Gorbi, G., Vescovi, L., 1996. Toxic effect of heavy metals on the activated sludge protozoan community, ***Wat. Res.,*** **30:** 135 – 142.

Mahoney, J. J., Langmuir, D., 1991. ***Radiochim Acta,*** **54:** 139.

Malkoc, E., 2006. Ni(II) removal from aqueous solutions using cone biomass of *Thuja Orientalis.* ***J. Haz. Mat.,*** **B137:** 899 – 908.

Mancuso, T. F, Hueper, W. C., 1951. Occupational cancer and other health hazards in a chromate plant: a medical appraisal 1. Lung cancer in chromate workers, ***Ind. Med. Surg.,*** **20:** 358 – 363.

Mancuso T. F., 1975. Consideration of chromium as an industrial carcinogen. *International Conference on Heavy Metals in the Environment. Toronto, Ontario, Canada,* October 27 – 31**:** 343- 356.

Mandal, B. K; Suzuki, K. T., 2002. Arsenic round the world: a review, ***Talanta,*** **58:** 201–235.

Mandal, S., Padhi, T., Patel, R.K., 2011. Studies of the removal of arsenic(III) from water by a novel hybrid material, ***J. Haz. Mater.,*** **192:** 899 – 908.

Manzano, M., Ayora, C., Domenech, C., Navrette, P., Garralon, A., Torrero, M.J. 1999. The impact of the Aznalcollar mine tailing spill on groundwater, ***Sci. Total Environ.***, **242:** 189 – 202.

Matschullat, J., 2000, Arsenic in the geosphere – a review, ***Sci. Total Environ.,*** **249(1-3):** 297 – 312.

McBride, M.B., 1997. A critique of diffuse double layers models applied to colloid and surface Chemistry, ***Clays & Clays Minerals,*** **45:** 598 – 608.

Mehta, S.K., Gaur, J.P., 2005. Use of algae for removing heavy metal ions from wastewater: progress and prospects, ***Crit. Rev. in Biotechnol.,*** **25:** 113 – 152.

Mehta, A., 2011. Ultraviolet-Visible (UV-Vis) Spectroscopy-Principle, *Analytical Chemistry.*

Meng, X., Letterman, R.D., 1993. Modeling ion adsorption on aluminum hydroxide modified silica, ***Environ. Sci. Technol.,*** **27 *:*** 1924 – 1929.

Meng, X., Letterman, R.D., 1996. Modeling cadmium and sulfate adsorption by $Fe(OH)_3$ /SiO_2 mixed oxides. ***Wat. Res.,*** **30:** 2148 – 2154.

Meng, X., Bang, S., Korfiatis, G.P., 2000. Effect of silicate, sulfate and carbonate on arsenic removal by ferric chloride, ***Wat. Res.,*** **34:** 1255–1261.

Merkle, P.B., Knocke, W.R., Gallagher, D.L., Junta – Rosso, J., Solberg, T., 1996. Characterizing filter media mineral coatings, ***J. Am. Water Works Assoc.,*** **88**: 62 – 73.

Merkle, P.B., Knocke, W.R., Gallagher, D.L., 1997. Method for coating filter media with synthetic manganese oxide, ***J. Environ. Eng.,*** **123:** 642 – 649.

Mesquita, M.E., Vieira e Silva, J.M., 2002. Preliminary study of pH effect in the application of Langmuir and Freundlich isotherms to Cu – Zn competitive adsorption, ***Geoderma,*** **106:** 219 – 234.

Mikhail, E.M., Misak, N.Z., 1988. Sorption of cesium and cobalt radionuclides on a new manganese oxide, ***J. Appl. Radiat. Isot.,*** **39(11):** 1121 – 1124.

Mishra, S.P., Singh, T.B., 1986. Radiotracer technique in adsorption study—III: Adsorption of phosphate ions on cobalt metal powder, ***J. Appl. Radiat. Isot.,*** **37:** 1121 – 1127.

Mishra, S.P., Singh, S.N., 1987. Radiotracer technique in adsorption study Part VI. Adsorption of chromate ions on chromium(IV) powder, ***J. Appl. Radiat. Isot.,*** **38:** 541.

Mishra, S.P., Singh, S.N., Tiwary, D., 1991. Radiotracer technique in adsorption study Part VII. Adsorption of iodide ions on chromium(IV) oxide powder, ***Appl. Rad. Isot.,*** **42:** 1177.

Mishra, S.P., Tiwary, D., 1991. *Proc. Int. Symp. (DAE), Bombay, India,* RC – 44.

Mishra, S.P., Tiwary, D., 1993. Radio tracer technique in adsorption studies X. Efficient removal of Ba(II)from aqueous solutions by hydrous manganese oxide, ***J. Radioanal. and Nucl. Chem. Articles,*** **170:** 133 – 141.

Mishra, S.P., Singh, V. K., 1995. Efficient removal of cadmium ions from aqueous solutions by hydrous ceric oxide. A radiotracer study, ***Radiochim. Acta.,*****68:** 251 – 256.

Mishra, S.P., Singh, V. K., Tiwari, D., 1996. Radiotracer technique in adsorption study XV. Removal behaviour of Barium titanate for mercury ions, ***Radiochim. Acta,*** **73:** 49 – 53.

Mishra, S.P., Tiwari, D., Dubey, R.S., Mishra, M., 1998. Biosorptive behavior of casein for Zn^{2+}, Hg^{2+} and Cr^{3+} effects of physic – chemical treatments, ***Bioresour. Technol.,*** **63:** 1 – 5.

Mishra, S. P., Dubey, S. S., Tiwari, D., 2004. Inorganic particulates in removal of heavy metal toxic ions IX. Rapid and efficient removal of Hg(II) by hydrous manganese and tin oxides, ***J. Colloids & Interface Sci.,*** **279:** 61 – 67.

Mott, N. F., Gurney, R. W., 1950. *Electronic processes in ionic Crystals,* Oxford Univ. Press. London.

Muir, G. M. 1977. *Hazards in the Chemical Laboratory,* 2nd edn. Pergamon Press, Oxford.

Murray, D.J., Healy, T.H., Fuerstenau, D.W., 1968. ***Adv. Chem. Ser.,*** **79:** 74

Music, S., Ristic, M., 1988. ***J. Radional. Nucl. Chem.,*** **120:** 289.

Namasivayam, C., Ranganathan, K., 1995. Removal of Pb(II), Cd(II)and Ni(II) and mixture of metal ions by adsorption onto waste Fe(III)/Cr(III) hydroxide and fixed bed studies, ***Environ. Technol.,*** **16:** 851–860.

Naqvi, S. M., Chetana, V., Singh, H, 1994. Toxicity and metabolism of arsenic in vertebrates. In: Arsenic in the Environment. Part II: Human Health and Ecosystem Effect. New York: John Wiley & Sons, Inc, **27:** 55–91.

Nariagu, O., Jerome and John. B., Sprangu. 1983. Cadmium on the aquatic environment, **9 A.** Wietly Interscience Publication.

National Research Council, 1999. Arsenic in drinking water: Washington D C: National Academy Press.

Ng, J. C., Wang, J., Shraim, A. A., 2003. Global health problem caused by arsenic from natural sources, ***Chemosphere,*** **52(9):** 1353 – 1359.

Nielson, P.B., Christensen, T.C., Vendrup, M., 1997. Continous removal of heavy metals from PGD wastewater in a fluidized bed without sludge generation, ***Wat. Sci. Technol.,*** **36:** 391 – 397.

Nikolaidis, N. P., Dobbs, G .M., Lackovic. J. A., 2003. Arsenic removal by zero valent iron: field, laboratory and modelling studies, ***Wat. Res.,*** **37:** 1417 – 1425.

Nordberg, G.F., 2004. Cadmium and health in the 21st century--historical remark and trends for the future, ***Biometals,*** **17(5):** 485 – 489.

Nouri, L., Ghodbane, L., Hamdouri, O., Chiha, M., 2007. Batch sorption and dynamic equilibrium for the removal of cadmium ions from aqueous phase using wheat bran, ***J. Hazard. Mater.,*** **149(1):** 115 – 125.

Nriagu, J. O., 1988. A 47 silent Epidemic of Environmental metal poisoning? ***Environ. pollut.,*** **50:** 139 -161.

NRC. Arsenic in drinking water: 2001. Update. National Research Council. Washington D C: National Academy Press.

O’Connor, J.T., 2002. Arsenic in drinking water. Part 2: human exposure and health effects, ***Water Eng. Manage.,*** **149(3):** 35–37.

Ottewill, H.H., Shaw, J. N., 1968. ***J. Colloid & interface Sci.,*** **26:** 110.

Oura, K., Lifshits, V. G., Saranin, A. A., Zotov, A. V. Katayama, M., 2003. *Surface Science, An Introduction*. Berlin: Springer.

Park, S., Kim, Y., 2005. Adsorption behaviours of heavy metal ions onto electro- chemically oxidized activated carbon fibers, ***Mater. Sci. Eng., A*** **391(1-2):** 121 – 123.

Pakholkov, V.S., Rychkov, V.N., Abramov, N.V., 1983. ***Chem. Abstr.,*** **98:** 41256

Patrick, W.A., Long, J.S., 1925. ***J. Phys. Chem.,*** **29:** 336

Patterson, J.W., Minear, R, A., 1975. *Physical – Chemical Methods of Heavy Metals Removal,* Pergamon Press: Oxford**,** p. 156.

Pauling, L., 1939. *The nature of the Chemical bond*, Cornell Univ. Press, Ithaca, New York.

Pehlivan, E., Altun, T., 2008. Biosorption of Chromium(VI) ion from aqueous solution using walnut, hazelnut and almond shell, ***J. Hazard Mater.,*** **155:** 378 – 384.

Penrose, W.R.,1974. Arsenic in the marine and aquatic environments. Analysaism occurrence \ and significance, ***CRC Critical. Rev. Environ. Control.***, **4:** 465.

Petrov, A. M., 1958. ***Khim. Tr. Tekhnol.,*** **1(2):** 229.

Pinto, A.P., Mota, A. M., De Varennes, A., Pinto, F.C., 2004. Influence of organic matter on the uptake of cadmium, zinc, copper and iron by sorghum plants. ***Sci Total Environ.,*** **326:** 239–274.

Polanyi, M., 1914. ***Verh. Dent Physik. Ges.,*** **16:** 1012.

Polanyi, M., 1920. ***Phiysik Z.,*** **2:** 117.

Pretorious, P. J., Peter, W. L., 2001. The adsorption characteristics of δ-manganese dioxide: a collection of diffuse layer constants for the adsorption of H^+, Cu^{2+}, Ni^{2+}, Zn^{2+}, Cd^{2+} and Pb^{2+}, ***Appl. Geochem.,*** **16:** 1067 – 1082.

Puziy, M., Poddubnaya, O. I., Zaitsev, V. N., Konoplitska, O. P., 2004. Modeling of heavy metal ion binding by phosphoric acid activated carbon, ***Appl. Surf. Sci.***, **221(1-4):** 421 – 429.

Qdais, H.A., Moussa, H., 2004. Removal of heavy metals from wastewater by membrane processes: a comparative study, ***Desal.,*** **164(2):** 105 – 110.

Raji, C., Anirudhan, T.S., 1998. Batch Cr(VI) removal by polyacrylamide grafted sawdust: kinetics and thermodynamics, ***Wat. Res.,*** **32(12):** 3772 – 3780.

Reed, B.E., Jamil, M., Thomas, B., 1996. Effect of pH, empty bed contact time and hydraulic loading rate on lead removal by granular activated carbon columns, ***Wat. Environ. Res.,*** **68:** 877 – 882.

Remembrance, L. N., 2003. *Arsenic removal from drinking Water* [Dissertation]. University of Idaho.

Robers, J. K., 1935. ***Proc. Roy. Soc. (London)*** **Ser. Al., 52:** 445

Rozovskaya, N.G., 1960. ***Radiokhimiya,*** **2:** 21.

Ruiz-Manriquez, A., Magaña, P. I., Lopez, R., and Guzman, R., 1998. Biosorption of Cu by *Thiobacillumferrooxidans,* ***Bioprocess Eng.,*** **18:** 113 – 118.

Rydberg, J., Rydberg, B., 1952. ***Sven Kem. Tidsk.,*** **64:** 200

Saha, J. C., Dikshit, A. K., Bandyopadhyay, M., Saha, K. C., 1999. A review of arsenic poisoning and its effects on human health, ***Crit. Rev. Envi. Sci. Tech.,*** **29:** 281 – 313.

Sanders, J.R., El-kherbawy, M. I., 1987. The effect of pH on zinc adsorption equilibria and exchangeable zinc pools in soils, ***Environ. Pollut.,*** **44:** 165 – 176.

Sankararamakrishnan, N., Dixit, A., Iyengar, L., Sanghi, R., 2006. Removal of hexavalent Cr using a novel cross linked xanthated chitosan, ***Bioresour. Technol.,*** **97:** 2377– 2382.

Sansalone, J.J., Buchberger, S.G., 1995. An filtration device as a best management practice for immobilizing heavy metal in urban highway runoff, ***Water Sci. Technol.,*** **32:** 119 – 125.

Sansalone, J. J., 1999. Adsorptive–infiltration of metals in urban drainage – media Characteristics, ***Sci. Total Environ.,*** **235:** 179 – 188.

Satpathy, J. K., Chaudhuri, M., 1995. Treatment of cadmium-plating and chromium-plating wastes by iron oxide-coated sand, ***Wat. Environ. Res.,*** **67:** 788 – 790.

Schore, G.,1972. Electronic Equipment and Ion Exchange for Use in Activated Treatment Systems, *27th Purdue Industrial Waste Conf., Lafayette, Indiana.*

Scheidegger, A., Borkovec, M., Sticher, H., 1993. Coating of silica sand with goethite: preparation and analytical identification, ***Geoderma,*** **58:** 43 – 65.

Schmuhl, R., Krieg, H. M., Keizer, K., 2001. Adsorption of Cu (II) and Cr(VI) ions by chitosan: kinetics and equilibrium studies, ***Water SA,*** **27:** 1–7.

Schöller, M., Dijk, J., Wilms, D., 1987. Recovery of heavy metals by crystallization, ***Met. Finish.,*** **85:** 31 – 34.

Schöller, M., Dijk, J., Wilms, D., 1991. Fluidized bed pellet reactor to recovery metals or anions, ***Met. Finish.,*** **89:** 46 – 50.

Schultz, M. F., Benjamin, M. M., Ferguson, J. F., (1987). Adsorption and desorption of Metals on ferrihydrite: reversibility of the reaction and sorption properties of the regenerated solid, ***Environ. Sci. Technol. ,*** **21(9):** 863 – 869.

Schwuger, M. J., Smolka, M. J., 1976. ***Colloid. Polymer Sci.,*** **254:** 1062.

Schwertmann, U., Taylor, R.M., 1989. Iron oxide in Minerals in Soil Environments, (Edited by J. B. Dixon and S. B. Weed), 2nd edn, ***Soil Sci. Sot. of Am. J.,*** 379 – 428. Madison, Wisconsin.

Seco, A., Marzal, P., Gabaldon, C., 1997. Adsorption of heavy metals from aqueous solutions onto activated carbon in single Cu and Ni systems and in binary Cu – Ni, Cu – Cd and Cu – Zn systems, ***J. Chem. Tech. Biotechnol.,*** **68:** 23 – 30.

Sekar, M., Sakthi, V., Rengaraj, S. 2004. Kinetics and equilibrium adsorption study of lead(II) onto activated carbon prepared from coconut shell, ***J. Colloid Interf. Sci.,*** **279(2):** 307 – 313.

Sen, A. K., De, A. K., 1987. Adsorption of mercury(II) by coal fly ash, ***Wat. Res.,*** **21:** 885 – 888.

Singh, D.K., Lal, J., 1992. Removal of toxic metal ions from wastewater by coal based adsorbents, ***J. Pollut. Res.,*** **11:** 37.

Singh, A., Kumar, D., Gaur, J.P., 2007. Copper(II) and lead(II) sorption from aqueous solution by non living biomass of *Spirogyra neglecta*, ***Bioresour. Technol.,*** **98:** 3622 – 3629.

Singh, A., Kumar, D., Gaur, J.P., 2012. Continous metal removal from solution and industrial effluents using *Spirogyra* biomass-packed column reactor, ***Wat. Res.,*** **46:** 779 – 788.

Sips, R., 1948. On the structure of a catalyst surface, ***J. Chem. Phys.,*** **16:** 490.

Skoog, *et al.,* 2007. *Principles of Instrumental Analysis.* 6th ed. Thomson Brooks/Cole. 169 – 173.

Skulskii, A., Lyubimov, A.A., 1971. ***Radiokhimiya,*** **13:** 272.

Smedley, P.L., Kinniburgh, D.G., 2002. A review of the source, behaviour and distribution of arsenic in natural waters, ***J. Appl. Geochem.,*** **17:** 517 – 568.

Sonia A Dean, John M Tobin, 1999. Uptake of chromium cations and anions by milled peat, ***Resources, Conservation and Recycling,*** **27(1-2):** 151 – 156.

Sparks, D.L, 1995. *Environmental Soil Chemistry*, Academic Press, San Diego. pp. 99.

Srivastava, S. K., Tyagi, R., Pant, N., 1989. Adsorption of heavy metal ions on Carbonaceous material developed from the waste slurry generated in local fertilizer plants, ***Wat. Res.,*** **23:** 1161 – 1165.

Stahl, R. S., James, B. R., 1991(a). Zinc sorption by iron – oxide coated sand as a function of pH, ***Soil Sci. Sot. Am. J.,*** **55:** 1287 – 1290.

Stahl, R. S., James, B. R. 1991(b) . Zinc sorption by manganese – oxide – coated sand as a function of pH, ***Soil Sci. Soc. Am. J.,*** **55:** 1291 – 1294.

Stasinakis, A. S., Thomaidis, N.S., Mamais, D., Karivali, M., Lekkas, T.D., 2003. Cr species behaviour in the activated sludge process, ***Chemosphere,*** **52:** 1059 – 1067.

Stryker, L. J., Manjevic, E., 1968. ***Advan. Chem. Ser.,*** **79:** 44.

Su, C., Puls, R., 2001(a). Arsenate and arsenite removal by zero valent iron: kinetics, redox transformation and implications for in situ groundwater remediation, ***Environ. Sci. Technol.,*** **35:** 1487 – 1492.

Su, C., Puls, R. W., 2001(b). Arsenate and arsenite removal by zero valent iron: effect of phosphate, silicate, carbonate, borate, sulfate, chromate, molybdate and nitrate, relative to chloride, ***Environ. Sci. Technol.,*** **35:** 4562 – 4568.

Sud, D., Mahajan, G., Kaur, M.P., 2008. Agricultural waste material as Potential Adsorbent for Sequestering Heavy Metal Ions from Aqueous Solutions – A review. ***Bioresour. Technol.,*** **99(14):** 6017 – 6027.

Suhybani, A.I., 1989. ***Isotopen Praxis,*** **25:** 381.

Sun, H., Wang, L., Zhang, R., Sui, J., Xu, G., 2006. Treatment of groundwater polluted by arsenic compounds by zero valent iron, ***J. Hazard. Mater.,*** **129(1 – 3):** 297–303.

Tamura, H. and Nagayama, M., 1984. ***Batt. Mater. Symp. Proc.,*** 88.

Tamura, H., Sasaki, K., Katayama, N., Nakai, T., Nagayama, M., 1986, ***Bunseki Kagaku,*** **35:** 996.

Tan, T.C., Teo, W. K., 1987. Combined effect of carbon dosage and initial adsorbate concentration on the adsorption isotherm of heavy metals on activated carbon, ***Wat. Res.,*** **21:** 1183 – 1188.

Taylor, R.S., Sickman, V.D., 1932. ***J. Am. Chem. Soc.,*** **54:** 602.

Taylor, H.S., 1932. ***Am. J. Chem. Soc.,*** **53:** 578.

Ternes, T.A., 1998. Occurrence of drugs in German sewage treatment plants and rivers, ***Wat. Res.,*** **32:** 3245 – 3260.

Tewari, P.H., Cambell, A.B., Lee, W., 1972. ***Can. J. Chem.,*** **50:** 1642.

Thirunavukkarasu, O.S., Viraraghavan, T., Subramanian, K.S., 2003. Arsenic removal from drinking water using iron oxide coated sand, ***Wat. Air Soil Pollut.,*** **142:** 95 – 111.

Thomas, H.C., 1944. Heterogeneous ion exchange in a flowing system, ***J. Am. Chem. Soc.,*** **66:** 1664 – 1666.

Tien, C. T., Huang, C. P., 1987. Adsorption behaviour of Cu(II) onto sludge particulate surfaces, ***ASCE J. Environ. Eng.,*** **113:** 285 – 299.

Tiwari, D., Mishra, S. P., Mishra, M., Dubey, R. S., 1999. Biosorptive behaviour of Mango (*Mangifera indica*) and Neem (*Azadirachta indica*) bark for Hg^{2+}, Cr^{3+} and Cd^{2+} toxic ions from aqueous solutions: a radiotracer study, ***Appl. Radiat. Isot.,*** **50:** 631 – 642.

Tiwari, D., Kim, H. U., Lee, S. M., 2006. Applications of sericite in waste water treatment: Removal of Cu(II) and Pb(II) from aqueous solutions. ***Kor. Soc. Environ. Engineers,*** **11(6):** 303 – 310.

Tiwari, D., Kim, H. U., Lee, S. M., 2007(a). Removal behaviour of sericite for Cu(II) and Pb(II) from aqueous solutions: Batch and column studies, ***Sep. Purif. Technol.,*** **57:** 11 – 16.

Tiwari, D., Yu, M. R., Kim, M. N., Lee, S. M., Kwon, O. H., Choi, K. M., Lim, G. J., Yang, J. K., 2007(b). Potential application of manganese coated sand in the removal of Mn(II) from aqueous solutions, ***Wat. Sci. Technol.,*** **56:** 153 – 160.

Tiwari, D., Laldanwngliana, C., Choi, C.H., Lee, S.M., 2011. Manganese – modified natural sand in the remediation of aquatic environment contaminated with heavy metal toxic ions, ***Chem. Eng. J.,*** **171:** 958 – 966.

Tiwari, D., Lee, S.M., 2011. Biomass - derived materials in the remediation of heavy metal contaminated water: Removal of Cadmium(II) and Copper(II from aqueous solutions, ***Wat. Environ. Res.,*** **83(9):** 874 – 881.

Theis, T. L., Lyer, R., Ellis, S. K., 1992. Evaluating a New granular Iron Oxide for removing Lead from Drinking Water, ***J. AWWA***, 101 – 105.

Upien, R.M., 1986. ***Int. Sci. Eau.,*** **2(4):** 109

Vaishya, R.C., Gupta, S.K., 2002. Modelling of arsenic(III) adsorption from water by sulfate modified iron oxide-coated sand (SMIOCS), ***J. Chem. Technol. Biotechnol.,*** **78:** 73 – 80.

Viraraghavan, T., Sapach, R., Rao, G.A. K., 1990. *Proc. Am. Conv. West. Can. Water Waste water Assoc.,* **42:** 85.

Viraraghvan, T., Subramanian, K. S., Aruldoss, J. A., 1999. Arsenic in drinking water problems and solutions, ***Wat. Sci. Technol.,*** **40:** 69 – 76.

Volkenshtein, F. F., 1949. Zhur. Fiz. Khim., **23:** 917.

Wahl, A.C., Bonner, N.A., (Eds), 1951. *Radioactivity Applied to Chemistry*, John Wiley and sons, New York.

Walsh, A., 1955, The application of atomic absorption spectra to chemical analysis, ***Spectrochim. Acta,*** **7:** 108 – 117.

Wang, J., Bejan, D., Bunce, N., 2003. Removal of arsenic from synthetic acid mine drainage by pH adjustment and co-precipitation with iron hydroxide, ***Environ. Sci. Technol.,*** **37:** 4500 – 4506.

Wang, T. C., 1995. *Copper and cadmium removal and recovery by iron oxide-coating granular activated carbon*. Ph. D. Dissertation, Illinois Institute of Technology, Chicago, II.

Wartelle, L.H., Marshall, W.E., 2006. Quaternized agricultural byproducts as anion exchange Resins, ***J. Environ. Manage.,*** **78:** 157 – 162.

Wells, M.J.M., Morse, A., Bell, K.Y., Pellegrin, M.L., Fono, L.J., 2009. Emerging pollutants, ***Wat. Environ. Res.,*** **81:** 2211 – 2254.

Welz, B., Sperling, M., 1999. *Atomic Absorption Spectrometry,* Wiley – VCH, Weinheim, Germany, ISBN 3-527-28571-7.

Weisz, P.B., 1953**. *J. Chem. Phys.,* 21:** 1531.

WHO (World Health Organisation), 1981. *Environmental Health Criteria, 18: Arsenic,* World Health Organisation, Geneva,

Wilms, D.A., Vercamst, K., Dijk, J.C., 1992. Recovery of silver by crystallization of silver carbonate in a fluidized bed reactor, ***Wat. Res.*, 26:** 235 – 239.

Williams, A. M., 1918. ***Proc. Roy. Soc. Edinburg.*, 38:** 23.

Wong, K.K., Lee, C.K., Low, K.S., Haron, M.J. 2003. Removal of Cu and Pb by tartaric acid modified rice husk from aqueous solutions, ***Chemosphere*, 50(1):** 23 –28.

Wolkentein, T., Peshev, O., 1965. ***Kinetika Kataliz.*, 6:** 95.

Wolkentein, T., Peshev, O., 1965. The electron factor in the kinetics of chemisorption on semiconductors, ***Catalysis, J.*, 4:** 301 – 309.

Xu, Y.H., Nakajima, T., Ohki, A., 2002. Adsorption of arsenic(V) from drinking water by aluminium - loaded Shirasu – zeolite, ***J. Hazard. Mater.*, B92:** 275 – 287.

Xu, Y., Axe, L., 2005. Synthesis and characterization of iron oxide-coated silica and its effect on metal adsorption. ***J. Colloid Inter. Sci.*, 282:** 11 – 19.

Xu, R.K., Wang, Y., Tiwari, D., Wang, H. 2009. Effect of ionic strength on adsorption of As(III) and As(V) on variable charge soils, ***J. Environ. Sci.*, 21:** 927 – 932 .

Yan, G., Viraraghavan, T., 2011. Heavy metal removal in a biosorption column by immobilized *M. Rouxii* biomass, ***Bioresour. Technol.*, 78:** 243 – 249.

Yang, J. K., Chang, Y. Y., Lee, S. I., Choi, H. J., Lee, S. M., 2005. Application of iron coated sand on the treatment of toxic metals, ***Wat. Sci. Technol.: Wat. Supply*, 4:** 335 – 341.

Yebra – Biurrun, M.C., Bermejo – Barrera, A., Bermejo – Barrera, M. P., Barciela – Alonso, M.C., 1995. Determination of trace metals in natural waters by flame atomic Absorption spectrometry following on-line ion exchange pre-concentration, ***Analytica Chim. Acta*, 303:** 341 – 345.

Younger, P.L., Banwart, S.A., Hedin, R.S. 2002. *Mine Water: Hydrology, Pollution, Remediation,* Kluwer Academic Publishers: Dordrecht, The Netherlands.

Yoyutsky, S., 1978. *Colloids Chemistry,* Mir publication, Moscow.

Yu, L.J., Shukla, S. S., Dorris, K. L., Shukla, A., Margrave, J. L., 2003. Adsorption of chromium from aqueous solutions by maple HA, ***J. Hazard. Mater.,*** **B100:** 53 – 63.

Zachara, J. M., Gaussman, P. L., Smith, S. C., Taylor, D., 1995. Oxidation of Co-EDTA^2 complexes in subsurface materials with iron and manganese oxide grain coatings, ***Geochim. Cosmochim. Acta,*** **59:** 4449-4463.

Zhong, Z.Y., Prozorov, T., Felner, I., Gedanken, A., 1999. Sonochemical synthesis and Characterization of iron oxide coated on submicro spherical alumina: a direct observation of interaction between iron oxide and alumina, ***J. Phys. Chem.,*** **B103:** 947 – 956.

Zouboulis, A. I., Kydros, K. A., Matis, K. A., 1993. Arsenic(III) and (V) removal from solutions by pyrite fines, ***Sep. Sci. Technol.,*** **28:** 2449 – 2463.

Zsingmondy, R. Z., 1911. ***Anorg. Chem.,*** **71:** 356.

REMOVAL BEHAVIOUR OF IRON COATED SAND (ICS) AND MANGANESE COATED SAND (MCS) FOR HEAVY METAL TOXIC IONS FROM AQUEOUS SOLUTIONS

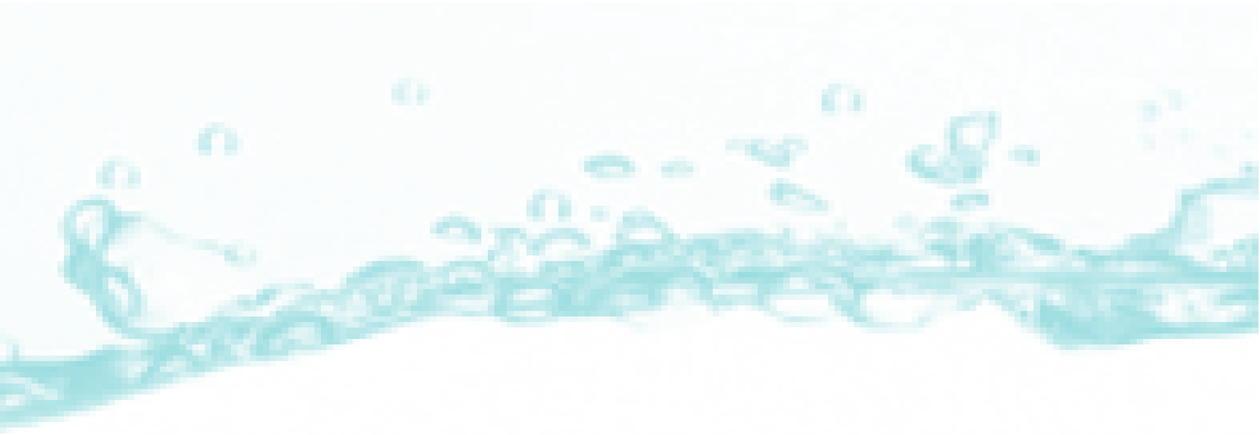

List of Publications

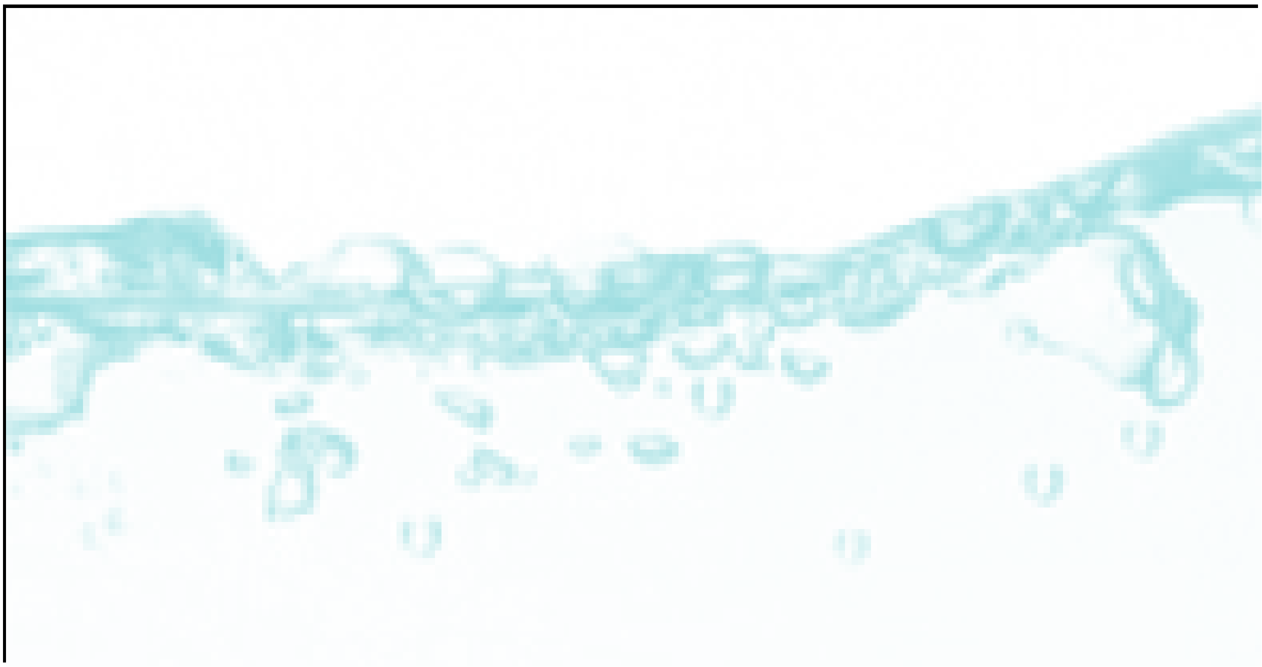

LIST OF PUBLICATIONS

(A) Journals :

1. Seung-Mok Lee, Won-Gee Kim, **C. Laldawngliana**, and Diwakar Tiwari, 2010. Removal behaviour of Surface modified sand for Cd(II) and Cr(VI) from aqueous solutions, ***Journal of Chemical & Engineering Data,*** **55:** 3089–3094.

2. Diwakar Tiwari, **C. Laldanwngliana**, Chul-Ho Choi, Seung Mok Lee, 2011. Manganese – modified natural sand in the remediation of aquatic environment contaminated with heavy metal toxic ions, ***Chemical Engineering Journal,*** **171:** 958–966.

3. Seung-Mok Lee, **C. Laldawngliana**, Diwakar Tiwari, 2012. Iron oxide nano–particles–immobilized-sand materials in the treatment of Cu(II), Cd(II) and Pb(II) contaminated waste waters, ***Chemical Engineering Journal,*** **195–196:** 103–111.

(B) Conference / Symposiums:

1. **C. Laldawngliana**, Diwakar Tiwari, Kyu-Man Choi, Seung-Mok Lee. Removal behaviour of surface modified sand for Cr(VI) and Cd(II)ions from aqueous solutions. *Proceedings of American Society of Civil Engineers/ Environmental and Water Resources Institute 3rd International Perspective on Current & Future State of Water Resources & the Environment,* January 5–7, 2010, IIT Madras, Chennai, India.

2. **C. Laldawngliana,** Diwakar **Tiwari**, Seung-Mok Lee. Surface Modified Sand in the Removal of Cr(VI) from Aqueous Solutions. *Proceedings of American Society of Civil Engineers/Environmental and Water Resources Institute. 4th International Perspective on Water Resources & the Environment,* January 4–6, 2011, National University of Singapore.

3. Diwakar Tiwari, **C. Laldawngliana**, Munui Kim, Seunk Mok Lee. Iron modified natural sand in the remediation of Arsenic contaminated waters. *Proceeding of 1st International conference on Green Environmental Technology 2011,* August 21 – 24, 2011, BEXCO, Busan, Korea.

4. **C. Laldawngliana,** Diwakar Tiwari. Manganese-modified sand in removal of heavy metal toxic ion contaminants in aquatic environment. *National Seminar cum Training Program on Green & Environmental Chemistry, Chemistry Department, Mizoram University,* 30th March 2011.

5. **C Laldawngliana,** Diwakar Tiwari and Seung Mok Lee. .Iron Impregnated Natural Sand (IINS), the effective adsorbent for treatment of Cu(II) and Pb(II) contaminated waste water. *Proceedings of International Conference on Advances in Environmental Chemistry (AEC-2011),* 16th-19th November, 2011, Mizoram University, Aizawl, Mizoram, India.

6. Lalramnghaki Pachuau, **C. Laldawngliana**, Diwakar Tiwari and Seung Mok Lee. Organo – inorgano – sericite, the promising adsorbent for waste water treatment. *Proceedings of International Conference on Advances in Environmental Chemistry (AEC-2011),* 16th-19th November, 2011, Mizoram University, Aizawl, Mizoram, India.

REMOVAL BEHAVIOUR OF IRON COATED SAND (ICS) AND MANGANESE COATED SAND (MCS) FOR HEAVY METAL TOXIC IONS FROM AQUEOUS SOLUTIONS

Appendix

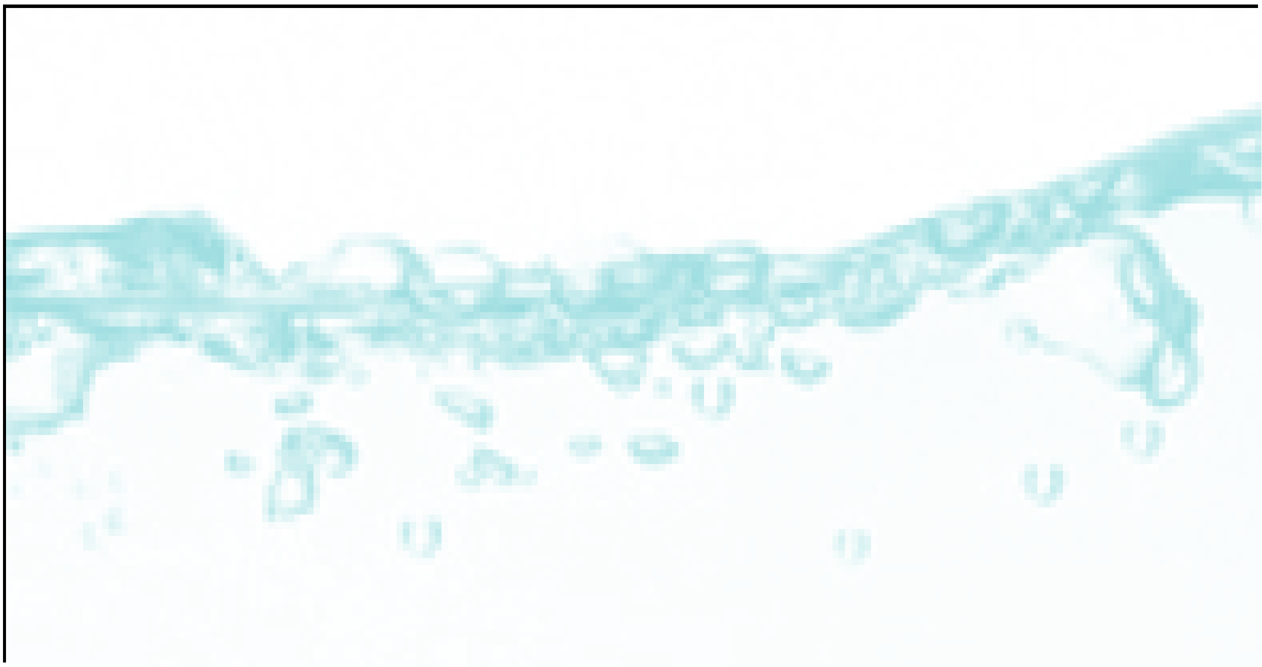

J. Chem. Eng. Data **2010,** *55,* 3089–3094

Removal Behavior of Surface Modified Sand for Cd(II) and Cr(VI) from Aqueous Solutions

Seung-Mok Lee,[†] Won-Gee Kim,[†] C. Laldawngliana,[‡] and Diwakar Tiwari*[,‡]

Department of Environmental Engineering, Kwandong University, Gangnung 210-701, Korea, and Department of Chemistry, Mizoram University, Tanhril Campus, Aizawl 796009, India

---

Sand which is a good filter medium and widely used in wastewater treatments possesses a very insignificant sorption capacity for several heavy metal toxic ions. However, surface-modified sand as impregnated with manganese is supposed to possess fair removal capacity at least for the low level removal of several heavy metal toxic ions from aqueous solutions since manganese is likely to be aggregated onto the sand surface as manganese dioxide which is a good adsorbing material. The present investigation intends to exploit the use of sand obtained from the river Tlawng, Sairang site, Aizawl, Mizoram, India. The sand sample was impregnated with Mn(II) by a wet method. Further, the surface morphology of this manganese-impregnated sand (MIS) was obtained using scanning electron microscopy, which showed that the manganese oxide occupied the surface of the sand and clustered on it. The particle size of coated manganese oxide was found to be in the nanoscale range. Moreover, the specific surface area of the sand was also increased with this impregnation. Further, the removal efficiency of MIS was assessed for two important heavy metal toxic ions, that is, Cr(VI) and Cd(II). The study was carried out for the pH and concentration dependence of sorptive solutions. Results obtained for the concentration dependence were further analyzed by the Freundlich and Langmuir adsorption isotherms.

Introduction

The contamination of surface or ground waters by toxic heavy metals is one of environmental and public concern because of the fact that these ions are virtually nonbiodegradable and tend to accumulate in living organisms, causing various biological disorders.[1] Although several heavy metals are reported to be essential trace ions, enhanced intake causes several adverse effects toward humans. Further, the increased level of industrialization and urbanization is one of the major sources of contamination of water bodies. The removal of toxic heavy metal ions from wastewaters has received increased attention recently for global awareness of the underlying detriment of heavy metals in the environment. Applications of traditional treatment techniques have enormous cost and continuous input of chemicals, which becomes impracticable and also causes further environmental damage.[2] Chemical precipitation has been traditionally employed to remove toxic heavy metal ions from aqueous solutions. However, metal removal via coagulation or flocculation is, in many cases, insufficient to meet strict regulatory requirements.[3] Hence, interest lies toward more effective, economic, and eco-friendly techniques to be developed for the fine-tuning of effluent and wastewater treatment.[4,5] In this regard inorganic ion-exchangers play a predominant role for the removal or speciation of several cationic and anionic species from wastewaters, and if the adsorbent is chosen so carefully and the solution chemistry adjusted accordingly, it can provide an effective waste treatment technique even over a wide range of solution pH.[6−10]

Heavy metals such as cadmium (Cd) and chromium (Cr) often are present in industrial wastewaters, are known to be hazardous to the aquatic ecosystem, and pose serious health hazards toward human beings. Cadmium is one of the dangerous pollutants, originating from metal plating, metallurgical alloying, mining, ceramics, and other industrial operations.[11] Cadmium toxicity may be observed by a variety of syndromes and effects including renal dysfunction, hypertension, hepatic injury, lung damage, and tetragenic effects.[12] Similarly, Cr(VI) is poisonous to most living organisms and has many applications including in-wood preservation.[13] Humans are exposed to excessive amounts of Cr(VI) through food, drinking water, and inhaling air that contains chromium. The average daily intake from air, water, and food is estimated to be (0.01 to 0.03) μg, 2.0 $\mu g \cdot L^{-1}$, and 60.0 μg, respectively.[14] Cr(VI) is known to be toxic to both plants and animals, as a strong oxidizing agent and potential carcinogen.[15] Cr(VI) is considered by the IARC (International, Agency for Research on Cancer) as a powerful carcinogenic agent that modifies the DNA transcription process, causing important chromosomic aberrations.[16] Therefore, the presence of Cr(VI) in water causes several environmental problems, and as mentioned by Muir,[17] the NIOSH (National Institute for Occupational Safety and Health) recommends that the levels of Cr(VI) in water should be reduced to 0.1 $mg \cdot L^{-1}$.

Sand is widely used as a filter medium for the treatment of wastewaters, and it was found that during the treatment, manganese and iron, if present in wastewater, are to be deposited on the surface of the sand in the form of their oxides. Moreover, either naturally or laboratory coated sand with manganese has been found to be fairly effective for the removal of several toxic heavy metal ions due to its high exchange capacity and selectivity toward these toxic ions.[18,19] Moreover, it may also provide removal efficiency even down to the trace level. Hence,

---

* Corresponding author. E-mail: diw_tiwari@yahoo.com. Tel/fax: +91-389-2330860.
[†] Kwandong University.
[‡] Mizoram University.

10.1021/je901094h

keeping this in view, the present study is conducted as to impregnate sand with Mn(II) and to characterize the impregnated sand. The suitability and selectivity of this manganese-impregnated sand (MIS) is then assessed for the low level removal of two important toxic heavy metal ions, namely, Cd(II) and Cr(VI), from aqueous solutions.

Experimental Section

Preparation of Manganese-Impregnated Sand (MIS) Samples. Manganese-coated sand was prepared by taking 120 g of sand ((30 to 60) BS in size) obtained from the local river Tlawng at the Sairang site, Aizawl, Mizoram, India and 100 mL of 0.05 M manganese chloride solution at pH = 9.0 in a beaker. The mixture was constantly stirred at (60 to 70) °C until the volume was reduced to about 10 mL. The solution was then kept in a drying oven at (90 to 100) °C for the complete evaporation of water. The sample was then kept at 160 °C for about 3 h for complete drying and better coating stability of the manganese. It was cooled to room temperature and again washed with distilled water several times. Finally the MIS sample was dried in a drying oven at 70 °C overnight. This dried MIS sample was used for the present investigation.

Batch Experiments. The pH_{PZC} is defined as the pH value where the net surface charge is zero. Hence, to evaluate the pH_{PZC}, the usual acid and base titrations were carried out by taking 5 g of a MIS sample in 500 mL of distilled water and titrated against the 0.1 $mol \cdot L^{-1}$ HNO_3 or NaOH solutions, and the corresponding pH was recorded using a pH meter. The titration data were further utilized to evaluate the pH_{PZC}. The pH_{PZC} for MIS was found to be 6.28.

Batch experiments were carried out to study the effect of pH on Cr(VI) and Cd(II) sorption by taking potassium dichromate solutions and cadmium nitrate solutions of (20 and 10) $mg \cdot L^{-1}$ concentrations, respectively, at different pH values of 2 to 10. The pH of the sorptive solutions was adjusted by adding drops of concentrated HNO_3/NaOH solutions. To 100 mL of each of these sorptive solutions, 0.5 g of the MIS sample was added. The solutions were constantly shaken for about 24 h in a rotary shaker at (25 ± 1) °C. The solutions were filtered with a 0.45 μm syringe filter, and the filtrates were then subjected to UV−visible spectrophotometry (Thermo Electron Corporation, England; model: UV1) analysis for Cr(VI) determination and AAS (Varian Spectra AA-300) for total cadmium determinations.

Similarly, the concentration dependence study was carried out varying the sorptive concentrations from (5 to 100) $mg \cdot L^{-1}$ (for Cr(VI)) and (1 to 20) $mg \cdot L^{-1}$ (for Cd(II)), keeping the solution pH constant (3.0 for Cr(VI) and 6.0 for Cd(II)). The 100 mL sorptive solutions were equilibrated with 0.5 g of MIS at (25 ± 1) °C for 24 h in a rotary shaker. The solutions were filtered with a 0.45 μm syringe filter, and the filtrates were then analyzed to measure the bulk sorptive concentrations.

Results and Discussion

Characterization of MIS. The effective coating of manganese onto the surface of sand was determined by using the US EPA method 3050B and was found to be 1446 $mg \cdot kg^{-1}$. Further, scanning electron microscopy (SEM) images (using FE-SEM model: SU-70, Hitachi, Japan) showed that the bare sand possessed a very compact and disordered surface structure with few pores on its surface (see Figure 1). Moreover, it contained several aggregated particles of silica. On the other hand MIS samples showed distinct micropores on its surface and a higher specific surface area, owing to the aggregation of manganese likely in the form of manganese dioxide on the sand surface. They were very orderly clusters onto the sand surface, and the particle size of manganese seems to be of the order of nanometers.

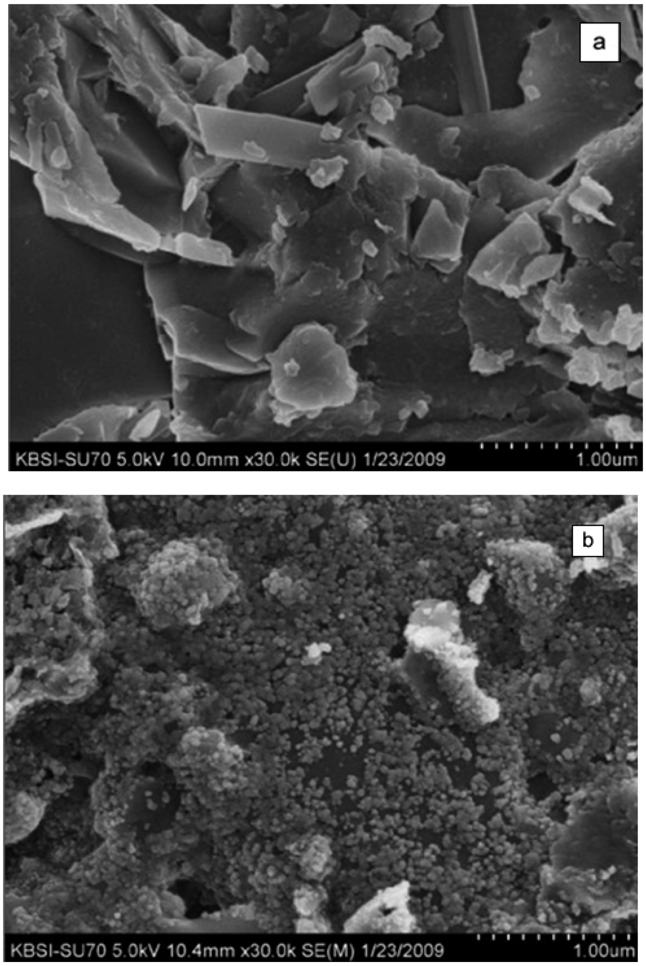

Figure 1. SEM images of (a) bare sand and (b) MIS.

Table 1. Physical Parameters Obtained with the Brunauer−Emmett−Teller (BET) Analyzer

	BET surface area	pore volume	pore size
	$m^2 \cdot g^{-1}$	$cm^3 \cdot g^{-1}$	nm
sand	8.51	$3.54 \cdot 10^{-3}$	1.96
MIS	9.21	$2.02 \cdot 10^{-3}$	2.14

Further, the physical properties of bare sand and MIS were obtained with a surface area and porosimetry system (model ASAP 2020, Micromeritics, USA) and are returned in Table 1. The MIS apparently possessed a relatively higher specific surface area.

Speciation Study of Cr(VI) and Cd(II). The speciation of Cr(VI) (20 $mg \cdot L^{-1}$) and Cd(II) (10 $mg \cdot L^{-1}$) were obtained using the MINEQL geochemical simulation program keeping the ionic strength (0.01 $mol \cdot L^{-1}$) and temperature (25 °C) constant as a function of solution pH. The equilibrium constants used are given in Table 2. The outcome of the results are shown in Figures 2 parts a and b respectively for Cr(VI) and Cd(II). Figure 2a clearly indicates that Cr(VI) exists as the soluble anionic species of CrO_4^{2-}, $HCrO_4^-$, or $Cr_2O_7^{2-}$ throughout the pH region, that is, 2 to 10. However, up to a pH of about 5.5, the major species of Cr(VI) is $HCrO_4^-$, and beyond pH 5.5 the predominant species is the CrO_4^{2-}. On the other hand the Cd(II) speciation showed (*cf* Figure 2b) that even up to pH 9.0 cadmium exists predominantly as the Cd^{2+} soluble cationic

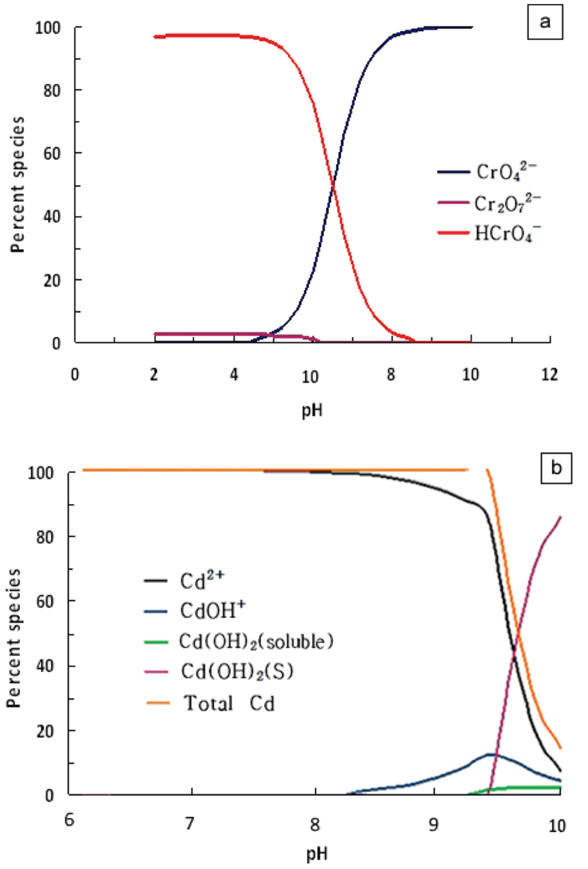

Figure 2. Speciation of (a) Cr(VI): 20 mg·L and (b) Cd (II): 10 mg·L^{-1} as a function of pH.

Table 2. Various Equilibrium Constants Used for the Speciation of Cr(VI) and Cd(II) in Aqueous Solutions at 25 °C and 0.01 mol·L^{-1} KNO_3 Ionic Strength

equilibrium	log *K*
$2CrO_4^{2-} + 2H^+ \leftrightarrow Cr_2O_7^{2-} + H_2O$	14.560
$CrO_4^{2-} + H^+ \leftrightarrow HCrO_4^-$	6.510
$CrO_4^{2-} + 2H^+ \leftrightarrow H_2CrO_4$ (aq)	6.419
$Cd^{2+} + 3H_2O \leftrightarrow Cd(OH)_3^- + 3H^+$	−32.505
$Cd^{2+} + 4H_2O \leftrightarrow Cd(OH)_4^{2-} + 4H^+$	−47.288
$Cd^{2+} + H_2O \leftrightarrow Cd(OH)^+ + H^+$	−10.097
$Cd^{2+} + 2H_2O \leftrightarrow Cd(OH)_2$ (aq) $+ 2H^+$	−20.294
$2Cd^{2+} + H_2O \leftrightarrow Cd_2(OH)^{3+} + H^+$	−9.397

species. Beyond pH 9.0 cadmium turns into the insoluble $Cd(OH)_2$ species. In between, a maximum of about 12 % of the $Cd(OH)^+$ species occurred at pH 9.4.

Removal Behavior of MIS for Cr(VI) and Cd(II). Effect of pH. The pH dependence data for the removal behavior of Cr(VI) and Cd(II) by MIS are obtained and presented graphically in Figure 3. Figure 3 clearly demonstrates the percent removal of these two ions as a function of pH. It is to be noted that in increasing the pH from 2.0 to 11.0 the removal percentage of Cd(II) increased from 14 % to 99 %, respectively, whereas the percent removal of Cr(VI) for a similar increase in pH, that is, from 2 to 10, decreased from 85 % to 72 %. The pH dependence data obtained by MIS may be explained with the help of the surface properties of MIS as well as the properties of the adsorbing species present in solution. Since MIS is likely to possess a manganese dioxide layer on its surface, the pH_{PZC} for manganese dioxide[20] is reported to be 5.5 against the experimentally obtained value of 6.28. The different values of pH_{PZC} may be because of the mineralogical species of manganese oxide; also possibly this value is due to the combination of the bare sand surface and the manganese-coated surface. Hence, the surface is supposed to be positively charged below pH 6.2, and beyond that it becomes negatively charged (see eq 1).

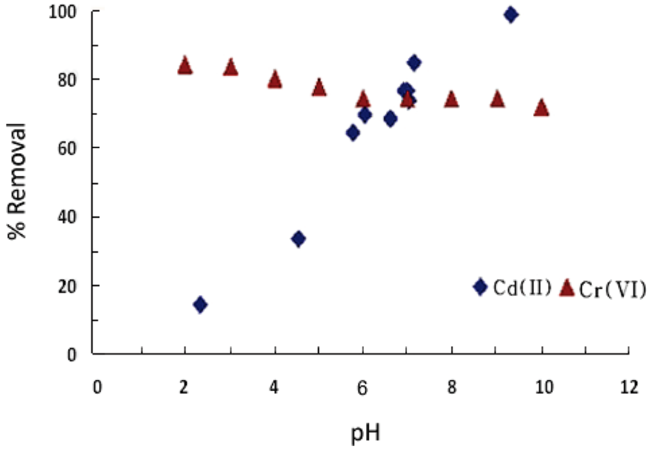

Figure 3. Effect of pH on the sorption of Cr(VI) and Cd(II) onto the surface of MIS [initial concentration of Cr(VI): 20 mg·L^{-1} and Cd(II): 10 mg·L^{-1}].

$$\equiv SH_2^+ \leftrightarrow \equiv SH^0(pH_{PZC}) \leftrightarrow \equiv S^- \quad (1)$$

The higher uptake of Cr(VI) at very low pH may be explained because of the anionic species of Cr(VI) present ($HCrO_4^-$, CrO_4^{2-}, $Cr_2O_7^{2-}$; see Figure 2a), which preferred the positively charged solid surface. However, the decrease in adsorption at higher pH values may be due to the competitiveness of the oxyanions of chromium and OH^- ions in the bulk solutions. In this region perhaps the repulsion of negatively charged surface to Cr(VI) anion also reduced the adsorption of Cr(VI) at higher pH. Moreover, the processes of oxo group protonation and Cr(VI) reduction are lowered because both of these reactions require protons.[21,22] Similar pH dependent results have also been reported for Cr(VI) on various sorbents previously.[23−25]

On the other hand, cadmium mostly exists in the cationic form in the pH range 2 to 9.0; hence, a sharp increase in adsorption occurred after pH 5.5, since the surface apparently becomes negatively charged and a further increase in pH beyond pH 9.0 leads to almost 100 % Cd(II) removal perhaps due to the mixed effect of adsorption and formation of insoluble species of cadmium, that is, $Cd(OH)_2$ (see Figure 2b). Moreover, below the pH 5.5 the removal of Cd(II) was greatly hindered, since the surface itself possesses a positive charge and the cadmium occurs in its cationic form, that is, Cd^{2+} in this pH region. In general the specific surface reactions may occur as follows.[18,26]

$$\equiv MnOH + Cd^{2+} \rightarrow \equiv MnO^-Cd^{2+} + H^+ \quad (2)$$

$$\equiv MnO^- + Cd^{2+} \rightarrow \equiv MnO^-Cd^{2+} \quad (3)$$

$$2(\equiv MnOH) + Cd^{2+} \rightarrow (\equiv MnO^-)_2Cd^{2+} + 2H^+ \quad (4)$$

$$2(\equiv MnO^-) + Cd^{2+} \rightarrow (\equiv MnO^-)_2Cd^{2+} \quad (5)$$

Further, it is interesting to note that at neutral pH conditions, that is, usual water pH, the employed solid MIS caused the removal of almost 80 % of these two pollutants, present in the aqueous solutions (see Figure 3). Hence, the material showed potential applicability to effectively decontaminate water polluted with Cr(VI) or Cd(II) at neutral pH conditions.

Effect of Sorptive Concentration. It has been mentioned that the initial concentration of a metal ion provides an important driving force to overcome all mass transfer resistances of the

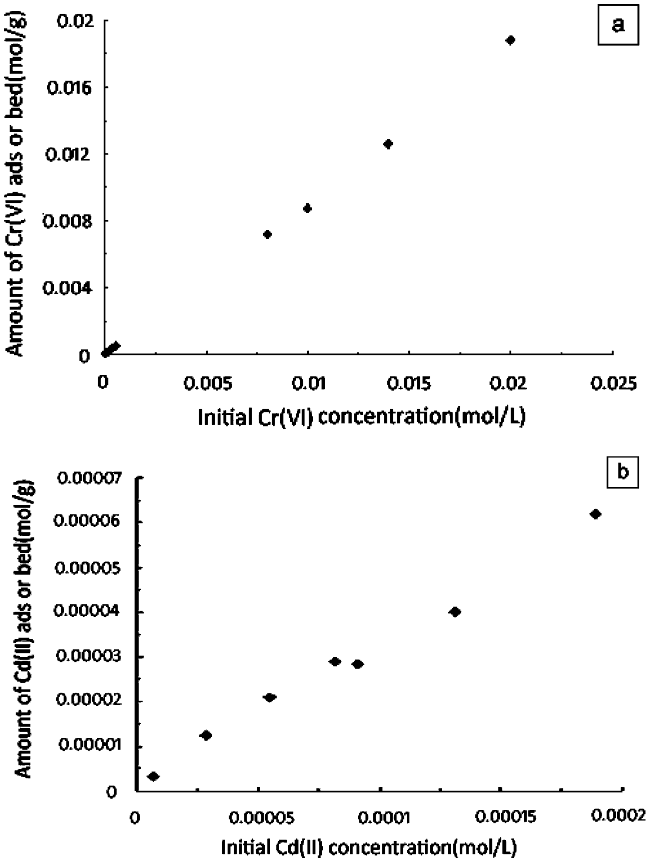

Figure 4. Effect of concentration on the sorption of (a) Cr(VI) pH: 3.0 and (b) Cd(II) pH: 6.0 onto the surface of MIS.

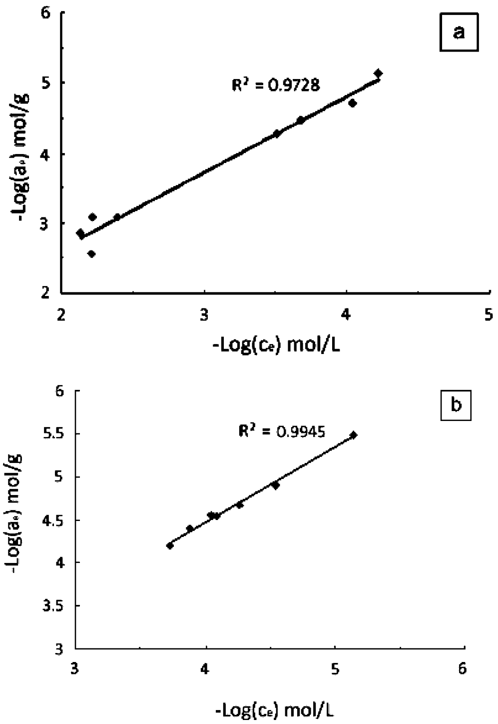

Figure 5. Freundlich adsorption isotherm for the sorption of (a) Cr(VI) and (b) Cd(II).

metal ion between aqueous and solid phases.[27] The effect of sorptive concentration on the removal behavior of MIS for Cr(VI) and Cd(II) was obtained by varying the sorptive concentration from $(9.63 \cdot 10^{-5}$ to $2.00 \cdot 10^{-2})$ $\text{mol} \cdot \text{L}^{-1}$ for Cr(VI) at pH 3.0 and $(7.30 \cdot 10^{-6}$ to $1.89 \cdot 10^{-4})$ $\text{mol} \cdot \text{L}^{-1}$ for Cd(II) at pH 6.0. The results obtained are shown in Figure 4 parts a and b respectively for Cr(VI) and Cd(II). It is to be noted that increasing the initial concentration apparently caused an increase in uptake of these two metal cations by the MIS. Further, by quantitatively increasing the concentration of Cr(VI) from $(9.63 \cdot 10^{-5}$ to $2.00 \cdot 10^{-2})$ $\text{mol} \cdot \text{L}^{-1}$, the amount of Cr(VI) removed was increased from $(8.44 \cdot 10^{-5}$ to $1.88 \cdot 10^{-2})$ $\text{mol} \cdot \text{g}^{-1}$. Similarly, the Cd(II) was increased from $(8.54 \cdot 10^{-7}$ to $6.47 \cdot 10^{-5})$ $\text{mol} \cdot \text{g}^{-1}$ for an increase in initial sorptive concentration from $(7.30 \cdot 10^{-6}$ to $1.89 \cdot 10^{-4})$ $\text{mol} \cdot \text{L}^{-1}$. Similar observations are reported by several authors along with our report as well.[2,23,28,29]

The concentration dependence data obtained at equilibrium between solid and solution interfaces were further utilized to build the adsorption isotherms, and it was found that these were fitted well by the Freundlich adsorption isotherm (eq 6), rather than the Langmuir isotherm. A reasonably good linearity was obtained while plotting the values of log a_e versus log C_e (see Figure 5.).

$$\log a_e = \frac{1}{n} \log C_e + \log K_f \qquad (6)$$

where a_e and C_e are the amount adsorbed $(\text{mol} \cdot \text{g}^{-1})$ and bulk sorptive concentration $(\text{mol} \cdot \text{L}^{-1})$ at equilibrium, respectively, and K_f and $1/n$ are the Freundlich constants referring to adsorption capacity and adsorption intensity or surface heterogeneity, respectively.[30] Further, in the case of $1/n = 1$, the partition between the two phases is independent of the concentration, and the case of $1/n < 1$ (the most common) corresponds to a normal L-type Freundlich isotherm,[31] while $1/n > 1$ is indicative of a cooperative sorption, which involves strong interactions between the molecules of the adsorbate.[32,33] These constants, that is, K_f and $1/n$, are estimated respectively by intercepts and slopes of the straight lines obtained while plotting log a_e versus log C_e (Figure 5a,b). The Freundlich constants along with the coefficient of determination (R^2) values obtained for these two systems are given in Table 3. The estimated adsorption capacities (i.e., K_f) for Cr(VI) and Cd(II) toward the MIS were found to be (0.326 and 0.111) $\text{mol} \cdot \text{g}^{-1}$, respectively. These results suggest that MIS possesses a relatively higher removal capacity for Cr(VI) compared to Cd(II). Further, the values obtained for the $1/n$ are less than one for Cd(II), whereas it is more than one for Cr(VI). As indicated previously, that is, $1/n > 1$, the Cr(VI) may have strong interactions within the sorbate molecules accompanied with cooperative sorption. Similar results are also reported for the Cr(VI) removal using the green alga *Ulva lactuca* and its activated carbon.[34] On the other hand Cd(II) possesses $1/n < 1$, which indicates that the MIS solid contains a heterogeneous nature and also points it toward the exponential distribution of adsorption sites.[35] On the other hand, the nonapplicability of the Langmuir adsorption isotherm is indicative of chemisorption, or perhaps an ion-exchange type uptake process took place at the surface. Moreover, the multilayer coverage along with the lateral interaction of sorbed ions could take place at the solid surface.

Further, the sorption capacity of MIS for these two pollutants, that is, Cr(VI) and Cd(II), obtained using the Freundlich fitting method are compared to the sorption capacities of different materials employed for these two pollutants in Table 4. Table 4 clearly demonstrates that MIS possesses very comparable sorption capacities for these two pollutants and, hence, is likely to be a possible alternative material for the treatment of waste waters contaminated with these pollutants.

Table 3. Freundlich Constants Obtained for the Cr(VI) and Cd(II) Sorption onto the Surface of MIS

Cr(VI)			Cd(II)		
$1/n$	K_f ($\text{mol}\cdot\text{g}^{-1}$)	R^2	$1/n$	K_f ($\text{mol}\cdot\text{g}^{-1}$)	R^2
1.076	0.326	0.973	0.879	0.111	0.994

Table 4. Adsorption Capacities Obtained for Cr(VI) and Cd(II) Using Different Materials

sorbents	sorption capacity of Cr(VI) $\text{mg}\cdot\text{g}^{-1}$	sorption capacity of Cd(II) $\text{mg}\cdot\text{g}^{-1}$	refs
Afsin-Elbistan fly ash		0.2306[a]	36
Seyitomer fly ash		0.0925[a]	36
food waste (areca)		1.086[b]	37
MnO_2 loaded D301 resin		77.88[a]	38
palygorskite clay	58.5[a]		39
maghemite nanoparticles	1.9[b]		40
bauxite	0.5[a]		41
Escherichia coli biofilm supported on kaolin	1.5[c]	1.1[c]	42
aniline formaldehyde condensate coated silica gel	0.89[b]		43
moss (*Hylocomium splendens*)		32.5[a]	44
MIS	6.27[b]	0.99[b]	present study

[a] Langmuir. [b] Freundlich. [c] Kinetic.

Conclusions

Manganese-coated sand (MIS) was prepared by the wet coating method, and SEM images of MIS showed that the manganese oxide occupied the surface and pores of the sand and clustered on it. The particle and pore size of coated manganese oxide was found to be in the nanoscale range. The amount of manganese coated was found to be 1446 $\text{mg}\cdot\text{kg}^{-1}$. Further, the MIS sample was exploited for the low level removal of Cr(VI) and Cd(II) from aqueous solutions. Results obtained showed that the lower pH values favored the uptake of Cr(VI), whereas the moderate-to-higher pH region favored Cd(II) removal. Moreover, relatively high uptake of these two pollutants at neutral pH conditions enhances the applicability of MIS to decontaminate water contaminated with Cr(VI) or Cd(II) at this pH. Similarly, the concentration dependence data fitted well the Freundlich adsorption isotherm rather than the Langmuir isotherm. The sorption capacity was obtained to be (0.326 and 0.111) $\text{mol}\cdot\text{g}^{-1}$, respectively, for Cr(VI) and Cd(II) ions. This work was partly supported by a Korea Science and Engineering Foundation (KOSEF) grant funded by the Korean Government (MEST) (No. 2009-0078010).

Acknowledgment

One of the authors, C.L., is thankful to the Higher and Technical Education Department, Govt. of Mizoram for granting him study leave to pursue his Ph.D. programme at the Chemistry Department, Mizoram University, Aizawl, India.

Literature Cited

(1) Martin, R. B. *Metal ions in Biological systems*; Sigel, H., Ed.; Marcel Dekker: New York, 1985.

(2) Tiwari, D.; Kim, H. U.; Lee, S. M. Removal behaviour of sericite for Cu(II) and Pb(II) from aqueous solutions: Batch and column studies. *Sep. Purif. Technol.* **2007**, *54*, 11–16.

(3) Lee, S. M.; Davis, A. P. Removal of Cu(II) and Cd(II) from aqueous solution by seafood processing waste sludge. *Water Res.* **2001**, *35*, 534–540.

(4) Chiron, N.; Guilet, R.; Deydier, E. Adsorption of Cu(II) and Pb(II) onto a grafted silica: isothermal and kinetic models. *Water Res.* **2003**, *37*, 3079–3086.

(5) Kadirvelu, K.; Namasivayam, C. Activated carbon from coconut coirfith as metal adsorbents: adsorption of Cd(II) from aqueous solution. *Adv. Environ. Res.* **2003**, *7*, 471–478.

(6) Benjamin, M. M.; Leckie, J. O. Effects of complexation by Cl, SO_4, S_2O_3 on adsorption behaviour of Cd on oxide surfaces. *Environ. Sci. Technol.* **1982**, *16*, 162–170.

(7) Davis, J. A.; Leckie, J. O. Effect of adsorbed complexing ligands on trace metal uptake by hydrous oxides. *Environ. Sci. Technol.* **2006**, *12*, 1309–1315.

(8) Elliot, H. A.; Huang, C. P. Adsorption of some copper(II)-amino acid complexes at the solid-solution interface. Effect of ligand and surface hydro- phobicity. *Environ. Sci. Technol.* **1999**, *14*, 87–93.

(9) Mishra, S. P.; Dubey, S. S.; Tiwari, D. Inorganic particulates in removal of heavy metal toxic ions IX. Rapid and efficient removal of Hg(II) by hydrous manganese and tin oxides. *J. Colloids Interface Sci.* **2004**, *279*, 61–67.

(10) Gupta, V. K.; Gupta, M.; Sharma, S. Process development for the removal of lead and chromium from aqueous solutions using red mud an aluminium industry waste. *Water Res.* **2001**, *35*, 1125–1134.

(11) Davis, T. A.; Volesky, B.; Vieira, R. H. S. F. Sagassum seaweed as biosorbent for heavy metals. *Water Res.* **2000**, *34*, 4270–4278.

(12) Hajialigol, S.; Taher, M. A.; Malekpour, A. A new method for the selective removal of cadmium and zinc ions from aqueous solution by modified clinoptilolite. *Adsorpt. Sci. Technol.* **2006**, *24*, 487–496.

(13) Lakatos, J.; Brown, S. D.; Snape, C. E. Coals as sorbents for the removal and reduction of hexavalent Cr from aqueous waste streams. *Fuel* **2002**, *81*, 691–698.

(14) Donais, M. K.; Henry, R.; Rettberg, T. Cr speciation using an automated liquid handling system with inductively coupled plasma mass spectro-metric detection. *Talanta* **1999**, *49*, 1045–1050.

(15) Costa, M.; Klein, C. B. Toxicity and carcinogenicity of chromium compounds in humans. *Crit. Rev. Toxicol.* **2006**, *36*, 155–163.

(16) IARC Monographs on the evolution of the carcinogenetic risk of chemical to humans, Supplement 4; IARC: Lyon, France, 1982.

(17) Muir, G. M. *Hazards in the Chemical Laboratory*, 2nd ed.; Pergamon Press: Oxford, 1977.

(18) Han, R.; Zou, W.; Zhang, Z.; Shi, J.; Yang, J. Removal of copper(II) and lead(II) from aqueous solutions by manganese coated sand I. Characterization and kinetic study. *J. Hazard. Mater.* **2006**, *B137*, 384–395.

(19) Viraraghvan, T.; Subramanian, K. S.; Aruldoss, J. A. Arsenic in drinking water - problems and solutions. *Water Sci. Technol.* **1999**, *40*, 69–76.

(20) Koulouris, G. Dynamic studies on sorption characteristics of 226Ra on manganese dioxide. *J. Radioanal. Nucl. Chem.* **1995**, *193*, 269–279.

(21) Cimino, G.; Passerini, A.; Toscano, G. Removal of toxic cations and Cr(VI) from aqueous solution by hazelnut shell. *Water Res.* **2000**, *34*, 2955–2962.

(22) Gode, F.; Pehlivan, E. Removal of cr(VI) from aqueous solution by two Lewatit-anion exchange resins. *J. Hazard. Mater.* **2005**, *119*, 175–182.

(23) Pehlivan, E.; Altun, T. Biosorption of chromium(VI) ion from aqueous solution using walnut, hazelnut and almond shell. *J. Hazard. Mater.* **2008**, *155*, 378–384.

(24) Gode, F.; Atalay, E. D.; Pehlivan, E. Removal of Cr(VI) from aqueous solutions using modified red pine sawdust. *J. Hazard. Mater.* **2008**, *152*, 1201–1207.

(25) Bhattacharya, A. K.; Naiya, T. K.; Mandal, S. N.; Das, S. K. Adsorption, kinetics and equilibrium studies on removal of Cr(VI) from aqueous solutions using different low-cost adsorbents. *Chem. Eng. J.* **2008**, *137*, 529–541.

(26) Pretorious, P. J.; Peter, W. L. The adsorption characteristics of δ-manganese dioxide: a collection of diffuse layer constants for the adsorption of H^+, Cu^{2+}, Ni^{2+}, Zn^{2+}, Cd^{2+} and Pb^{2+}. *Appl. Geochem.* **2001**, *16*, 1067–1082.

(27) Malkoc, E. Ni(II) removal from aqueous solutions using cone biomass of *Thuja orientalis*. *J. Hazard. Mater.* **2006**, *B137*, 899–908.

(28) Gode, F.; Atalay, E. D.; Pehlivan, E. Removal of Cr(VI) from aqueous solutions using modified red pine sawdust. *J. Hazard. Mater.* **2008**, *152*, 1201–1207.

(29) Mishra, S. P.; Tiwari, D. Inorganic particulates in removal of toxic metal ions: Part-IX. Rapid and efficient removal of Hg(II) by hydrous manganese and tin oxides. *J. Colloid Interface Sci.* **2004**, *279*, 61–67.

(30) Benjamin, M. M. Effects of competing metals and competing ligands on trace metal adsorption at the oxide/solution interface. Ph.D. Thesis, Stanford University, CA, 1978.

(31) Reed, B. E.; Matsumoto, M. R. Modeling of Cd adsorption in single and binary adsorbent (PAC) systems. *J. Environ. Eng.* **1993**, *119*, 332–348.

(32) Haghesresht, F.; Lu, G. Adsorption characteristics of phenolic compounds onto coal-rejected-derived adsorbents. *Energy Fuels* **1998**, *12*, 1100–1107.

(33) Khezami, L.; Capart, R. Removal of chromium(VI) from aqueous solution by activated carbons: kinetic and equilibrium studies. *J. Hazard. Mater.* **2005**, *B123*, 223–231.

(34) El-Sikaily, A.; El-Nemr, A.; Khaled, A.; Abdelwehab, O. Removal of toxic chromium from wastewater using green alga *Ulva lactuca* and its activated carbon. *J. Hazard. Mater.* **2007**, *148*, 216–228.

(35) Benes, P.; Majer, V. *Trace Chemistry of Aqueous Solutions*; Elsevier: Amsterdam, 1980; pp 200.

(36) Bayat, B. Comparative study of adsorption properties of Turkish fly ash II. The case of chromium(VI) and cadmium(II). *J. Hazard. Mater.* **2002**, *B95*, 275–290.

(37) Zheng, W.; Li, X.-M.; Wang, F.; Yang, Q.; Deng, P.; Zeng, G.-M. Adsorption removal of cadmium and copper from aqueous solution by areca-A food waste. *J. Hazard. Mater.* **2008**, *157*, 490–495.

(38) Zhu, Z.-L.; Ma, H.-M.; Zhang, R.-H.; Ge, Y.-X.; Zhao, J.-F. Removal of cadmium using mnO_2 loaded D301 resin. *J. Environ. Sci.* **2007**, *19*, 652–658.

(39) Potgieter, J. H.; Potgieter-Vermaale, S. S.; Kalibantonga, P. D. Heavy metals removal from solution by palygorskite clay. *Miner. Eng.* **2006**, *19*, 463–470.

(40) Hu, J.; Chen, G.; Lo, I. M. C. Removal and recovery of Cr(VI) from wastewater by maghemite nanoparticles. *Water Res.* **2005**, *39*, 4528–4536.

(41) Erdem, H.; Altundogan, H. S.; Tllman, F. Removal of hexavalent chromium by using heat-activated bauxite. *Miner. Eng.* **2004**, *17*, 1045–1052.

(42) Quintelas, C.; Rucha, Z.; Silva, B.; Fonseca, B.; Figueiredo, H.; Tavares, T. Removal of Cd(II), Cr(VI), Fe(III) and Ni(II) from aqueous solutions by an *E. Coli* biofilm supported on kaolin. *Chem. Eng. J.* **2009**, *149*, 319–324.

(43) Kumar, P. A.; Ray, M.; Chakraborty, S. Hexavalent chromium removal from wastewater using aniline formaldehyde condensate coated silica gel. *J. Hazard. Mater.* **2007**, *143*, 24–32.

(44) Sari, A.; Mandil, D.; Tuzen, M.; Soylak, M. Biosorption of Cd(II) and Cr(III) from aqueous solution by moss (*Hylocohnium spendens*) biomass: Equilibrium, kinetic and thermodynamic studies. *Chem. Eng. J.* **2008**, *144*, 1–8.

Received for review December 30, 2009. Accepted May 16, 2010.

JE901094H

Chemical Engineering Journal 171 (2011) 958–966

Contents lists available at ScienceDirect

Chemical Engineering Journal

journal homepage: www.elsevier.com/locate/cej

Manganese-modified natural sand in the remediation of aquatic environment contaminated with heavy metal toxic ions

Diwakar Tiwari[a], C. Laldanwngliana[a], Chul-Ho Choi[b], Seung Mok Lee[b,*]

[a] *Department of Chemistry, School of Physical Sciences, Mizoram University, Aizawl 796004, India*
[b] *Department of Environmental Engineering, Kwandong University, Gangneung, Gangwondo, Republic of Korea*

ARTICLE INFO

Article history:
Received 12 March 2011
Received in revised form 19 April 2011
Accepted 20 April 2011

Keywords:
Manganese-modified natural sand
Pb(II)
Cu(II)
Freundlich isotherm
Sorption

ABSTRACT

The present communication aims towards the possible exploitation of modified natural sand materials in the remediation of the heavy metal toxic ions contaminated aquatic environment. The surface of the sand was modified as depositing the nano-particles of manganese (i.e., manganese-modified natural sand: MMNS) and the mineral phase of manganese was perhaps depicted to be pyrolusite as indicated by the XRD analytical data. The *d*-spacings of quartz was significantly enhanced with the manganese modification indicated the manganese caused an apparent increase in basal spacing of sand structure. SEM images and the EDX analysis showed that manganese nano-particles are evenly distributed onto the surface of sand. The BET surface area of the MMNS was increased significantly. The amount of manganese aggregated was found to be 1002.6 mg/Kg of sand and the stability tests suggested that the nano-particles aggregated onto the sand surface are fairly stable within the pH region 3–10. Further, the removal behavior of this MMNS was employed for the attenuation of two important heavy metal toxic ions i.e., Pb(II) and Cu(II) in aqueous medium. The uptake of these two metal ions followed the Freundlich adsorption isotherm. The removal capacity of MMNS estimated with the Freundlich approximation was found to be 0.4596 mg/g for Cu(II) and 2.996 mg/g for Pb(II). Further, the 1000 times increase in ionic strength caused for relatively insignificant change in uptake of these two ions onto the solid surface points it a predominant strong chemical binding involved at the solid/solution interface. The column experiments and the breakthrough curves suggested that material possessed significantly high removal capacity i.e., 0.190 and 0.895 mg/g, respectively, for Cu(II) and Pb(II) even under the dynamic conditions.

1. Introduction

The increasing scarcity of freshwater and its supplies led to the utilization of reclaimed water i.e., the treated wastewaters, in a variety of reuse applications. The planned potable reuse, a process by which reclaimed water is eventually incorporated into drinking water supplies, is one of the sources for diverse water portfolios. The reclaimed water is, however, contained with unregulated contaminants of emerging concern (CECs), which include pharmaceuticals, household chemicals, personal care products, disinfection by products, insecticides, and suspended endocrine disruptors along with the heavy metals toxic ions [1–4]. Although, many of these contaminants are present at very low levels; however, the toxicity and fate of these CECs makes a greater concern in the aquatic environment.

Similarly, increased use of toxic metals in various industrial processes caused an increased industrial effluent/wastewaters contaminated with these non-degradable toxic ions, which is entering into our aquatic environment. The extended persistence of these pollutants in the biological systems and tendency to accumulate within the bio-system as they move up with the food chain, represent important environmental and occupational hazards [5]. Hence, proper and effective attenuation/speciation of these, environmentally important, contaminants from the industrial effluents is one of the safe guards to protect the aquatic environment [6–8]. In this regard, the naturally occurring manganese oxides tend to attenuate the trace metals in the soil, sediments and rocks through their seemingly dominant sorptive capacities towards these ions because of its specific properties *viz*., high surface area, micropores available on its surface, possessed with –OH functional groups capable of forming strong chemical bond with several sorbing metal ions, including phosphate and arsenic etc. [9]. Hence, because of its unique properties manganese dioxide widely employed for the removal/speciation of several heavy/radio toxic ions from aqueous solutions [10–18]. However, the oxide of manganese is in the form of fine powders or is generated *in situ* in aqueous medium as hydroxide floc or gel. Under these conditions, solid/liquid separation is fairly difficult and the metal oxide alone is not suitable to be

---

* Corresponding author. Tel.: +82 33 649 7535; fax: +82 33 642 7635.
E-mail address: leesm@kwandong.ac.kr (S.M. Lee).

1385-8947/$ – see front matter © 2011 Elsevier B.V. All rights reserved.
doi:10.1016/j.cej.2011.04.046

used as filter medium since it possess significantly low hydraulic conductivity [19]. Therefore, keeping in view the modifications of the solid substrate materials *viz.*, sand or minerals are being exploited as coated with the manganese to obtain the materials like manganese-coated sand or manganese-coated minerals. The selection of sand because of it showed an excellent natural filter medium which could be possessed with cost effectiveness. Moreover, the stability and easy use may further enhance its exploitation for the purpose. Manganese coated sand or manganese coated minerals showed reasonably good sorption efficiency towards the variety of pollutants. Additionally, it provides a good filter medium for better performance of the materials towards its possible use in the waste water treatment plants [19–21]. It has also been observed that in natural medium the flux of Fe(II) and Mn(II) ions from the raw water facilities caused the formation of iron oxide coatings on the sand grains. The coatings formed normally have manganese oxides embedded within the substrate. These iron and manganese oxides (e.g., Fe_2O_3, FeOOH, MnO_2) in the sand mineral coating enhance adsorption of in-coming Fe(II) and Mn(II) ions. Certain oxides in the mineral coating, especially MnO_2 catalyses the oxidation of adsorbed Mn(II) in the presence of dissolved oxygen and favorable pH [22]. Consequently, the new adsorption sites are generated thus preventing saturation of adsorption capacity. The presence of high amount of these catalytic oxides on the sand grains is therefore paramount for the rapid start-up of manganese and other pollutants removal from the sand filters. The similar mechanism was proposed earlier for the batch reactor speciation of manganese from aqueous solutions using the manganese-coated sand and calcined starfish [23–25]. The removal efficiency of manganese-coated sand for Mn(II) was enhanced significantly by the addition of very small dose of sodium hypochlorite i.e., 3 ppm [23,24].

The report previously showed that manganese as in the mixed form of +3 and +4 state occurred with amorphous in nature onto the sand surface [19]. In a line reports indicated that manganese is mostly accumulated as in amorphous form on the carbon nano-tubes [26]. However, the manganese-coated sand was obtained using the $KMnO_4$ for the impregnation showed that manganese aggregated with multi crystallites of the pyrolusite (MnO_2), γ-Mn_2O_3 and $Mn(OH)_4$ onto the sand surface [27]. Manganese-oxide-coated zeolite was prepared using the $KMnO_4$ precursor and was further employed for the removal of uranium(VI), Cu(II) and Pb(II) under the column experimentation [28,29]. The fixed-bed column experiments were then employed to assess the applicability of the manganese-coated zeolite for the removal of lead and copper from aqueous solutions [30]. Further, the same group obtained the manganese-coated sand and employed this for the low-level removal of Cu(II) and Pb(II) under the single and binary removal of these pollutants from the aqueous solutions. However, the mineralogical study of the solid was not discussed [31]. Similarly, pyrolusite (δ-MnO_2 or β-MnO_2) was reported with the precursor Mn(II) as manganese nitrate was used for the preparation of MCS [20,32]. Alumina was chosen as the supporting material for the preparation of manganese-coated alumina using the manganese(II) chloride solution and the XRD results showed the manganese is coated as MnO_2. The material is further found to be useful in the defluoridation of drinking water [33]. The natural bentonite was impregnated with manganese(II) chloride in highly alkaline medium. Based on the XRD, IR and acid base titrations, it was concluded that manganese accumulated onto the surface of bentonite as manganese(IV) dioxide and possessed with very enhanced removal capacity for the Pb(II) from aqueous solutions [34]. In a line the study previously conducted showed the use the manganese-coated sand in the removal of some heavy metal cations/anions *viz.*, Cd(II) and Cr(VI) from aqueous solutions [35]. It was assumed that the manganese was associated as manganese(IV) dioxide onto the sand surface. The material showed a significant sorption capacity of manganese-coated sand towards these two heavy metal toxic ions. In a line the present communication aims to obtain indigenously the nano-sized manganese particles onto the natural sand surfaces with its mineralogical composition. Further, the material is to be assessed for its applicability in the removal of two important heavy metal toxic ions *viz.*, Cu(II) and Pb(II) from aqueous solution under the batch reactor as well the fixed-bed column reactor.

2. Materials and methods

2.1. Materials

Natural sand was obtained from the local river Tlawng at the Sairang site, Aizawl, Mizoram, India. It was washed with water, 0.2 mol/L HNO_3 and then again with distilled water. It was then sieved to obtain the 30–60 BS Mesh size using the simple sieve. Manganese nitrate as $Mn(NO_3)_2.6H_2O$; 97% Extra Pure, Junsei Chemical, Japan was used. The other chemicals *viz.*, copper sulfate ($CuSO_4.5H_2O$; GR Reagent, Duksan Pure Chemicals Co. Ltd., Korea and lead ($Pb(NO_3)_2$; GR Reagent, Shinyo Pure Chemicals Co. Ltd., Japan) are obtained and used without any further purification. HNO_3 and NaOH are used of AR grade and the water was used as de-ionized distilled water (18 MΩ-cm) using the Millipore water purification system (Milli-Q+).

2.2. Methodology

2.2.1. Nano-particle deposition onto sand

The sand surface was activated with taking the sand samples in the 0.1 mol/L HNO_3 solution overnight and hence washed with plenty of water and dried at 90 °C in a drying oven and stored in a stoppered bottle. 100 mL manganese nitrate i.e., 0.05 mol/L solution was taken in the flask and the pH of this solution was adjusted to 9.0 and then cleaned and dried 120 g sand was taken in this flask. This was rotated in the rotary evaporator with the slow speed of 30 rpm in the water bath at 70 °C and 90% of the water was very slowly removed applying the vacuum in the rotary evaporator. The sample was then taken into beaker and abruptly dried at 90 °C in the drying oven. Further, it was kept at 160 °C for about 8 h for the thermal stabilization of aggregated small-sized particles onto the sand surface. The MMNS sample was cooled at room temperature and washed with distilled water several times and again dried at 90 °C and stored in the stoppered polyethylene bottles.

2.2.2. Characterization of solid sample

The solid MMNS sample was characterized by using the SEM (Scanning Electron Microscope) machine (FE-SEM-Model: SU-70, Hitachi, Japan) equipped with energy dispersive X-ray Spectroscopy EDX system. XRD data was collected using the X-ray diffraction machine i.e., PANalytical, Netherland (vide model-X'Pert PRO MPD). The data was collected with the scan rate of 0.034 of 2θ illumination and the applied voltage was 45 kV with the observed current 35 mA and using the CuKα radiation having wavelength 1.5418 Å.

2.2.3. Stability of solids

The manganese particles aggregated onto the sand surface were assessed for its stability against the pH effect by varying the solution pH from 2 to 11. To this effect, 0.5 g of solid was equilibrated in 100 mL of distilled water at different initial pH values and then kept in an automatic shaker at 25 °C for 24 h. The solutions were then filtered using the 0.45 μm syringe filter and the filtrates were subjected for its total manganese content using the Atomic Absorption

Table 1
Various equilibrium constants used for the speciation of Cu(II and Pb(II) in aqueous solutions at 25 °C.

Equilibrium	log *K*
$2Cu^{2+} + 2\ H_2O \leftrightarrow Cu_2(OH)_2{}^{2+} + 2H^+$	−10.594
$Cu^{2+} + 3\ H_2O \leftrightarrow Cu(OH)_3{}^-$	−26.879
$Cu^{2+} + 4H_2O \leftrightarrow Cu(OH)_4{}^{2-} + 4H^+$	−39.980
$Cu^{2+} + H_2O \leftrightarrow Cu(OH)^+ + H^+$	−7.4970
$Cu^{2+} + 2\ H_2O \leftrightarrow Cu(OH)_2$ (aq.) + $2H^+$	−16.497
$Pb^{2+} + 2H_2O \leftrightarrow Pb(OH)_2$ (aq) + $2H^+$	−17.094
$Pb^{2+} + H_2O \leftrightarrow Pb(OH)^+ + H^+$	−7.597
$4Pb^{2+} + 4\ H_2O \leftrightarrow Pb_4(OH)_4{}^{4+} + 4H^+$	−19.988
$2Pb^{2+} + H_2O \leftrightarrow Pb_2(OH)_3{}^+ + H^+$	−6.397
$Pb^{2+} + 3\ H_2O \leftrightarrow Pb(OH)_3{}^- + 3H^+$	−28.091
$Pb^{2+} + 4H_2O \leftrightarrow Pb(OH)_4{}^{2-} + 4H^+$	−39.699
$3Pb^{2+} + 4H_2O \leftrightarrow Pb_3(OH)_4{}^{2+} + 4H^+$	−23.888

Spectrometer (AAS; Fast Sequential Atomic Absorption Spectrometer Model AA240FS, Varian).

2.2.4. pH_{PZC} determination of solid

The pH_{PZC} (point of zero charge) of manganese-modified natural sand was defined as the pH value at which the surface carries net zero charge. Hence, to evaluate the pH_{ZPC}, the acid and base titrations were carried out by taking 5 g of the solid sample in 500 mL of distilled water and titrated against the 0.1 mol/L of HNO_3 or NaOH solutions, and the corresponding pH was recorded using a pH meter (HANNA pH 213, Microprocessor pH meter, USA). The titration data were further utilized to evaluate the pH_{PZC}.

2.2.5. Speciation studies

Speciation of copper(II) and lead(II) were conducted separately using the MINEQL+ (Version 4.5) a geochemical computer simulation program. The input parameters were taken as initial concentration of Cu(II):20 mg/L; Pb(II): 40 mg/L; at constant temperature: 25 °C. Further, the thermodynamic equilibrium constants used were given in Table 1.

2.2.6. Batch reactor experiments

The stock solution i.e., 1000 ppm of Cu(II) and Pb(II) was prepared by dissolving the appropriate amounts of their salts in the distilled water and the desired concentration for the batch/column reactor experiments were obtained by successive dilution. The 10 mg/L of Cu(II)/or 20 mg/L of Pb(II) solution (100 mL) was taken into the polyethylene bottle and the pH was adjusted by the addition of drops of conc. HNO_3/NaOH solutions. 0.5 g of solid i.e., MMNS was then added. The bottles are kept in the automatic shaker (KUKJE, Shaking Incubator, Korea model 36-SIN-125) for 24 h at 25 ± 1 °C in order to complete the sorption process and an apparent equilibrium may likely to be attained between the solid/solution interfaces. The samples were taken out from the shaker and filtered using a 0.45 μm syringe filter and the pH was again checked and reported as the final pH. The filtrates were then subjected for its bulk sorptive concentration measurements using the AAS. Further, the percentage removal of the target metal ion was calculated using Eq. (1):

$$\%\text{Removal} = \frac{C_0 - C_e}{C_0} \times 100, \tag{1}$$

where C_0 and C_e, respectively, were the initial and bulk sorptive concentrations.

The kinetics of the sorption of Cu(II) and Pb(II) by the MMNS were carried out by obtaining the percent removal of these two cations as a function of time. The initial sorptive concentration i.e., 10 mg/L for Cu(II) and 20 mg/L for Pb(II) and the solution pH 4.0 was kept constant.

Further, the sorptive dependence data were collected taking the sorptive concentration from 1 to 20 mg/L (for Cu(II)) and from 1 to 40 mg/L (for Pb(II)) at the constant pH 4.0 and temperature 25 °C. Results obtained were then reported in terms of sorptive concentration and respective amount of Cu(II)/or Pb(II) removed. This concentration dependence data was then employed for the adsorption isotherm modeling using the Freundlich and Langmuir Adsorption isotherms Eqs. (2) and (3), respectively:

$$\text{Log}\ q_e = \text{Log}\, K_F + \frac{1}{n} \times \text{Log}\, C_e \tag{2}$$

$$\frac{C_e}{q_e} = \frac{1}{bq_m} + C_e\left(\frac{1}{q_m}\right), \tag{3}$$

where 'C_e' is the equilibrium concentration of Cu(II)/or Pb(II) in the solution (mg/L), 'q_e' is the amount of Cu(II)/or Pb(II) adsorbed at equilibrium (mg/g). The constants 'K_F' and n were known as the Freundlich constants and were representing, respectively, the adsorption capacity (mg/g) and adsorption intensity. On the other hand, the constants 'b' and 'q_m' were known as the Langmuir constants and referred, respectively, to the adsorption equilibrium constant (L/mg) and maximum adsorption capacity (mg/g) of solid.

Similarly, the ionic dependence study was conducted varying the background concentration of sorptive solution using the different concentrations i.e., from 0.001 to 0.1 mol/L of $NaNO_3$ solution. The sorptive pH (4.0) and temperature (25 °C) was kept constant throughout the experiments. The results were reported as percent removal as a function of the ionic strength.

2.2.7. Column experiments

The column experiments were performed using a glass column (1 cm inner diameter) packed with 2 g of solid MMNS sample (kept in the middle of column) and below and above to the MMNS, it was filled with the glass beads. Sorptive solution of Cu(II)/or Pb(II): 10 mg/L (prepared with back ground 0.01 mol/L $NaNO_3$ solution) and at constant pH 4.0 was pumped upward from the bottom of the column using Acuflow Series II, High-pressure liquid chromatograph, at a constant flow rate of 1.25 mL/min. Effluent samples were then collected using Spectra/Chrom CF-1 fraction collector. Furthermore, these collected samples were filtered using a 0.45 μm syringe filter and the total bulk sorptive concentrations were measured using AAS.

Further, the breakthrough data obtained were simulated for its removal capacity using the Thomas Eq. (4) [36]:

$$\frac{C_e}{C_0} = \frac{1}{1 + e^{(K_T(q_0 m - C_0 V))/Q}}, \tag{4}$$

where C_e is the Cu(II)/or Pb(II) concentration in the effluent (mg/L); C_0 is the Cu(II)/or Pb(II) concentration in the feed (mg/L); K_T the Thomas rate constant (L/min/mg); q_0 is the maximum amount of the Cu(II)/or Pb(II) can be loaded (mg/g) under the specified column conditions; m the mass of adsorbent loaded (g); V the throughput volume (L); and Q is the flow rate (L/min). A non-linear regression of the breakthrough data was performed for the least square fitting of two unknown parameters i.e., K_T and q_0.

3. Results and discussion

3.1. Surface morphology and mineralogical analysis of solid

The SEM images of sand and MMNS were obtained and shown in Fig. 1a and b, respectively, for the sand and MMNS. The SEM images clearly indicated that the bare sand possessed with very compact and disordered surface structure. It hardly has the meso- or micropores onto its surface. However, the surface structure of manganese-modified natural sand is completely different as the manganese is aggregated very orderly onto the surface of sand

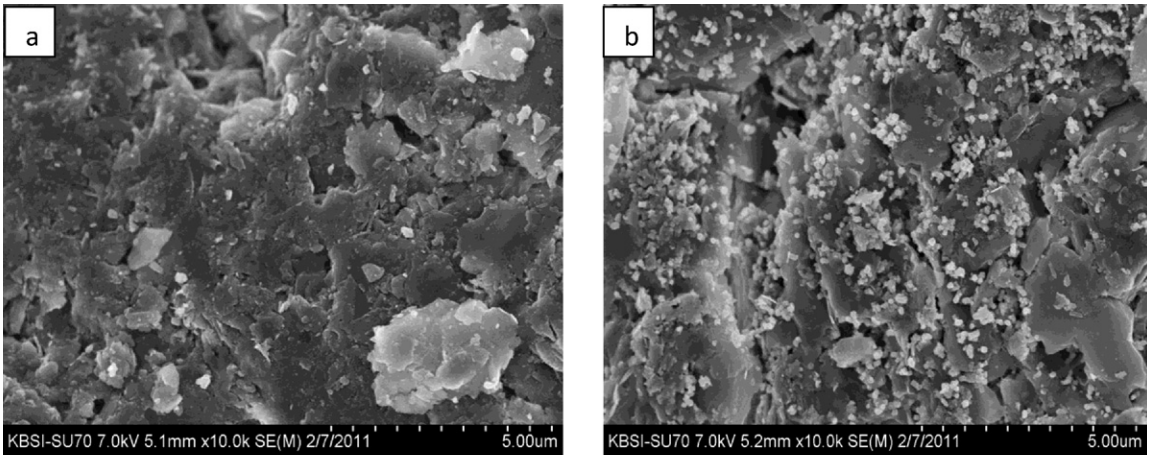

Fig. 1. SEM images of (a) sand and (b) manganese-modified natural sand.

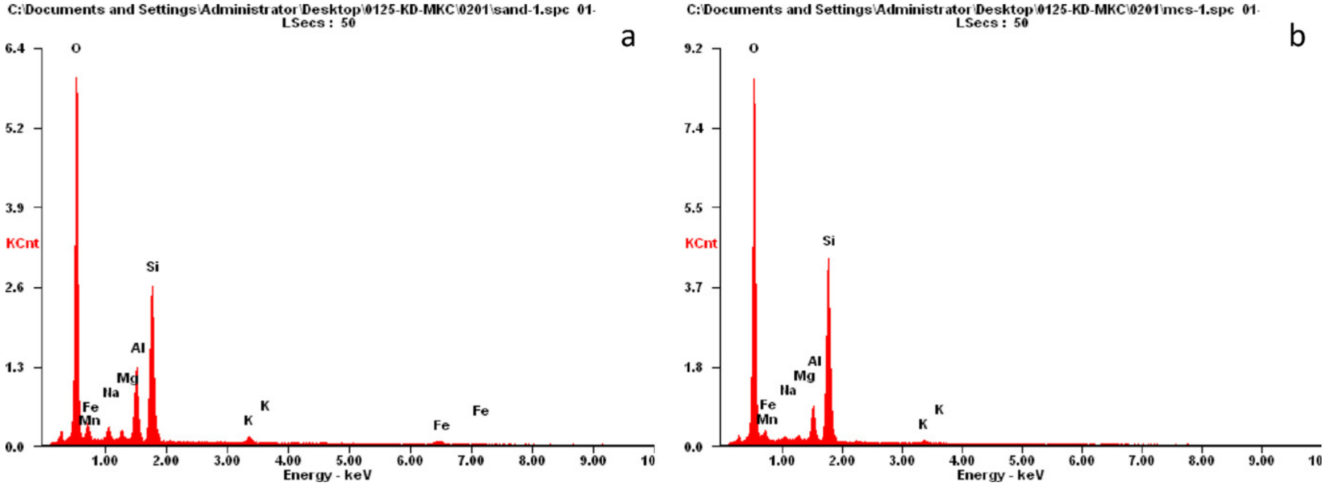

Fig. 2. EDX analytical data for (a) sand and (b) manganese-modified natural sand.

and the average size of these particles was estimated to be Ca. 200–300 nm. At places the particles were partially clustered. Further, the EDX analysis was performed and the results obtained were shown in Fig. 2a and b, respectively, for the sand and MMNS. Sand showed distinct peaks for the silica, iron, aluminum, magnesium etc. along with very weak peak of manganese (Ca. 0.25%). But the MMNS showed relatively distinct peak for the manganese i.e., Ca. 4.54% (weight percent). These results again confirmed the low-level aggregation of the manganese onto the surface of sand. Earlier, it was noted that significantly high manganese content was aggregated onto the sand surface making dense clustering onto the substrate [19] as was prepared by the different preparative route. Moreover, total manganese coated onto the sand was reported to be relatively much higher.

Further, the XRD data obtained for the sand and MMNS were shown in Fig. 3. The figure clearly possessed the distinct peaks at the 2θ value of 21.04, 26.76, 36.64, 39.58, 42.62, 50.24, 55.44, 60.04, 68.42, 81.57 etc. because of the reflections due to silica in both the samples. The *d*-spacings along with the relative intensities obtained for these reflections were then reported in Table 2. The data published by the Joint Committee on Powder Diffraction standards (JCPDS) were used to identify the crystalline phases of silica (SiO_2) in sand. Further, it was noted that the introduction of manganese caused for an apparent shift of the d-values, as mentioned in Table 2. This indicated that interlayer of sand structure was propped up significantly. Moreover, possibly due to the very low content of manganese onto the surface of sand, could not provide very sharp reflections of the mineral phases of manganese. These results were in accordance to the previous reports in which the pyrolusite was coated onto the clay surface using very low loading of pyrolusite. The pyrolusite was not detected by the XRD analysis because of the reasons that there may be inhibition of oxide crystallization or that the oxide nucleated as nanometer particles which were not detected by XRD [21]. This observation is also in accordance to the poorly crystalline lepidocrocite-coated montmorillonite [37]. However, the other reports indicated that it mainly contained with the pyrolusite (δ-MnO_2) [32]. Moreover, Hu et al. reported that the manganese was aggregated onto sand

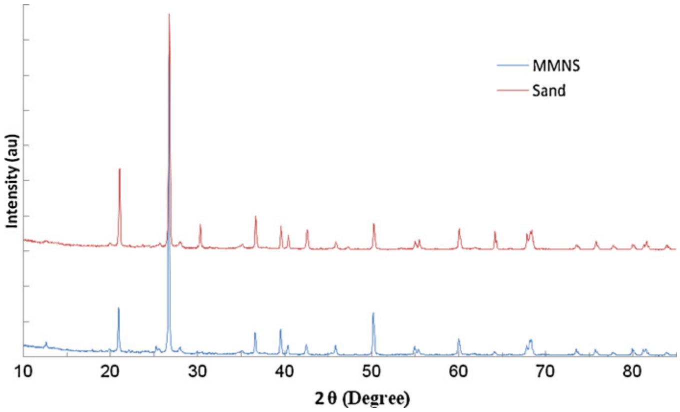

Fig. 3. XRD pattern of sand and manganese-modified natural sand.

Table 2
The *d*-spacing and relative intensities for sand and manganese-modified natural sand using the XRD data.

Sand	MIS					Difference with *d*-spacing
2θ	*d*-spacing	I/I_0	2θ	*d*-spacing	I/I_0	
21.0441	4.2215	34.59	20.9141	4.2474	16.02	0.0259
26.7641	3.3308	100	26.7121	3.3372	100	0.0064
36.6441	2.4523	14.61	36.5920	2.4557	7.88	0.0034
39.5821	2.2768	10.29	39.5301	2.2797	8.99	0.0029
42.6241	2.1211	8.88	42.4941	2.1273	4.09	0.0062
50.2421	1.8159	11.35	50.1641	1.8185	14.58	0.0026
55.4421	1.6573	4.90	55.3641	1.6594	2.38	0.0021
60.0441	1.5408	9.34	59.9921	1.5420	5.94	0.0012
68.4161	1.3712	8.84	68.3381	1.3726	5.61	0.0014
81.5721	1.1801	4.16	81.4941	1.1810	2.31	0.0009

as randomly stacked pyrolusite (MnO_2), γ-Mn_2O_3 and $Mn(OH)_4$ [27].

3.2. *Stability of solids*

The stability test data showed that the manganese strongly occupied the surface within the pH region 3–11 since no significant amount of manganese occurred in the bulk solution. Whereas, it was slightly unstable at pH 2 since Ca. 24 mg/L of total manganese was desorbed from the solid surface. These results suggested that manganese occupied the surface of sand firmly and likely to have some strong chemical binding with the substrate. Moreover, the solid is useful to employ it in water purification purposes over the wide pH range.

Further, the manganese content aggregated onto the surface of sand was also obtained by using the United States Environmental Protection Agency (US EPA) standard method 3050B. The amount of manganese aggregated effectively was found to be 1002.6 mg/Kg of sand. The low dose of manganese used (i.e., 0.05 mol/L) for the modification of activated sand samples likely to cause for less amount of manganese aggregated onto the sand surface and the other studies showed that very fine particles, orderly arranged onto the sand surface.

The pH_{ZPC} of the MMNS solid was obtained by the usual acid/base titrations and it was found to be 6.28. This value is somewhat higher than the pH_{ZPC} of the manganese dioxide as reported to be 5.5 [38]. This may be because of the mixed effect of sand and manganese content possibly in the form of manganese dioxide.

The specific surface area of the solids is obtained using a Brunauer–Emmett–Teller (BET) specific surface area analyzer (Mountech, Japan model MacSorb HM model-1200 Series). The BET multipoint surface area of the sand and manganese-modified natural sand was found to be, respectively, 8.51 and 11.03 m^2/g. This clearly showed that the manganese-modified natural solid possessed with significantly higher specific surface area compared to the bare sand sample.

3.3. *Speciation of Cu(II) and Pb(II)*

The speciation data obtained by the MINEQL+ geochemical program is returned in Fig. 4 for the Cu(II) and Pb(II). These results are important to elucidate the mechanism involved at solid solution interface. Moreover, it intends to describe, under the specified conditions, the sorptive ions are distributed in aqueous solutions with what specific species at the varied pH region i.e., pH 2–11. Fig. 4 clearly showed that both copper and lead exist to their ionic forms i.e., Cu^{2+} and Pb^{2+} up to the pH region ~5.8. But beyond that both started precipitating as the Cu(II) converted to tenorite and lead precipitated to $Pb(OH)_2(s)$ and around pH 7.0 these two were completely precipitated. The batch and column experiments conducted further, much lower sorptive concentrations (i.e., for Cu(II) 10 mg/L and Pb(II) 20 mg/L) and at pH 4.0 so that both the sorptive species existed to their ionic form and a plausible explanation was made based on these species.

3.4. *Batch experiments*

3.4.1. *Effect of pH*

The effect of pH on the sorption of Cu(II) (10 mg/L) and Pb(II) (20 mg/L) was conducted at constant temperature (25 °C) and the results in terms of percent adsorption were shown in Fig. 5. These results indicated that a sharp initial increase of removal attained

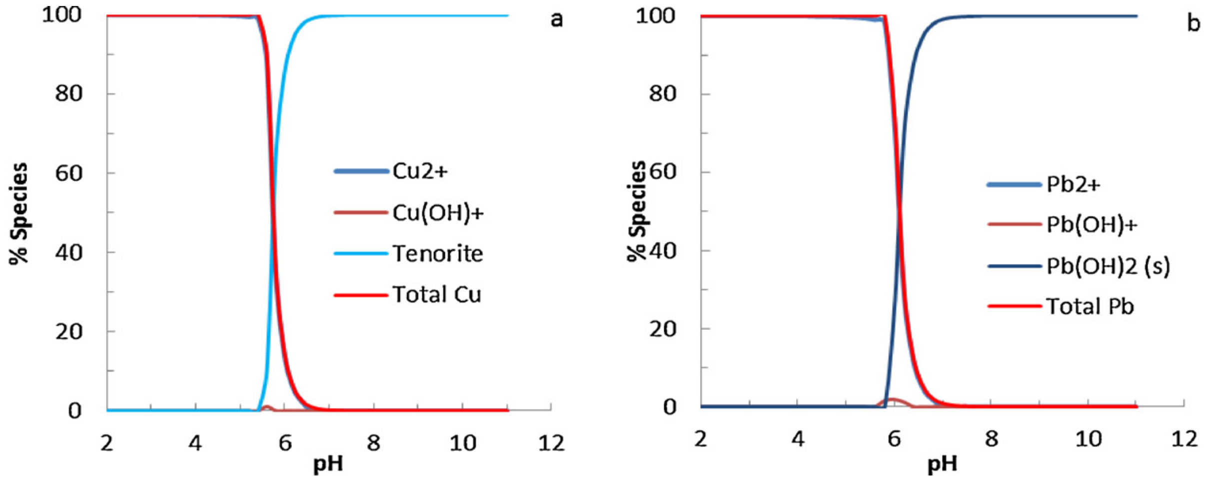

Fig. 4. Percentage distribution of various species of (a) Cu(II) and (b) Pb(II) as a function of pH.

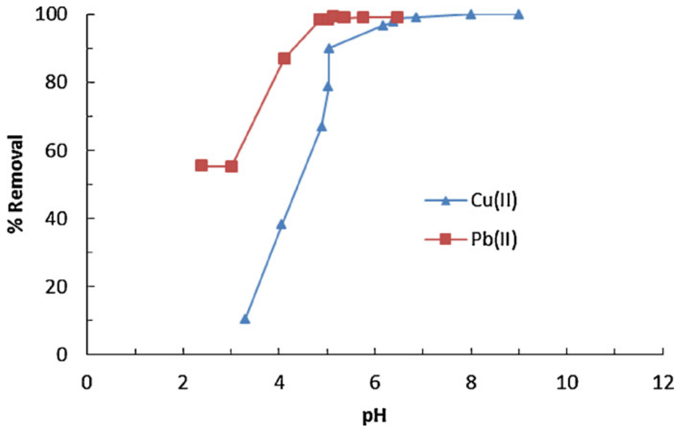

Fig. 5. Effect of pH on the removal of Cu(II) and Pb(II) by the MMNS. Initial [Cu(II)]: 10 mg/L and [Pb(II)]: 20 mg/L.

a maximum of almost 100% removal beyond pH 6.38 (for Cu(II)) and 4.85 (for Pb(II)). More quantitatively, increasing the pH from 3.30 to 9.00 the respective increase in Cu(II) removal was from 10.25% to 100.00%. Similarly, the Pb(II) removal was increased from 55.39% to 99.00% for the corresponding increase in pH i.e., from 2.39 to 6.48. The increase of percent removal using MMNS mainly depends upon the mixed effect of sorbing species and the surface properties of solids. The earlier observation showed that the manganese-modified natural sand has pH_{PZC} value of 6.28 against the manganese dioxide reported pH_{PZC} value of 5.5 [38]. Hence, it was expected that the manganese fine particles are aggregated as manganese dioxide on the surface of sand. Hence, the surface properties of MMNS were dependent on the manganese dioxide. The surface of MMNS becomes negatively charged beyond the pH 6.2 and below this it could possess the positive charge (Eq. (5)):

$$\equiv SH_2^+ \leftrightarrow \equiv SH^0(pH_{PZC}) \leftrightarrow \equiv S^- \quad (5)$$

On the other hand, below pH 6.2, the dominant species of Cu(II) and Pb(II) were the cationic species *viz.*, Cu^{2+} and Pb^{2+} or insignificant $Pb(OH)^+$ etc. Hence, increasing the pH above 6.2, surface of MMNS favored to attract the positively charged cations; however, the pH below 6.2 hindered the attraction of positively charged cations. Hence, based on these observations, it was assumed that relatively low uptake occurred at the lower pH values [35]. Additionally, relatively very high uptake of Cu(II) and Pb(II) occurred even at lower pH values may be explained with the possible specific chemisorption of these cations to the manganese-modified surfaces Eqs. (6)–(10) [19,35,39,40]:

$$\equiv MnOH + M^{2+} \rightarrow \equiv Mn{-}O{-}M^+ + H^+ \quad (6)$$

$$\equiv Mn{-}O^- + M^{2+} \rightarrow \equiv Mn{-}O{-}M^+ \quad (7)$$

$$2(\equiv Mn{-}OH) + M^{2+} \rightarrow (\equiv Mn{-}O^-)_2M^{2+} + 2H^+ \quad (8)$$

$$2(\equiv Mn{-}O^-) + M^{2+} \rightarrow (\equiv Mn{-}O^-)_2M^{2+} \quad (9)$$

$$\equiv Mn{-}OH + M^{2+} + H_2O \rightarrow \equiv Mn{-}O{-}M{-}OH + 2H^+ \quad (10)$$

where M denoted to Cu or Pb. Hence, the reactions (6, 8 and 10) were supposed to be predominant below pH 6.2. Moreover, the significant decrease in pH after adsorption as observed for these ions particularly for the Pb(II) (data not shown) indicated the occurrence of reactions (6,8 and 10). The chemisorption of these cations were further investigated using the background electrolytes i.e., the effect of ionic strength using the $NaNO_3$ solutions.

Moreover, further increase in pH i.e., beyond pH 6.2, there might be a mixed effect of adsorption and co-precipitation of metal ions on the surface of solids. Hence, apparently, it caused for very high uptake of metal ions in this pH region.

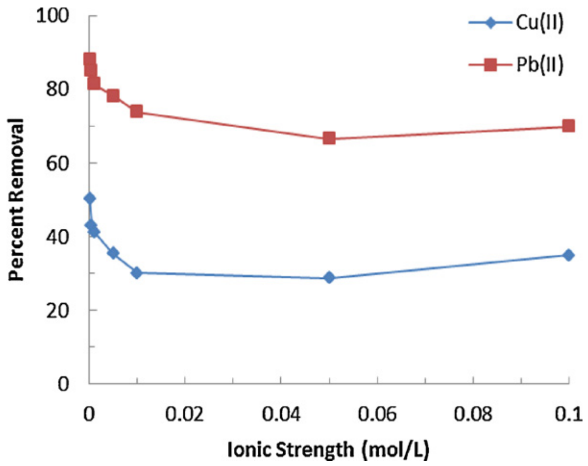

Fig. 6. Variation of percent removal of Cu(II) and Pb(II) by the MMNS as a function of ionic strength. Initial [Cu(II)]: 10 mg/L and [Pb(II)]: 20 mg/L; pH: 4.0.

The percent uptake of Cu(II) and Pb(II) as a function of time were obtained and it was found that the uptake of these two ions saturated within 10 min of contact. Quantitatively, Ca. 42% of Cu(II) and Ca. 73% of Pb(II) were removed at pH 4.0. No further change in uptake of these two cations was obtained even after 24 h of contact. This clearly demonstrated that sorption of Cu(II) and Pb(II) on the MMNS solids occurred in a single step and was not accompanied by any complexity.

3.4.2. *Effect of ionic strength*

Further, the change of ionic strength is one of the important parameter determining the nature of binding of the sorptive of ions onto the surface of solids. The ionic strength dependence data by soil minerals is usually used to distinguish between non-specific and specific adsorption. Outer sphere complexes involved only electrostatic interaction and are strongly affected by the ionic strength of the aqueous phase, whereas inner sphere complexes involved much stronger covalent or ionic binding and are only weakly affected by the ionic strengths [41,42]. Hence, the background electrolyte i.e., $NaNO_3$ was increased from 0.0001 to 0.1 mol/L and hence the removal of Cu(II) and Pb(II) was monitored keeping the initial sorptive concentration 10 mg/L (for Cu(II)) and 20 mg/L (for Pb(II)), temperature 25 °C and pH 4.0 was kept constant. The results obtained were presented graphically in Fig. 6. The figure clearly demonstrated that the increase in ionic strength i.e., from 0.0001 to 0.1 mol/L of $NaNO_3$ caused for decrease in percent removal, respectively, from 50.36 to 34.97% (for Cu(II)) and 87.94–69.81% (for Pb(II)). This indicated that the 1000 times increase in ionic strength caused only for the decrease in percent removal of 15.39% (for Cu(II)) and 18.13% (for Pb(II)). These results clearly inferred that the sorbing ions are predominantly bound by the strong forces and form the inner sphere complexes onto the surface of MMNS. These results again supported the mechanism suggested previously (vide reactions 6–10) or the applicability of the Freundlich sorption isotherm. The similar results also obtained for the removal of Cu(II) and Pb(II) by sericite [42]; Ni(II) and Cd(II) by rice straw [43] etc.

3.4.3. *Effect of Cu(II) and Pb(II) concentration*

It was reported that the initial concentration of a metal ion provides an important driving force to overcome all mass transfer resistances of the metal ion between aqueous and solid phase [44]. The concentration dependence data was obtained increasing the Cu(II) concentration from 1 to 20 mg/L for Cu(II) and 1 to 40 mg/L for Pb(II) keeping the solution pH 4.0 and temperature 25 °C as

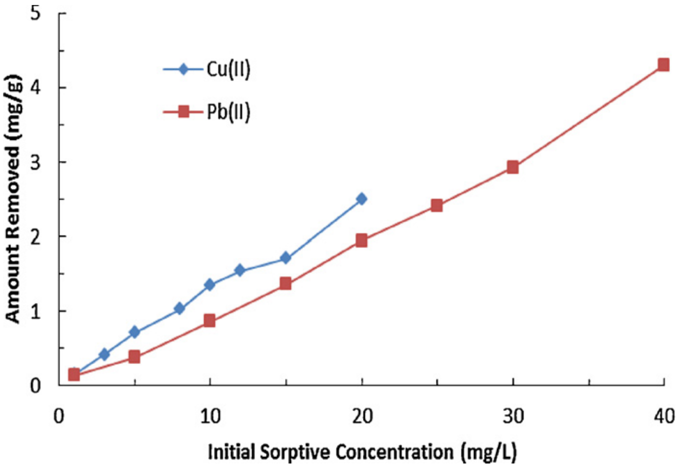

Fig. 7. Amount of Cu(II) and Pb(II) removed by the MMNS as a function of sorptive concentration. pH: 4.0.

constant. Results obtained were presented as a function of amount removed in Fig. 7. The figure clearly indicated that increasing the concentration from 1 to 20 mg/L of Cu(II) caused to increase an amount removed, respectively, from 0.151 to 2.498 mg/g. Similarly, for the Pb(II) ions the increase in sorptive concentration from the 1 to 40 mg/L increased the removal content, respectively, from the 0.138 to 4.3 mg/g. However, on the other hand the percent sorption was decreased, respectively, from 81.65 to 54.04% (for Cu(II)) and 99.00–75.02% (for Pb(II)) for the respective increase in concentration i.e., 1–20 mg/L for Cu(II) and 1–40 mg/L for Pb(II). This decrease in percent uptake of metal cations may be explicable on the basis that less number of active sites are available at the solid surface at higher concentration of sorbing ions [45,46].

3.4.4. Equilibrium modeling

The concentration dependence study was further utilized to model it towards the known Freundlich adsorption isotherm (Eq. (2)). The Freundlich model assumed with the assumption that the sorption occurs on an energetically heterogeneous surface on which the sorbed molecules interact laterally. The plots were drawn between Log C_e vs. Log q_e and reasonably a good straight line was obtained having the R^2 value of 0.980 for Cu(II) and 0.941 for Pb(II) (cf. Fig. 8a and b). Further, using the fitting equation, the Freundlich constants $1/n$ and K_F were evaluated. The $1/n$ values for the Cu(II) and Pb(II) were found to be 0.623 and 0.276, respectively. The fractional values of $1/n$ $(0 < 1/n < 1)$ obtained referred to the heterogeneous nature of the solid surface along with the exponential distribution of sorption sites [47,48]. On the other hand, K_F which estimates the maximum removal capacity of the solid was found to be 0.4596 mg/g for Cu(II) and 2.996 mg/g for the Pb(II). Relatively fair uptake capacity was obtained for these two solids. Comparing these two cations MMNS showed better capacity for the lead ions than copper ions. The applicability of Freundlich adsorption isotherm again points it towards the chemisorptive type of sorption taking place at the solid/solution interface. The similar results were obtained for the sorption of other cations using different sorbents [46,49,50].

Table 3
Thomas constants for the removal of Cu(II) and Pb(II) by the manganese-modified natural sand.

Cu(II)		Pb(II)	
q_m (mg/g)	K_T (L/min/mg)	q_m (mg/g)	K_T (L/min/mg)
0.1904	1.42×10^{-2}	0.8946	5.67×10^{-3}

Further, the applicability of Langmuir adsorption isotherm was tested to deduce the mechanism of sorption process, based on the assumptions that the monolayer coverage of sorbing species took place along with non-lateral interaction within the sorbed ions. The plots were drawn between the C_e vs. C_e/q_e but the linear least square fitting was unacceptably very high as the R^2 value was found to be 0.776 for Cu(II) and 0.841 for Pb(II). Hence, further the estimation of Langmuir constants was not estimated.

3.5. Column experiments

The applicability of the manganese-modified natural sand was assessed under the dynamic conditions for the removal of Cu(II) and Pb(II) from aqueous solution using the column experiments. The column parameters were maintained as mentioned before and the breakthrough curves obtained were presented graphically in Fig. 9. Fig. 9 clearly demonstrated that the breakthrough started at the throughput volume of 0.037 L for Cu(II) and 0.137 L for Pb(II). Further, the complete breakthrough occurred at the throughput volume of 0.145 L for Cu(II) and 0.225 L for Pb(II). These results again supported the fact that MMNS possessed better affinity towards the Pb(II) removal. The breakthrough data is further used for the non-linear fitting to the Thomas equation (Eq. (4)) for the two unknown parameters i.e., q_m and K_T. Reasonably a good fitting was observed and the calculated line was shown in Fig. 9. Further, the Thomas constants were evaluated and returned in Table 3. The removal capacity of manganese-modified natural sand was found to be

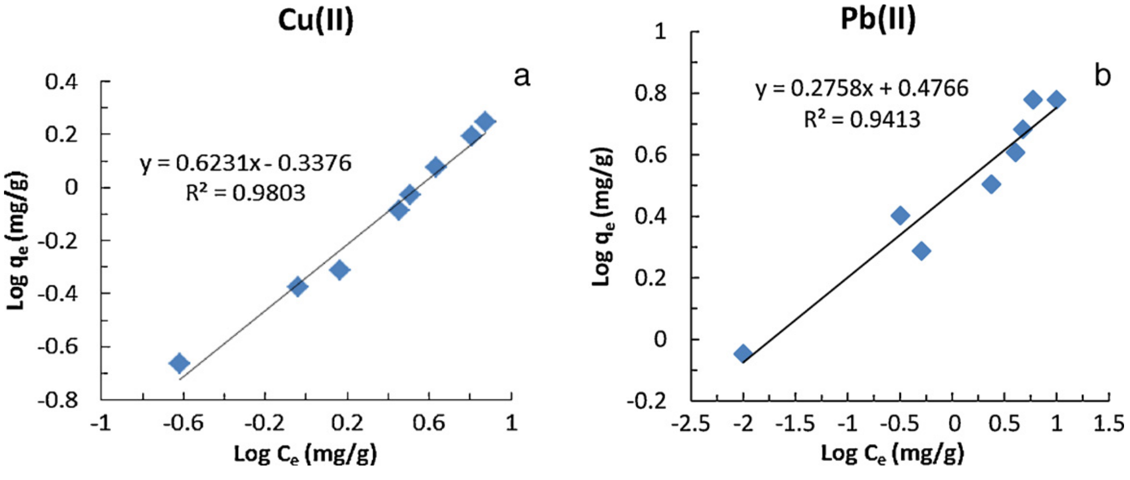

Fig. 8. The Freundlich adsorption isotherm for (a) Cu(II) and (b) Pb(II).

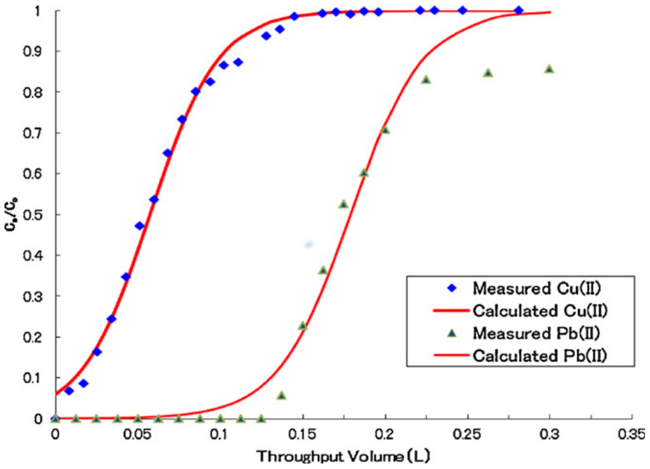

Fig. 9. Breakthrough curves for the removal of Cu(II) and Pb(II) by MMNS fitted for the Thomas model.

higher for Pb(II) than Cu(II). However, the value was significantly lower than the capacity evaluated using the Freundlich model. This difference may be explicable on the basis that the insufficient time of contact provided for the sorption of these metal cations onto the surface of solid under the dynamic conditions [42,51].

4. Conclusions

The manganese-modified natural sand was obtained in the laboratory. The nano-particles of manganese were evenly distributed onto the surface of sand which was characterized by the SEM and XRD analyses. Further, the EDX analysis of the MMNS solid showed relatively distinct peak of Mn. Moreover, the XRD data inferred that introduction of manganese caused an apparent shift of the d-values which indicated the interlayer spacings of sand propped up significantly. The BET data suggested that significantly higher specific surface area, possessed by the manganese-modified natural sand. The material was efficient for the low-level removal of Cu(II) and Pb(II) ions from aqueous solutions. The removal of these two ions was favored with increasing the sorptive pH and concentration, however, slightly decreased with increasing solution ionic strength. The concentration dependence data followed the Freundlich adsorption isotherm rather the Langmuir isotherm. The maximum sorption capacity obtained by the Freundlich adsorption isotherm was found to be 0.4596 mg/g for Cu(II) and 2.996 mg/g for Pb(II). The mechanism involved at solid/solution interface was predominantly the 'chemisorptive' type. The column data was fitted well for the Thomas equation hence, the maximum removal capacity of this solid under the dynamic conditions was found to be 0.1904 mg/g for Cu(II) and 0.8946 mg/g for Pb(II). The material comparatively showed better removal capacity for Pb(II) than Cu(II) from aqueous solutions.

Acknowledgements

One of the authors DT is thankful to the Head, Department of Chemistry, Mizoram University for allowing us to carry part of the research work in the department. This research was supported by the National Research Foundation of Korea (NRF) funded by the Korea government (MEST) (No. 2010-0000295).

References

[1] B.V. Laws, E.R.V. Dickenson, T.A. Johnson, S.A. Snyder, J.E. Drewes, Attenuation of contaminants of emerging concern during surface-spreading, Sci. Tot. Environ. 409 (2011) 1087–1094.

[2] T.A. Ternes, Occurrence of drugs in German sewage treatment plants and rivers, Water Res. 32 (1998) 3245–3260.

[3] D.W. Kolpin, M. Skopec, M.T. Meyer, E.T. Furlong, S.D. Zaugg, Urban contribution of pharmaceuticals and other organic wastewater contaminants to stream during differing flow conditions, Sci. Tot. Environ. 328 (2004) 119–130.

[4] M.J.M. Wells, A. Morse, K.Y. Bell, M.L. Pellegrin, L.J. Fono, Emerging pollutants, Water Environ. Res. 81 (2009) 2211–2254.

[5] K. Rout, M. Mohapatra, B.K. Mohapatra, S. Anand, Pb(II), Cd(II) and Zn(II) adsorption on low grade manganese ore, Int. J. Eng. Sci. Technol. 1 (2009) 106–122.

[6] F.N. Allouche, N. Mameri, E. Guibal, Pb(II) biosorption on *Posidonia Oceanica* biomass, Chem. Eng. J. 168 (2011) 1174–1184.

[7] A. El-Sikaily, A. El Nemr, A. Khaled, Copper sorption onto dried red alga *Ptero Cladia capillacea* and its activated carbon, Chem. Eng. J. 168 (2011) 707–714.

[8] A.P. Vieira, S.A.A. Santana, C.W.B. Bezerra, H.A.S. Silva, J.C.P. de Melo, E.C.S. Filho, C. Airoldi, Copper sorption from aqueous solution and sugar cane spirits by chemically modified babassu coconut (*Orbignya speciosa*) mesocarp, Chem. Eng. J. 161 (2010) 99–105.

[9] M.S. Al-Sewailem, E.M. Khaled, A.S. Mashhady, Retention of copper by desert sands coated with ferric hydroxides, Geoderma 89 (1999) 249–258.

[10] M. Ajmal, R.A.K. Rao, B.A. Siddiqui, Adsorption studies and the removal of dissolved metals using pyrolusite as adsorbent, Environ. Monit. Assess. 38 (1995) 25–35.

[11] X.H. Feng, L.M. Zhai, W.F. Tan, F. Liu, J.Z. He, Adsorption and redox reactions of heavy metals on synthesized Mn oxide minerals, Environ. Pollut. 147 (2007) 366–373.

[12] R.R. Gadde, H.A. Laitinen, Studies of heavy metal adsorption by hydrous iron and manganese oxides, Anal. Chem. 46 (1974) 2022–2026.

[13] G. Koulouris, B. Slowikowslei, R. Pilvio, T. Bostrom, M. Bickel, Preconcentration of actinides from waters: a comparison of various sorbents, Appl. Radiat. Isot. 53 (2000) 279–287.

[14] S.P. Mishra, Vijaya, Removal behviour of hydrous manganese oxide and hydrous stannic oxide for Cs(I) from aqueous solutions, Sep. Purif. Technol. 54 (2007) 10–17.

[15] S.P. Mishra, S.S. Dubey, D. Tiwari, Inorganic particulates in removal of heavy metal toxic ions IX: rapid and efficient removal of Hg(II) by hydrous manganese and tin oxide, J. Colloid Interface Sci. 279 (2004) 61–67.

[16] S. Nour, A. Ei-Sharkawy, W.C. Burnett, E.P. Horwitz, Radium-228 determination of natural waters via concentration on manganese dioxide and separation using diphonix ion exchange resin, Appl. Radiat. Isot. 61 (2004) 1173–1178.

[17] R.S. Sidhu, P. Hoff, Rapid determination of environmental plutonium in large water samples by means of manganese dioxide coprecipitation and extraction chromatographic separation, Radiochim. Acta 84 (1999) 89–93.

[18] S.S. Tripathy, K. Bersillon, G. Krishna, Adsorption of Cd2+ on hydrous manganese dioxide from aqueous solutions, Desalination 194 (2006) 11–21.

[19] R. Han, W. Zou, Z. Zhang, J. Shi, J. Yang, Removal of copper(II) and lead(II) from aqueous solution by manganese oxide coated sand. I. Characterization and kinetic study, J. Hazard. Mater. B137 (2006) 384–395.

[20] H. Guha, J.E. Saiers, S. Brooks, P. Jardine, K. Jayachandran, Chromium transport, oxidation and adsorption in manganese-coated sand, J. Contam. Hydrol. 49 (2001) 311–334.

[21] T. Boonfueng, L. Axe, Y. Xu, Properties and structure of manganese oxide-coated clay, J. Colloid Interface Sci. 281 (2005) 80–92.

[22] T. Stambel, M. Markic, N. Ribicic, F. Briski, L. Sipos, Removal of ammonia, iron and manganese from ground waters of northern Croatia: pilot plant studies, Process Biochem. 40 (2005) 327–335.

[23] D. Tiwari, M.R. Yu, M.N. Kim, S.M. Lee, O.H. Kwon, K.M. Choi, G.J. Lim, J.K. Yang, Potential application of manganese coated sand in the removal of Mn(II) from aqueous solutions, Water Sci. Technol. 56 (2007) 153–160.

[24] D. Tiwari, J.K. Yang, H.Y. Lee, K.M. Choi, S.M. Lee, Removal of Mn(II) from aqueous solutions using manganese coated sand, J. Chem. Eng. Data 54 (2009) 1823–1828.

[25] S.M. Lee, W.G. Kim, J.K. Yang, D. Tiwari, Sorption behavior of manganese-coated calcined starfish and manganese-coated sand for Mn(II), Environ. Technol. 31 (2010) 445–453.

[26] S.G. Wang, W.X. Gong, X.W. Liu, Y.W. Yao, B.Y. Gao, Q.Y. Yue, Removal of lead(II) from aqueous solution by adsorption onto manganeseoxide-coated carbon nanotubes, Sep. Purif. Technol. 58 (2007) 17–23.

[27] P.Y. Hu, Y.H. Hsieh, J.C. Chen, C.Y. Chang, Characteristics of manganese-coated sand using SEM and EDAX analysis, J. Colloid Interface Sci. 272 (2004) 308–313.

[28] W. Zou, L. Zhao, R. Han, Removal of uranium(VI) by fixed bed ion-exchange column using natural zeolite coated with manganese oxide, Sep. Sci. Eng. Chin. J. Chem. Eng. 17 (2009) 585–593.

[29] W. Zou, R. Han, Z. Chen, Z. Jinghua, J. Shi, Kinetic study of adsorption of Cu(II) and Pb(II) from aqueous solutions using manganese oxide coated zeolite in batch mode, Colloids Surf. A Physicochem. Eng. Aspects 279 (2006) 238–246.

[30] R. Han, W. Zou, H. Li, Y. Li, J. Shi, Copper(II) and lead(II) removal from aqueous solution in fixed-bed columns by manganese oxide coated zeolite, J. Hazard. Mater. B137 (2006) 934–942.

[31] R. Han, Z. Lu, W. Zhou, W. Daotong, J. Shi, J. Yang, Removal of copper(II) and lead(II) from aqueous solution by manganese oxide coated sand. II. Equilibrium study and competitive adsorption, J. Hazard. Mater. B137 (2006) 480–488.

[32] Y.Y. Chang, K.H. Song, J.K. Yang, Removal of As(III) in a column reactor packed with iron-coated and manganese-coated sand, J. Haz. Mat. 150 (2008) 565–572.

[33] S.M. Maliyekkal, A.K. Sharma, L. Philip, Manganese-oxide-coated alumina: a promising sorbent for defluoridation of water, Water Res. 40 (2006) 3497–3506.

[34] E. Eren, B. Afsin, Y. Onal, Removal of lead ions by acid activated and manganese oxide-coated bentonite, J. Hazard. Mater. 161 (2009) 677–685.

[35] S.M. Lee, W.G. Kim, C. Laldawngliana, D. Tiwari, Removal behavior of surface modified sand for Cd(II) and Cr(VI) from aqueous solutions, J. Chem. Eng. Data 55 (2010) 3089–3094.

[36] H.C. Thomas, Heterogeneous ion exchange in a flowing system, J. Am. Chem. Soc. 66 (1944) 1664–1666.

[37] H. Green-Pederson, N. Pind, Preparation, characterization, and sorption properties for Ni(II)of iron oxyhydroxide-montmorillonite, Colloids Surf. A 168 (2000) 133–145.

[38] G. Koulouris, Dynamic studies on sorption characteristics of ^{226}Ra on manganese dioxide, J. Radioanal. Nucl. Chem. 193 (1995) 269–279.

[39] Z. Aksu, Determination of the equilibrium, kinetic and thermodynamic parameters of the batch biosorption of lead(II) ions onto *Chlorella vulgaris*, Process Biochem. 38 (2002) 89–99.

[40] C.I. Lee, W.F. Yang, C.I. Hsieh, Removal of copper(II) by manganese-coated sand in a liquid fluidized-bed reactor, J. Hazard. Mater. B114 (2004) 45–51.

[41] D.L. Sparks, Environmental Soil Chemistry, Academic Press, San Diego, 1995, pp. 99.

[42] D. Tiwari, H.U. Kim, S.M. Lee, Removal behavior of sericite for Cu(II) and Pb(II) from aqueous solutions: batch and column studies, Sep. Sci. Technol. 57 (2007) 11–16.

[43] G.O. El-Sayed, H.A. Dessouki, S.S. Ibrahim, Biosorption of Ni(II) and Cd(II) ions from aqueous solutions onto rice straw, Chem. Sci. J. 9 (2010) 1–11.

[44] E. Malkoc, Ni(II) removal from aqueous solutions using cone biomass of *Thuja orientalis*, J. Hazard. Mater. B137 (2006) 899–908.

[45] M.S. Kim, J.G. Chung, Removal of copper(II) ion by kaolin in aqueous solutions, Environ. Eng. Res. 7 (2002) 49–57.

[46] D. Tiwari, S.P. Mishra, M. Mishra, R.S. Dubey, Biosorptive behavior of Mango (*Mangifera indica*) and Neem (*Azadirachta indica*) bark for Hg^{2+}, Cr^{3+} and Cd^{2+} toxic ions from aqueous solutions: a radiotracer study, Appl. Radiat. Isot. 50 (1999) 631–642.

[47] P. Benes, V. Majer, Trace Chemistry of Aqueous Solutions, Elsevier, Amsterdam, 1980.

[48] S.P. Mishra, D. Tiwari, R.S. Dubey, M. Mishra, Biosorptive behavior of casein for Zn^{2+}, Hg^{2+} and Cr^{3+}: effects of physic-chemical treatments, Bioresour. Technol. 63 (1998) 1–5.

[49] A. Agarwal, K.K. Sahu, Kinetic and isotherm studies of cadmium adsorption on manganese nodule residue, J. Hazard. Mater. B137 (2006) 915–924.

[50] M.E. Mesquita, J.M. Vieira e Silva, Preliminary study of pH effect in the application of Langmui and Freundlich isotherms to Cu-Zn competitive adsorption, Geoderma 106 (2002) 219–234.

[51] M.V. Sivaiah, P. Venkatesan, R.M. Sasidhar, J. Krishna, J. Murthy, Ion exchange study of cerium (III) on uranium antimonite, J. Nucl. Radiochem. Sci. 5 (2004) 7–10.

Chemical Engineering Journal 195-196 (2012) 103–111

Contents lists available at SciVerse ScienceDirect

Chemical Engineering Journal

journal homepage: www.elsevier.com/locate/cej

Iron oxide nano-particles-immobilized-sand material in the treatment of Cu(II), Cd(II) and Pb(II) contaminated waste waters

Seung-Mok Lee [a], C. Laldawngliana [b], Diwakar Tiwari [b],*

[a] Department of Environmental Engineering, Kwandong University, Gangneung 210-701, South Korea
[b] Department of Chemistry, School of Physical Sciences, Mizoram University, Aizawl, Mizoram 796 004, India

HIGHLIGHTS

- Iron oxide nanoparticle immobilized sand (INS) was obtained.
- INS was characterized by XRD and SEM analysis.
- INS assessed for remediation of aquatic environment.
- Batch and column reactor operations.
- Cu(II), Cd(II) and Pb(II) removal.

ARTICLE INFO

Article history:
Received 10 March 2012
Received in revised form 23 April 2012
Accepted 23 April 2012
Available online 30 April 2012

Keywords:
Iron oxide nano-particles-immobilized-sand
Sorption
pH
Concentration
Adsorption isotherm
Cu(II)
Cd(II)
Pb(II)

ABSTRACT

The aim of this investigation was to obtain iron-oxide nano-particles-immobilized sand (INS) by simple impregnation process. For the purpose, locally available sand was used with prior acid activation. The INS sample was characterized by XRD and SEM/EDX analytical methods. Further, the solid was employed for its possible implication in the removal of several toxic heavy metal ions *viz*., Cu(II), Cd(II) and Pb(II) from aqueous solutions under the static and dynamic experimental conditions. Batch experiments were carried out analyzing various physico-chemical parametric studies *viz*., effect of solution pH, ionic strength and sorptive concentration. The equilibrium state data obtained by concentration dependence study was utilized to obtain the Langmuir and Freundlich adsorption modeling. INS sample was also employed to assess the suitability of material in the removal of these heavy metal toxic ions under the dynamic conditions i.e., in column studies. The breakthrough data obtained by column studies were then utilized to model it with Thomas equation and hence, estimated the loading capacity of Cu(II)/or Cd(II)/or Pb(II) under the specified column conditions. Results obtained showed that INS is found to be one of promising and effective solid material and could be used in several wastewater treatment strategies in particular the treatment wastewaters contaminated with these heavy metal toxic ions.

1. Introduction

The contamination of surface and ground waters by heavy metal toxic ions became serious environmental issues because of the fact that these ions were virtually non-biodegradable and tends to accumulate in living being and cause for various biological disorders. Although, several heavy metals were found to be essential at trace level however, enhanced uptake caused for several toxic effects. Moreover, the heavy metals can form compounds within the bio-system which tends to be potentially carcinogenic and mutagenic even at very low levels [1,2].

Copper, cadmium and lead were common pollutants often to occur in our aquatic environment. Copper was one of essential trace element for humans and living organism which catalyzed the heme synthesis and iron absorption. An excess intake of copper, however, caused for stomach and intestinal distress, liver and kidney damage, anemia, etc. [3]. Cadmium was a non-essential metal ion caused several biological disorders *viz*., diarrhea, nausea, muscle cramp and damage of bone marrow. Moreover, it was considered as carcinogenic and responsible to stones formation in kidney [4,5]. Similarly, lead was also intended as non-essential heavy metal toxic ion and reported biological effects towards living being were anemia, encephalopathy, hepatitis and nephritic syndrome [6,7]. Severe toxicity of lead was associated with sterility, abortion, stillbirths and neo-natal death [8]. Therefore, because of several toxic effects of these heavy metal toxic ions, the US EPA recommended permissible

---

* Corresponding author. Tel.: +91 986 2323015; fax: +91 389 2330834.
E-mail address: diw_tiwari@yahoo.com (D. Tiwari).

1385-8947/$ - see front matter © 2012 Elsevier B.V. All rights reserved.
http://dx.doi.org/10.1016/j.cej.2012.04.075

limit in drinking water to be significantly low i.e., 1.3 mg/L for Cu(II), 0.005 mg/L for Cd(II) and 0.015 mg/L for Pb(II).

Various methods including ion-exchange, sorption, precipitation, coagulation/flocculation, membrane filtration, electrolysis, etc. were demonstrated to the treatment of aqueous wastes contaminated with these non-degradable pollutants [9–15]. Among these the sorption method based on suitable and selective materials gaining momentum for these studies because of several reasons including significantly high efficiency, low level removal of target ions, cost effectiveness, selectivity, etc. [10,14–16]. The natural sand which was provided a natural filter media employed primarily for filtration of water however, the removal capacity of sand material was found to be insignificant for various heavy metal toxic ions [17–20]. However, a suitable surface modification of sand perhaps showed enhanced suitability even for several heavy metal toxic ions. Impregnation of sand with manganese or iron could enable it suitable for the removal of heavy metal toxic ions from aqueous solutions [17–25]. The reclaimed iron oxide coated sand as obtained by the fluidized and air aerated bed reactor, which was designed to remove ferrous ions, produced by the reduction reaction occurred with nitrate and Fe(0) [26–28], were further used for the arsenic removal from aqueous solutions [29,30]. Similarly, the natural iron-oxide coated sand was employed in the effective adsorptive removal of Ni(II) and Cu(II) ions from aqueous solutions [31]. The silica was coated with iron by simple sol–gel method and was further employed in the removal of Cd(II) ions. The uptake process was reported to be spontaneous and greatly affected with solution pH [32]. The previous studies indicated the possible use of manganese nitrate in order to obtain the manganese impregnated natural sand and this was obtained by the low dose addition of manganese nitrate solution. Moreover, the active surface of sand was capable enough to aggregate the nano-sized particles of manganese oxide onto the sand surface. This solid was further employed for the low level removal of various heavy metal cations including, Mn^{2+}, Cu^{2+}, Pb^{2+} and Cd^{2+} or anion *viz*., Cr(VI), etc. The solid showed enhanced affinity towards the removal/speciation of these toxic ions from aqueous solutions [17,18,23,33,34]. Hence keeping in view the present study is an extension of our several previous studies in which the manganese-modified sand was employed. This is an attempt to modify the natural sand with low dose of iron as to obtain the iron oxide nanoparticles-immobilized sand and further it was employed to the removal of several heavy metal toxic ions *viz*., Cu(II), Cd(II) and Pb(II) from aqueous solutions. The batch and column studies were performed to simulate the experimental data in the treatment of wastes contaminated with these heavy metal toxic ions.

2. Materials and methods

2.1. Materials

Natural sand was collected from local river the Tlawng at the Sairang site, Aizawl, India. Cupric sulfate was obtained from DSP, Korea. Similarly, the cadmium nitrate was obtained from Duksan Pure Chemicals, Korea. Lead nitrate and iron(III) nitrate were obtained respectively from Junsei Chemicals Co. Ltd., Japan and Kanto Chemical Co. Ltd., Japan. The 1000 ppm standard solutions of copper, lead and cadmium were obtained from Wako Pure Chemicals, Japan. The nitric acid and sodium hydroxide were used of AR grade. The deionized water was further purified (18 MΩ-cm) using Millipore water purification system (Milli-Q+).

2.2. Methodology

2.2.1. Iron oxide-nanoparticles-immobilized sand preparation

Sand was washed thoroughly with purified water and kept in 0.2 mol/L HNO_3 solution overnight followed by washed with purified water and dried at 90 °C in a drying oven. Iron oxide-nanoparticles-immobilized sand (INS) was prepared by taking 120 g of dried sand (30–60 BSS in size) with 100 ml of 0.05 iron nitrate solutions at pH = 9.0 in a rotary flask and kept at 70 °C at the rotary evaporator speed of 30 rpm in a water bath. Almost 90% of the water was very slowly removed applying vacuum in the rotary evaporator. This sample was taken into a beaker and abruptly dried at 90 °C in a drying oven. The sample was heated at 160 °C for *Ca.* 8 h which could enable it for complete drying and perhaps better coating stability of iron onto the sand surface. The small-sized particles of iron oxide were aggregated onto the sand surface. It was then cooled to room temperature and again washed with purified water for several times. It was dried again in a drying oven at 90 °C overnight and stored in a stoppered polyethylene bottle. This dried INS sample was used for the present investigation. Moreover, the amount of iron impregnated onto the sand surface was analyzed with the standard US EPA method as mentioned elsewhere [23].

2.2.2. Characterization of INS sample

The INS sample was characterized by the XRD data which was collected by using an X-ray diffraction (machine PAnalytical, Netherland vide model X'Pert PRO MPD). The data was collected with the scan rate of 0.034 of 2θ illumination and the applied voltage was maintained at 45 kV and the observed current was 35 mA. Moreover, the Cu Kα radiation possessed with wavelength of 1.5418 Å. Similarly, the morphology of the solid was discussed by taking its SEM (Scanning Electron Microscope) images using the SEM machine (FE-SEM, Model: SU-70, Hitachi, Japan) equipped with energy dispersive X-ray Spectroscopy EDX system.

2.2.3. pH_{PZC} determination of INS

The pH_{PZC} (point of zero charge) of INS was defined as the pH value at which the surface carries no net charge. The pH_{PZC} was obtained by the acid and base titrations. Five grams of INS was taken in 500 mL of purified water and titrated with standard 0.10 mol/L of HNO_3 or NaOH solutions, and the corresponding pH values were recorded using a pH meter (Dual pH meter Istek, Korea, Model 740P). The pH data obtained against the standard addition of acid/or base was then utilized to evaluate the pH_{PZC} of the INS.

2.2.4. Speciation studies

The speciation studies were performed separately for Cu(II), Cd(II) and Pb(II) using the MINEQL+(Version 4.5) a geochemical computer simulation program. The input parameters were taken as initial concentration of Cu(II)/or Cd(II)/or Pb(II): 10 mg/L; Temperature: 25 °C.

2.2.5. Batch reactor experiments

Stock solutions of Cu(II), Cd(II) and Pb(II) 1000 mg/L were prepared by dissolving appropriate amount of respective metal salts in purified water. Further, the required concentration of these metal ions was obtained by successive dilutions. However, the blank check was always performed analyzing the diluted solution with AAS (Atomic Absorption Spectrometer; Fast Sequential Atomic Absorption Spectrometer Model AA240FS, Varian). The pH dependence data was obtained by taking 100 mL 10 mg/L of Cu(II)/or Cd(II)/or Pb(II) solutions into different polyethylene bottles and its pH was adjusted from pH 2 to 10 by small addition of conc. HNO_3/NaOH solutions. 0.5 g of solid INS was added to each bottle and these bottles were kept in an automatic shaker for 24 h at 25 ± 1 °C in order to complete the sorption process. These samples were taken out from the shaker and filtered using 0.45 μm syringe filter. The solution pH was again checked and reported throughout as final pH. The filtrates were taken for its bulk sorptive concentration measurements using AAS. Further, the percentage removal of these metal ions was calculated using the following the known equation as given elsewhere [23].

Similarly, concentration dependence data were obtained by taking the sorptive solution having varied concentration from 1 mg/L to 20 mg/L for Cu(II) and Cd(II) whereas it was taken from 1 to 50 mg/L for Pb(II). The solution pH was kept constant as the final pH recorded as 4.5 and adsorption process was conducted at constant temperature 25 °C. Moreover, the sorption procedures were followed as described before. Further, the concentration dependence data were presented graphically in terms of percent removal against the initial sorptive concentration.

The equilibrium state concentration dependence data was then employed for the adsorption isotherm modeling using the known Freundlich and Langmuir linear adsorption isotherm Eqs. (1) and (2) respectively:

$$\mathrm{Log}\, q_e = \mathrm{Log}\, K_F + \frac{1}{n} \times \mathrm{Log}\, C_e \qquad (1)$$

$$\frac{C_e}{q_e} = \frac{1}{bq_m} + C_e\left(\frac{1}{q_m}\right) \qquad (2)$$

where 'C_e' was the equilibrium bulk concentration of Cu(II)/or Cd(II)/or Pb(II) in solution (mg/L), 'q_e' was the amount of Cu(II)/or Cd(II)/or Pb(II) adsorbed at equilibrium (mg/g). The constants 'K_F' and '$1/n$' were implied to the Freundlich constants and were represented, respectively, to adsorption capacity (mg/g) and adsorption intensity. On the other hand, the constants 'b' and 'q_m' were referred to Langmuir constants respectively represented to adsorption equilibrium constant (L/mg) and maximum adsorption capacity (mg/g), respectively.

The ionic strength dependence data was obtained varied the background electrolyte concentration of sorptive solution from 0.001 to 1.0 mol/L using $NaNO_3$ solution. The sorptive pH (~4.0) and temperature (25 ± 1 °C) was kept constant throughout the experiments. Results were presented as percent removal as a function of ionic strength.

2.2.6. Column studies

Column data was obtained by using a glass column (1 cm inner diameter) annexed with a peristaltic pump and fraction collector. The glass column was packed with 0.5 g of INS solid (kept in the middle of column) and below and above to the INS 2 g of bare sand was packed followed by the glass beads to pack completely the column. Cu(II)/or Cd(II)/or Pb(II) 10 mg/L solution (pH 4.0) was pumped upward from bottom of the column using a peristaltic pump at a constant flow rate of 1.2 mL/min. Effluent samples were then collected using Spectra/Chrom CF-1 fraction collector. The samples collected were filtered using 0.45 μm syringe filter and subjected for bulk sorptive concentrations using AAS.

Moreover, the column/breakthrough data obtained was further simulated for its removal capacity estimation using the Thomas Eq. (3) [35]:

$$\frac{C_e}{C_0} = \frac{1}{1 + e^{(K_T(q_0 m - C_0 V))/Q}} \qquad (3)$$

where C_e was the Cu(II)/or Cd(II)/or Pb(II) concentration in the effluent (mg/L); C_0 was the Cu(II)/or Cd(II)/or Pb(II) concentration in the feed (mg/L); K_T the Thomas rate constant (L/min/mg); q_0 was the maximum amount of the Cu(II)/or Cd(II)/or Pb(II) could be loaded (mg/g) under the specified column conditions; m was the mass of adsorbent loaded (g); V the throughput volume (L); and Q the flow rate of pumped sorptive solution (L/min). A non-linear regression analysis of the breakthrough data was conducted using the least square fitting method implying for two unknown parameters i.e., K_T and q_0.

3. Results and discussions

3.1. Characterization of INS Sample

The solids INS and sand were analyzed using the X-ray diffraction data. The diffraction data obtained was represented in Fig. 1. INS or sand samples showed very characteristics and distinct diffraction reflections occurred at the 2θ values of 20.88, 26.68, 36.58, 39.50, 50.18, 59.96, 67.73, 68.30, etc. These reflections were because of the presence of silica as compared with the standards mentioned by Joint Committee on Powder Diffraction Standards (JCPDSs). Moreover, the relative intensities with the d-values were obtained and returned in Table 1. The difference in d-value was insignificant for these two solids inferred that iron oxide was hardly to prop-up the silicate layer hence, mostly it was aggregated onto the surface or within the accessible pores of the sand. Further, there were no additional sharp reflections occurred by the INS indicated that no mineral phase of iron was present onto the sand surface. This was because of the fact that very low content of iron aggregated onto the surface of sand [19,23]. Earlier studies were also mentioned that an amorphous iron oxide was coated onto sand which was converted to goethite and hematite at 150 °C and hematite above 300 °C [36]. Similarly, γ-Fe_2O_3 was occurred at 400 °C while iron was coated onto alumina [37]. Similarly, mixture of hematite and goethite were obtained by Chang et al. [38].

SEM images of sand and INS were obtained and shown in Fig. 2a and b, respectively for sand and INS solids. The SEM image of bare sand (*cf* Fig. 2a) showed, the surface structure of sand was very compact and disordered. It was not possessed with micro- or meso-pores on it. However, surface roughness and cracks were clearly visible onto it. On the other hand, the surface morphology of INS showed (*cf* Fig. 2b) that an intense deposition of nano-sized particles of iron oxide which were partly clustered at places. However, mostly, these nano-sized particles were very orderly arranged onto the sand surface. The average size of these particles was estimated to be *Ca* < 200–300 nm. Further, the EDX data (*Cf* Fig. 3a and b; Table 2) indicated that the sand itself possessed with low content of iron i.e., 6.82% however, it was increased significantly to 12.96% (weight percent) by the iron impregnation. These results showed that a low content of iron was impregnated onto the sand surface. Earlier studies showed that iron is mostly concentrating within the rough areas available onto the sand surface, with non-uniform Fe and Si distribution [19,39,40]. Moreover, it was previously obtained by very high dose of iron i.e., 2 M ferric nitrate solution [12]. Further, the present study showed that almost evenly distributed iron oxide particles were occurred onto the sand surface. Further, the content of iron obtained by the digestion method

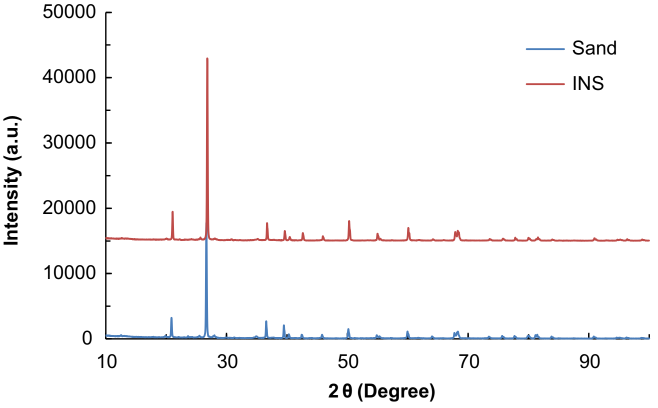

Fig. 1. XRD pattern of sand and INS.

Table 1
The *d*-values and relative intensities for sand and INS obtained by XRD analysis.

Sand			INS			Difference with *d*-value
2θ	*d*-Value	$I/I_0 \times 100$	2θ	*d*-Value	$I/I_0 \times 100$	
20.8811	4.25074	18.12	21.1151	4.20415	16.05	0.04659
26.6791	3.33867	100	26.8351	3.31959	100	0.01908
28.0051	3.18351	3.11	28.1091	3.17197	1.40	0.01154
36.5851	2.4542	15.19	36.7411	2.44414	9.83	0.01006
39.4971	2.27971	11.71	39.6791	2.26967	5.54	0.01004
40.3291	2.23458	3.95	40.5111	2.22496	2.25	0.00962
42.4611	2.12718	3.59	42.6691	2.11729	4.41	0.00989
50.1831	1.81646	8.48	50.3391	1.8112	10.98	0.00526
59.9591	1.54155	6.33	60.1411	1.53732	7.21	0.00423
67.7331	1.3823	5.16	67.9151	1.37903	4.96	0.00327
68.3051	1.37211	6.29	68.3311	1.37165	5.64	0.00046

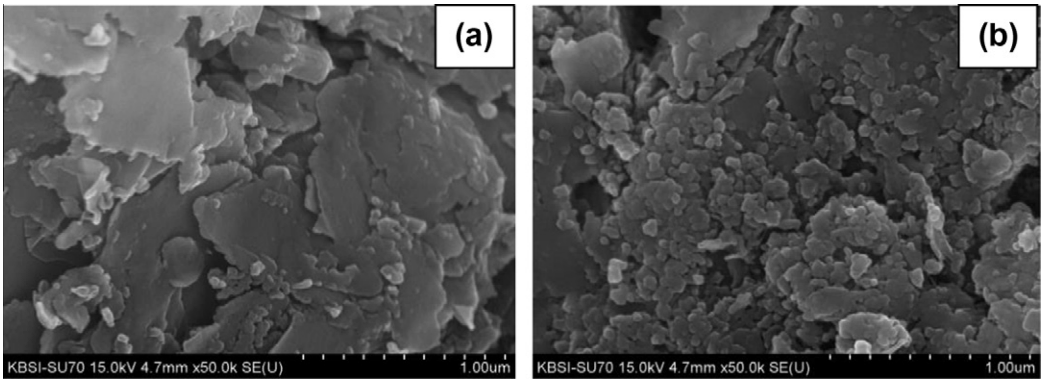

Fig. 2. SEM images of (a) sand and (b) INS solid.

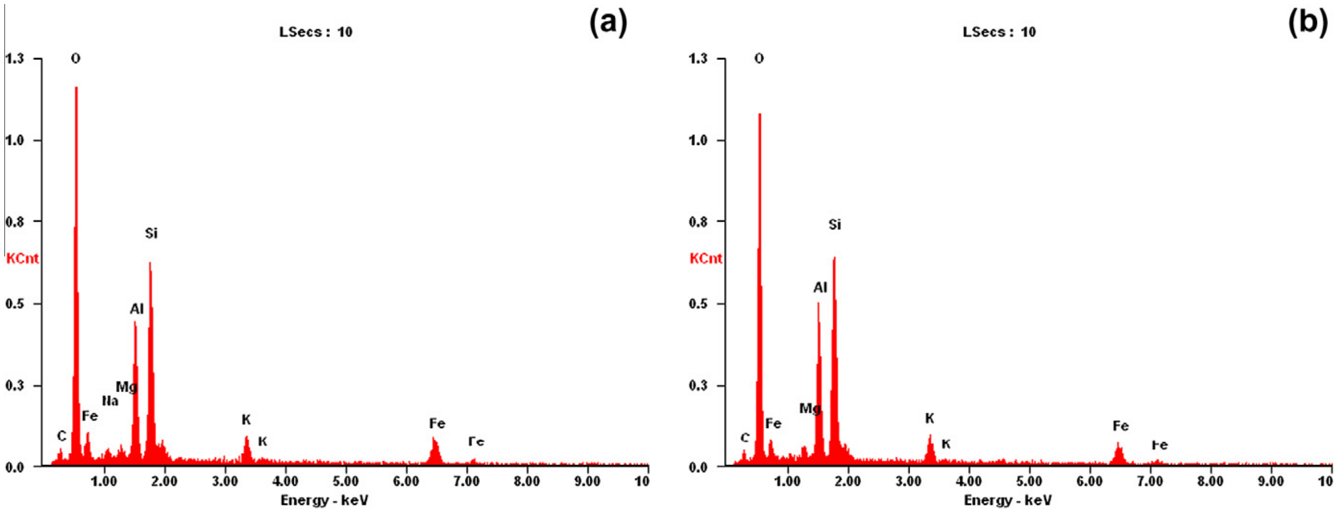

Fig. 3. EDX analytical results for (a) sand and (b) INS solid.

was found to be 5.7 mg of Fe/g of sand, which is having lower iron content compared to the other methods of iron impregnation onto silica.

3.2. Speciation studies of Cu(II), Cd(II) and Pb(II)

The speciation data obtained by the MINEQL geochemical program were presented graphically in Fig. 4a–c respectively for Cu(II), Cd(II) and Pb(II). These results were greatly helpful in elucidating the mechanism involved at solid solution interface at various pH conditions. Results showed that both copper and lead were occurred to its ionic forms i.e., Cu^{2+} and Pb^{2+} even up to the pH ~5.8. But beyond that both started precipitating as the Cu(II) was converted to insoluble tenorite phase and lead was precipitated as $Pb(OH)_2(S)$; beyond pH 7.0 these two species were completely dominated. However, in between these two species insignificant formation of $Cu(OH)^+$ (max. 1.4%) was occurred at pH 5.8. Similarly, $Pb(OH)^+$ was occurred at pH 6.2 with a maximum of 3.9%. On the other hand the speciation data obtained for Cd(II) showed, the Cd^{2+} ionic species were stable even up to the solution pH of 8.8 but beyond pH 9.4 the dominant species was the insoluble $Cd(OH)_2$ (S). Similar to Cu(II) and Pb(II), it also existed with the insignificant species of $Cd(OH)^+$ (maximum of 4.8%) but at pH 8.8.

Table 2
EDX Data for Sand and INS solid.

Element	Wt%		At%	
	Sand	INS	Sand	INS
CK	15.29	07.30	24.00	12.59
OK	41.72	42.65	49.18	55.19
NaK	01.97	01.10	01.62	00.99
MgK	00.70	01.42	00.54	01.21
AlK	07.35	08.53	05.14	06.54
SiK	24.37	23.57	16.36	17.37
KK	01.77	02.46	00.86	01.30
FeK	06.82	12.96	02.30	04.81

3.3. pH dependence sorption

The pH dependence data were obtained for the studied metal cations using INS and the results were presented graphically in Fig. 5. The uptake of these metal cations was greatly affected with the change in solution pH. It was noted that during initial range of pH the uptake of these ions were increased gradually. However, at the latter stage of pH i.e., beyond pH 7, it was attained with almost a constant value of sorption. Quantitatively, increasing the pH from 1.76 to 8.18 the respective increase of Cu(II) was from 1.87% to 98.26%. The Cd(II) was increased from 2.87% to 97.28%, respectively for the increase in pH from 2.37 to 9.12. Similarly, the Pb(II) sorption was increased from 2.05% to 94.91%, increasing the respective pH from 2.09 to 7.62.

The pH dependence data obtained for these metals ions using INS was explained by the surface properties of INS as well the nature of sorbing species in present in solution. The nano-particles of iron oxide mostly covered the surface of sand hence, the bulk sand properties was changed markedly in presence of impregnated iron oxide. Moreover, the pH_{PZC} of INS sample was found to be 6.23 which, was very close to the reported pH_{PZC} of ferric hydroxide 6.28 [41]. The other studies indicated the pH_{PZC} of reclaimed IOCS was found to be 7.0 ± 0.4 [29] and 6.5–8.5 [42]. Similarly, Stenkamp and Benjamin [43] found the pH_{PZC} close to 7.5 for iron oxide-coated sand. Hence, our values of pH_{PZC} for INS were slightly different from the previously reported values. The surface of INS was carried with positive charge below pH 6.23 and became negatively charged beyond this:

$$\equiv SOH_2^+ \underset{pH_{PZC}}{\leftrightarrow} \equiv SOH^0 \leftrightarrow \equiv SO^- \qquad (4)$$

On the other hand up to the pH 5.8 both the ions Cu(II) and Pb(II) were dominantly existed as positively charged species of Cu^{2+} and Pb^{2+} whereas even up to pH 8.8 Cd(II) existed as cationic species of Cd^{2+} (MINEQL studies). At extreme low pH region i.e., pH between 2 and 4 both solid surface of INS and sorbing species were possessed with enhanced positive charge which ultimately caused for strong electrostatic repulsion. Therefore, seemingly it caused for significantly low uptake of these metal cations. However, the further increase in pH i.e., beyond 4.0 the partial acidic dissociation of solid INS surface may perhaps cause for some electrostatic attraction of these metal cations which showed a gradual increase in metal uptake. The similar results were occurred for different metal cations uptake by the manganese coated sand [17,18,33]. However, the only electrostatic attraction could not be ascribed to

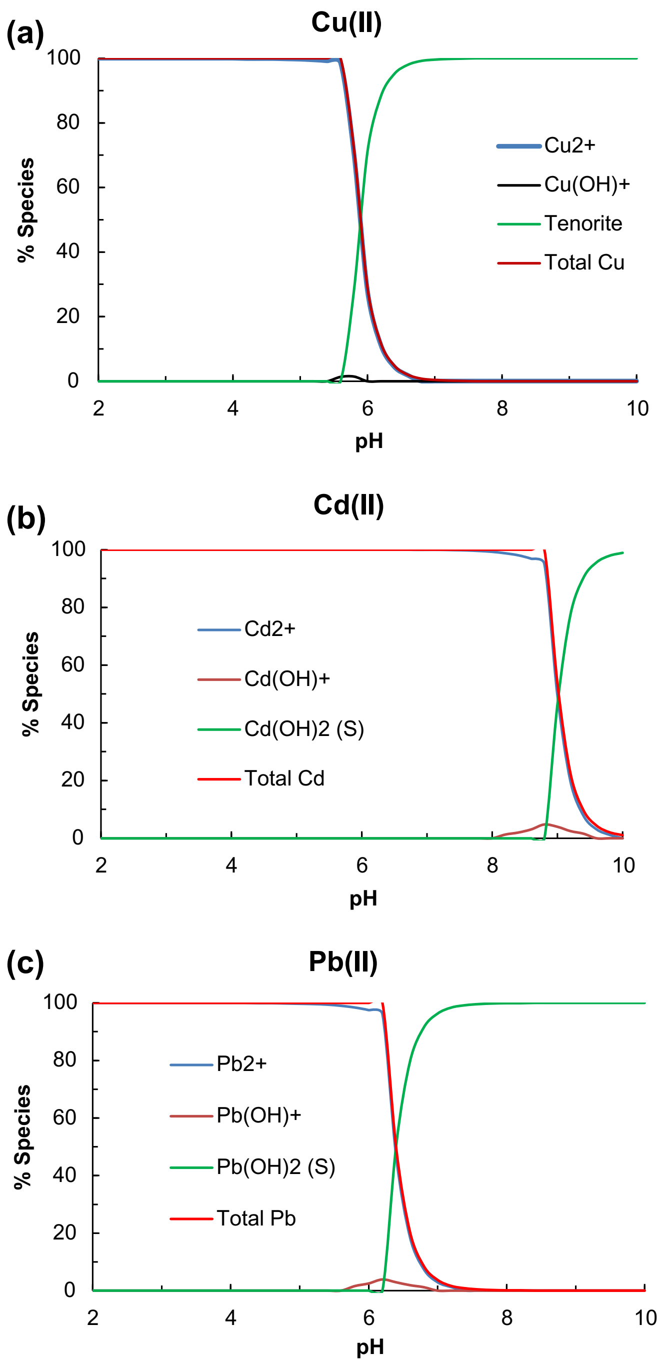

Fig. 4. Percentage distribution of various species of (a) Cu(II); (b) Cd(II); and (c) Pb(II) as a function of pH.

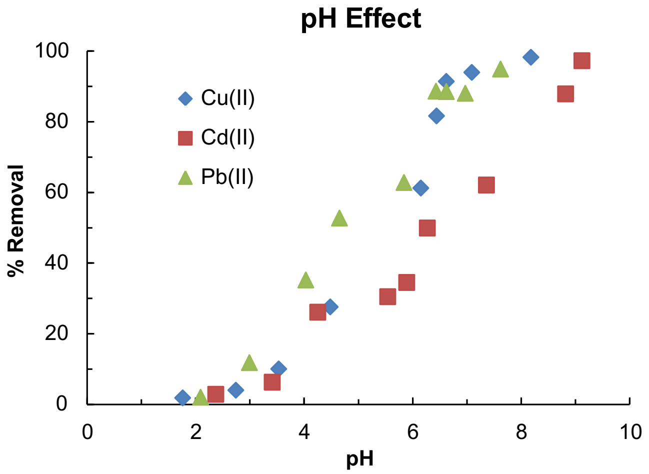

Fig. 5. Effect of pH on the percent sorption of Cu(II), Cd(II) and Pb(II) from aqueous solutions by the INS.

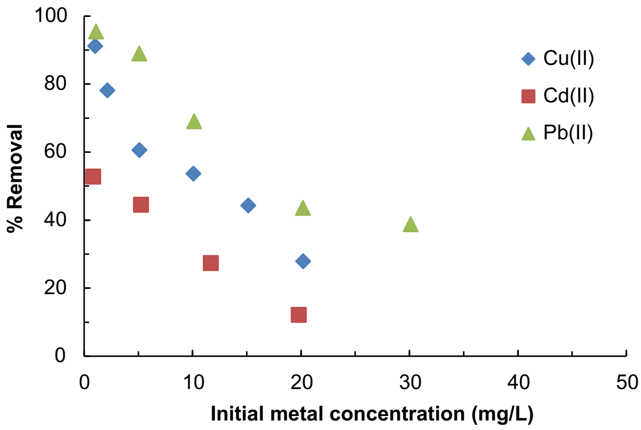

Fig. 6. Effect of sorptive concentration in the percent removal of Cu(II), Cd(II) and Pb(II) from aqueous solutions by INS.

explain the sorption of these metal cations since surface carries a net negative charge beyond pH 6.23 (pH_{PZC} of INS) hence, in addition to partial electrostatic attraction, the surface complexation through ion-exchange process was also postulated for enhanced uptake of these metal cations M(II) (M(II): Cu(II), Cd(II) and Pb(II)) within the pH region 4–6.0 [24,44] and this was suggested with Eqs. (5) and (6) whereas between the pH region 6.2 to 8.8 for (Cd(II)), additional mechanism was suggested by Eqs. (7) and (8):

$$M^{2+} + \equiv SOH_2^+ \leftrightarrow \equiv S{-}OM^+ + 2H^+ \qquad (5)$$

$$M(OH)^+ + \equiv SOH_2^+ \leftrightarrow \equiv S{-}OM(OH)^0 + 2H^+ \qquad (6)$$

$$Cd^{2+} + \equiv SO^- \leftrightarrow \equiv S{-}OCd^+ \qquad (7)$$

$$Cd(OH)^+ + \equiv SO^- \leftrightarrow \equiv S{-}O{-}Cd(OH)^0 \qquad (8)$$

Similar ion exchange mechanism was suggested for the uptake of cadmium by goethite coated sand [24], iron-oxide coated sand [44] or even metal oxide surfaces [45]. Further, increase in pH i.e., beyond pH 6.0 for Cu(II) and Pb(II) and above pH 8.8 for Cd(II) there could be a mixed effect of sorption with co-precipitation or even coagulation of these metal cations [33,46,47] which caused for almost 100% removal of these studied metal cations. These results were in conformity to the speciation studies conducted for these cations previously.

3.4. Effect of sorptive concentrations

The concentration dependence data were shown graphically in Fig. 6 as initial metal concentration against the percent removal of these metal ions. Increasing the sorptive concentration apparently caused for a decrease in percent removal of these ions or decreasing the concentration favored for percent uptake of metal removal. This could be ascribed because of the fact that at low sorptive concentrations, more and more active sites are available for relatively lesser number of sorbing species. Hence, an enhanced percentage of sorption was observed at low sorptive concentration [48]. More quantitatively, increasing the Cu(II) and Cd(II) concentration from 1 mg/L to 20 mg/L caused for a decrease of percent uptake respectively from 91.17% to 27.92% (for Cu(II); from 52.81% to 12.16% for Cd(II). Similarly, increasing the sorptive concentration from 1 to 50 mg/L was caused for a decrease in percent uptake of Pb(II) from 95.45% to 20.03%, respectively.

Further, these concentration dependence data obtained at equilibrium stage between the solid/solution interfaces were utilized to build the known adsorption isotherms i.e., Freundlich and Langmuir adsorption models. It was found that these were fitted to the Freundlich and Langmuir linear adsorption models. However, it was noted that the fitting was relatively better for the Langmuir adsorption model comparing to the Freundlich adsorption model. Fitting data were then used to evaluate the Freundlich and Langmuir constants. These constants along with the R^2 values were returned in Table 3. The marked difference in capacity estimated by these two models is attributed to the different basic nature and assumptions of the models. It was observed that apparent removal capacity for Pb(II) was relatively higher than the Cu(II) and Cd(II). Previously also observed that the removal capacity of Pb(II) was comparatively higher than the Cu(II) using sericite sorbent [47]. Moreover, the low value of sorption capacity for Cd(II) towards the INS showed its less affinity towards the solid surfaces. Similar, observation was observed previously as the tree bark samples showed enhanced removal capacity for Hg^{2+} and Cr^{3+} whereas Cd^{2+} was removed insignificantly [48]. Similar, trend was also reported by the others for the bioaccumulation of Zn^{2+} and Cd^{2+} by the *Saccharomyces cerevisiae* biomass applied for the uptake of these two cations from aqueous solutions [49].

Further, the fractional value of Freundlich constant, i.e., $1/n$ which relates to the sorption intensity of the solid, obtained for these systems indicated a heterogeneous surface structure of solids with an exponential distribution of surface active sites [23,50]. Similarly, the Langmuir constant '*b*' reflected to the strength and affinity of the solid towards the sorbing species [12]. Also it was related to the equilibrium constant of the process: M(II) + Solid = -M(II)…Solid (surface adsorption complex).

3.5. Effect of background electrolyte

In order to demonstrate the specific and non-specific adsorption of metal cations onto the surface of solid, the effect of ionic strength on metal cation partitioning was enabled the plausible data to explain the mechanism involved at solid/solution interface [51]. It was reported that the specific adsorption was unaffected with the change in ionic strength, whereas the non-specific adsorption was greatly influenced by the change of ionic strength because of the competitive adsorption with counter ions. Hence keeping in view the study was conducted to observe the change in background electrolyte concentration i.e., $NaNO_3$ in the adsorption behavior of INS at least to the removal of studied metal cations i.e., Cu(II), Cd(II) and Pb(II). The background electrolyte concentration was increased from 0.001 mol/L to 1.0 mol/L $NaNO_3$. Results were presented with percent removal of Cu(II), Cd(II) or Pb(II) vs the background electrolyte concentrations and presented graphically in Fig. 7. In general, it was observed that increasing the background electrolyte concentration caused for an apparent decrease in percent removal of Cu(II), Cd(II) or Pb(II) by INS. Quantitatively, increasing the background electrolyte concentration from 0.001 mol/L to 1.0 mol/L $NaNO_3$, the corresponding decrease in percent uptake was occurred, respectively from 52.95% to 49.56% for Cu(II) (i.e., decreased by only 3.39%); from 45.83% to 11.69% for Cd(II) (i.e., decreased by 34.14%); from 62.55% to 25.29% for Pb(II) (i.e., decreased by 37.26%). These results showed that 1000 times increase in background electrolyte concentration was not hampered greatly the uptake of Cu(II).

Table 3
Freundlich and Langmuir constants for the adsorption of Cu(II), Cd(II) and Pb(II) by INS.

System	Freundlich constants			Langmuir constants		
	K_f (mg/g)	$1/n$	R^2	q_m (mg/g)	b (L/mg)	R^2
INS-Cu(II)	0.4867	0.4013	0.9615	1.2649	1.0005	0.9729
INS-Cd(II)	0.1788	0.4912	0.8062	0.5282	1.5729	0.9582
INS-Pb(II)	0.7845	0.3402	0.9117	2.0877	1.3705	0.9912

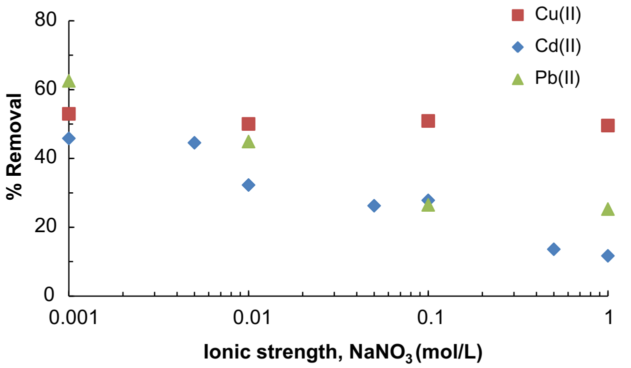

Fig. 7. Effect of background electrolyte concentration (NaNO3) in the percent removal of Cu(II), Cd(II) and Pb(II) from aqueous solutions by INS.

However, it was affected to a significant level in the removal of Cd(II) or Pb(II) ions. Hence, this indicated that Cu(II) was sorbed specifically by the INS whereas the Cd(II) and Pb(II) were sorbed partly by the electrostatic attraction along with the 'ion-exchange' process. Earlier, it was shown that copper was singly coordinated to the surface OH groups of present on Al hydroxides [52]. Similarly, Benjamin and Leckie [53] suggested that copper formed an inner-sphere complex along with ion-exchange process onto the surface of iron oxide coated sand. On the other hand, the uptake of Pb(II) by iron-oxide coated sepiolite was significantly affected decreased increasing the background electrolyte concentrations [54]. These results were in a line to our experimental findings and favored the mechanism proposed.

3.6. Column reactor studies

Applicability of the INS was further assessed in the removal of Cu(II), Cd(II) and Pb(II) under the dynamic conditions. These data were of direct practical importance in the possible large scale or pilot scale implication of the material. The column conditions were maintained as stated before and the results were presented graphically in Fig. 8a–c respectively for the Cu(II), Cd(II) and Pb(II). The complete breakthrough was occurred for the throughput volume of 0.176L, 0.261L and 0.454L respectively for Cu(II), Cd(II) and Pb(II). These results inferred that INS possessed significantly high removal capacity for these metal ions even under the dynamic conditions as well which pointed it a potential and promising sorbent material.

Further, the breakthrough data was used to the non-linear fitting of Thomas equation (Eq. (2)) and hence estimated the two unknown parameters *viz.*, q_0 and K_T which were referred respectively to maximum amount of Cu(II)/or Cd(II)/or Pb(II) to be loaded in the column under the specified column conditions and Thomas rate constant, respectively. Reasonably, fairly a good fitting of breakthrough data obtained for these systems as shown in Fig. 8a–c. Similar results were also reported previously where the metal ions were removed by using the biosorbents or manganese coated sands, etc. [23,55,56]. The Thomas constants i.e., q_0 and K_T were estimated for these solids and returned in Table 4. The data showed that the solid INS possessed with significantly high removal capacity for these metal cations. Previous studies showed that the biomass *Spirogyra*-packed column possessed the removal capacity of 18.87 and 29.50 mg/g respectively for the Cu(II) and Pb(II) at relatively low flow rate of 0.6 mL/min [55]. On the other hand the biomass *Macrophthalmus rouxii* showed the removal capacity of 4.06 (at the flow rate 2.28 mL/min) and 1.25 mg/g (at the flow rate 2.60 mL min), respectively for the Pb(II) and Cd(II) [56]. These results indicated that the removal capacity of a material primarily depends on its affinity towards the metal cations which further affected with the column conditions *viz.*, flow rate, influent pH and, ionic strength, etc. of the influent solution.

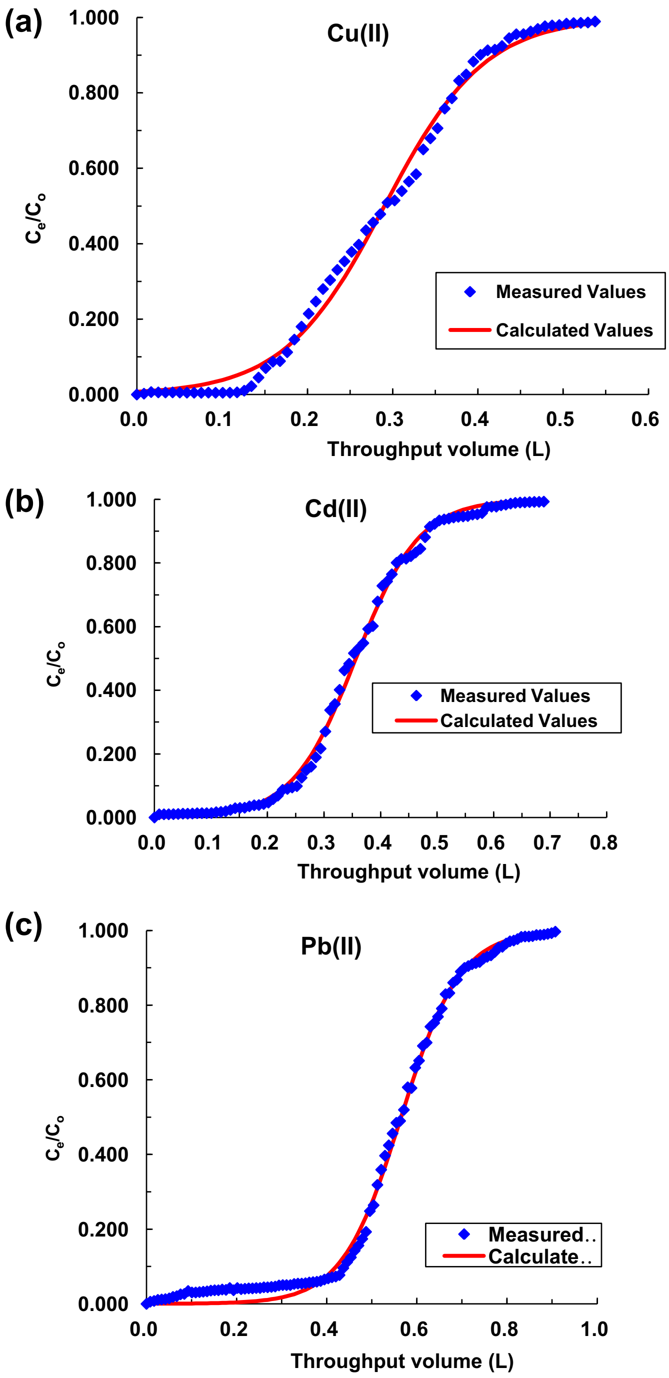

Fig. 8. Breakthrough curves for the removal of (a) Cu(II); (b) Cd(II); and (c) Pb(II) by INS fitted for the Thomas model.

Table 4
Thomas constants for the removal of Cu(II), Cd(II) and Pb(II) from aqueous solutions by INS solid.

Systems	q_0 (mg/g)	$K_T \times 10^{-3}$ (L/min/mg)
INS-Cu(II)	5.81	2.03
INS-Cd(II)	7.13	2.14
INS-Pb(II)	11.30	1.83

However, among these, Pb(II) possessed with higher removal capacity compared to the Cd(II) or Cu(II). These results are in accordance to the batch data obtained. However, unlikely to the batch trend obtained particularly the removal capacity of Cd(II) which was relatively higher than the Cu(II) under the batch experiments. This is possibly because of relatively higher effluent pH was recorded for Cd(II) i.e., *Ca* 5.5 whereas the effluent pH of Cu(II) was recorded as 4.5.

4. Conclusions

Nano-sized-iron oxide-immobilized-sand (INS) was obtained by simple impregnation process. INS was characterized by the XRD and SEM/EDX analytical data. Total amount of iron aggregated onto the sand surface was found to be 5.7 mg/g of sand. INS was further employed for the low level removal of Cu(II), Cd(II) and Pb(II) from aqueous solutions under the batch and column experimentation. Batch data revealed that increase in sorptive pH, increased the uptake of these ions whereas increase in sorptive concentration (1–20 mg/L for Cu(II) and Cd(II) and 1–50 mg/L for Pb(II)) caused for decrease in percent uptake of these metal cations. Moreover, 1000 times increase in background electrolyte concentration (from 0.001 to 1 mol/L NaNO$_3$) was caused for significant decrease in Cd(II) and Pb(II) removal whereas Cu(II) was almost unaffected with this increase. These, results implied that the sorption of copper follow 'ion-exchange' along with inner-sphere surface complexation whereas Cd(II) and Pb(II) sorption was presumably proceeded with ion-exchange along with electrostatic attraction by the solid surface. Equilibrium state modeling of adsorption models showed a good applicability of Freundlich and Langmuir adsorption isotherms. Accordingly, the estimated Langmuir sorption capacity was found to be 1.2649, 0.5282 and 2.0877 mg/g respectively for Cu(II), Cd(II) and Pb(II) by INS. Moreover, the breakthrough data was demonstrated well to the Thomas equation which was used to optimize the loading capacity of these metal ions within the column. The obtained capacity was found to be 5.81, 7.13 and 11.30 mg/g respectively for Cu(II), Cd(II) and Pb(II). These results, therefore, showed that INS could found to be one of efficient material, which could have potential application in the remediation of wastewaters contaminated with heavy metal toxic ions *viz.*, Cu(II), Cd(II) and Pb(II).

References

[1] R.B. Martin, Metal ions in biological systems, in: H. Siegel, (Ed.), Arcel Dekker, New York, 1985.

[2] P. Madoni, D. Davoli, G. Gorbi, L. Vescovi, Toxic effect of heavy metals on the activated sludge protozoan community, Water Res. 30 (1996) 135–142.

[3] J.L. Gardea-Torresdey, L. Tang, J.M. Salvador, Copper adsorption by esterified and unesterified fractions of *Sphagnum* peat moss and its different humic substances, J. Hazard. Mater. 48 (1996) 191–206.

[4] B.B. Johnson, Effects of pH, temperature and concentration on the adsorption of cadmium on goethite, Environ. Sci. Technol. 24 (1990) 112–118.

[5] M. Waseem, S. Mustafa, A. Naeem, G.J.M. Koper, K.H. Shah, Cd^{2+} sorption characteristics or iron coated silica, Desalination 277 (2011) 221–226.

[6] L. Friberg, G.F. Nordberg, B. Vouk, Handbook on the toxicology of metals, Elsevier, North-Holland, Biomedical press, Amsterdam, 1979.

[7] W. Lo, H. Chua, K.H. Lam, S.H. Bi, A comparative investigation on the biosorption of lead by filamentous fungal biomass, Chemosphere 39 (1999) 2723–2736.

[8] J. Goel, K. Kadirvelu, C. Rajagopal, V.K. Garg, Removal of lead(II) by adsorption using treated granular activated carbon: batch and column studies, J. Hazard. Mater. B125 (2005) 211–220.

[9] A. Demirbas, Heavy metal adsorption onto agrobased waste materials: a review, J. Hazard. Mater. 157 (2008) 220–229.

[10] D. Sud, G. Mahajan, M.P. Kaur, Agricultural waste material as potential adsorbent for sequestering heavy metal ions from aqueous solutions – a review, Bioresour. Technol. 99 (2008) 6017–6027.

[11] S.P. Singh, L.Q. Ma, M.J. Hendry, Characterization of aqueous lead removal by phosphatic clay: equilibrium and kinetic studies, J. Hazard. Mater. 136 (2006) 654–662.

[12] V.K. Gupta, V.K. Saini, N. Jain, Adsorption of As(III) from aqueous solutions by iron oxide-coated sand, J. Colloid Interface Sci. 288 (2005) 55–60.

[13] G. Zhang, J. Qu, H. Liu, R. Liu, R. Wu, Preparation and evaluation of a novel Fe–Mn binary oxide adsorbent for effective arsenite removal, Water Res. 41 (2007) 1921–1928.

[14] I. Ali, V.K. Gupta, Advances in water treatment by adsorption technology, Nat. Protocols 1 (2006) 2661–2667.

[15] S.M. Lee, D. Tiwari, Organo- and inorgano–organo-modified clays in the remediation of aqueous solutions: an overview, Appl. Clay Sci. in press, doi: 10.1016/j.clay.2012.02.006.

[16] D. Mohan, C.U. Pittman Jr., Arsenic removal from water/wastewater using adsorbents – a critical review, J. Hazard. Mater. 142 (2007) 1–53.

[17] D. Tiwari, M.R. Yu, M.N. Kim, S.M. Lee, O.H. Kwon, K.M. Choi, G.J. Lim, J.K. Yang, Potential application of manganese coated sand in the removal of Mn(II) from aqueous solutions, Water Sci. Technol. 56 (2007) 153–160.

[18] S.M. Lee, W.G. Kim, C. Laldawngliana, D. Tiwari, Removal behavior of surface modified sand for Cd(II) and Cr(VI) from aqueous solutions, J. Chem. Eng. Data 55 (2010) 3089–3094.

[19] Y. Xu, L. Axe, Synthesis and characterization of iron oxide-coated silica and its effect on metal adsorption, J. Colloid Interface Sci. 282 (2005) 11–19.

[20] C.H. Lai, S.L. Lo, H.L. Chiang, Adsorption/desorption properties of copper ions on the surface of iron-coated sand using BET and EDAX analyses, Chemosphere 41 (2000) 1249–1255.

[21] M. Edwards, M.M. Benjamin, Adsorptive filtration using coated sand: a new approach for treatment of metal bearing wastes, J. WPCF 61 (1989) 1523–1533.

[22] R.P. Bailey, T. Bennett, M.M. Benjamin, Sorption onto and recovery of Cr(VI) using iron-oxide-coated sand, Water Sci. Technol. 26 (1992) 1239–1244.

[23] D. Tiwari, C. Laldanwngliana, C.H. Choi, S.M. Lee, Manganese-modified natural sand in the remediation of aquatic environment contaminated with heavy metal toxic ions, Chem. Eng. J. 171 (2011) 958–966.

[24] C.H. Lai, C.Y. Chen, B.L. Wei, S.H. Yeh, Cadmium adsorption on goethite-coated sand in the presence of humic acid, Water Res. 36 (2002) 4943–4950.

[25] M.G. Mostafa, Y.H. Chen, J.S. Jean, C.C. Liu, Y.C. Lee, Kinetics and mechanism of arsenate removal by nanosized iron oxide-coated perlite, J. Hazard. Mater. 187 (2011) 89–95.

[26] C. Ruangchainikom, C.H. Liao, J. Anotai, M.T. Lee, Innovative process using Fe^0/CO$_2$ for the removal of nitrate from groundwater, Water Sci. Technol. Water Supply 5 (2005) 49–56.

[27] C. Ruangchainikom, C.H. Liao, J. Anotai, M.T. Lee, Characteristics of nitrate reduction by zero-valent iron powder in the recirculated and CO$_2$-bubbled system, Water Res. 40 (2006) 195–204.

[28] C. Ruangchainikom, C.H. Liao, J. Anotai, M.T. Lee, Effects of water characteristics on nitrate reduction by the Fe^0/CO$_2$ process, Chemosphere 63 (2006) 335–343.

[29] J.C. Hsu, C.J. Lin, C.H. Liao, S.T. Chen, Removal of As(V) and As(III) by reclaimed iron-oxide coated sands, J. Hazard. Mater. 153 (2008) 817–826.

[30] J.C. Hsu, C.J. Lin, C.H. Liao, S.T. Chen, Evaluation of the multiple-ion competition in the adsorption of As(V) onto reclaimed iron-oxide coated sands by fractional design, Chemosphere 72 (2008) 1049–1055.

[31] N. Boujelben, J. Bouzid, Z. Elouear, Adsorption of nickel and copper onto natural iron oxide-coated sand from aqueous solutions: study in single and binary systems, J. Hazard. Mater. 163 (2009) 376–382.

[32] M. Waseem, S. Mustafa, A. Naeem, G.J.M. Koper, K.H. Shah, Cd^{2+} sorption characteristics of iron coated silica, Desalination 277 (2011) 221–226.

[33] D. Tiwari, J.K. Yang, H.Y. Lee, K.M. Choi, S.M. Lee, Removal of Mn(II) from aqueous solutions using manganese coated sand, J. Chem. Eng. Data 54 (2009) 1823–1828.

[34] S.M. Lee, W.G. Kim, J.K. Yang, D. Tiwari, Sorption behaviour of manganese-coated calcined-starfish and manganese-coated sand for Mn(II), Environ. Technol. 31 (2010) 445–453.

[35] H.C. Thomas, Heterogeneous ion exchange in a flowing system, J. Am. Chem. Soc. 66 (1944) 1664–1666.

[36] S.L. Lo, H.T. Jeng, C.H. Lai, Characteristics and adsorption properties of iron-coated sand, Water Sci. Technol. 35 (1997) 63–70.

[37] Z.Y. Zhong, T. Prozorov, I. Felner, A. Gedanken, Sonochemical synthesis and characterization of iron oxide coated on submicrospherical alumina: a direct observation of interaction between iron oxide and alumina, J. Phys. Chem. B 103 (1999) 947–956.

[38] Y.Y. Chang, K.H. Song, J.K. Yang, Removal of As(III) in a column reactor packed with iron-coated sand and manganese-coated sand, J. Hazard. Mater. 150 (2008) 565–572.

[39] M. Edwards, M.M. Benjamin, Adsorption filtration using coated sand: a new approach for treatment of metal-bearing wastes, J. Water Pollut. Control Fedn. 61 (1989) 1523–1533.

[40] A. Scheidegger, M. Borkovec, H. Sticher, Coating of silica sand with goethite: preparation and analytical identification, Geoderma 58 (1993) 43–65.

[41] G. Koulouris, Dynamic studies on sorption characteristics of ^{226}Ra on manganese dioxide, J. Radioanal. Nucl. Chem. 193 (1995) 269–279.

[42] R.M. Cornell, Schwertmann, The Iron Oxides: Structure, Properties, Reactions, Occurrence and Use, Wiley-VCM, New York, 1996.

[43] V.S. Stenkamp, M.M. Benjamin, Effect of iron oxide coatings on sand filtration, J. AWWA 86 (1994) 37–50.

[44] M.M. Benjamin, R.S. Sletten, R.P. Bailey, T. Bennett, Sorption and filtration of metals using iron-oxide-coated sand, Water Res. 30 (1996) 2609–2620.

[45] K.F. Hayes, J.O. Leckie, Modeling ionic strength effects on cation adsorption at hydrous oxide/solution interfaces, J. Colloid Interface Sci. 115 (1987) 564–572.
[46] K.S. Hui, C.Y.H. Chao, S.C. Kot, Removal of mixed heavy metal ions in wastewater by zeolite 4A and residual products from recycled coal fly ash, J. Hazard. Mater. B127 (2005) 89–101.
[47] D. Tiwari, H.U. Kim, S.M. Lee, Removal behavior of sericite for Cu(II) and Pb(II) from aqueous solutions: batch and column studies, Sep. Purif. Technol. 57 (2007) 11–16.
[48] D. Tiwari, S.P. Mishra, M. Mishra, R.S. Dubey, Biosorptive behaviour of Mango (*Mangifera indica*) and Neem (*Azadirachta indica*) bark for Hg^{2+}, Cr^{3+} and Cd^{2+} toxic ions from aqueous solutions: a radiotracer study, Appl. Radiat. Isot. 50 (1999) 631–642.
[49] Y.P. Ting, W.K. Teo, Uptake of cadmium and zinc by yeast: effect of co-metal ions and physical chemical treatment, Bioresour. Technol. 50 (1994) 113–117.
[50] P. Benes, V. Majer, Trace Chemistry of Aqueous Solutions, Elsevier, Amsterdam, 1980.
[51] K.F. Hayes, C. Papelis, J.O. Leckie, Modeling ionic strength effects on anion adsorption at hydrous oxide/solution interfaces, J. Colloid Interface Sci. 125 (1988) 717–726.
[52] M.B. McBride, Cu^{2+} adsorption characteristics of aluminum hydroxide and oxyhydroxides, Clays Clay Miner. 30 (1982) 21–28.
[53] M.M. Benjamin, J.O. Leckie, Multiple-site adsorption of Cd, Cu, Zn and Pb on amorphous iron oxyhydroxide, J. Colloid Interface Sci. 79 (1981) 209–236.
[54] E. Eren, H. Gumus, Characterization of the structural properties and Pb(II) adsorption behavior of iron oxide coated sepiolite, Desalination 273 (2011) 276–284.
[55] A. Singh, D. Kumar, J.P. Gaur, Continuous metal removal from solution and industrial effluents using *Spirogyra* biomass-packed column reactor, Water Res. 46 (2012) 779–788.
[56] G. Yan, T. Viraraghavan, Heavy metal removal in a biosorption column by immobilized *M. rouxii* biomass, Bioresour. Technol. 78 (2011) 243–249.